

Modelling traffic in the Randstad using a dynamic zone model based on the Network Fundamental Diagram

Mark Slood

MODELLING TRAFFIC IN THE RANDSTAD USING A DYNAMIC ZONE MODEL BASED ON THE NETWORK FUNDAMENTAL DIAGRAM

by

Mark Slood

in partial fulfillment of the requirements for the degree of

Master of Science
in Civil Engineering

at the Delft University of Technology,
to be defended publicly on Monday April 1, 2019 at 17:00 PM.

Thesis committee:	Prof. dr. ir. J.W.C. van Lint,	TU Delft (CEG)
	Dr. V. L. Knoop,	TU Delft (CEG)
	Dr. K. Yuan,	TU Delft (CEG)
	Prof. dr. ir. A. Verbraeck,	TU Delft (TPM)

An electronic version of this thesis is available at <http://repository.tudelft.nl/>.

ABSTRACT

This master thesis focusses on the usability of a dynamic zone-based traffic assignment model for large areas, using the concept of the Network Fundamental diagram. These kinds of models differ from the traditional traffic assignment models, because the conventional models are suitable for modelling traffic networks consisting of links, rather than zones.

The most simple traffic assignment models are all static models. These models are capable of modelling traffic networks with constant network parameters for single time periods with a stationary demand. The travel times are determined using a link travel time function, which is a monotonically increasing function for an increasing flow. The principle for determining the route flows is the principle that each traveller optimizes its own travel time, so the traffic assignment results in a User Equilibrium (UE).

Dynamic traffic models are more advanced models, that can model multiple time periods with varying demand. Those models also set capacity restrictions at intersections and bottlenecks. The traffic surplus at bottlenecks is stored in horizontal queues. The travel times are determined with the fundamental diagram. A drawback of dynamic models is the computational effort, especially for large networks.

An alternative to dynamic and static models are the quasi-dynamic models. Those models are static models that incorporate some properties of dynamic models, like flow-metering and spillback. This results in computationally efficient models that can produce realistic travel times and flow patterns.

This research describes an alternative to the aforementioned model types, and applies it in a case study for the Randstad, which is the area enclosed by the Dutch cities Amsterdam, Den Haag, Rotterdam and Utrecht. The model that is used is a dynamic zone model.

This model makes use of the concept of the Network Fundamental Diagram (NFD), which relates the average internal flow (production) and speed in a network to the number of vehicles in the network (accumulation). The production is related linearly to the output of the network, which is the sum of the outflow at the boundaries of the network and the trip completion rate in the network.

An example of a dynamic zone model is the Network Transmission Model (NTM). In this model the flow between two neighbouring zones is determined by the demand in the upstream zone, the supply in the downstream zone, and the capacity of the boundary between these zones. The total amount of traffic that a certain zone receives can not exceed the supply of that zone. The demand and supply are derived from the NFDs for both zones. In this case, the NFD is used that gives the relation between accumulation and performance.

The NTM has some limitations. It may not perform well under rapidly changing conditions, because the outflow of a zone changes instantly when the accumulation changes. Besides that, all vehicles inside one zone have the same average trip lengths, regardless of their paths.

The simulation model that is used in this case study for the Randstad is a newly developed model inspired by the Network Transmission Model. It differs from the NTM in the way the demand is determined. The demand of a zone is not derived directly using the NFD, but instead by the number of vehicles that have completed their trip inside that zone. For all vehicles a trip length is determined on beforehand. Each simulation step is then calculated how much distance is travelled by this vehicle during that time step, using the current average speed inside the zone, which is derived from the NFD. The trip is completed when the traversed distance equals the predetermined trip length.

The simulation program generates new trips for small sets of vehicles. Such a set of vehicles represents multiple travellers with the same destination, same path and the same departure time. The number of vehicles in the set is determined by the OD-matrix and the normalized demand pattern. The fastest route from the origin to the destination under the current traffic conditions is assigned to the set of vehicles.

The OD-matrix is determined using the first two steps of the four-step model, namely trip generation and trip distribution. In the trip generation step, the number of departures and arrivals for each zone is estimated

using a formula, based on the number of households and the number of jobs in each zone. The number of departures and arrivals for the external areas are derived from observed data.

For the trip distribution step the doubly constrained gravity model is used. The attractiveness of travelling between two zones is represented by the cost function, with the euclidean distance between the zones as generalized costs. The OD matrix is then estimated by means of an iterative procedure, during which the number of trips between each pair is updated after each iteration. Convergence has been reached as soon as the OD-matrix no longer changes as a result of the iterations.

The trip distribution phase leads to an OD-matrix for 24 hours. The next step is that this OD matrix has to be translated to a full demand pattern over the day. The demand pattern is unknown, but based on the observed data, the internal flow pattern can be determined. If this internal flow pattern is divided by the total production for 24 hours, it gives the normalized demand pattern. This normalized demand pattern can be multiplied by the total departures or arrivals for the zone, resulting in the 24-hour OD-matrix.

During each simulation step, the distance travelled by each set of vehicles is updated. Afterwards, the demand for each zone is calculated. As mentioned, the demand is the number of vehicles that has traversed its predetermined trip length. In the next step, it is determined whether the capacities of the boundaries between the zones are sufficient for the demands. If not, the values for the demand are reduced such that the total demand does not exceed the boundary capacity. This results in the effective demand.

When the effective demand is calculated for each zone, the next step is to verify whether the supply of the zones is further restricting the flows. If this is the case, the flows are reduced again such that the supply is not exceeded. When this is finished, the sets of vehicles are moved between the zones. Finally, the state of each zone is updated. The new accumulation for a zone is the accumulation in the previous step plus the sum of the inbound flows, reduced by the outbound flows. The whole procedure is repeated until all time steps are fulfilled.

Before the simulation can be performed, the study area has to be divided into zones, and for each zone an NFD has to be constructed. The area is divided into zones by clustering the existing municipalities in the study area into 16 zones. For each zone that is located at the border of the study area an external zone is added to the simulation, in order to incorporate traffic with an external origin or destination.

The NFDs are constructed in three steps. First the NFD for the freeway network is constructed based on loop detector data. Then the NFDs for the local network are estimated based on a theoretical fundamental diagram and characteristics of the road network. Finally, these NFDs are combined to one NFD per zone.

The NFD for the freeway network is constructed using data requested from NDW (Nationale Databank Wegverkeersgegevens). This data consists of flows (veh/h/lane) and speeds (km/h) measured with loop detectors on fixed locations. By taking the weighted average of the flow and the accumulation for each time period, the production and accumulation are obtained for each zone.

For the local network, the NFD is estimated using an analytical approach. Motorways are now left out, because for these roads the NFD has already been estimated using detector data. In this step, information from OpenStreetMap is used to determine the total lane length of each road type in each zone. The same road classification as used by OpenStreetMap is used in this stage. The lower-hierarchy-roads (residential, living street, service and unclassified roads) are left out. For each of the remaining road types, a triangular-shaped fundamental diagram is assumed, based on the speed limits on these road types.

The final step in the NFD estimation process is to combine the NFDs for each road type to one final NFD for the full network, by averaging the speeds on each road for a given average density. Differences in occupancy between the different road types are taken into account by means of a fixed ratio between these densities. Based on data from the NDW, an average ratio between the density on freeways and primary roads of 1.38 is defined. For the secondary roads, the square of this value is used (1.90), and for tertiary roads the cube (2.63).

Now, the final NFD can be constructed. For each observed density on the freeway network the corresponding densities on the lower-hierarchy roads are calculated, as well as the weighted average density for the full network. With these densities and the fundamental diagrams, the weighted average network flow is calculated. The resulting weighted average densities and flows are then plotted in the K, P -diagram and a multi-linear line is fitted through the points.

With this input, the simulation can be performed. The simulation results are analyzed on three aspects, which are the outflow and accumulation patterns of the zones, and the trip durations between the zones.

These outflow and accumulation patterns are compared to observed patterns, and for some OD-pairs the trip durations are compared to data from Google Maps. For the accumulation and outflow patterns it is desired that the difference with the observed patterns over 24 hours and during peak hours is less than 20%.

Generally, the model is able to reproduce the shapes of the outflow patterns, taking into account the desired range of 20%, but some zones show large deviations. Especially for the zones Den Haag and Rotterdam the outflow is particularly during morning peak much higher than the observed values.

For the accumulation patterns, the majority of the zones have an accumulation pattern for which the deviation from the expected patterns is larger than desired. This is especially the case for Gouda and Zaanstad, for which the accumulation is between 2 and 3 times higher than the expected accumulations based on the observed values for freeways.

One of the plausible explanations for these results is that the trip lengths inside the zone are overestimated. This statement is tested by reducing the internal distances for four zones. After this reduction, the accumulation patterns improved, but the reduction is not in all cases large enough.

Lastly, the travel times are compared to travel times obtained from Google Maps. From the results it becomes clear that in general the travel times are highly overestimated by the simulation model for long-distance trips and underestimated for short-distance trips. An explanation for these findings is that all traffic in a zone drives with the same speed, regardless of the traffic purpose, and the origin or destination. Through traffic on a freeway has then the same speed as the local traffic inside the zone. It would be more realistic to distinguish multiple types of traffic.

Based on the first simulation results, three possible improvements to the simulation model have been tested. In the original simulation, all traffic was assigned to the shortest path. A possible addition is to distribute traffic over multiple routes instead of using an all-or-nothing assignment, by means of a logit model. In order to test the effect of assigning vehicles to different routes, multiple logit parameters have been evaluated, but it has not lead to improved simulation results. For smaller parameters, the changed distribution of the traffic over a network leads to a gridlock in some of the zones. For larger parameters the logit distribution converges to an all-or-nothing assignment, so the differences with regard to the original simulation are small.

Even when all traffic uses the same path on zone level, it does not necessarily mean that all traffic uses the same roads. An example is traffic between Leiden and Rotterdam via Den Haag. In the zone of Den Haag, traffic can still choose between the A4 and A13, so there are two feasible paths through the same zones. Therefore, a plausible explanation for the simulation results is that routing happens more inside the zones than one zone-level.

The second improvement that is tested is to make distinction between trips based on the origins and destinations. Two main types of traffic are distinguished, which are local traffic and through traffic. Vehicles crossing a zone with both an external origin and destination are classified as through traffic, and vehicles with both an internal origin and destination are classified as local traffic. For both types a separate NFD is defined, which gives the relation between the accumulation and the average speed. The accumulation is the total accumulation of the zone, consisting of both the local and the through traffic.

Apart from through traffic and local traffic, a third type is introduced, called mixed traffic. This category covers all vehicles with either an internal origin and external destination or an external origin and internal destination. For this type, no separate NFD is determined, but it is assumed that this type of traffic drives with a speed which is the average of the local and through traffic speed.

Because the OD-matrix remains the same, the outflow patterns do not change significantly. The accumulation patterns overall show a major improvement with respect to the base case. For most zones, the difference between the simulated and observed accumulation patterns falls in the desired range of 20%.

The most important reason for making distinction between local and through traffic is the travel times between the zones. When the travel times are compared to observations by Google Maps, it is concluded that the results improved with respect to the original simulation case. This improvement is especially visible for the long-distance trips. For some short-distance trips no clear improvement is visible in the results. But overall it can be concluded that the distinction between local and through traffic has lead to improved results.

The last change to the original simulation setup that is tested is the OD-matrix estimation process. Originally, the OD-matrix has been estimated using a doubly-constrained gravity model with the euclidean distance between the centers of each OD-pair as the generalized costs for travelling between that OD-pair. Alternatively, the travel time between the origin and destination could be used as an estimator for the generalized

costs, which has been tested in the last simulation. In this last test, also three types of traffic are distinguished, each with its own NFD in terms of speed. These free-flow speeds combined with the internal distance matrices are used to calculate the travel times between each OD-pair.

Overall, the simulation results show that the new OD matrix has just a small effect on the accuracy of the outflow patterns. For some zones the outflow pattern improved, but for other zones the situation got worse, therefore no general conclusion can be drawn from these results. The accumulation patterns and travel times also do not show a clear improvement with respect to the base case.

Although the changed OD-matrix did not improve the results, it is still preferred to estimate the OD-matrix using travel times rather than the euclidean distance, because for the original OD matrix it was necessary to reduce the total departures and arrivals for some zones, to end up with a suitable results, while for the new OD-matrix this was not necessary. Besides that, it is more intuitive to use travel times as an indicator for the generalized costs than euclidean distances.

The objective of this research is to develop a zone-based dynamic traffic model that can be applied on large areas, like the Randstad. The final model that is proposed is based on the Network Transmission Model, but some modifications have been made to make the model suitable for the Randstad. The main difference is that a trip-based approach is used, so that for each vehicle its own trip length can be defined. This has a positive effect on the performance of the model.

Another adjustment is that distinction is made between through traffic and local traffic. For both traffic types a separate NFDs is defined. This addition is necessary for the model to be able to estimate the travel times accurately. When one single NFD is used for all traffic, it results in inaccurate travel times. For through traffic, the travel times are overestimated, while for local traffic the travel times are underestimated. For smaller-scale networks this distinction is probably not necessary, because the speed differences are much smaller.

For so far, the all-or-nothing routing assignment has given the best results. Distributing traffic over multiple routes using the logit model did not work well, because it has lead to a gridlock in some of the zones.

The simulation of this model has given promising results, and it is expected that improving the input to the model can result in more reliable outflow and accumulation patterns and travel times. Especially the OD-matrix estimation can be improved, because in this research only a simple approach has been used to construct the OD-matrix. besides that, the internal distance matrix and the NFDs for local traffic also need further improvement. Before the model could be applied in practice, some further research is therefore needed. The model has now been applied to one area, but it is recommended to test this model for other large areas, also with different zone sizes, to check whether this approach could be used as a universal approach for modelling traffic on a macroscopic level.

CONTENTS

Abstract	iii
1 Introduction	1
1.1 Background	1
1.2 Problem statement	1
1.3 Research objective	2
1.4 Report structure.	4
2 Literature review	7
2.1 Static traffic models	7
2.2 Dynamic traffic models	7
2.3 Quasi-dynamic models	8
2.4 Dynamic zone model based on the Network Fundamental Diagram	9
2.4.1 Network Fundamental Diagram	9
2.4.2 Network Transmission Model	12
2.4.3 Trip-based model	13
3 Methodology	15
3.1 Simulation model	15
3.1.1 Model steps	15
3.2 Zone division	18
3.3 NFD construction.	18
3.3.1 Detector data	19
3.3.2 Analytical approach	19
3.3.3 Combination.	20
3.3.4 Calculating the state of the system	22
3.4 OD-pattern estimation	24
3.4.1 Trip generation	24
3.4.2 Trip distribution	25
3.4.3 Demand pattern over time	27
3.5 Routing strategy.	27
3.6 Performance analysis	28
4 Model application	29
4.1 Zone division	29
4.2 NFD Construction	32
4.2.1 NFD for the freeway networks	32
4.2.2 NFD for the local networks.	34
4.2.3 NFD for the full network	37
4.3 OD-pattern estimation	40
4.3.1 Trip generation	40
4.3.2 Distance matrix estimation	40
4.3.3 Trip distribution	43
4.3.4 OD-patterns over time	46
4.4 Routing	47
5 Simulation results	49
5.1 Analysis of the outflow patterns.	49
5.2 Analysis of the accumulation patterns	50
5.2.1 Sensitivity analysis of the internal distance matrix	51

5.3	Analysis of the travel times	54
5.4	Supply and boundary capacity restriction.	60
5.5	Conclusion	61
6	Improvements to the simulation	63
6.1	Multiple routes	63
6.1.1	Methodology.	63
6.1.2	Results	63
6.1.3	Conclusion.	65
6.2	Separation local and through traffic.	66
6.2.1	Methodology.	66
6.2.2	Application	69
6.2.3	Results	73
6.2.4	Conclusion.	82
6.3	OD-matrix based on travel times	83
6.3.1	Methodology.	83
6.3.2	Application	83
6.3.3	Results	84
6.3.4	Conclusion.	89
7	Discussion	93
7.1	Discussion on the methodology.	93
7.2	Discussion on the results	94
8	Conclusions and recommendations	97
	Bibliography	103
A	Freeway NFDs	107
B	NFD plots	113
B.1	Full network	113
B.2	Local & through traffic	118
C	OD-matrix	125
C.1	Base-case	126
C.2	OD-matrix based on travel times	128
D	Outflow plots	131
E	Accumulation plots	149
F	Travel times	167
E1	Free-flow travel times	167
E2	Morning peak travel times	176
E3	Afternoon peak travel times	181
G	Technical information	187

1

INTRODUCTION

In this chapter, the motivation for this research is discussed, and the research objective is introduced. This results in six research questions that are answered in the remainder of this report.

1.1. BACKGROUND

The Network Fundamental Diagram (NFD) relates the number of vehicles in a traffic network (accumulation) to the average speed or internal flow (Production) in that network. The production is also related to the performance of the network, which is the outflow plus the number of completed trips per time interval for that network. The ratio between the production and performance is the average internal trip length as a fraction of the total lane length of the network. Observations based on real life data have shown that aggregating traffic data for individual detectors for a network can result in a curve with hardly any scatter. This resulting curve is the NFD. [13] [12]

Based on the Network Fundamental Diagram, traffic models have been developed, like the Network Transmission Model (NTM). The NTM does not model traffic in individual road sections, but instead complete networks are considered. Urban areas are divided in multiple zones, in which the traffic should be more or less homogeneously distributed. Traffic in these zones is aggregated, and flows in accordance to the NFD defined for that zone. Other models use a trip-based or an event-based approach.

1.2. PROBLEM STATEMENT

The NFD has been developed for urban areas with homogeneous traffic conditions. The same holds for the simulation models that are based on this NFD. It is therefore unknown how such a model performs when it is applied to a larger region, because it has not been implemented and tested yet.

Major differences can be identified between small-scale simulations for urban areas and larger regions. One of the main differences is that larger regions consist of both urban and non-urban areas. These urban areas are interconnected by motorways. Traffic on motorways behaves differently from urban traffic for multiple reasons. One reason is that on motorways a phenomenon called hysteresis is observed. This phenomenon has two main causes: [14]

- **Spatial heterogeneity:** The spatial distribution of the origins over the network is different from the distribution of destinations. Origins are more evenly distributed over the network than destinations.
- **Capacity drop:** The queue-discharge rate of a congested freeway is usually smaller than the capacity before the onset of congestion.

For this reason the NFD may not be well-defined like in urban areas. Secondly, since the scale of the simulation is larger than usual, the zones will also be larger. However, it is unclear whether the NFD will also hold for large zones. Since homogeneity is a requirement for the NFD, the NFD may not be well-defined for larger zones.

1.3. RESEARCH OBJECTIVE

The objective of this master thesis is to model the Randstad area using a dynamic zone-based model, with the Network Fundamental Diagram defined for each zone. The Randstad is roughly defined as the area covered by the four major cities in the Netherlands (Amsterdam – The Hague – Rotterdam – Utrecht) and their surroundings, see the shaded area in fig. 1.1. Those cities and their agglomerations form the urban areas in the model, while the regions in between are mainly rural areas with some smaller cities. The cities are connected by motorways.



Figure 1.1: The Randstad area

The model that is used is a trip-based approach. On this point it differs from the Network Transmission Model, which is an accumulation-based approach. With the trip-based approach a specific path with its own trip length can be defined for each vehicle. The hypothesis is that this has a positive effect on the performance of the model. The exact model will be described in section 3.1. With this model, a traffic simulation will be performed. The results of this simulation will be analyzed and validated with real data. The purpose of this analysis is to check the performance (goodness of fit) of this zone-based model for larger areas.

The main question is how the Randstad can be modelled using a zone-based dynamic traffic model, and whether the results of this simulation model are representative enough, so that the model can probably replace static link-based models for large areas. This can lead to a significant decrease in the duration of the simulations.

RESEARCH QUESTIONS

Resulting from the research objective, the main research questions formulated:

- **How can traffic in the Randstad be modelled using a zone-based dynamic traffic model?:**

The core purpose of this research is to develop and implement a zone-based dynamic traffic model for the Randstad. Based on the initial simulation results, the setup of the simulation model can be changed to improve the results, and make the model appropriate for large areas such as the Randstad.

Six sub-questions are formulated to answer this main question. Those questions will be addressed in this report. In this section the research questions are explained in short:

SQ 1 How should the Randstad be divided into zones for a dynamic simulation based on the Network Fundamental Diagram:

The first step in the implementation of the model is to decide which areas should be included in the simulation. A clear definition of the Randstad should be made. Next, the Randstad area has to be divided into zones. An important question in this step is the question how to cope with the non-urban regions, as those regions have a less homogeneous distribution of traffic. These areas are crossed by motorways connecting the four main agglomerations. The traffic on motorways is also far from homogeneous, and hysteresis is observed. The aim of this research question is to come up with a step-by-step approach which can be applied to any area, like the Randstad.

SQ 2 Can a clear NFD be defined for large zones including higher-hierarchy roads?:

The next step is that for each zone an NFD has to be estimated. The main interest is to define a clear NFD, although traffic on freeways is often not homogeneously distributed, and hysteresis is observed. Because of the network level, this research has to cope with multiple road types with a variety of characteristics, like the maximum speed and capacity. All these roads with their own characteristics have to be combined into one NFD for each zone. It is likely that hysteresis loops will be visible in the NFDs. Hysteresis means that the state of the system not only depends on the input variables, but also on its history. For freeway traffic it is observed that there is a difference between the network flow (Production) during the onset and offset of congestion. The aim of this research question is therefore to analyze whether it is possible to produce well-defined NFDs for large zones, and how hysteresis can be taken into account in the simulation.

SQ 3 Which paths does the traffic take inside the zones?:

In real traffic, the trip length of one vehicle inside a zone depends on the location where the vehicle enters the zone, and the location where it leaves the zone. This means that for each pair of neighbouring zones a different travel time or trip length can be defined. In the classic NTM, which is an accumulation-based approach, this difference in trip length is ignored. In this research, the trip lengths are defined based on the path of the vehicle. Simple approaches exist to estimate these trip lengths, so for this research it is not necessary to develop an own strategy.

SQ 4 How can an OD-matrix be estimated for the Randstad?:

The Origin & Destination Matrix is an essential input to the simulation. It is also one of the components that highly influences the outcomes of the simulation. Since OD-matrices are not available on this scale, it has to be estimated. A possible approach is to calculate the OD-matrix using a transport model, based on socio-economic characteristics like the number of households and jobs in the zone, and the generalized costs of travelling between each pair of zones.

SQ 5 What is the routing strategy of the traffic between the zones?:

The OD-matrix contains the flows between each pair of origins, but for the simulation the flow between each pair of neighbouring zones is required. Therefore, routes have to be determined for each OD-pair. It is not necessary to develop a routing strategy for this research, because an existing strategy will be sufficient. One of the things that has to be determined is whether traffic is divided over multiple routes, or just one single route.

SQ 6 What is the performance of the zone-based simulation model for the Randstad?:

The last step is to analyze the performance of the model for the Randstad. This can for example be done based on the estimated travel times between the zones. These travel times can be compared to real traffic data. In an earlier stage, before running the simulation, criteria have to be defined for analyzing the performance of the model. Based on the simulation results, the setup of the simulation can be changed to improve the results. Changes can for example be made in the routing strategy, estimation method of the OD-matrix, or the definition of the zones. These changes will be implemented and the results will be analyzed in the same way as the original simulation.

1.4. REPORT STRUCTURE

In chapter 2 the existing literature on the Network Fundamental Diagram and the models based on this diagram, like the Network Transmission model is reviewed. Then, chapter 3 discusses the methodology that is used for the simulation, and in chapter 4 this methodology is applied to a case study for the Randstad. After executing the simulation, the results are presented and discussed in chapter 5. Finally, in chapter 8 the conclusions with respect to the research questions of section 1.3 are given.

The structure of the report is summarized in table 1.1, for each section is indicated which research questions are related to the contents of that section. **RQ** stands for the main research question, **SQ** stands for the sub question, followed by the number of the sub question.

Table 1.1: Structure of the report

Section	Title	Research Questions
1	Introduction	
2	Literature Review	
2.1	Static traffic models	-
2.2	Dynamic traffic models	-
2.3	Quasi-dynamic traffic models	-
2.4	Dynamic zone model based on the Network Fundamental Diagram	RQ
3	Methodology	
3.1	Simulation model	RQ, SQ3
3.2	Zone division	SQ1
3.3	NFD construction	SQ2
3.4	OD-pattern estimation	SQ4
3.5	Routing strategy	SQ5
3.6	Performance analysis	SQ6
4	Model application	
4.1	Zone division	SQ1
4.2	NFD construction	SQ2
4.3	OD-pattern estimation	SQ4
4.4	Routing	SQ3, SQ5
5	Simulation results	
5.1	Analysis of the outflow patterns	SQ6
5.2	Analysis of the accumulation patterns	SQ4, SQ6
5.3	Analysis of the travel times	SQ6
5.4	Conclusion	SQ4, SQ5, SQ6
6	Improvements to the simulation	
6.1	Multiple routes	SQ5, SQ6
6.2	Separation local and through traffic	RQ, SQ2, SQ6
6.3	OD-matrix based on travel times	SQ4, SQ6
6.4	Conclusion	RQ, SQ2, SQ4, SQ5, SQ6

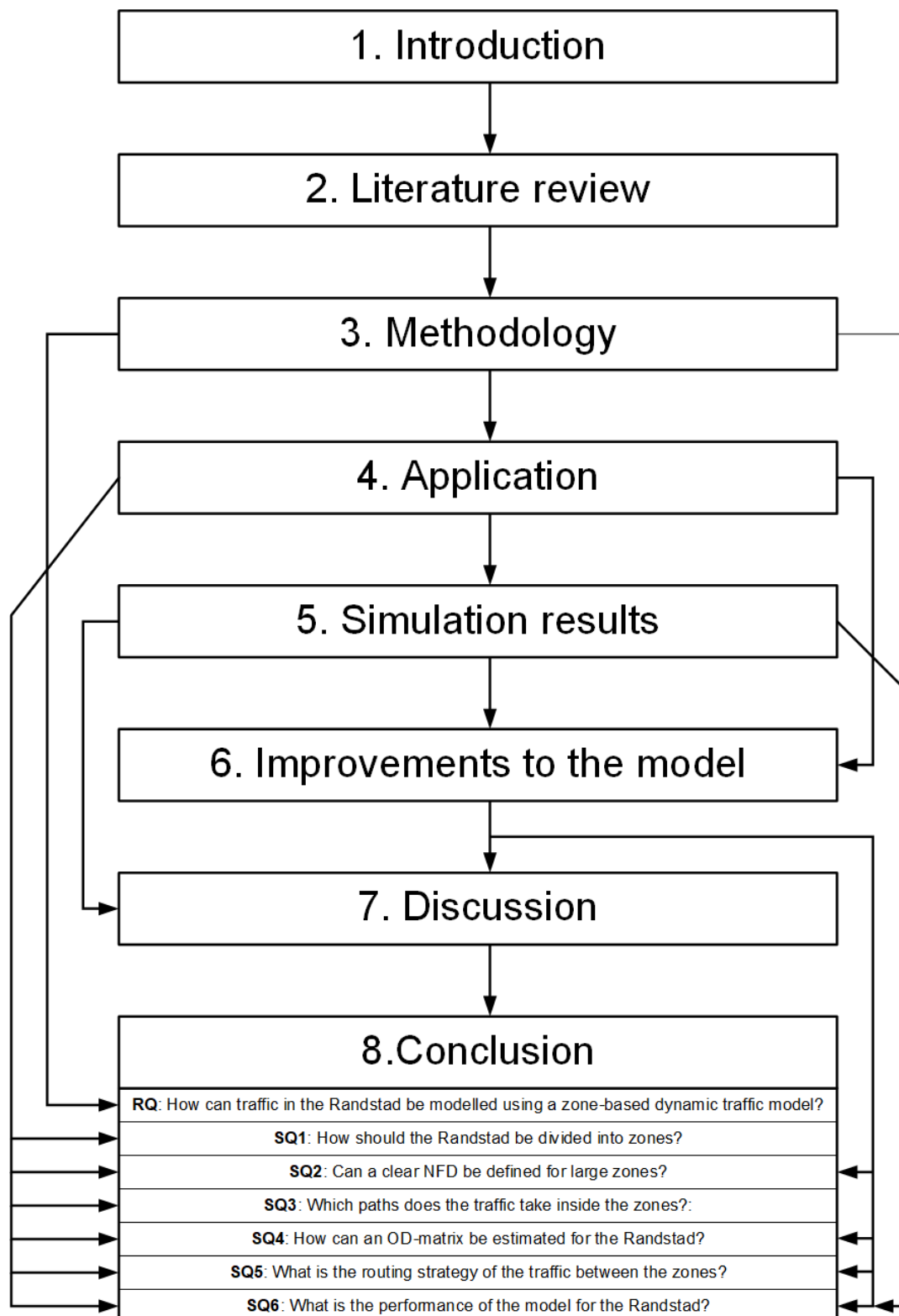


Figure 1.2: Report structure diagram

2

LITERATURE REVIEW

This research focusses on the usability of a dynamic zone-based model for large areas, using the concept of the Network Fundamental diagram. In this chapter, the literature about this modelling concept is reviewed. Large traffic networks can be modelled in different ways. Therefore, other ways of modelling traffic in large areas are also discussed in this chapter, to place the concept of dynamic zone models in the wide context of the existing ways of modelling large traffic networks.

2.1. STATIC TRAFFIC MODELS

The most simple traffic assignment models are all static models. Those static traffic assignment models only consider one single time period with a stationary demand, and constant network parameters. The traditional static models do not incorporate any capacity restrictions, although some extended models exist which include capacity constraints [1]. With these simplifications, static models are computationally efficient.

Travel times are determined using a link travel time function. For these functions, the travel time is monotonically increasing with an increasing flow [6]. It is possible that the flow exceeds the capacity. The most used travel time function is the BPR function [27], which gives the travel time on a link i for flow q_i :

$$t_i(q_i) = t_i^0 \cdot (1 + \alpha_i \cdot (\frac{q_i}{C_i})^{\beta_i})$$

In which t_i^0 is the free-flow travel time for link i and C_i is the capacity of link i . The coefficients α_i and β_i are link parameters.

The route flows have to satisfy Wardrop's equilibrium law, which states that for all used routes from an origin A to a destination B , the travel times are equal, and no unused route has a shorter travel time [29]. Each traveller optimizes its own travel time, so the traffic assignment results in a User Equilibrium (UE).

Due to the absence of capacity constraints, the link flows are unlimited, and spillback effects are ignored. Therefore, the static traffic assignment models fail to reconstruct real traffic patterns, which often results in unrealistic travel times [1].

2.2. DYNAMIC TRAFFIC MODELS

Contrary to static models, dynamic models can model multiple time periods with varying demand. Besides that, dynamic models take spillback effects into account, because those models use capacity restrictions at intersections and bottlenecks. The travel times are not determined using a link travel time. but with the fundamental diagram instead.

An example of a dynamic traffic model is the Cell Transmission Model, which has been developed by Daganzo [6]. This model works with discrete time steps, and after each time step the traffic conditions are updated. The road is divided into small homogeneous cells, with a length equal to the distance that is traversed by a vehicle under free-flow conditions. This means that with low traffic each vehicles moves to the next cell each time step. [6]

The number of vehicles in a cell i at time moment t is denoted by $n_i(t)$. The inflow of this section i is limited by the demand from the upstream cell $i - 1$ and the supply in cell i . [6]

$Q_i(t)$ is the maximum number of vehicles that can flow from cell $i - 1$ to cell i at time moment t , which is the minimum of the capacity flow of the cells $i - 1$ and i . [6]

$N_i(t)$ is the maximum number of vehicles that can be stored in cell i at time moment t . This is equal to the jam density multiplied by the length of the cell. The supply of cell i is the maximum storage capacity reduced by the number of vehicles in cell i . [6]

The flow from cell $i - 1$ towards i is then the minimum of the number of vehicles in cell i , the capacity flow between cell $i - 1$ and cell i , and the supply of cell i [6]:

$$q_{i-1}^i = \min(n_{i-1}(t), Q_i(t), N_i(t) - n_i(t))$$

Each time step, the cell occupancys are updated, by adding the inflow and subtracting the outflow [6]:

$$n_i(t + 1) = n_i(t) + q_{i-1}^i(t) - q_i^{i+1}(t)$$

The inflow to the network is modelled using a source cell and a gate cell at the start of the road. The source cell contains an infinite number of vehicles, and the gate cell has an infinite storage capacity. The vehicles flow from the source cell to the gate cell. This gate cell has an inflow capacity which is equal to the desired input to the road. The gate cell makes sure that the vehicles enter the road at the desired rate, and it is capable of storing all vehicles that are unable to enter the road due to capacity restrictions. [6]

Daganzo [7] further developed this model to a model suitable for complete freeway networks. The network is described by nodes, representing the cells, and links, representing the interactions between the nodes. Three types of cells are distinguished: merging, diverging and ordinary cells. Merging cells are cells with two incoming links and one outgoing links, diverging cells are cells with one incoming and two outgoing links and ordinary cells have both one incoming and one outgoing link. For most freeway networks these types are sufficient. [7]

Between two ordinary cells, the flow is again the minimum of the demand in the upstream cell and the supply in the downstream cell. For a merging cell, the situation is more complicated. If the sum of the demand from both upstream cells exceeds the supply of the merging cell, the flows from both upstream cells have to be restricted. For the diverging cells, if the supply one of the downstream cells is smaller than the demand, the flow towards the other downstream cell is also restricted. [7]

A drawback of this model are that it is developed for rather simple networks, that can only contain diverging and merging conflicts. Although it is possible to extend the model, it is most suitable for small networks. For larger networks, comparable in size to the network that is modelled in this research, too much computational effort is required.

2.3. QUASI-DYNAMIC MODELS

The aim of quasi-dynamic models is to combine the properties of static and dynamic models in one model that is computationally efficient, but still can produce realistic travel times.

An example of a quasi-dynamic model is STAQ (Static Traffic Assignment with Queuing), as described by Brederode et al. [1]. The aim of this model is to develop a static traffic assignment model with capacity constraints, spillback and shockwaves [1]. The model is based on the Link Transmission Model, but instead only one time period is modelled with a stationary demand.

Because only one time period is modelled, the model has some shortcomings with respect to dynamic models. Brederode et al. [1] mention two consequences for the simulation results:

- The results are average values over all traffic in the study period
- An assumption has to be made about the network load at the start and after the end of the study period. It is often assumed that initially the network is empty, and that the demand is set to zero after the study period, so that each vehicle in the network has the chance to reach its destination.

The traffic network used by STAQ consists of links, nodes and junctions, which are a special type of nodes. At the nodes constraints are set to the flows from the upstream links, to account for capacity restrictions

on the downstream links. At junctions additional constraints are set, because of the conflicting flows at the junction. Besides that, turn delays are established for the flows on the junctions. [2]

The algorithm has two submodels that are linked with each other: Network loading and routing. The network loading submodel uses the route flows to calculate the link travel times and the resulting route travel times. The routing submodel then uses the route travel times to calculate the demand per route again. [2]

The network loading submodel has two phases:

1. **Squeezing:** For all links where the flow exceeds the capacity, the flows are reduced to the capacity and the surplus traffic is stored in a point queue at the start of the congested link [2]. This phase has no time variable, because the travel demand is stationary [1].
2. **Queuing:** Using an assumed fundamental diagram, the point queues are translated into spatial queues at the upstream links, by means of shockwaves [2]. In this phase, a time variable is used for the propagation of the shockwaves [1]. The algorithm is an event-based approach, with three types of events that can occur. As soon as a backward shockwave reaches an upstream link, there is spillback. Conversely, a forward shockwave can reach the downstream link. Besides that, it is possible that two shockwave meet, and continue has one shockwave. [1]

Already after the squeezing phase a prediction for the travel times can be calculated, with more realistic results than provided by a travel time function [1]. However, the queuing phase is necessary to account for the spillback effects [1]. After the queuing phase the route travel times are calculated by adding up all link travel times and the turn delays at the junctions. The link travel times are determined using the cumulative inflow and outflow curves. [2]

The routing submodel calculates the demand per route, using the route travel times obtained from the network loading submodel. No specific routing algorithm is developed for the STAQ model, so this submodel is interchangeable, as long as the model is able to produce route demands based on the network and the route travel times [2].

The STAQ model has been applied in multiple case studies and it has proven that is able to reconstruct real traffic situations including congestion and spillback effects more accurately than the existing static models, with acceptable computation times (contrary to dynamic models) [2].

The drawback of this model is that only one time period can be modelled, with a stationary travel demand. In real traffic, the demand is changing continuously over the day. This means that with STAQ only a short time period can be modelled. The model assumes that no queues are present at the start of the study period, and at the end of the study period can not grow anymore.

2.4. DYNAMIC ZONE MODEL BASED ON THE NETWORK FUNDAMENTAL DIAGRAM

An alternative to (quasi-)dynamic link models is a dynamic zone model, which uses zones rather than links. The dynamic zone model that is used in this study makes use of the concept of the Network Fundamental Diagram (NFD). This section therefore first explains this concept and discusses the existing literature about the NFD. Secondly, the Network Transmission Model is explained. Lastly, a trip-based model approach is considered.

2.4.1. NETWORK FUNDAMENTAL DIAGRAM

The concept of modelling traffic in cities in a macroscopic way, using the Network Fundamental Diagram has been proposed by Geroliminis and Daganzo [11] in 2007.

The idea of investigating traffic flows on the network level, by identifying fundamental traffic flow variables for networks and the principal relationships between these variables, is not new, as multiple researchers have written about this in the past, among which Mahmassani et al. [20].

The fundamental variables for traffic networks are related to the average density, flow and speed. Several studies in the past came up with functional relationships between these variables, like the relationship that the average speed would decrease with increasing density, which also holds on link-level.

This presumption was generally accepted, but no empirical evidence existed yet for these statements, since it can only be verified using large-scale data analysis, and this data was not available for a long time. Due to the complexity of traffic networks, it could not be proven analytically either. [20]

The fundamental variables in network flow theory are:

- **Accumulation** $K(t)$: The total number of moving vehicles in the network, which may or may not be divided by the total network length (veh or veh/km). This quantity is equivalent to the average density.
- **Production** $P(t)$: The total internal flow in the network (veh/h). This quantity is equivalent to the average flow.
- **Performance** $\hat{P}(t)$: The output of the network, which includes both the outflow at the boundaries and the rate at which vehicles reach their destination inside the network (veh/h).

The ratio between the total production and the performance is the average trip length inside the zone, normalized by the total network length [11].

NFD CONSTRUCTION

Courbon and Leclercq [5] identified three methods for estimating the Network Fundamental diagram:

1. **Trajectory-based approach**: This method uses Edie's formulas for the calculation of the average flow and density for a specific space-time window $(\Delta x, \Delta t)$,
2. **Detector data approach**: For this method the data from loop-detectors or other measurements is aggregated. The approach is similar to the trajectory-based approach, where Edie's formulas are used for the calculation of the network flow and density [13].
3. **Analytical approach**: Using an analytical approach, the NFD is estimated based on traffic flow theory. Daganzo and Geroliminis [8] for example defined an analytical model that provides an upper bound to the NFD.

A fourth one can be added to that list:

4. **Simulation-based approach**: In this approach the estimate for the NFD is based on trajectories or virtual loop detector data obtained from a traffic simulation.

If the Network Fundamental Diagram is constructed using loop detector data, for the accumulation and production both a weighted and an unweighted average can be calculated. The weighted values account for the spacing between the detectors, while the unweighted values don't.

The weighted values are defined as $P^w = \sum_i q_i l_i / \sum_i l_i$ and $K^w = \sum_i k_i l_i / \sum_i l_i$, and the unweighted values as $P^u = \sum_i q_i / \sum_i 1$ and $K^u = \sum_i k_i / \sum_i 1$. In this equations q_i and k_i are respectively the flow and density measured at link i , and l_i is the length of the link i , which is essentially the spacing between the detectors.

Geroliminis and Daganzo [12] have shown in their Yokohama test case that both the weighted and unweighted averages for the flow and density can be used to produce a well-defined NFD.

When the weighted averages are used, the detectors should be at representative locations, since the detector measurements are regarded to be normative for the entire road section. If the aggregation time step is large enough compared to the traffic signal cycles, the resulting flow will always be representative, but the same cannot be said for the density if the density is determined using the detector occupancy. [13][12]

An important finding is that the congested part of the NFD is often not clearly visible in the results for freeway network, because usually small parts of the network are congested at the same time, while the majority of the network is still uncongested. The NFD gives an average of the congested and uncongested states. Fully congested network states are never observed. [14] [17]

EFFECT OF INHOMOGENEITY ON THE NFD

Geroliminis and Daganzo [12] state that the NFD holds for homogeneously congested cities. Buisson and Ladier [3] question this homogeneity requirement, using data that was collected from the Toulouse road network. This data contains measurements from loop detectors on the urban highway network and the surface network. The data shows that congestion is not homogeneously distributed over the highways.

With regard to inhomogeneity, Buisson and Ladier [3] conclude that the locations of the detectors have a strong impact on the NFD, especially when detectors are located close to traffic signals. This was also found by Geroliminis and Daganzo [12]. They also conclude that when multiple road types are present in the network, it highly influences the shape of the NFD, because the different road types have different NFD shapes. [3]

Lastly, hysteresis loops are visible in the NFDs, even with a homogeneous dataset [3]. This is confirmed by Gayah and Daganzo [10] with their simulation model for a grid network. They also show that this hysteresis effect can be prevented when drivers avoid congestion by adapting their routes real-time, because driver adaptivity leads to a more uniform distribution of traffic over the network [10].

Hysteresis phenomena are not only observed in traffic, but in many fields of study. In general it means that the state of the system not only depends on the input variables, but also on its history. It can be some lag between the input and output of a physical system, which is the case for traffic systems.

Especially for freeway traffic it is observed that there is a difference between the network flow (Production) during the onset and offset of congestion. Geroliminis and Sun [14] analyze the causes and mechanisms of hysteresis for traffic networks, using data obtained from the Twin Cities Metropolitan Area (Minneapolis-St. Paul). First they analyzed the data for the entire freeway network, and subsequently for two subnetworks, to reveal more specific aspects of the hysteresis phenomenon.

For the freeway network, they plotted the average network flow and the variance in occupancy, both versus the average network occupancy. The plots for the flow show clockwise hysteresis loops, which means that during the offset of the congestion the flow is lower than during onset. Although the density (Accumulation) recovers during the offset, the flow does not increase to its original level. [14]

The plots for the variance in occupancy show counter-clockwise hysteresis loops, meaning that the variance is higher during the offset than during the onset of congestion. During the offset, the distribution of the traffic over the network is more inhomogeneous than during the onset. The same average occupancy with larger variance means lower average network flows. [14]

Geroliminis and Sun [14] explain this by an analogy of two parallel servers with separate queues. Suppose that the demand is spread equally over both queues, then the system operates at its capacity. But when the demand is not spread equally over the queues, the system will operate below the capacity, since one server is not fully exploited.

The spatial heterogeneity is confirmed by mapping the origins and destinations of the traffic. It is shown that the origins are divided more evenly over the area, while destinations are more concentrated at specific locations, like the center. [14]

After analyzing the freeway network, two subnetworks are considered by Geroliminis and Sun [14]. One of the subnetworks consists of 100 detectors at the most congested locations in the network.

For those detectors, the distribution of the occupancy is plotted for 5 different time instances during onset and offset of the congestion. When two time instances with the same mean occupancy, one during onset and one during offset, were compared, it turned out that the distributions of the occupancy are similar for both moments in time. But hysteresis is still observed in the NFDs, and that is not due to spatial heterogeneity, since the variance of the occupancy is the same during onset and offset of congestion. [14]

This can be attributed to the existence of transient states and to the capacity drop phenomenon that is widely observed on freeways. The existence of transient states means that it takes time to return to the original state. [14]

Summarizing, two main causes for hysteresis can be identified:

- **Spatial heterogeneity:** The same average density for the network does not necessarily result in the same average flow, since the distribution of the density may be different.
- **Transient states & capacity drops:** The same density for an individual detector does not necessarily result in the same flow. The response to the density depends on the history of the system.

Geroliminis and Sun [14] conclude that freeway networks do not have well-defined NFDs, due to the presence of hysteresis loops [14]. This however does not mean that the NFD is not usable for networks with freeways. If the hysteresis loops are consistent, and the effect of hysteresis can be quantified, the NFDs could still be valuable with some modifications.

Shi and Lin [25] analyze the NFD shapes for the Shanghai urban expressway network. They selected the data of one week in 2009, containing a typical weekday, a weekend, a national holiday, and one weekday before that national holiday. The plots of the NFDs for the urban expressway network show hysteresis loops, except for the holiday, where the traffic is still in free-flow conditions. The Saturday also deviates from the other days, because it has one irregular hysteresis loop during the afternoon.

The hysteresis loops for one day are further analyzed. Similar to the results of Geroliminis and Sun [14], the hysteresis loops are clockwise. All the detectors that are used to construct the NFD are classified in seven types, and for each type a separate NFD is plotted. One type is the detectors that are all in free-flow condition, and one type contains the detectors that are all on the NFD curve without hysteresis. Three types show hysteresis loops, of which two types are clockwise hysteresis loops, and one gives eight-shaped hysteresis loops. The remaining two types do not show clear hysteresis loops, but scattered NFDs.[25]

The results show that especially the two detector types resulting in clockwise hysteresis loops determine the shape of the NFD of the full network. When the standard deviation of the occupancy is plotted, it results in counter-clockwise hysteresis loops are, similar to the results of Geroliminis and Sun [14]. The plots for the other types of detectors do not show clear hysteresis loops for the standard deviation.[25]

Shi and Lin [25] show that the hysteresis loops are caused by the transitions between free flow and congested traffic. These transitions do not occur immediately, but happen over time, since drivers need time to decelerate before entering a congested state from free-flow state. The same applies for the acceleration from congested to free-flow state. This means that in the transition from congestion to free-flow and vice versa the traffic states are not on the fundamental diagram, but below the capacity between the free-flow and congested branch.

Knoop et al. [16] study the effect of inhomogeneity on the NFD, using two methods. The first method is to construct the NFDs using randomly drawn traffic states from a uniformly distributed random variable. This method does not incorporate traffic dynamics, it is assumed that there is no correlation between traffic states. The second method is a simulation for a grid network using the Cell Transmission Model. This model incorporates traffic dynamics.

Using this simulation Knoop et al. [16] identified the nucleation effect, which is the phenomenon that congested areas attract more congestion. Congestion starts at the nucleation point, and from there a queue builds up, which can lead to spillback at other links. When congestion dissolves again, it gradually dissolves at the head of the queue, and it increases the spatial inhomogeneity of the density.

Based on their findings, Knoop et al. [16] come up with a Generalized Macroscopic Fundamental Diagram, which gives the average internal flow as a function of the accumulation and the inhomogeneity, which is the standard deviation of the density. These diagrams show that the smaller the production (internal flow) of the network decreases with increasing inhomogeneity.

For very small values of inhomogeneity their simulation however also shows a reduction of the production, because a fully homogeneous network is only occurs when the network is empty or it is fully congested, but that is a matter of their interpolation method. [16]

From these researches, it is concluded that inhomogeneity highly influences the shape of the NFD in multiple ways. This can therefore not be ignored in this research. The most discussed effect of inhomogeneity is hysteresis. It has been proven that during the onset of congestion, flows are larger than during the offset of congestion, which is related to the inhomogeneity of traffic. This hysteresis phenomenon will therefore be considered in this research.

2.4.2. NETWORK TRANSMISSION MODEL

The Network Transmission Model (NTM) is a macroscopic dynamic traffic model based on the Network Fundamental Diagram, proposed by Knoop and Hoogendoorn [15]. This model divides an urban area in multiple zones, in which the traffic should be more or less homogeneously distributed.

The approach is similar to the Cell Transmission Model (CTM). The simulation is performed in discrete time steps. For each time step, the traffic state of each zone is updated. The flow between two neighboring zones is determined by [15]:

- The demand from zone i to zone j .
- The capacity of the boundary between zone i and j
- The supply in zone j

The total demand (D_i) for a certain zone i is derived from the NFD, which gives the relation between accumulation and performance. Then, all destinations for the traffic in that zone are considered separately. The demand for each possible destination f is calculated: $D_{i,f} = \zeta_f \cdot D_i$. [15]

The fraction of this demand that is going from zone i to a specific zone j is $\eta_{i,f}^j$. So, the demand from zone i to zone j is $D_i^j = \sum_{f \in F} \eta_{i,f}^j \cdot D_{i,f}$ with F as the set of destinations. [15]

However, this demand is restricted by the capacity of the boundary between these zones. If the demand exceeds the capacity, the effective demand is reduced to match the capacity: $\tilde{D}_i^j = \min(D_i^j, C_i^j)$. The ratio between the effective demand and the demand is $\theta_i^j = \tilde{D}_i^j / D_i^j$. For each destination the demand is reduced proportionally to this ratio: $\tilde{D}_{i,f}^j = \theta_i^j \cdot \eta_{i,f}^j \cdot D_{i,f}$ [15]

Then, the demands towards each zone is calculated, as the summation of all demands from its neighbours. If the total demand D^j towards zone j is larger than the supply S^j , the effective demand for each zone has to be reduced further, so that the supply is not exceeded. [15]

The ratio between the supply and demand is the the fraction of the traffic that can enter zone j : $\psi^j = \min(S^j / D^j, 1)$. [15]

The flow leaving from a zone i is restricted by the minimum restricting factor of all neighbouring zones with a nonzero effective demand from zone i . The set containing these neighbours is denoted as N_i . The factor restricting the outflow from zone j is then: $\psi_i = \min_{j \in N_i} (\psi^j)$. [15]

The sum of the inflows and outflows for one zone, multiplied by the time step gives the change in accumulation for that particular zone. This new accumulation is used in the next time step. The accumulation is stored for each destination separately. Adding up these accumulations gives the total accumulation for each zone. [15]

2.4.3. TRIP-BASED MODEL

The Network Transmission Model proposed by Knoop and Hoogendoorn [15] might not perform well under rapidly changing conditions. When a zone is in the uncongested state and the accumulation increases rapidly, caused by a large inflow, the outflow also increases immediately. In reality, there will be some delay between the increase in accumulation and outflow, because the outflow increases as soon as the entered vehicles complete their trip inside the zone, and not as soon as they enter the zone. This means that in the NTM, information propagates with infinite speed, which indeed is not the case. [19]

Besides that, the NTM does not take into account the factual trip lengths inside the zones. These trip lengths inside each zone, and so the times spent in each zone, depend on the origins and destinations. The NTM ignores this, and rather uses a fixed trip length independent of the path of each vehicle. [21]

Lamotte and Geroliminis [19], therefore describe an alternative approach. Instead of an accumulation-based model, they describe the trip-based model, which is further developed into an event-based approach by Mariotte et al. [21]. The difference between the trip-based and event-based approach is that in the trip-based approach the simulation is performed in small time steps, while in the event-based approach the traffic conditions remain fixed until the next event.

The key principle of both approaches is that the outflow of a zone is determined by the number of vehicles that have completed their trip. When the trip length is denoted as L_0 for a vehicle entering the zone at time moment t_0 and leaving the zone at $t_0 + \tau$, the following equation by Lamotte and Geroliminis [19] holds:

$$L_0 = \int_{t_0}^{t_0 + \tau} U(K(\tilde{t})) d\tilde{t}$$

In which $U(K)$ is the speed corresponding with accumulation K . This speed is the common speed for the zone, defined by the NFD: $U(K) = P(K)/K$. With this relationship, the trip length can be rewritten in terms of production and accumulation [21]:

$$L_0 = \int_{t_0}^{t_0+\tau} \frac{P(K(\tilde{t}))}{K(\tilde{t})} d\tilde{t}$$

This equation makes clear that the trip-based model takes into account the development of the accumulation over time [21].

An advantage of this approach is also that for each vehicle in a zone, an individual trip length based on its origin and destination can be determined. The vehicles then travel with the current average speed in the zone, which is updated every simulation step. Once the vehicle has completed its trip length, it can leave the zone. [21]

Although it is possible to define a fixed trip length for all travellers in the trip-based model, it is not desirable, since real traffic is much more complex and it is a major simplification to assume that all vehicles in one zone have the same trip length.

3

METHODOLOGY

In this chapter, the research methodology is discussed. A general approach will be given, independent of the research case study. Each step that is taken to come to the final results will be described in the coming sections.

First of all, the simulation model that will be used is explained in detail. The simulation requires some essential information as an input to the simulation process. In the remainder of this chapter it is explained how this information is obtained, how it is processed to the desired input, and how this input is used during the simulation. This information includes the construction of the zone map, because the research area has to be divided into zones. Then, for each zone an NFD has to be constructed based on detector data and/or an analytical approach, and the OD-matrix has to be estimated. Next, the routing strategy has to be selected that will be used to determine a path between each OD-pair during the simulation. Finally, the performance criteria are defined, based on which the simulation results are analyzed and discussed.

3.1. SIMULATION MODEL

The simulation model that is used is based on the Network Transmission Model as proposed by Knoop and Hoogendoorn [15] and the trip-based model as described by Mariotte et al. [21]. The approach that is used in this research differs from the NTM in the way the demand is determined. According to the NTM, the demand from a zone i is given by the NFD, with the current accumulation as input. So, the model is an accumulation-based approach. This research instead makes use of a trip-based approach for calculating the demand.

When a trip is generated, a path through the network is assigned to the vehicle. In general, this will be the shortest path from its origin to the destination. The path is constructed based on the internal distance matrices of the zones.

Each zone z_0 has its own internal distance matrix, containing the path length inside zone z_0 for each combination of a previous zone z_{-1} and next zone z_{+1} . As soon as a vehicle is generated, or it enters a new zone z_0 , its trip length inside that zone is determined from this internal distance matrix.

Each simulation step is then calculated how much distance is travelled by this vehicle during that time step, using the current average speed inside the zone, which is derived from the NFD. The demand D_i of zone i is the number of vehicles inside zone i that has completed this predetermined trip length.

The line of reasoning behind this trip-based approach is that a vehicle can leave a zone as soon as it has travelled a predetermined distance inside that zone. This distance is a fixed amount of kilometers, depending on the previous and the next zone on its route. Vehicles with the same previous and next zone will have to cover the same distance.

3.1.1. MODEL STEPS

The simulation is performed in discrete time steps with a fixed duration of τ seconds. During each time period, seven steps are taken, each of which will be explained in this section.

GENERATE NEW TRIPS

New trips are generated in small sets of vehicles. Such a set of vehicles represents n vehicles (n is not necessarily an integer) with the same destination, same path and the same departure time.

The number of vehicles in the set is determined by the OD-matrix and the normalized demand pattern. The number of trips (Departures/arrivals) for an OD-pair (i, j) is denoted by DA_i^j and the normalized demand pattern for zone i is given by $\overline{D}_i(t)$.

The number of vehicles with origin i and destination j that is generated during the k th time step is:

$$n_i^j(k) = \int_{t=\tau \cdot k}^{t=\tau \cdot (k+1)} DA_i^j \cdot \overline{D}_i(t) dt$$

UPDATE TRAVELLED DISTANCES

Each set of vehicles has a parameter x , which gives the distance to be travelled before the vehicle can leave the current zone. At the moment a vehicle is generated, or it enters a new zone, this parameter x is determined. This distance is the length of the path crossing zone z_0 , with previous zone z_{-1} and next zone z_{+1} .

During each simulation step, the distance travelled during that step is subtracted from this parameter, which is the duration of one simulation time step (τ) multiplied by the average speed in the current zone at that moment. The average speed is derived from the NFD: $U(K) = P(K)/K$.

The vehicle can leave the zone as soon as $x = 0$, which is the moment when sum of the travelled distances during each time steps equals the predetermined trip length.

CALCULATE DEMAND

The demand $D_{i,f}^j$ from a zone i to a neighbour j and final destination f , at any time during the simulation is the total number of vehicles in zone i for which the next zone is j , the final destination is s , and the parameter $x = 0$.

The total demand for a zone i is then:

$$D_i = \sum_{j \in N_i} \sum_{f \in F_i} D_{i,f}^j$$

with N_i as the set of neighbours of zone i and F_i as the set of final destinations for zone i .

APPLY BOUNDARY CAPACITY RESTRICTION

It is determined whether the capacities of the boundaries between the zones are sufficient for the demands. If not, the values for the demand are reduced such that the total demand does not exceed the boundary capacity, conform the method described in section 2.4.2.

The demand D_i^j for a zone i to a neighbour j is:

$$D_i^j = \sum_{f \in F_i} D_{i,f}^j$$

Then, the effective demand is calculated, which is the demand D_i^j limited to the capacity C_i^j of the boundary between zone i and j :

$$\tilde{D}_i^j = \min(D_i^j, C_i^j)$$

The ratio between the effective demand and the demand is:

$$\theta_i^j = \tilde{D}_i^j / D_i^j$$

For each destination the demand is reduced proportionally to this ratio:

$$\tilde{D}_{i,f}^j = \theta_i^j \cdot D_{i,f}^j$$

APPLY SUPPLY RESTRICTION

The next step is to verify whether the supply of the zones is further restricting the flows. If this is the case, the flows are reduced again conform the approach mentioned in section 2.4.2. The supply of a zone j is $S_j = \hat{P}_j(K_j)$.

For each zone, the incoming demand is calculated, as the summation of all demands from its neighbours:

$$D^j = \sum_{i \in N_j} \sum_{f \in F_j} \tilde{D}_{i,f}^j$$

with N_j as the set of neighbours of zone j and F_j as the set of final destinations for the traffic entering zone j .

If the total demand D^j towards zone j is larger than the supply S^j , the effective demand has to be reduced further, so that the supply is not exceeded [15].

The ratio between the supply and demand is the the fraction of the traffic that can enter zone j : $\psi^j = \min(S^j/D^j, 1)$. [15]

The flow leaving from a zone i is restricted by the minimum restricting factor of all neighbouring zones with a non-zero effective demand from zone i . The set containing these neighbours is denoted as N_i . The factor restricting the outflow from zone j is then: $\psi_i = \min_{j \in N_i}(\psi^j)$. [15]

The final flow from zone i to zone j with final destination f is then:

$$Q_{i,f}^j = \psi_i \cdot \tilde{D}_{i,f}^j$$

The flow from zone i to zone j is then the result summed for all destinations:

$$Q_i^j = \sum_{f \in F_j} Q_{i,f}^j$$

The outflow for zone i is:

$$O_i = \sum_{j \in N_i} Q_i^j$$

And the inflow for zone j is:

$$I_j = \sum_{i \in N_j} Q_i^j$$

MOVE VEHICLES BETWEEN ZONES

In the previous step the final flow from each zone i to zone j with final destination f is calculated, and represented by the variable $Q_{i,f}^j$.

The next step is to move the sets of vehicles between the zones. For each zone combination of a sender i , receiver j and final destination f , sets of vehicles are moved from zone i to j , in the same order as these sets entered the zone. If necessary, one set can be split into two different sets of vehicles, if the number of vehicles in the set exceeds the permitted flow $Q_{i,f}^j \cdot \tau$.

UPDATE SYSTEM STATE

Finally, the state of each zone is updated according to the sum of the inbound and outbound flows for the zones. The new system state is used in the next time step.

The new accumulation for a zone i becomes:

$$K_i(t + \tau) = K_i(t) + (I_i - O_i) \cdot \frac{\tau}{L_i}$$

The sum of the inflows and outflows for one zone, multiplied by the time step gives the change in accumulation for that particular zone. This new accumulation is used in the next time step. The procedure is repeated until all time steps are fulfilled.

3.2. ZONE DIVISION

The attempt is to create a zone map, with zones matching the service area of each major city. Therefore, as a first step, all cities or municipalities with a number of inhabitants above a predefined threshold are selected. Each selected city/municipality forms one zone, and the areas between these cities have to be assigned to one of these zones. The coordinates of the center (centroid) of the zones are determined, so that the area between the cities can be assigned to the zone with the closest centroid.

This approach results in a zone division which is the starting point for the creation of the final zone map. After this step, it can be necessary to change the zone map, by adding or removing zones to the map and repeating the same procedure. In first instance, each location is assigned to the closest centroid, without taking into account any existing or natural borders. The result will therefore not directly be used, but it rather forms the basis for the final zone map. The final zone map is then created by assigning each municipality or district in the region to a zone. It basically means that the straight line boundaries obtained in the previous step are shifted towards the already existing borders of the municipalities.

Because traffic can enter and leave the study area at the boundaries, a special type of zone is introduced, which is the external zone. These external zones do not have an NFD, but they have a demand pattern. Traffic inside external zones and between external zones mutually is not modelled. For each zone that is located at the boundary of the study area, one external zone is added, adjacent to the original zone. Traffic is only able to move between the external zone and the corresponding zone inside the study area.

3.3. NFD CONSTRUCTION

For constructing the NFD, the traffic network of each zone is split into two subnetworks: One subnetwork containing all road sections for which loop detector data is available, and a subnetwork containing all roads without loop detectors. For the latter one, the NFDs are estimated for each road type separately using an analytical approach. Finally, the NFD for both subnetworks are combined into one single NFD for the entire zone, by calculating the weighted average of both diagrams.

In fig. 3.1 the steps that are taken during the NFD-estimation process are shown schematically.

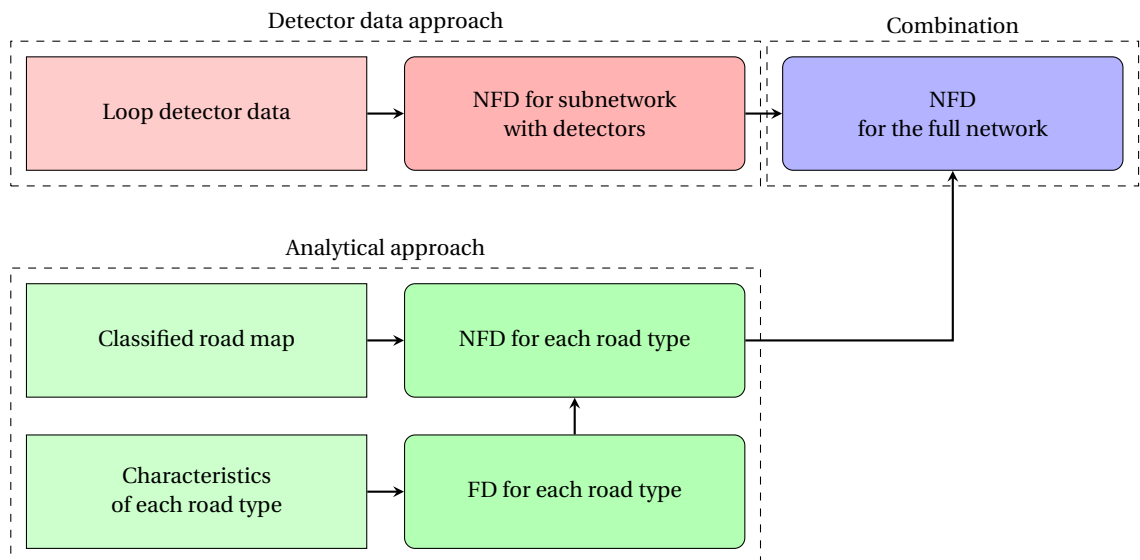


Figure 3.1: Scheme for the estimation of the NFD in terms of Production

3.3.1. DETECTOR DATA

The network production and accumulation are calculated as follows for a network with single-lane roads: [5]

$$\begin{cases} P^w(t) = \frac{\sum_i q_i(t) \cdot l_i}{\sum_i l_i} \\ K^w(t) = \frac{\sum_i k_i(t) \cdot l_i}{\sum_i l_i} \end{cases}$$

With $P^w(t)$ and $K^w(t)$ as the production and accumulation at time instance t respectively. Note that these values are the weighted averages for the flow and density.

The variables q_i and k_i are the flow and density measured at the detector at location i , and l_i is the total length of the section at this location, which equals half of the distance between the first detector downstream and the first detector upstream. The density k_i is not measured directly by the detectors, but it is calculated using the measurements for the flow q_i and the speed u_i , using the relation $k_i = q_i / u_i$.

The resulting values are plotted in the K, P -diagram. The congested branch then has to be extended to until the jam density (around 125 veh/km), because the jam density state is seldomly observed in reality, since the NFD gives the average of the traffic states in the network.

A line will be fitted through the plot in the last step, when the NFD for the freeway network is combined with the underlying network.

3.3.2. ANALYTICAL APPROACH

For the subnetwork for which no loop detector data is available, an analytical approach is used to estimate the NFD. This approach is based on an presumed theoretical fundamental diagram (FD) for a specific road type, based on the characteristics (speed limit) of that road type.

FUNDAMENTAL DIAGRAM

The general shape that is used for the fundamental diagram is the triangular fundamental diagram, characterized by the following variables:

- v : Free-flow speed
- q_{\max} : Flow capacity
- k_j : Jam density
- $k_1 = q_{\max} / v$: Critical density
- $w = -q_{\max} / k_j$: Jam-wave speed

The theoretical capacity q_{\max} can be determined by assuming a minimum time headway between two successive vehicles, an average vehicle length, and a maximum jam density, which is the inverse of the minimum space headway between two vehicles. The capacity depends on the minimum headway time and the average vehicle length. If a normal passenger car is around 4.5 meters long, and a truck between 12 and 16.5 meters, this results in an average vehicle length of 5.5 meters under the assumption that 10% of the traffic is freight traffic. As a starting point it is then assumed that a road with a speed limit of 100 km/h has a capacity of 2000 veh/h, resulting in a minimum time headway of 1.6 seconds. The capacity of the other roads is then derived from this minimum time headway of 1.6 seconds and the average vehicle length of 5.5 meters. For 50 km/h-roads this for example gives a capacity of 1800 veh/h.

The fundamental diagram is only valid for situations with unrestricted flow, which is definitely not the case in traffic networks, due to flow restrictions at intersections. For these restrictions is accounted by applying a fixed multiplier to the fundamental diagrams, reducing the capacity to a smaller level in order to match the capacity of the system. This multiplier depends on the road type. It seems logical to set this multiplier equal to the weighted average ratio of green time over the cycle time of an intersection [18]. This weighted average value also accounts for the differences in capacity between the branches of an intersection, using the fact that the branches with larger flows also get more green time. It is therefore reasonable to assume that this multiplier will on average be larger than 0.5, but the value will likely depend on the road type. For lower-hierarchy roads, like living streets, values lower than 0.5 are appropriate, since these roads will have more capacity restrictions at intersections. Conversely, for higher-hierarchy roads, like motorways, values for the multiplier between 0.5 and 1.0 will be more appropriate. The multipliers will be determined in section 4.2.2.

DERIVING ROAD MAP DATA

From the road map, it can be derived how much length of each road type is present in the zone. When this information is combined with the theoretical fundamental diagram of each road type, and the NFD of the freeway network, this results in an estimate for the NFD of the full network. This NFD is the weighted average of the fundamental diagrams for each distinctive road type.

The road maps can be extracted from OpenStreetMap, using the Overpass API [22], which provides XML-shaped files including the nodes and links of the traffic network. The links also provide information on the link type.

Processing the XML data files results in a set of nodes with a number (id) and a coordinate (longitude,latitude), and a set of links with including a number (id), the link type, the number of lanes, and a list containing the nodes that are crossed by the link.

OpenStreetMap classifies the roads into the following types [23]:

- **motorway / motorway_link**: Restricted-access divided highway (or: *freeway*). Generally with two or more lanes per direction and emergency shoulders.
- **trunk / trunk_link**: Limited-access highways. The second road type in the road hierarchy, after motorways. The directions can be separated, but this is not necessarily the case.
- **primary / primary_link**: Major roads linking larger towns, without physical separation of directions, and major urban arterials.
- **secondary / secondary_link**: Roads linking smaller towns or urban distributor roads. The directions are usually not separated
- **tertiary / tertiary_link**: Local roads connecting villages or residential areas.
- **residential**: Roads that function as access road for housing
- **living-street**: Residential streets where pedestrians have priority over cars.
- **service**: Small roads providing access to a building, parking, etc.
- **unclassified**: Minor roads without residential functions, lower in hierarchy than tertiary roads.
- **road**: Roads of unknown type.

The *_link* road types are mainly used for ramps and turning-lanes.

Other link types that can be ignored for constructing the NFD include among others cycleways and foot-paths, or special road types like tracks for motor racing.

In order to determine the length of each link, the longitude & latitude coordinates of the nodes are first converted to the local x,y-coordinate system. Then, the length of each link is calculated by adding up the Euclidean distance between each two successive nodes on the link.

3.3.3. COMBINATION

Based on the NFD for the freeway and the non-freeway network, an NFD is constructed for the entire network. This has to be a weighted average of both, taking into account that the occupancy is not the same for freeways and other roads.

A fixed ratio between the densities of the different road types is assumed. This ratio has to be calculated from observed data, provided that this data is available. For each observed freeway density, the densities on lower-hierarchy roads are calculated using the fixed ratios obtained from observed data or assumptions. Using the total lane length and the NFD, the production is obtained and the weighted average density:

$$K_{avg} = \frac{\sum_{r \in R} k_r \cdot L_r}{\sum_{r \in R} L_r}$$

$$P(K_{avg}) = \frac{\sum_{r \in R} L_r \cdot P_r(k_r)}{\sum_{r \in R} L_r}$$

with R as the set of road types.

The resulting values are plotted in the K, P -diagram, and finally a shape is fitted through the plot. Multiple shapes for the NFD can be used, but for this research, a multi-linear shape with four branches is used. The shape for the NFD is visualized in fig. 3.2. The four branches that are distinguished are:

- Free flow:

$$P_1(K) = v \cdot K \quad \text{for } K \leq K_1$$

- Reduced-speed flow:

$$P_2(K) = \frac{K - K_1}{K_2 - K_1} \cdot P_{\max} + \frac{K_2 - K}{K_2 - K_1} \cdot v \cdot K_1 \quad \text{for } K_1 \leq K \leq K_2$$

- Capacity flow:

$$P_{\max} \quad \text{for } K_2 \leq K \leq K_3$$

- Congestion flow:

$$P_3(K) = -w \cdot (K_j - K) \quad \text{for } K_3 \leq K \leq K_j$$

Characterized by the following variables:

- v : Free-flow speed
- P_{\max} : Network capacity
- K_j : Jam density
- K_1 : First critical accumulation
- K_2 : Second critical accumulation
- K_3 : Third critical accumulation
- $w = P_{\max} / (K_3 - K_j)$: Jam-wave speed

The reasoning behind this shape is that at low densities, the separation between vehicles is so long that it does not affect the speed of the network users, so the traffic is in *free-flow*. When the density has passed the first critical density, the flow can still increase, but it leads to a reduced speed. When the second critical density is exceeded, it does not immediately lead to a reduction in internal flow, but the capacity of the network is maintained with a lower speed. The throughput decreases after the third critical density has been exceeded.

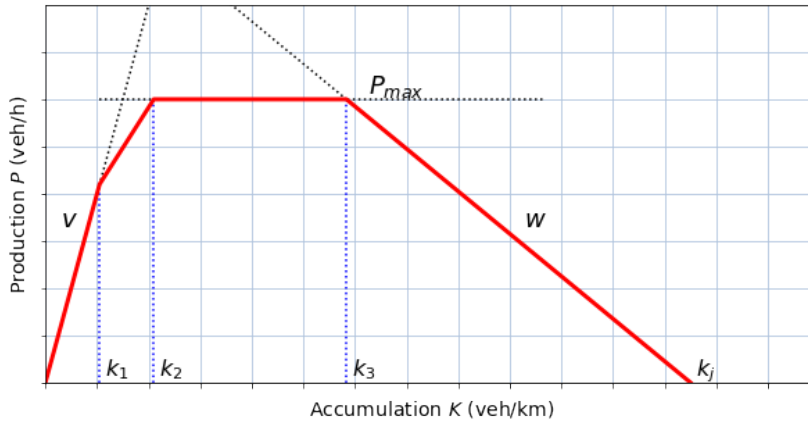


Figure 3.2: Example of a multi-linear NFD

The production equals:

$$P(k) = \min \begin{pmatrix} P_1(k) \\ P_2(k) \\ P_{\max} \\ P_3(k) \end{pmatrix}.$$

NFD IN TERMS OF PERFORMANCE

The performance (outflow + trip completion rate) and the production (internal flow) of a traffic network are related linearly by the average trip length [11]. As soon as the NFD is known in terms of production, it can be transformed to an NFD in terms of performance by simply multiplying it by the average trip length, unless the average trip length is known.

The exit rate of the network at the borders is not the same as the performance, since the performance also includes the trips that end inside the zone. It is assumed that the exit rate and trip completion rate are related to each other, but some difference between the morning and afternoon peak can be expected, especially for zones with a dominant inbound or outbound flow during morning and afternoon peak. Zones with a large amount of residents and a few amount of jobs will most likely have a dominant outbound flow during morning peak and a dominant inbound flow during afternoon peak. This means that the exit rate during morning peak will be close to the total performance, while during afternoon peak it will be much lower compared to the total performance. Initially, the variation over time is ignored in this research, and a fixed ratio between the exit rate and performance is used.

During the OD estimation step, the number of trips ending inside each zone is estimated as a total value for 24 hours. The outflow patterns at the boundaries of the zones are known from loop detector data. The total performance over 24 hours can therefore be calculated by taking the integral of the outflow pattern and adding the number of completed trips for 24 hours. When this total performance is divided by the sum of the outflow rate, it gives the ratio between the performance and the outflow. With this ratio, the performance pattern can be calculated by multiplying the outflow pattern by this multiplier. The average trip length is then defined as the maximum production for the zone, divided by the maximum performance, multiplied by the total network length.

3.3.4. CALCULATING THE STATE OF THE SYSTEM

During the stimulation, the state of the system is determined using the NFD. Two adjustments are made to the NFD:

In theory, it is possible that the jam density state is reached during the simulation, which means that a gridlock occurs. This has to be prevented, by setting a minimum for the outflow in congested state. The minimum is set to 10% of the maximum production or performance: $P_{min} = 0.1 \cdot P_{max}$.

This adds one extra restriction to the congested branch of the NFD:

$$P_3(K) = \max \begin{pmatrix} -w \cdot (K_j - K) \\ P_{min} \end{pmatrix}.$$

The resulting NFD is visualized in fig. 3.3a.

It is also likely that hysteresis loops will be visible in the NFDs based on measurement data, because this phenomenon is widely observed on higher-hierarchy roads, therefore has to be captured in the simulation. This is realized by the following approach: as soon as the third critical accumulation (K_3) in a zone is exceeded, the maximum production of that particular zone will be limited to the production corresponding with that density. When the accumulation decreases again, the production can not be increased again until the density has dropped till the free flow branch of the NFD again. As soon as the density reaches the free flow branch again, the temporary maximum production is released again. This basically means that the network capacity P_{max} is reduced to a temporary value $P_{max,t}$, which also induces a change in the values for the critical accumulations $K_{1,t}$, $K_{2,t}$ and $K_{3,t}$. For this reduced maximum production, a minimum value is set as a fixed fraction γ of the maximum production: $P_{max,t} \geq \gamma \cdot P_{max}$, in order to restrict the effects of hysteresis.

The approach is visualized in fig. 3.3 for the NFD in terms of the production.

At the start of the simulation, the temporary NFD is equal to the unrestricted NFD, so:

$$P_{max,t} = P_{max}$$

$$K_{1,t} = K_1$$

$$K_{2,t} = K_2$$

At any step during the simulation, the production is:

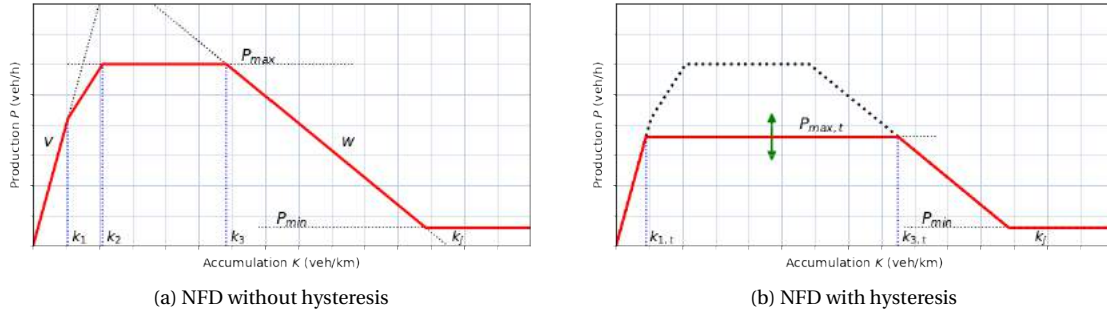


Figure 3.3: Hysteresis described in two figures

$$P(k) = \min \begin{pmatrix} P_1(k) \\ P_2(k) \\ P_{\max,t} \\ P_3(k) \end{pmatrix}.$$

As soon as the accumulation reaches the third critical accumulation, the shape changes. The values for the first and second critical accumulation and the maximum production are updated.

If $K > K_3$:

$$P_{\max,t} = \max \begin{pmatrix} \min(P_{\max,t}, P_3(k)) \\ \gamma \cdot P_{\max} \end{pmatrix}.$$

$$K_{1,t} = \begin{cases} \frac{P_{\max,t}}{v} & \text{for } P_{\max,t} < v \cdot K_1 \\ K_1 & \text{for } P_{\max,t} \geq v \cdot K_1 \end{cases}$$

$$K_{2,t} = \begin{cases} K_{1,t} & \text{for } P_{\max,t} < v \cdot K_1 \\ K_1 + \frac{P_{\max,t} - v \cdot K_1}{P_{\max} - v \cdot K_1} & \text{for } P_{\max,t} \geq v \cdot K_1 \end{cases}$$

As soon as the accumulation drops below K_2 (the temporary secondary critical accumulation), the original shape is restored again.

If $K \leq K_{2,t}$:

$$\begin{aligned} P_{\max,t} &= P_{\max} \\ K_{1,t} &= K_1 \\ K_{2,t} &= K_2 \end{aligned}$$

Using this approach, the history of the system influences the shape of the NFD. If necessary, this shape is updated in each simulation step.

A possible result is given in fig. 3.4, based on the examples in fig. 3.3.

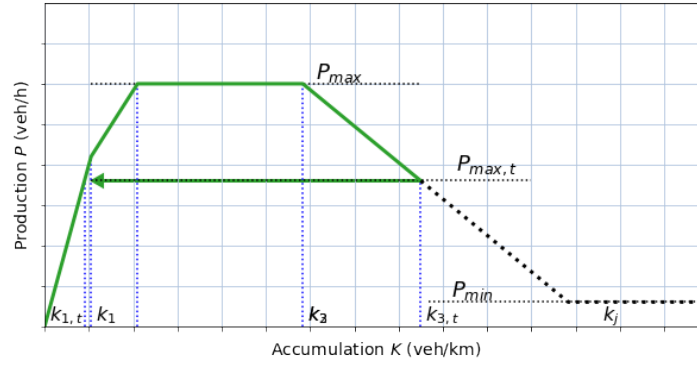


Figure 3.4: The resulting NFD with hysteresis

3.4. OD-PATTERN ESTIMATION

The OD-matrix (origin & destination matrix) gives the total demand between each pair (i, j) of zones for one day. For the estimation of this matrix, the first two steps of the four-step model, namely trip generation and trip distribution, are used.

Estimating the total demand between each pair of zones is though not sufficient, since the distribution of this demand over time is also required as an input to the simulation. In fig. 3.5 the steps that are taken during the OD-estimation process are shown schematically.

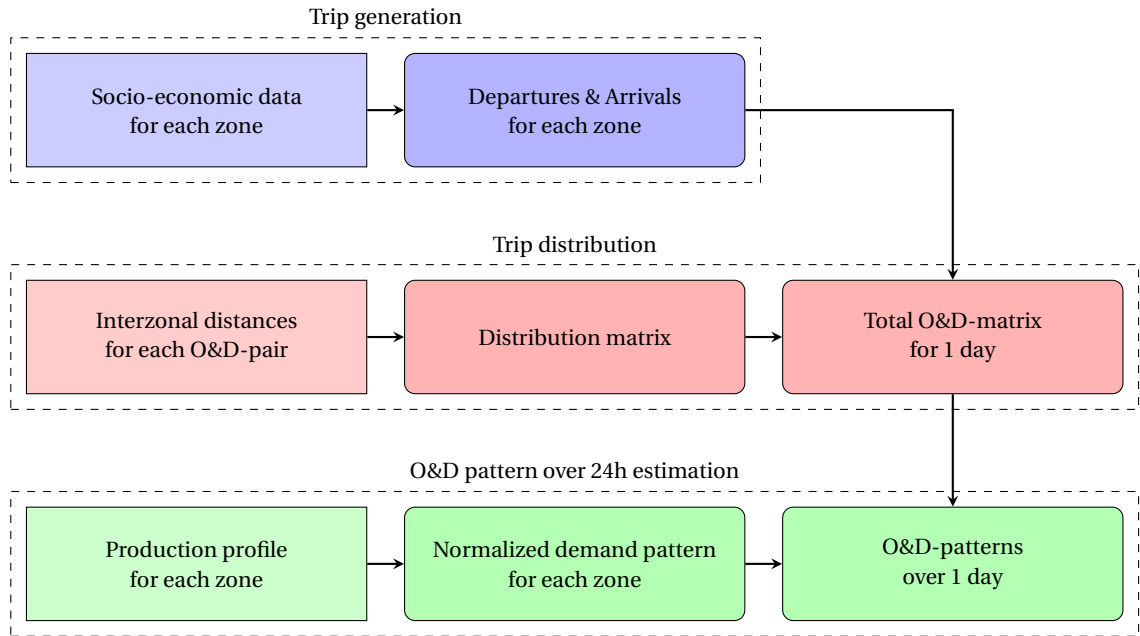


Figure 3.5: Scheme for the OD-estimation step

3.4.1. TRIP GENERATION

The number of departures and arrivals for each zone are estimated using a formula, based on the number of households and the number of jobs in the zone. If the departures and arrivals are calculated as totals for 24-hours, it can be assumed that both values are equal, implying that for each outbound trip a return trip is made within the same 24 hours.

The total departures and arrivals for a specific zone i for 24 hours is estimated at [28]:

$$DA_i = 6.5 \cdot \text{households}_i + 2.9 \cdot \text{jobs}_i$$

The resulting value for the departures and arrivals include all modes of traffic. Therefore, the number has to be reduced in compliance with the local modal split of the zone i . Only the share of car drivers should be taken into account, leaving out the car passengers, since the traffic model considers traffic at vehicle-level. The share of car traffic depends on the region.

The number of departures and arrivals for the external zones is derived from observed data, obtained from the detectors at the boundaries of the study area. For each zone at the border of the study area, the inflows and outflows are determined. Because the number of departures and arrivals must be equal, the inflow and outflow are averaged. The resulting value is the number of departures and arrivals for the external zone that is used in the simulation.

3.4.2. TRIP DISTRIBUTION

For the trip distribution step the doubly constrained gravity model is used.

The gravity model uses the attractiveness of travelling between two zones (i, j) , which is represented by the cost function (also called deterrence function) $f(c_{ij})$, with c_{ij} as the generalized costs value for travelling between each OD-pair (i, j) . The cost matrix (often called *skim matrix*) c is the starting point for this approach. This matrix is often, but not necessarily, symmetric. Using a symmetric cost matrix for trip generation leads to a symmetric OD matrix, which is consistent with the assumption that for each outbound trip the same return trip is made within the same 24 hours.

For the costs, the euclidean distance between the center of each pair of zones is taken. External zones do not have a center, because these zones account for all traffic between the study area and the surrounding area. The distance towards an external zone is therefore defined as the distance towards the neighbouring internal zone plus a predefined distance of 40 kilometers.

The generalized costs for internal trips are estimated based on the area of the zone. Each zone is simplified and represented by a circle with the radius $r = \sqrt{A/(2 \cdot \Pi)}$. The average internal distance is then obtained by calculating the average distance between two random points inside the circle. It is assumed that these points are uniformly distributed over the radius of the circle, which means that trips are more likely to start or end near the center than near the boundaries. This results in an average internal distance is $d \approx 0.72 \cdot r = 0.72 \cdot \sqrt{A/(2 \cdot \Pi)}$.

Several options exist for the cost function:

- Power function: $f(c_{ij}) = \alpha \cdot c_{ij}^{-\beta}$
- Exponential function: $f(c_{ij}) = \alpha \cdot e^{-\beta \cdot c_{ij}}$
- Top-exponential function: $f(c_{ij}) = \alpha \cdot e^{-\beta \cdot c_{ij}} \cdot c_{ij}^{\gamma}$
- Lognormal function: $f(c_{ij}) = \alpha \cdot e^{-\beta \cdot \ln^2(c_{ij} + 1)}$
- Top-lognormal: $f(c_{ij}) = \alpha \cdot e^{-\beta \cdot \ln^2(c_{ij}/\gamma)}$

α , β and γ are parameters that can be varied to fine-tune the outcomes. Note that the value for α will not influence the OD-matrix if the value is the same for all zones.

The power, exponential and lognormal functions are all monotonically decreasing functions, which means that the attractiveness decreases with increasing distance. Special cases are the top-exponential and top-lognormal function. These functions have the property that the attractiveness increases first with increasing distance up to a certain distance, and then it starts decreasing. By using these functions it can be taken into account that for short trips the car is less attractive as transport mode.

Using the cost function, the distribution matrix is calculated:

$$F_{ij} = f(c_{ij})$$

The OD matrix is then estimated by means of an iterative procedure, during which the number of trips between each pair is updated after each iteration. For the first iteration the number of trips T_{ij} between each zone-pair (i, j) is equal to the distribution matrix:

$$T_{ij}^1 = F_{ij}$$

This process is visualized in a table:

	Zone 1	Zone 2	...	Zone n	Sum
Zone 1	T_{11}^1	T_{12}^1	...	T_{1n}^1	$\sum_{i=1}^n T_{1i}^1$
Zone 2	T_{21}^1	T_{22}^1	...	T_{2n}^1	$\sum_{i=1}^n T_{2i}^1$
...	
Zone n	T_{n1}^1	T_{n2}^1	...	T_{nn}^1	$\sum_{i=1}^n T_{ni}^1$

Table 3.1: First iteration of the trip distribution step

Then, the values for T_{ij} are updated for the next step. The number of trips between each OD-pair (i, j) is scaled linearly, to make sure that the total number of trips originating at zone i matches the value for the departures that was determined in the trip generation step. This is done by using the formula:

$$T_{ij}^2 = DA_{i,\text{car}} \cdot \frac{T_{ij}^1}{\sum_{p=1}^n T_{ip}^1}$$

Leading to the following table:

	Zone 1	Zone 2	...	Zone n
Zone 1	T_{11}^2	T_{12}^2	...	T_{1n}^2
Zone 2	T_{21}^2	T_{22}^2	...	T_{2n}^2
...
Zone n	T_{n1}^2	T_{n2}^2	...	T_{nn}^2
sum	$\sum_{i=1}^n T_{i1}^2$	$\sum_{i=1}^n T_{i2}^2$...	$\sum_{i=1}^n T_{in}^2$

Table 3.2: Second iteration of the trip distribution step

Now, the number of trips T_{ij} between each OD-pair (i, j) is updated again to make sure that the total number of trips ending at zone j matches the value for the arrivals that was determined in the trip generation step. This is done by using the formula:

$$T_{ij}^3 = DA_{j,\text{car}} \cdot \frac{T_{ij}^2}{\sum_{p=1}^n T_{pj}^2}$$

The first iteration is now finished. The same procedure is then repeated until the OD matrix has converged, using the formula's:

$$T_{ij}^k = PA_{i,\text{car}} \cdot \frac{T_{ij}^{k-1}}{\sum_{p=1}^n T_{ip}^{k-1}} \quad \text{for } k = 2, 4, 6, \dots$$

$$T_{ij}^k = PA_{j,\text{car}} \cdot \frac{T_{ij}^{k-1}}{\sum_{p=1}^n T_{pj}^{k-1}} \quad \text{for } k = 3, 5, 7, \dots$$

Convergence has been reached as soon as the OD-matrix no longer changes as a result of the iterations. This means that the total number of trips starting at each zone i matches the production, and the total number of trips ending at each zone j matches the attraction for that particular zone.

3.4.3. DEMAND PATTERN OVER TIME

The trip distribution phase leads to an OD-matrix for 24 hours. The next step is that this OD matrix has to be translated to a full demand pattern over the day.

The outflow pattern provides a good representation of the demand pattern of a zone. The outflow is however not equal to the demand, since the outflow also includes the flows crossing the zone, while the intra-zonal demand is not present in this pattern. But still it seems reasonable to assume that this outflow pattern is a good estimate for the demand pattern. Since the performance and the production are related linearly by the average trip length [11], the production can also be used to estimate the demand pattern. The results should be equivalent. The production is then discretized for the simulation time step τ . The normalized demand pattern is obtained by dividing the discretized production by the total production for 24 hours:

$$\overline{D}_i^k = \frac{\int_{t=\tau \cdot k}^{t=\tau \cdot (k+1)} P_i(t) dt}{\int_{t=0}^{t=24h} P_i(t) dt}$$

With \overline{D}_i^k as the normalized demand pattern for zone i at the k th simulation time step, using τ as the duration of one time step (in hours). An example of a normalized demand pattern is given in fig. 3.6.

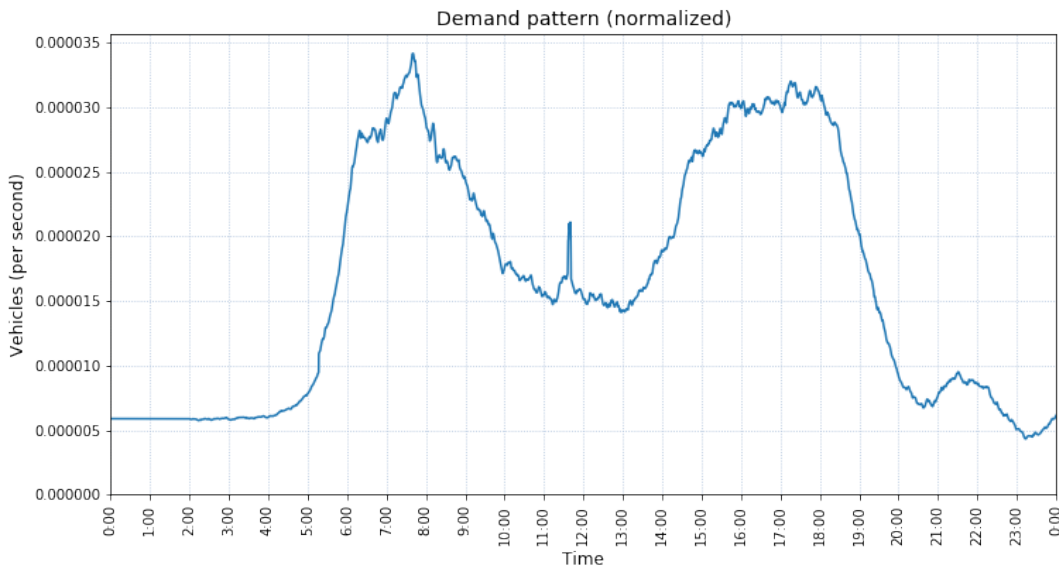


Figure 3.6: An example of a normalized demand pattern

The resulting normalized demand pattern multiplied by the total demand over one day gives the demand for each simulation time step:

$$D_{ij}^k = T_{ij} \cdot \overline{D}_i^k = T_{ij} \cdot \frac{\int_{t=\tau \cdot k}^{t=\tau \cdot (k+1)} P_i(t) dt}{\int_{t=0}^{t=24h} P_i(t) dt}$$

With D_{ij}^k as the demand from zone i to zone j at the k th simulation time step, using τ as the duration of one time step.

3.5. ROUTING STRATEGY

For each OD-pair three routes are defined before running the simulation. These three routes are the fastest routes under free-flow conditions.

During the simulation, the fastest route is assigned to each set of vehicles at the moment when these vehicles are generated. This means that the travel times for the routes have to be updated continuously based on the traffic conditions. For the time being it is assumed that the vehicles stick to the route during the trip, even when the traffic conditions have changed in the mean time.

3.6. PERFORMANCE ANALYSIS

After the simulation, the performance of the simulation is analyzed on three aspects:

- **Trip duration** between zone centers: The trip duration obtained from the simulation can be compared to observed travel times from Google Maps.
- **Density distribution** of each zone: The density distribution makes clear whether the simulation model is able to reconstruct congestion patterns correctly. Can it predict the locations where and time moments when congestion occurs? The density distribution is also useful for the calibration of the OD-matrix.
- **Outflow pattern** of each zone: The outflow pattern can be compared to the observed outflows, in order to calibrate the OD-matrix and the route set. Besides that, it is a useful addition to the comparison of the travel times, because a reliable prediction for travel times does not necessarily mean that the model used to calculate those travel times is reliable as well.

For the accumulation and outflow patterns, it is desired that the average deviation between the simulated and observed patterns is less than 20% over 24 hours, and also specifically during the peak hours (6:00 - 10:00 and 15:00 - 19:00). The value of 20% is chosen because this research is a first step in developing a dynamic zone-model for large areas, and some assumptions had to be made for the input to the simulation, like the OD-matrix estimation. It is therefore possible that large deviations can occur between the simulation results and the expected patterns.

4

MODEL APPLICATION

In this chapter, the model that has been described in section 3.1 will be applied in a case study for the Randstad. The Randstad is the area between and including the four largest cities in the Netherlands: Amsterdam, Den Haag, Utrecht and Rotterdam (see fig. 4.1). The area consists of both urban and rural areas. The cities are connected by a network of freeways and provincial roads.



Figure 4.1: The Randstad area

First of all the area is divided into ± 15 zones. For the defined zones an NFD is then constructed and an OD-matrix is estimated for the area. Also, the routes between the OD-couples are determined. These elements serve as an input for the simulation.

4.1. ZONE DIVISION

As a first step the Randstad is divided into zones by the following approach: All municipalities with more than 75,000 inhabitants are selected to form a zone. Then each location in the Randstad is assigned to the closest zone center. For this, first the GPS coordinate of the center of each zone is identified, based on the open data from Publieke Dienstverlening Op de Kaart (PDOK) [24].

The selected municipalities are listed in table 4.1.

The first step is to assign each location in the Randstad to the closest centroid. The centroids are the GPS locations of the center of each municipality. The result is shown in fig. 4.2a.

Table 4.1: Municipalities in the Randstad with >75,000 inhabitants

Province	Municipality	Inhabitants (x1000)	GPS [24]
Noord-Holland	Amsterdam	853	52.38, 4.90
	Haarlem	159	52.38, 4.65
	Zaanstad	154	52.46, 4.77
	Haarlemmermeer	146	52.30, 4.68
	Amstelveen	90	52.29, 4.85
	Hilversum	89	52.22, 5.17
	Purmerend	80	52.50, 4.97
Zuid-Holland	Rotterdam	640	51.92, 4.27
	Den Haag	526	52.07, 4.29
	Zoetermeer	125	52.06, 4.49
	Leiden	124	52.15, 4.49
	Dordrecht	118	51.78, 4.71
	Alphen a/d Rijn	109	52.11, 4.64
	Westland	106	52.00, 4.21
	Delft	101	52.00, 4.36
	Nissewaard	85	51.83, 4.28
	Schiedam	78	51.93, 4.39
Utrecht	Utrecht	344	52.09, 5.07
	Amersfoort	155	52.17, 5.38
Flevoland	Almere	202	52.40, 5.21

The area in the middle of the Randstad, called *Groene Hart* (Green Heart), is an area with sparse population. It is however an area with two important freeways (A12 and A20) connecting the cities in the Randstad. Besides that, the traffic dynamics in this area will most likely be different from urban areas. It is therefore desirable to add one extra zone in this area. The city of Gouda, which is the largest city in the region (71,000 inhabitants) is selected to be added as an extra zone. The zone *Westland* is removed, since this zone is part of the agglomeration of Den Haag, and the municipality itself does not contain any significant city.

The results of the second iteration are shown in fig. 4.2b.

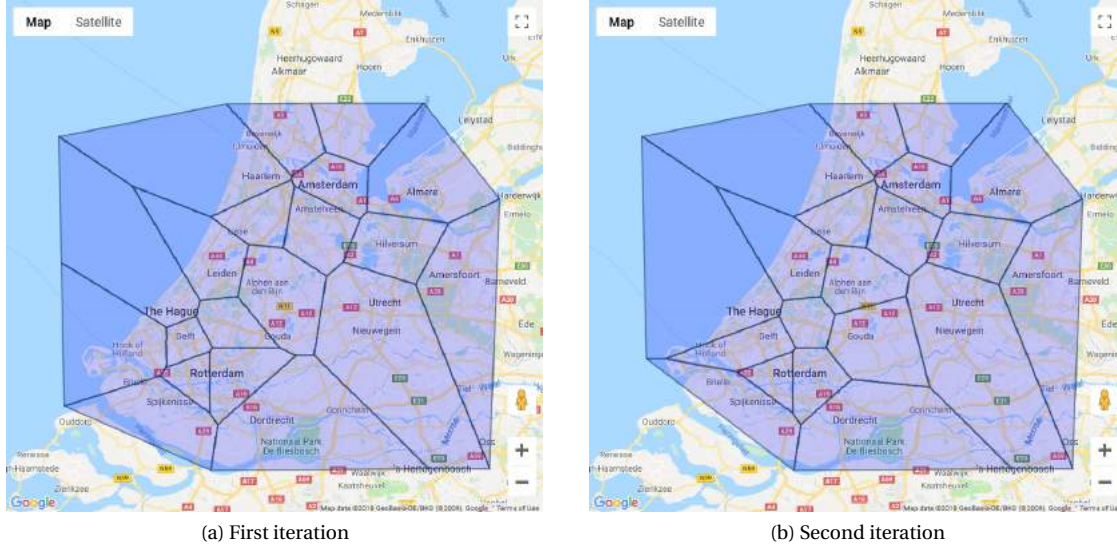


Figure 4.2: Raw zone maps created by assigning each location to the closest centroid.

This does not immediately give the desired results, mainly because some agglomerations are still split into multiple zones. Therefore again some zones are merged:

- Amsterdam & Amstelveen
- Den Haag & Delft
- Haarlem & Haarlemmermeer
- Rotterdam & Schiedam

The result is shown in fig. 4.3a. This map is the basis for the final zone map.

The final map is created by assigning each municipality in the Randstad to a zone, based on the map of fig. 4.3a, according to three guidelines:

- Municipalities that are fully enclosed by the boundaries of one zone are always assigned to that zone.
- Municipalities that are not fully enclosed by one zone, but belong to the agglomeration of a city are assigned to the same zone as the city.
- Other municipalities are assigned to the zone that contains the largest share of their area.

With this approach, the zones follow the boundaries of the municipalities. These boundaries include natural separations like waterways, for instance in the area of Rotterdam. The final zones are listed in table 4.2 and the final map is shown in fig. 4.3b. Seven of these final zones are located at the border of the study area (marked with a * in table 4.2). For each of those, an external zone is added to the simulation, in order to incorporate traffic with an external origin or destination.

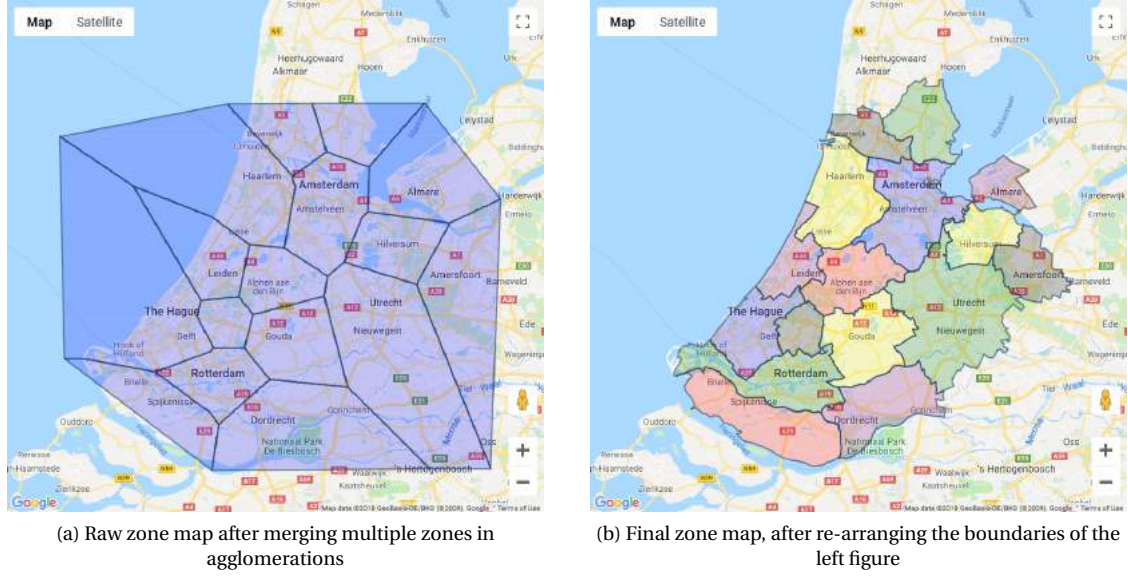


Figure 4.3: Final zone maps after merging zones and re-arranging the boundaries.

Table 4.2: List of the final zones

- | | |
|------------------------|------------------|
| 1. Den Haag | 9. Haarlem |
| 2. Nissewaard * | 10. Amsterdam |
| 3. Rotterdam | 11. Hilversum |
| 4. Dordrecht * | 12. Amersfoort * |
| 5. Gouda | 13. Utrecht * |
| 6. Zoetermeer | 14. Almere * |
| 7. Leiden | 15. Zaanstad * |
| 8. Alphen aan den Rijn | 16. Purmerend * |

4.2. NFD CONSTRUCTION

The NFDs are constructed in three steps. First the NFD for the freeway network is constructed based on loop detector data. Then the NFDs for the local network are estimated based on a theoretical fundamental diagram and characteristics of the road network. Finally, these NFDs are combined to one NFD per zone.

4.2.1. NFD FOR THE FREEWAY NETWORKS

Two days are selected: One with normal weather conditions (09 May 2017) and one with rainfall (7 December 2017). For both days, the data from the freeway network is requested from NDW (Nationale Databank Wegverkeersgegevens). This data consists of flows (veh/h/lane) and speeds (km/h) measured with loop detectors on fixed locations. The data is aggregated for time periods of 30 seconds and divided into segments with a fixed length of 200 meters. The number of lanes for each segment is also given.

Using the approach described in chapter 3, the production and accumulation is calculated for each zone. These numbers are the average flow and density for the zone during each time period. fig. 4.4 - fig. 4.6 show the results for three of the sixteen zones. More NFDs are added in appendix A

As expected, hysteresis loops are visible in the NFD plots. Particularly for Rotterdam on 7 December, a day with heavy rainfall, the clockwise hysteresis loop is clearly visible.

In the diagrams, just a part of the congested branch is visible, because congestion is not homogeneously divided over the network, instead just small parts of the network are fully congested, while the rest is still in free-flow. In the NFD these traffic states are averaged. A fully congested network is never observed, in line with Knoop et al. [17].

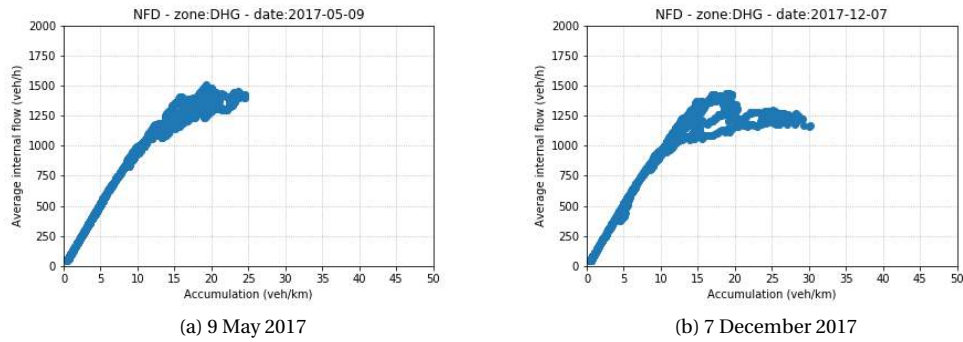


Figure 4.4: Network Fundamental Diagrams for the freeway network of Den Haag

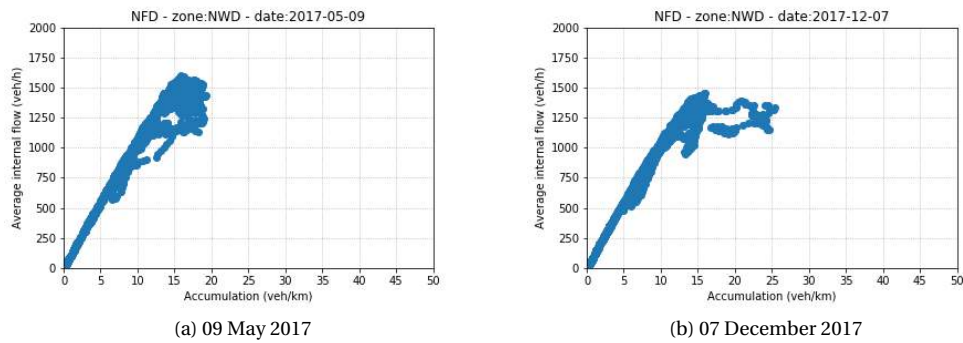


Figure 4.5: Network Fundamental Diagrams for the freeway network of Nissewaard

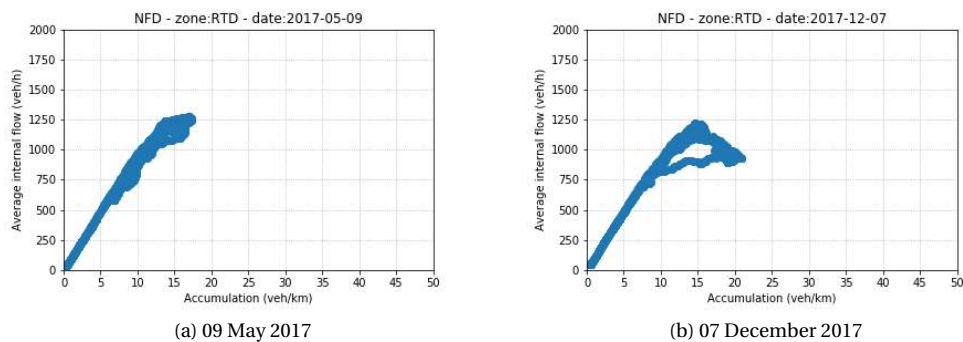


Figure 4.6: Network Fundamental Diagrams for the freeway network of Rotterdam

4.2.2. NFD FOR THE LOCAL NETWORKS

For the local network, the NFD is estimated using an analytical approach. Motorways are now left out, because for these roads the NFD has already been estimated using detector data.

For the calculation of the length of each road type, the number of lanes is also necessary. The data from OpenStreetMap does not always contain this information. If the number of lanes is available, it is used, otherwise the number has to be estimated based on the road type. The assumptions for the number of lanes are shown in table 4.3. Distinction is made between uni-directional and bi-directional roads. If it is unknown whether the road is one-way or two-way traffic, the value in the third column will be used. Living streets are assumed to have just one lane in all cases, because these streets are narrow, and the same space is shared by both directions,

Table 4.3: Default values for the number of lanes for each road type

Road type	One-way	Two-way	Unknown
Motorway	2	4	2
_link	1	2	1
Trunk	2	2	2
_link	1	2	1
Primary	2	2	2
_link	1	2	1
Secondary	1.5	2	2
_link	1	2	1
Tertiary	1	2	2
_link	1	2	1
Residential	1	2	2
Living-street	1	1	1
Service	1	2	2
Unclassified	1	2	2
Road	1	2	2

With the effective number of lanes for each road type, the total lane length of each road type can be determined for each zone. Using the results of this calculation, also the share of each road type in terms of lane length is determined. This is shown in the bar chart of fig. 4.8. Notable is the large amount of 'unclassified', residential and service roads, for most zones. These roads will have large impact on the NFD, because of the low speeds on these roads.

The lane length per area is also calculated and shown in the bar chart in fig. 4.9. Den Haag and Rotterdam have the most dense networks. More rural areas like Alphen aan den Rijn, Gouda and Nissewaard (the zone below Rotterdam) have the least dense networks.

This research is mainly focussing on through traffic. The lower-hierarchy-roads (residential, living street, service and unclassified) are therefore left out, since these roads are in general only used for local traffic. The share of each major road type in terms of lane length is shown in fig. 4.10.

Roads of the same type do not always have the same speed limit, because most road types can be found both inside and outside urban areas, with different characteristics. Therefore, an average value for the free-flow speed and the capacity is determined. It is assumed that the roads have a triangular-shaped fundamental diagram. The parameters of the fundamental diagrams are shown in table 4.4.



(a) Trunk road (1)



(b) Trunk road (2)



(c) Primary road (1)



(d) Primary road (2)



(e) Secondary road



(f) Tertiary road



(g) Residential road



(h) Living street



(i) Unclassified road



(j) Service road

Figure 4.7: Pictures of the road types (Source: Google Maps)

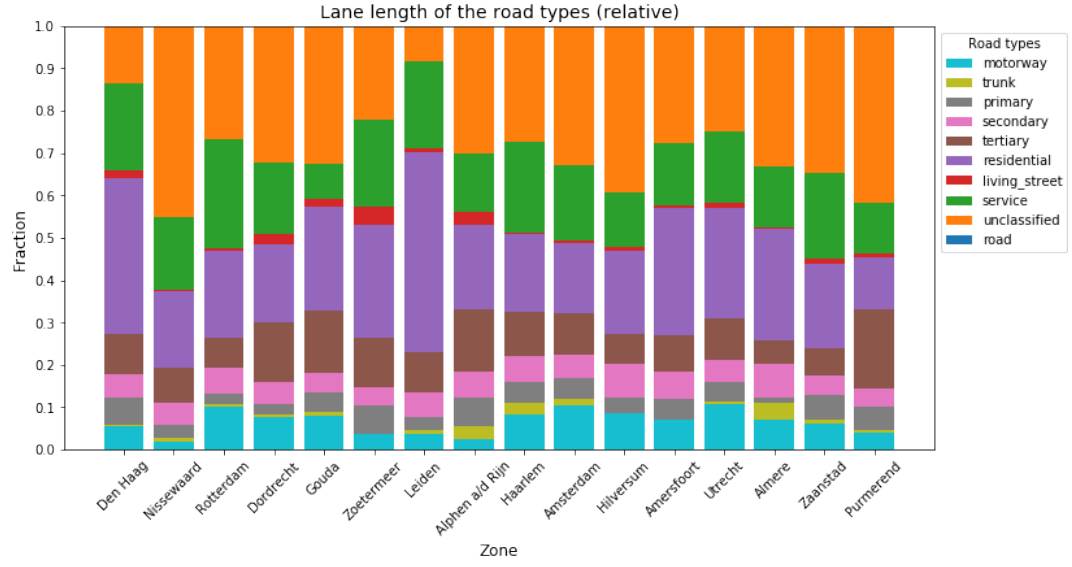


Figure 4.8: The fraction of each road type for each zone, based on the lane lengths

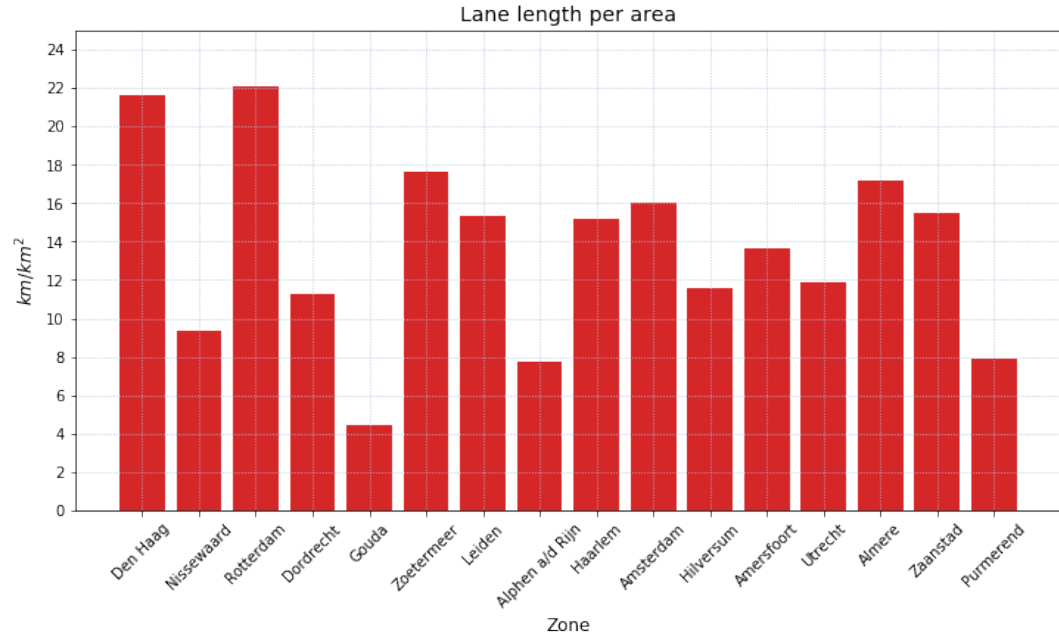
Figure 4.9: The total road (lane) length per area (km/km^2)

Table 4.4: FD Parameters for the different road types

Road type	Speed (km/h)	Capacity (veh/h)	Jam density (veh/km)	Capacity-Multiplier -
Trunk	90	1975	125	0.9
Primary	70	1900	125	0.8
Secondary	50	1800	125	0.7
Tertiary	50	1800	125	0.6

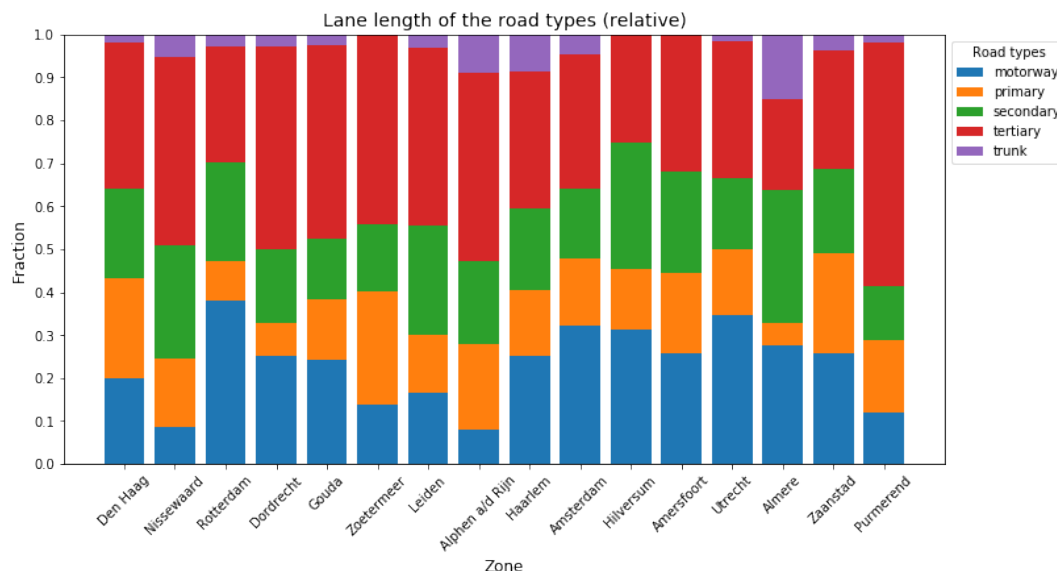


Figure 4.10: The fraction of each major road type for each zone, based on the lane lengths

4.2.3. NFD FOR THE FULL NETWORK

The final step in the NFD estimation process is to combine the NFDs for each road type to one final NFD for the full network, using the approach described in section 3.3.3.

Differences in occupancy between the different road types are taken into account by means of a fixed ratio between these densities. For a small part of the provincial road network, some data from loop detectors is available. This is often limited to one or two detectors on a long road stretch, and therefore not suitable for constructing entire NFDs, but it can be used to determine the ratio between the densities on freeways and primary roads.

For four zones, the ratio is calculated for each time instance by dividing the average density on the free-ways by the average density on the primary roads. The four zones that are selected for this approach are Amersfoort, Amsterdam, Leiden and Utrecht, because these zones have a reasonable amount of provincial roads with detector data. The amount of data for primary roads is however still small compared to the data for the freeway network.

For Amsterdam, the result is plotted in fig. 4.11. During night there is large variation in the ratio, but between 7:00 and 23:00 the ratio seems to be stable around 1.36, with some scatter.

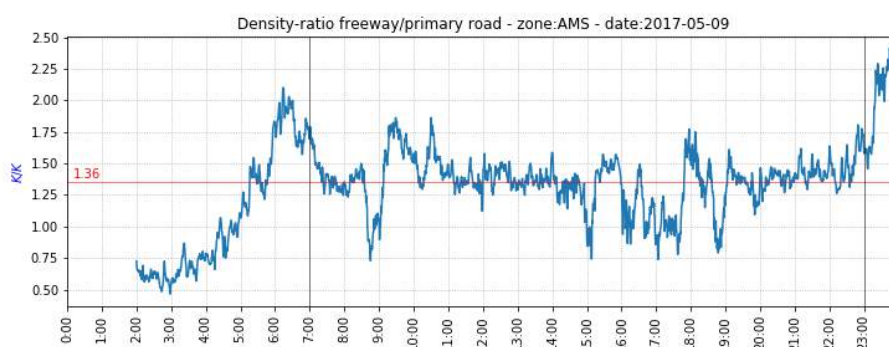


Figure 4.11: The ratio between the density on freeways and primary roads for Amsterdam on 09 May 2017

Similar results are observed for the other zones. The ratios for Amersfoort, Utrecht and Leiden are 1.36, 1.56 and 1.26 respectively. The average of these values is 1.38, which will be used in this remainder of this

research.

This ratio is only calculated for primary roads, but it is assumed that the same value counts for trunk roads. For the secondary roads, the square of this value is used (1.90), and for tertiary roads the cube (2.63), because in line with the hierarchical structure of the network the densities on these roads are expected to be lower, and no data is available to calculate the actual ratio.

Now, the final NFD can be constructed. For each observed density on the freeway network the corresponding densities on the lower-hierarchy roads are calculated, as well as the weighted average density for the full network. With these densities and the fundamental diagrams, the weighted average network flow is calculated. The resulting weighted average densities and flows are then plotted in the K, P -diagram and a multi-linear line is fitted through the points. The K, P -diagrams are given in appendix B.1.

These NFDs are defined in terms of the production (internal flow). The performance is the exit rate (out-flow) of a zone plus the trip completion rate inside the zone. The production and the performance are linearly related by the average trip length.

The outflow pattern is known, but the number of completed trips per day is unknown yet, this will be determined in section 4.3.1. Afterwards the average trip length can be calculated, using the method described in section 3.3.3.

The final parameters for the NFD are given in table 4.5 and an example is plotted in fig. 4.12 for the zone Utrecht.

Table 4.5: NFD Parameters for each zone

Zone	Free-flow speed (km/h)	Capacity (veh/h)	Critical density 1 (veh/km)	Critical density 2 (veh/km)	Critical density 3 (veh/km)	Jam density (veh/km)	Average trip length (km)	Network Length (km)
Den Haag	60	950	9	23	54	125	12.06	1754
Nissewaard	47	970	15	35	53	120	12.47	879
Rotterdam	68	860	10	27	58	125	14.67	2431
Dordrecht	66	890	9	31	57	120	11.65	1354
Gouda	68	900	9	25	56	120	8.48	585
Zoetermeer	56	930	10	24	55	120	8.33	611
Leiden	57	940	13	35	54	120	9.31	712
Alphen a/d Rijn	52	970	16	35	52	120	13.32	812
Haarlem	63	940	10	23	55	125	11.40	2094
Amsterdam	69	930	11	25	55	125	18.39	2502
Hilversum	70	940	10	27	56	120	9.65	706
Amersfoort	65	930	9	27	55	125	10.94	856
Utrecht	73	910	10	25	56	125	18.77	2905
Almere	70	960	9	24	55	125	9.35	612
Zaanstad	70	870	6	25	58	125	5.72	624
Purmerend	53	900	8	32	54	125	9.42	728

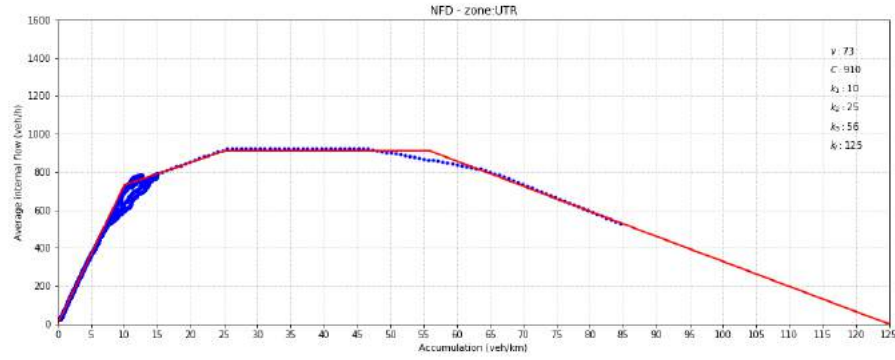


Figure 4.12: Example of an NFD fitted through the points

4.3. OD-PATTERN ESTIMATION

For the estimation of the OD-pattern, the first two steps of the four-step model are used, the trip generation and trip distribution, resulting in an OD-matrix for 24 hours. The pattern over the day is derived from the observed flows on the freeway network.

4.3.1. TRIP GENERATION

Before the OD-matrix can be estimated, first the number of departures and arrivals for each zone is calculated using the number of households and jobs in each zone. The production and attraction are totals including all modes of transport.

The production and attraction for car traffic is calculated by multiplying this value by the share of car drivers in the modal split of the zone. For the Netherlands this value is around 0.32. For larger cities, the modal split is published by EPOMM [9]. Their database contains results from mobility studies for the Netherlands like OVIN and MON. For the cities for which this information is not available, the value of 0.32 is used as an initial estimate. Generally, it can be stated that the share of car drivers is smaller for larger cities than for smaller towns and rural areas.

For each zone, the data on the number of households is collected from the Centraal Bureau voor Statistiek (CBS) [4] database and the number of jobs from the Stichting Lisa [26] database. Finally, the values are shown in table 4.6.

Traffic with an origin or destination outside the Randstad is taken into account using seven external zones. The demand from and towards those zones is calculated by taking the average of the observed inflow and outflow at the boundaries of the Randstad for one day. The observed inflow and outflows are calculated using loop detector data taken from the NDW database. The resulting demand is then increased by 10% to account for the lower-hierarchy roads without observations. The final values for the departures and arrivals for external areas are then given in table 4.7.

4.3.2. DISTANCE MATRIX ESTIMATION

Next, the distance matrix is constructed, containing the euclidian distance between the centroids of the zones. The matrix is given in table 4.8.

The distance towards the external zones is obtained by adding 40 kilometers to the distance towards the neighbours of the external zones. Together with the production and attraction values from table 4.6 this matrix forms the input to the OD-estimation process. Using the procedure in section 3.4 the OD-matrix is calculated.

Table 4.6: Departures & Arrivals estimation based on socio-economic data

Zone	Inhabitants	Households	Jobs	Departures Arrivals (Total)	Departures Arrivals (Car)
Den Haag	900,708	439,778	459,330	4,190,614	1,080,369
Nissewaard	239,732	105,236	76,920	907,102	290,273
Rotterdam	989,241	482,098	519,750	4,640,912	1,125,850
Dordrecht	366,479	157,484	172,460	1,523,780	550,455
Gouda	236,981	99,818	103,840	949,953	303,985
Zoetermeer	235,036	97,649	94,670	909,262	321,705
Leiden	349,846	163,505	160,910	1,529,422	459,294
Alphen a/d Rijn	169,620	71,325	71,990	672,384	215,163
Haarlem	501,373	225,216	271,590	2,251,515	843,507
Amsterdam	1,090,312	573,527	768,015	5,955,170	1,144,831
Hilversum	209,148	95,131	88,355	874,580	279,866
Amersfoort	273,742	117,825	136,080	1,160,495	395,128
Utrecht	779,389	362,803	464,170	3,704,313	891,852
Almere	198,145	82,509	81,030	771,296	269,953
Zaanstad	254,947	113,645	96,790	1,019,384	357,539
Purmerend	168,257	72,629	57,790	639,680	204,697

Table 4.7: Departures & Arrivals for external zones

External zone	Departures Arrivals (Car)
Nissewaard	40,235
Dordrecht	117,538
Amersfoort	114,688
Utrecht	156,938
Almere	36,855
Zaanstad	53,850
Purmerend	55,864

Table 4.8: Distance matrix (in kilometers)

-	1	2	3	4	5	6	7	8	9	10	11	12	13	14	15	16
Den Haag	7.02	23.8	13.32	39.07	29.59	12.27	20.81	29.02	41.99	51.8	64.39	74.23	52.21	75.35	59.32	70.23
Nissewaard	23.8	8.92	11.7	31.04	34.01	25.48	42.26	43.76	62.01	67.08	74.46	80.23	56.56	87.63	79.43	88.3
Rotterdam	13.32	11.7	8.3	29.32	26.02	14.07	30.57	32.91	50.42	56.45	65.51	72.88	49.51	78.05	67.87	77.13
Dordrecht	39.07	31.04	29.32	8.12	17.86	29.21	44.26	34.6	55.72	51.83	51.53	53.02	30.34	65.95	70.68	74.76
Gouda	29.59	34.01	26.02	17.86	8.12	17.41	27.82	16.74	37.89	35.87	40.49	46.87	23.54	53.97	53.27	58.59
Zoetermeer	12.27	25.48	14.07	29.21	17.41	4.66	17.95	19.1	36.57	42.66	53.25	62.31	40	65.05	53.96	63.07
Leiden	20.81	42.26	30.57	44.26	27.82	17.95	5.78	15.52	21.24	33.45	49.33	61.86	43.65	58.04	38.52	49.79
Alphen a/d Rijn	29.02	43.76	32.91	34.6	16.74	19.1	15.52	7.23	21.23	23.57	35.63	46.95	28.15	46.36	37.34	44.65
Haarlem	41.99	62.01	50.42	55.72	37.89	36.57	21.24	21.23	8.36	18.17	37.5	52.49	41.97	41.76	17.48	28.79
Amsterdam	51.8	67.08	56.45	51.83	35.87	42.66	33.45	23.57	18.17	8.93	19.44	34.71	29.24	24.73	22	22.93
Hilversum	64.39	74.46	65.51	51.53	40.49	53.25	49.33	35.63	37.5	19.44	6.1	15.49	21.77	14.52	38.77	32.75
Amersfoort	74.23	80.23	72.88	53.02	46.87	62.31	61.86	46.95	52.49	34.71	15.49	6.19	23.67	23.1	54.11	46.76
Utrecht	52.21	56.56	49.51	30.34	23.54	40	43.65	28.15	41.97	29.24	21.77	23.67	11.43	36.28	51.16	50.3
Almere	75.35	87.63	78.05	65.95	53.97	65.05	58.04	46.36	41.76	24.73	14.52	23.1	36.28	4.79	36.51	25.65
Zaanstad	59.32	79.43	67.87	70.68	53.27	53.96	38.52	37.34	17.48	22	38.77	54.11	51.16	36.51	5.26	14.51
Purmerend	70.23	88.3	77.13	74.76	58.59	63.07	49.79	44.65	28.79	22.93	32.75	46.76	50.3	25.65	14.51	6.77

4.3.3. TRIP DISTRIBUTION

The values from the distance matrix are substituted in the deterrence function, resulting in a new matrix containing the attractiveness of each OD-pair.

First, four different shapes for the deterrence function are analyzed. The parameters are given table 4.9 in and fig. 4.13 shows the functions in a plot.

Table 4.9: Parameters

#	Function type	Parameters			Function
		α	β	γ	
1	Power	1.0	2.0	-	$f(c_{ij}) = c_{ij}^{-2.0}$
2	Exponential	1.0	0.2	-	$f(c_{ij}) = e^{-0.2 \cdot c_{ij}}$
3	Lognormal	1.0	0.4	-	$f(c_{ij}) = e^{-0.5 \cdot \ln^2(c_{ij}+1)}$
4	Top-lognormal	1.0	0.5	2.0	$f(c_{ij}) = e^{-0.5 \cdot \ln^2(c_{ij}/2.0)}$

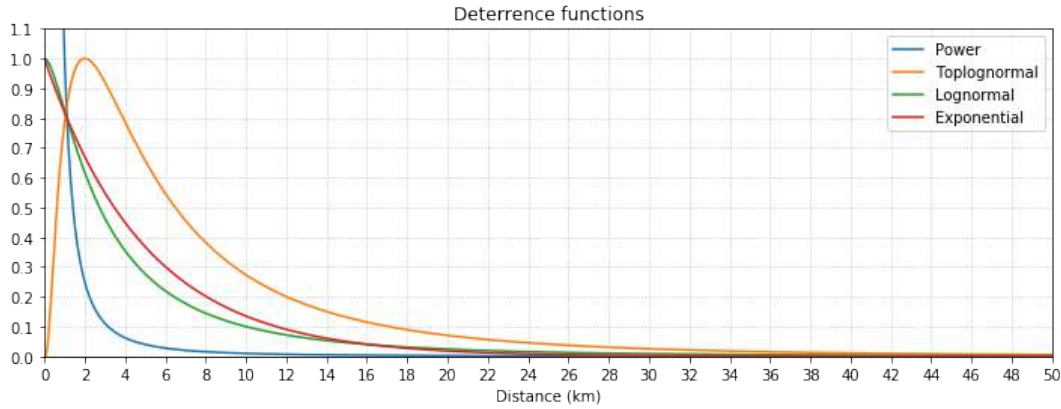


Figure 4.13: Plot with the four considered deterrence functions

The outflow of a zone includes the trips starting in the zone with a destination outside that zone, and all other trips with a path through that zone. So, the OD-matrix has to meet one extra requirement, which is that for each zone the number of non-internal trips has to be smaller than the total observed outflow. In this section, this first requirement is checked for the functions mentioned in table 4.9.

For these four functions, the results of the OD-estimation process are shown in table 4.10 (power function), table 4.11 (exponential function), table 4.12 (lognormal function) and table 4.13 (toplognormal function).

The tables list the number of internal and outbound trips, the observed outflows at the boundaries and the ratio between the outbound trips and the outflow. This ratio should be smaller than 1.0.

For all four deterrence functions, there are a couple of zones for which the number of outbound trips exceeds the observed outflows. This is mostly the case for Den Haag, Nissewaard, Rotterdam and Zoetermeer. Some other zones require attention as well, because even though the observed outflow is not exceeded, it is likely that the outflow will be exceeded in the simulation, due to the trips passing through that zones.

Reducing the total demand for the zones Den Haag, Nissewaard, Rotterdam, Zoetermeer and Amsterdam will lead to a reduction in both internal and outbound trips for these five zones, so the requirement that the number of outbound trips should be smaller than the observed outflow can be fulfilled.

Alternatively, the parameters of the deterrence functions can be changed. Increasing the β -parameter of the power, exponential or lognormal function will make the attractiveness of an OD-pair decrease faster with increasing distance, which will lead to a reduction of outbound trips, and an increase in internal trips.

Table 4.10: Power function with $\beta = 2.0$

Zone	Internal	Outbound	Observed outflow	Ratio
Den Haag	622,153	458,216	346,354	1.32
Nissewaard	81,846	208,427	151,939	1.37
Rotterdam	568,533	557,317	502,858	1.11
Dordrecht	310,619	239,836	345,294	0.69
Gouda	92,267	211,718	264,067	0.80
Zoetermeer	121,142	200,563	177,840	1.13
Leiden	248,251	211,043	268,090	0.79
Alphen a/d Rijn	55,607	159,556	257,164	0.62
Haarlem	454,589	388,918	447,221	0.87
Amsterdam	638,887	505,944	509,158	0.99
Hilversum	107,665	172,201	344,800	0.5
Amersfoort	230,072	165,056	256,033	0.64
Utrecht	456,095	435,757	586,861	0.74
Almere	159,490	110,463	140,859	0.78
Zaanstad	198,574	158,965	262,195	0.61
Purmerend	89,430	115,267	137,466	0.84

Table 4.11: Exponential function with $\beta = 0.2$

Zone	Internal	Outbound	Observed outflow	Ratio
Den Haag	723,751	356,432	346,354	1.03
Nissewaard	110,558	179,661	151,939	1.18
Rotterdam	650,486	475,163	502,858	0.94
Dordrecht	387,176	163,253	345,294	0.47
Gouda	172,018	131,956	264,067	0.50
Zoetermeer	126,449	195,208	177,840	1.10
Leiden	343,627	115,641	268,090	0.43
Alphen a/d Rijn	106,789	108,373	257,164	0.42
Haarlem	626,341	217,239	447,221	0.49
Amsterdam	897,501	247,458	509,158	0.49
Hilversum	145,485	134,422	344,800	0.39
Amersfoort	239,841	155,351	256,033	0.61
Utrecht	646,649	245,299	586,861	0.42
Almere	187,724	82,273	140,859	0.58
Zaanstad	215,129	142,450	262,195	0.54
Purmerend	110,235	94,488	137,466	0.69

Table 4.12: Lognormal function with $\beta = 0.4$

Zone	Internal	Outbound	Observed outflow	Ratio
Den Haag	616,833	463,536	346,354	1.34
Nissewaard	86,284	203,989	151,939	1.34
Rotterdam	564,662	561,188	502,858	1.12
Dordrecht	331,877	218,578	345,294	0.63
Gouda	95,823	208,162	264,067	0.79
Zoetermeer	98,494	223,211	177,840	1.26
Leiden	246,794	212,500	268,090	0.79
Alphen a/d Rijn	55,676	159,487	257,164	0.62
Haarlem	471,619	371,888	447,221	0.83
Amsterdam	660,892	483,939	509,158	0.95
Hilversum	98,610	181,256	344,800	0.53
Amersfoort	227,264	167,864	256,033	0.66
Utrecht	497,227	394,625	586,861	0.67
Almere	152,323	117,630	140,859	0.84
Zaandam	187,409	170,131	262,195	0.65
Purmerend	90,111	114,586	137,466	0.83

Table 4.13: Toplognormal function with $\beta = 0.5$ and $\gamma = 2.0$

Zone	Internal	Outbound	Observed outflow	Ratio
Den Haag	596,499	483,870	346,354	1.40
Nissewaard	83,376	206,897	151,939	1.36
Rotterdam	547,971	577,879	502,858	1.15
Dordrecht	324,471	225,984	345,294	0.65
Gouda	90,295	213,690	264,067	0.81
Zoetermeer	86,747	234,958	177,840	1.32
Leiden	233,392	225,902	268,090	0.84
Alphen a/d Rijn	51,247	163,916	257,164	0.64
Haarlem	457,154	386,353	447,221	0.86
Amsterdam	643,465	501,366	509,158	0.98
Hilversum	90,355	189,511	344,800	0.55
Amersfoort	217,714	177,414	256,033	0.69
Utrecht	489,428	402,424	586,861	0.69
Almere	142,892	127,061	140,859	0.90
Zaanstad	175,733	181,806	262,195	0.69
Purmerend	84,798	119,899	137,466	0.87

For the toplognormal function, adapting the parameters is more complicated, since it has one parameter extra. The OD-matrix can be improved by:

- Increasing the β -parameter, which will make the attractiveness of an OD-pair decrease faster with increasing distance, which will lead to a reduction of outbound trips, and an increase in internal trips.
- Changing the γ -parameter, which will shift the peak in the deterrence function. Increasing this parameter will shift the peak more towards larger distances, and decreasing it will shift the peak towards smaller distances.

The exponential function also requires some more attention. A closer look at the OD-matrix for the exponential function makes clear that for all zones, the majority of the non-internal trips already ends in one of its neighbouring zones, because trips to other zones farther away are too unattractive. Some examples are Den Haag - Utrecht and Den Haag - Amsterdam with 126 and 128 trips/day respectively, or Amsterdam - Rotterdam with just 54 trips/day.

Increasing the β -parameter or reducing the total demand will therefore not lead to a better result, because it will even reduce the attractiveness of those OD-pairs. Exponential functions are therefore not considered in the remainder of this research. The other three functions are optimized.

As an example, the effect of changing the β -parameter and reducing the demand is shown for the lognormal deterrence function. The β -parameter is increased from 0.4 to 0.45 and the demand for Den Haag, Rotterdam and Amsterdam is reduced with 30%, the demand for Zoetermeer is reduced with 20% and the demand for Nissewaard is reduced with 50%. The results are summarized in table 4.14. Now, for all zones the outbound flow is lower than the observed outflow. In chapter 5, this OD-matrix will be used for the simulation.

Table 4.14: Lognormal function with $\beta = 0.45$ and reduced demand

Zone	Internal	Outbound	Observed outflow	Ratio
Den Haag	452,893	303,365	346,354	0.88
Nissewaard	38,134	107,002	151,939	0.70
Rotterdam	425,322	362,773	502,858	0.72
Dordrecht	366,912	183,543	345,294	0.53
Gouda	119,413	184,572	264,067	0.70
Zoetermeer	93,952	163,412	177,840	0.92
Leiden	290,475	168,819	268,090	0.63
Alphen a/d Rijn	72,847	142,316	257,164	0.55
Haarlem	540,140	303,367	447,221	0.68
Amsterdam	462,048	339,334	509,158	0.67
Hilversum	119,676	160,190	344,800	0.46
Amersfoort	247,770	147,358	256,033	0.58
Utrecht	548,981	342,871	586,861	0.58
Almere	172,837	97,116	140,859	0.69
Zaanstad	212,480	145,059	262,195	0.55
Purmerend	106,245	98,452	137,466	0.72

The final OD-matrix is given in appendix C.1.

4.3.4. OD-PATTERNS OVER TIME

The OD-flows obtained from the trip distribution step are totals for 24 hours. Combined with the normalized OD-pattern, it gives the development of these flows over the day.

Based on the on the internal flows found during the NFD estimation process, the normalized demand pattern is calculated. The patterns are shown in fig. 4.14. This figure shows that the demand patterns are similar for all zones, so it could be simplified to one general demand pattern. In this research however the specific demand patterns for the sixteen zones are used.

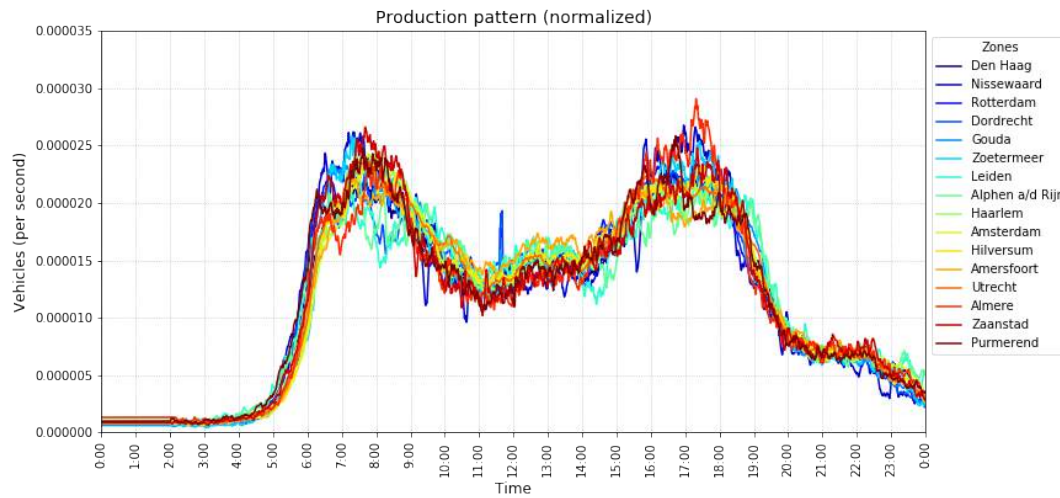


Figure 4.14: The normalized Production pattern for each zone

When the OD-flows calculated in the trip distribution step are multiplied with the normalized production pattern of the origin, the full OD-pattern is obtained. Some examples are shown in fig. 4.15.

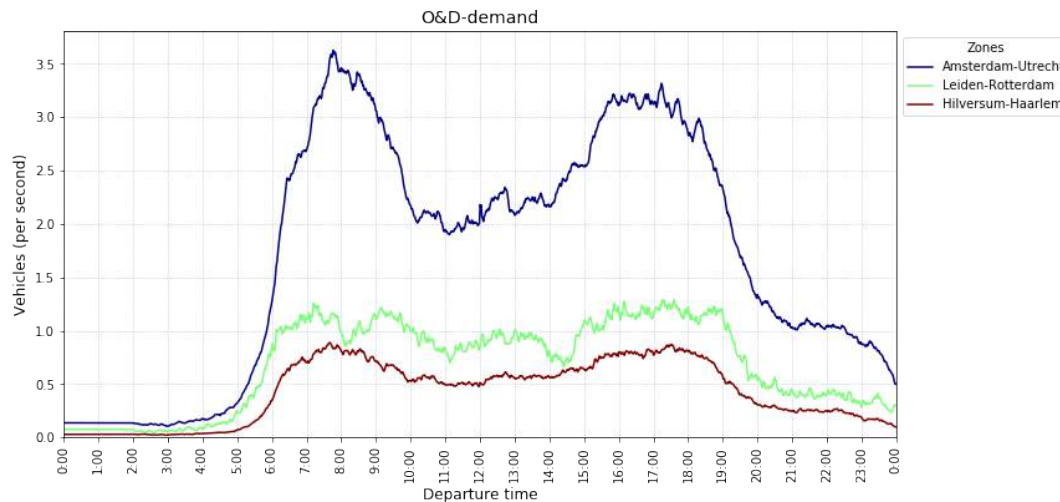


Figure 4.15: Three examples of OD-patterns

4.4. ROUTING

The internal distance matrices are constructed based on the distances obtained from Google Maps. This matrix is a specific matrix for each zone, containing the distances between each pair of its neighbours and the average distance from the zone itself to its neighbours.

Preliminary to the simulation, three distinct routes are generated for each OD-pair, which are the three fastest routes under free flow conditions. During the simulation, the travel times for these routes are updated each time step. The fastest route is always selected.

5

SIMULATION RESULTS

In this chapter the first simulation results are presented and analyzed on three aspects:

- **Outflow pattern** of each zone.
- **Density distribution** of each zone.
- **Trip duration** between each OD-pair.

From this results, conclusions are drawn and options for improvement of the simulation model are suggested. These improvements will be tested in chapter 6.

5.1. ANALYSIS OF THE OUTFLOW PATTERNS

In this section, the outflow patterns are discussed. The results for all zones are summarized in table 5.1. This table gives the ratio between the simulated outflow patterns and the observed patterns. The closer the values to one, the better the pattern matches the expected results. The columns give the mean value over the day, the minimum and maximum value of the ratio, and the mean values for the morning peak (6:00-10:00) and the afternoon peak (15:00-19:00).

In section 3.6 it was mentioned that an average deviation of maximum 20% from the expected pattern is desired over 24h and over the morning and afternoon peak periods. The values that fall within this range are shown in green and the values outside this range in red.

Generally, the model is able to reproduce the shapes of the outflow patterns, taking into account the desired range of 20%, but some zones show large deviations. The results can probably be improved by adjusting the OD-matrix. In addition to table 5.1, the plots of the outflow patterns can be found in appendix D for all sixteen zones. Some outstanding outflow patterns are discussed in this section, based on these figures.

- **Den Haag:** For Den Haag, the total demand for Den Haag had to be reduced during the OD-estimation process in section 4.3.3, to make sure that the total demand would not exceed the observed outflow. The outflow plots however show that the outflow is particularly during morning peak much higher than the observed values. This could be solved by further reducing the demand or slightly increasing the β -parameter of the deterrence function in the OD-estimation process. Over 24 hours, the average deviation between the simulated and observed pattern is slightly higher than 20%.
- **Nissewaard:** This zone is located south of Rotterdam. For this zone, the outflow during morning peak matches the observed values quite well, but during the afternoon peak, the model overestimates the outflow. The reason for this result is most likely that this zone has a dominant outbound flow during morning peak, but a dominant inbound flow during afternoon peak, probably because of the commuting traffic going from Nissewaard to Rotterdam in the morning, and returning during the afternoon.

Table 5.1: Ratio between the simulated and observed outflows.

Zone	Mean	Min	Max	AM peak	PM peak
Den Haag	<u>1.20</u>	0.91	1.53	<u>1.23</u>	1.11
Nissewaard	1.17	0.61	2.04	1.07	<u>1.53</u>
Rotterdam	1.13	0.71	1.50	<u>1.36</u>	1.17
Dordrecht	1.04	0.62	1.70	0.99	1.02
Gouda	1.12	0.74	1.71	0.93	0.87
Zoetermeer	<u>1.27</u>	1.00	2.28	1.15	1.13
Leiden	0.90	0.73	1.19	<u>0.79</u>	0.88
Alphen a/d Rijn	1.08	0.66	1.61	0.94	1.07
Haarlem	0.88	0.70	1.23	0.93	0.88
Amsterdam	1.18	0.79	1.69	<u>1.36</u>	1.08
Hilversum	<u>1.22</u>	0.80	1.85	1.15	1.14
Amersfoort	<u>1.25</u>	0.88	1.80	1.12	1.16
Utrecht	1.12	0.86	1.53	1.09	0.94
Almere	<u>1.26</u>	0.57	2.79	0.89	<u>1.26</u>
Zaanstad	1.08	0.73	1.55	0.93	0.96
Purmerend	<u>1.43</u>	1.07	2.10	<u>1.33</u>	<u>1.25</u>

- **Rotterdam:** Similar to Den Haag, the total demand for this zone was reduced during the OD-estimation process in section 4.3.3, to make sure that the total demand did not exceed the observed outflow. Although over 24 hours, the average deviation between the simulated and observed pattern remains below 20%, the outflow plots show that the outflow is during morning peak much higher than the observed values. The average difference during this peak is 36%. As mentioned, this could be solved by further reducing the demand or slightly increasing the β -parameter of the deterrence function in the OD-estimation process.
- **Dordrecht:** This is an example of a zone for which the outflow pattern matches the the observed values relatively well. On average, the deviation between the simulated and observed pattern is even less than 5%. The patterns however show that during the end of the afternoon peak there is a delay between the observed and simulated decrease in the outflow.
- **Zoetermeer:** This is also an example of a zone for which the outflow pattern matches the the observed values relatively well. Although the average deviation between the observed and simulated outflow pattern is more than the desired 20% over 24 hours, during the peak hours, the deviation stays within this range. This is also visible in the plots. Similar to Dordrecht, during the end of the afternoon peak there is a delay between the observed and simulated drop in the outflow.

5.2. ANALYSIS OF THE ACCUMULATION PATTERNS

In this section, the accumulation patterns are discussed. The results for all zones are summarized in table 5.2. This table gives the ratio between the simulated accumulation patterns and the expected patterns. The closer the values to one, the better the pattern matches the expected results. The columns give the mean value over the day, the minimum and maximum value of the ratio, and the mean values for the morning peak (6:00-10:00) and the afternoon peak (15:00-19:00).

In section 3.6 it was mentioned that an average deviation of maximum 20% from the expected pattern is desired over 24h and over the morning and afternoon peak period. The values that fall within this range are shown bold and in green and the values outside this range are underlined and shown in red.

Table 5.2: Ratio between the simulated and expected accumulation.

Zone	Mean	Min	Max	AM peak	PM peak
Den Haag	0.97	0.70	1.51	0.85	0.87
Nissewaard	1.53	0.70	2.73	1.29	1.52
Rotterdam	0.98	0.68	1.42	0.92	0.91
Dordrecht	1.39	0.84	2.80	1.35	1.63
Gouda	2.37	1.20	3.65	2.12	2.83
Zoetermeer	1.31	0.82	2.31	1.10	1.16
Leiden	0.95	0.37	1.67	0.70	0.90
Alphen a/d Rijn	1.08	0.56	1.91	0.90	1.08
Haarlem	1.31	0.80	1.92	1.28	1.16
Amsterdam	0.94	0.58	1.42	0.91	0.79
Hilversum	1.30	0.77	1.98	1.10	1.48
Amersfoort	1.22	0.83	2.08	1.23	1.28
Utrecht	1.20	0.83	1.86	1.20	1.13
Almere	1.00	0.64	1.55	0.90	0.96
Zaanstad	2.14	1.21	4.27	2.71	2.35
Purmerend	1.69	0.88	2.79	1.87	1.69

Overall, the model is able to reproduce the shapes of the accumulation patterns, but the accumulations are overestimated by more than 20% for most of the zones. The deviations are especially visible during the peak hours. In addition to table 5.2, the plots of the accumulation patterns can be found in appendix E. Some of those accumulation patterns are discussed in this section:

- **Rotterdam:** Rotterdam is an example of a zone for which the average deviation is less than 10%, both over 24 hours and during the peak hours.
- **Gouda:** The accumulation pattern for Gouda shows that the simulation results in an accumulation that is about 2 or 3 times higher than the expected accumulation pattern based on the observed values for freeways.
- **Leiden:** For Leiden, the average deviation over 24 hours and during the afternoon peak is less than 10%, but during the morning peak the difference is 30%. Between the peaks and at the boundaries of the peaks the model is able to predict the accumulation accurately, but during the peak hours, the top of the peak is for Leiden lower than expected.
- **Zaanstad:** The accumulation pattern for Zaanstad shows the same problem as the pattern for Gouda. The simulation gives an accumulation that is on average more than two times as high as the expected accumulation pattern based on the observed values for freeways.

The plots confirm the findings based in table 5.2. For the majority of the zones, the deviation from the expected patterns is larger than desired. This is especially the case for Gouda and Zaanstad, but some other zones face the same problem, but to a lesser extent. One possible cause for this problem is that the trip lengths from the internal distance matrix are probably too large, and vehicles are therefore kept in the zone for a too long period, leading to an overestimation of the accumulation. At the end of this section (see section 5.2.1) this will be checked.

5.2.1. SENSITIVITY ANALYSIS OF THE INTERNAL DISTANCE MATRIX

Some zones showed a large overestimation of the accumulation. This could be caused by too large internal distances. Therefore, some changes are made to the internal distance matrices. For four zones the internal

distances are reduced:

- **Dordrecht:** -10%
- **Gouda:** -20%
- **Zaanstad:** -20%
- **Purmerend:** -10%

The new accumulation plots are shown in fig. 5.1 for Dordrecht and Gouda and in fig. 5.2 for Zaanstad and Purmerend.

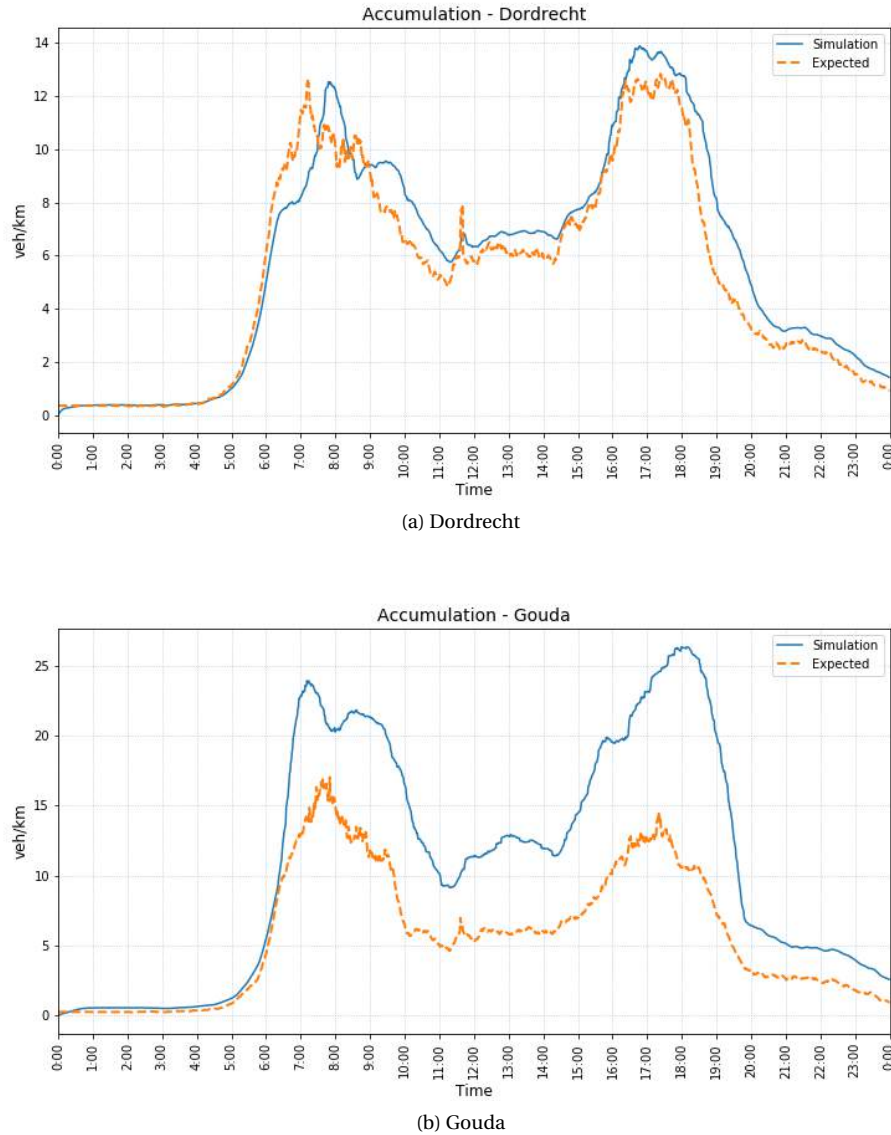
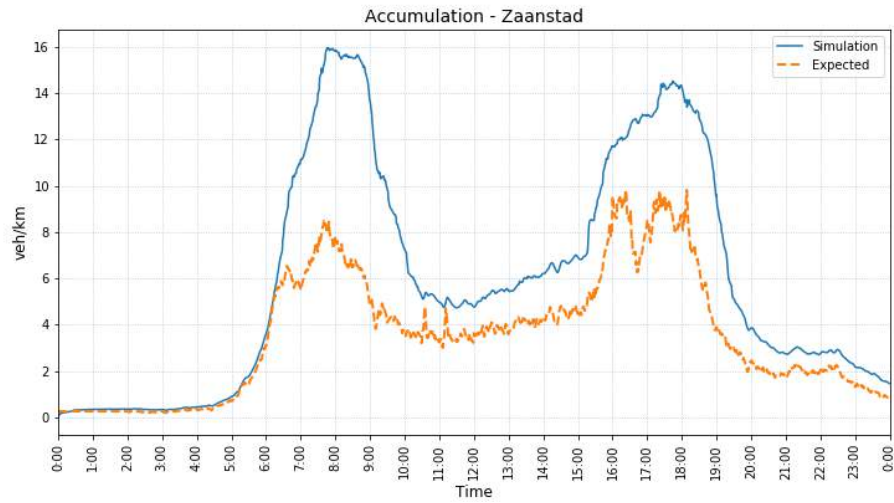
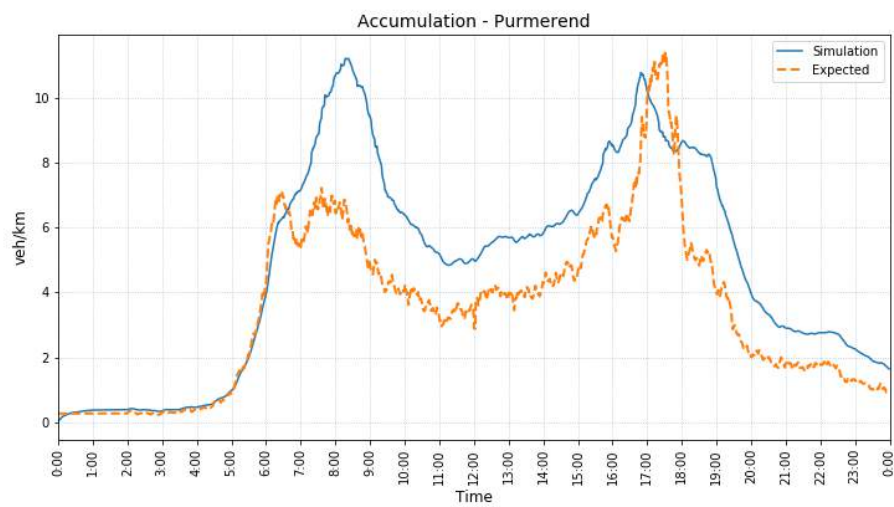


Figure 5.1: The resulting accumulation patterns for Dordrecht and Gouda for the reduced internal distance matrices.

All accumulation plots improved, but for three of the four zones the reduction is not large enough. Only Dordrecht now has an accumulation pattern that matches the expected values. For Gouda the maximum accumulation reduced from over 40 veh/km to a value of 25 veh/km and for Zaanstad the maximum accumulation reduced from more than 20 veh/km to 16 veh/km. For Purmerend the maximum accumulation reduced from 14 veh/km to 11 veh/km.



(a) Zaanstad



(b) Purmerend

Figure 5.2: The resulting accumulation patterns for Zaanstad and Purmerend for the reduced internal distance matrices.

The accumulation patterns for the other zones are not significantly influenced by the reduction of the internal distances for these for zones.

5.3. ANALYSIS OF THE TRAVEL TIMES

For all OD-pairs the free-flow travel time have been requested from Google Maps and HERE Maps. The full results can be found in appendix F. The differences between the free-flow travel times obtained from the simulation and those observed values are calculated in minutes, and the results are summarized in table 5.3. A positive value means that the travel time from the simulation is larger than the observed travel time.

Table 5.3: Deviation in free-flow travel times between the simulation and observed values (in minutes).

Statistics	Google Maps	HERE Maps
Mean	11.15	11.88
Median	9.92	10.40
Std. dev	11.28	11.25
Minimum	-11.18	-10.87
Maximum	41.82	43.07

From the mean and median values in this table it becomes clear that in general the travel times are highly overestimated by the simulation model. The maximum difference is even more than 40 minutes.

The travel times during peak hours are compared to data from Google Maps. For this comparison three routes are selected for the long distance:

- Den Haag - Amsterdam: fig. 5.3
- Den Haag - Amersfoort: fig. 5.4
- Dordrecht - Zaanstad: fig. 5.5

The plots give the average Google Maps travel time based on multiple days of observations. The travel time is measured between the centers of the zones, and an upper and lower bound, which are the travel time between the boundaries of the zones. The full observed travel time patterns are shown in appendix E2 and appendix E3.

The travel time patterns during peak hours confirm that the travel times are overestimated by the simulation model. For two of the three routes it even exceeds the upper bound. The model is not able to predict the travel time patterns accurately. The plots for Dordrecht - Zaanstad show however that the peak in travel time occurs approximately at the same moment as in reality.

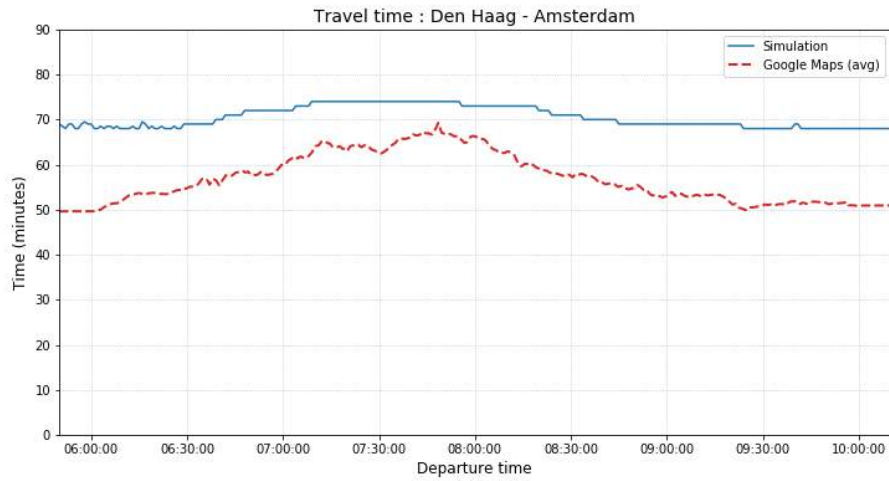
Additionally, three routes for the short distance are tested:

- Utrecht - Amersfoort: fig. 5.6
- Den Haag - Rotterdam: fig. 5.7
- Hilversum - Amsterdam: fig. 5.8

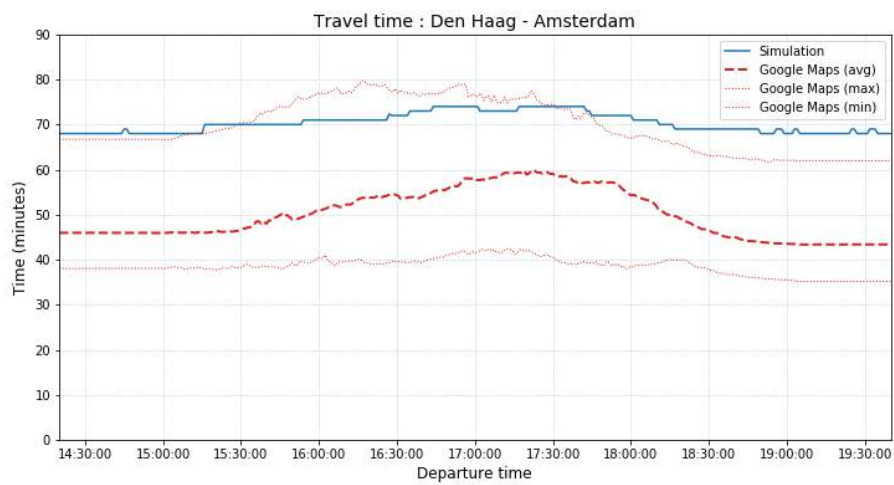
The plots give the average Google Maps travel time between the centers of the zones based on multiple days of observations. The full observed travel time patterns are shown in appendix E2 and appendix E3.

For Den Haag - Rotterdam, the simulation is not able to reconstruct the travel time pattern. The free-flow travel time is close to the real travel time, but the large peak with delays of around 15 minutes is not present in the results.

For Utrecht - Amersfoort, there is around 6 minutes difference between the free-flow travel times, but during the morning and afternoon peak the simulated and observed patterns match quite well. However, the

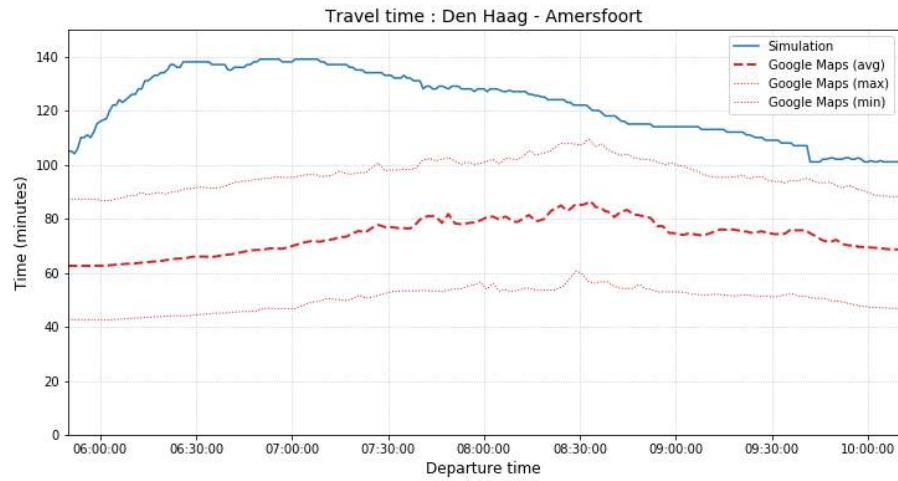


(a) Morning peak

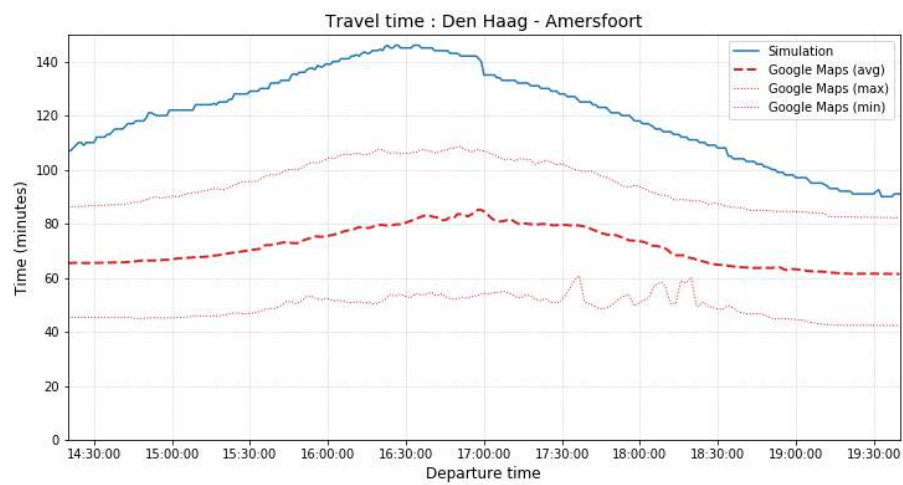


(b) Afternoon peak

Figure 5.3: The travel time plots for the route Den Haag - Amsterdam

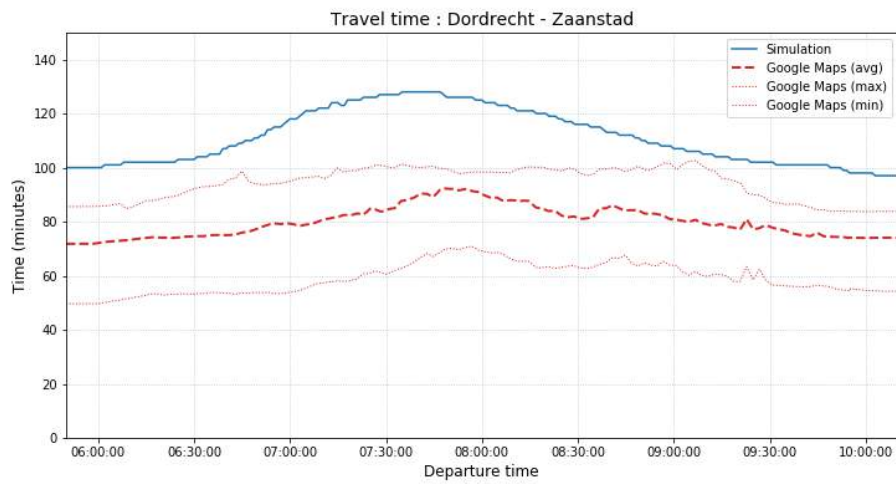


(a) Morning peak

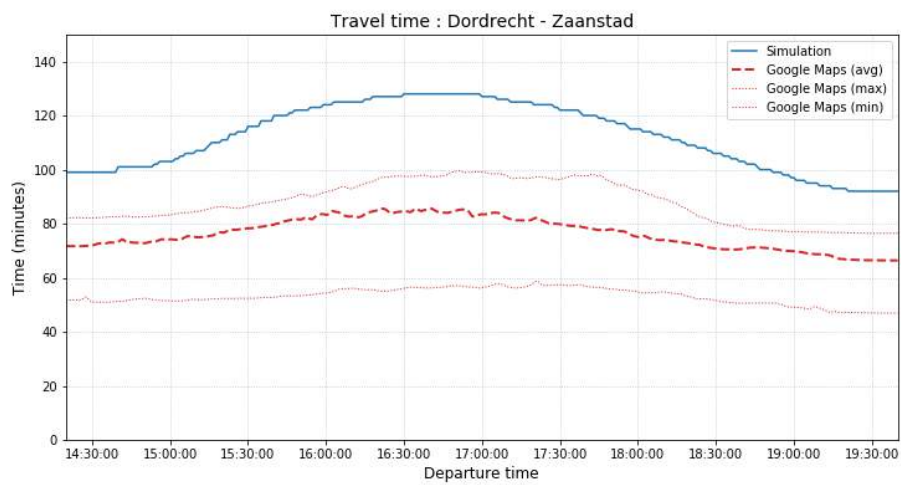


(b) Afternoon peak

Figure 5.4: The travel time plots for the route Den Haag - Amersfoort

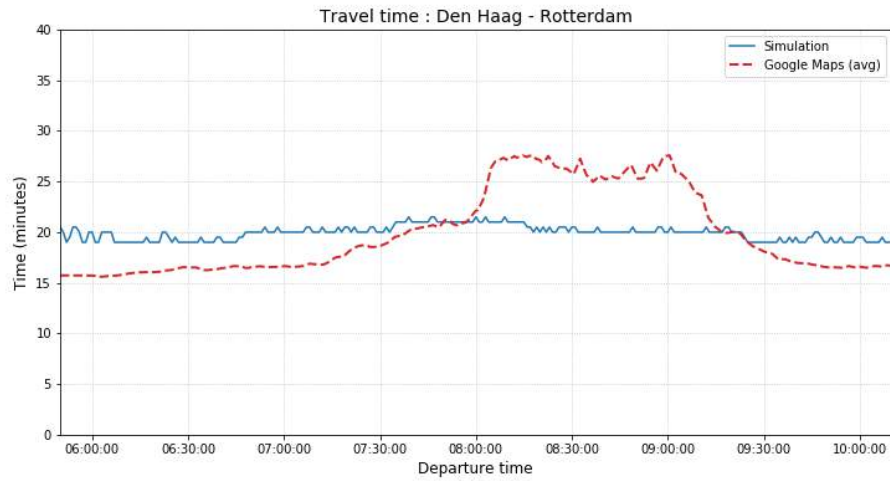


(a) Morning peak

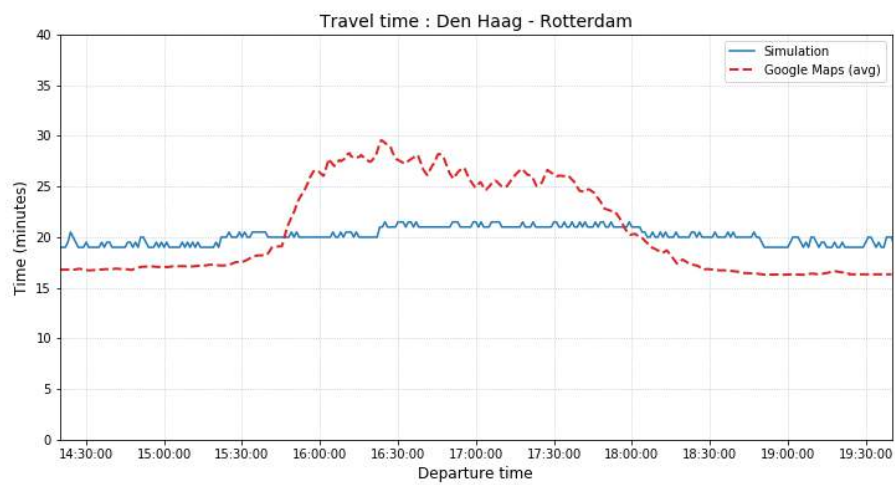


(b) Afternoon peak

Figure 5.5: The travel time plots for the route Dordrecht - Zaanstad

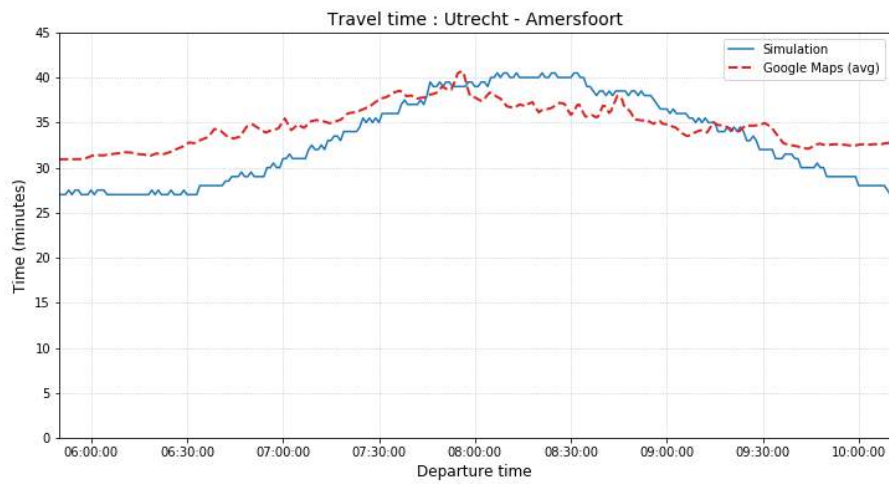


(a) Morning peak

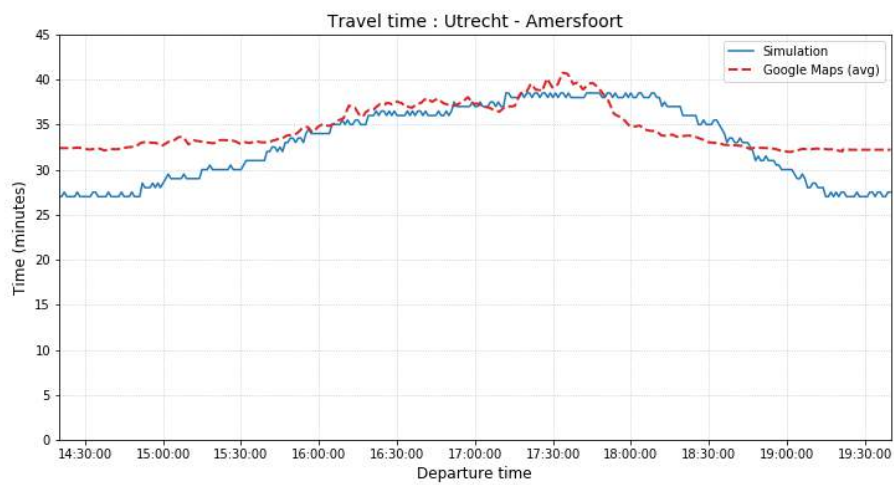


(b) Afternoon peak

Figure 5.6: The travel time plots for the route Den Haag - Rotterdam



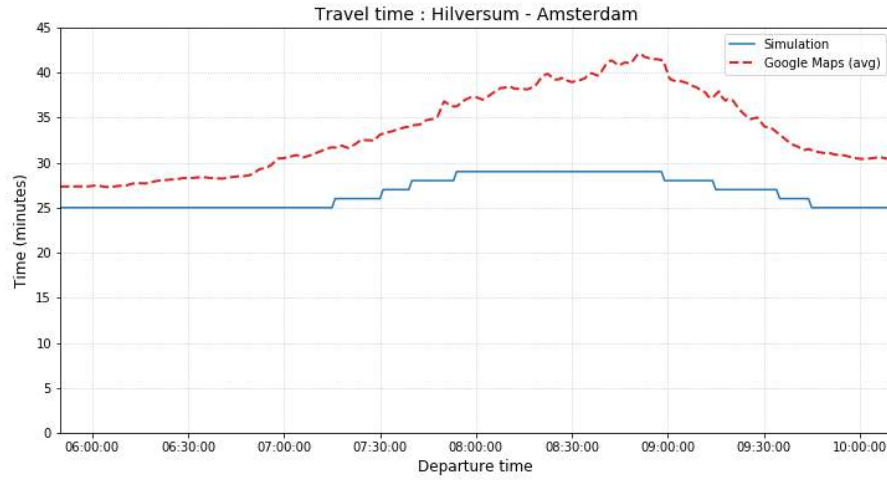
(a) Morning peak



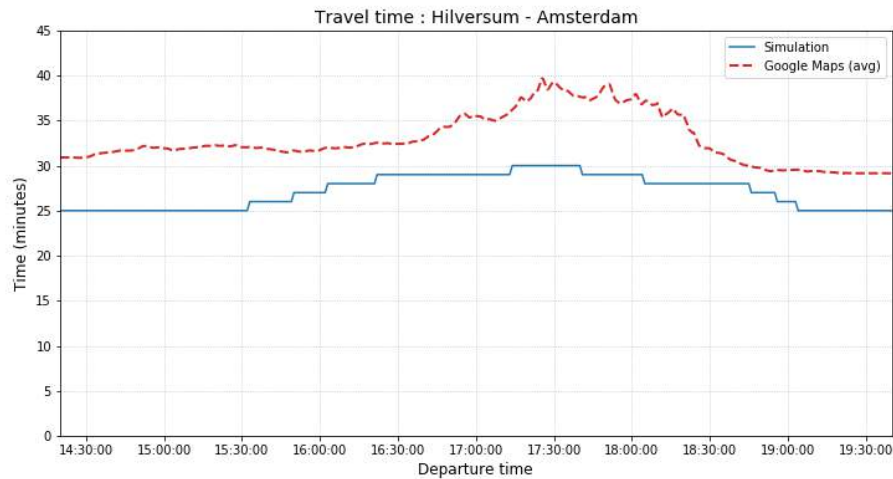
(b) Afternoon peak

Figure 5.7: The travel time plots for the route Utrecht - Amersfoort

delay with respect to the free-flow travel time is much larger in the simulation than in the observations.



(a) Morning peak



(b) Afternoon peak

Figure 5.8: The travel time plots for the route Hilversum - Amsterdam

For Hilversum - Amsterdam, the simulation model underestimates the free-flow travel times with a couple of minutes. During the peak, this difference increases to ten minutes. The delay in the observed situation is larger than the simulation indicates.

5.4. SUPPLY AND BOUNDARY CAPACITY RESTRICTION

The supply restriction did not limit the flow between two zones at any moment during the simulation. This means that congestion did not propagate from one cell to its neighbours. The traffic state of a zone is the average of all roads inside that zone, so although parts of the network may be congested, zones are never so congested that inflow of traffic is restricted. It can however occur that the inflow is blocked because congestion there is a chance that congestion occurs near the boundary between the zones.

Besides the supply restriction, the flow between two zones is also limited by the boundary capacity. The results of the simulation show that the boundary capacity restriction only limits the outflow for two zones:

Amsterdam and Purmerend. fig. 5.9 gives the outflow and the demand plots for these zones. From these results it can be concluded that the roads connecting these two zones are not capable of handling all traffic between these zones.

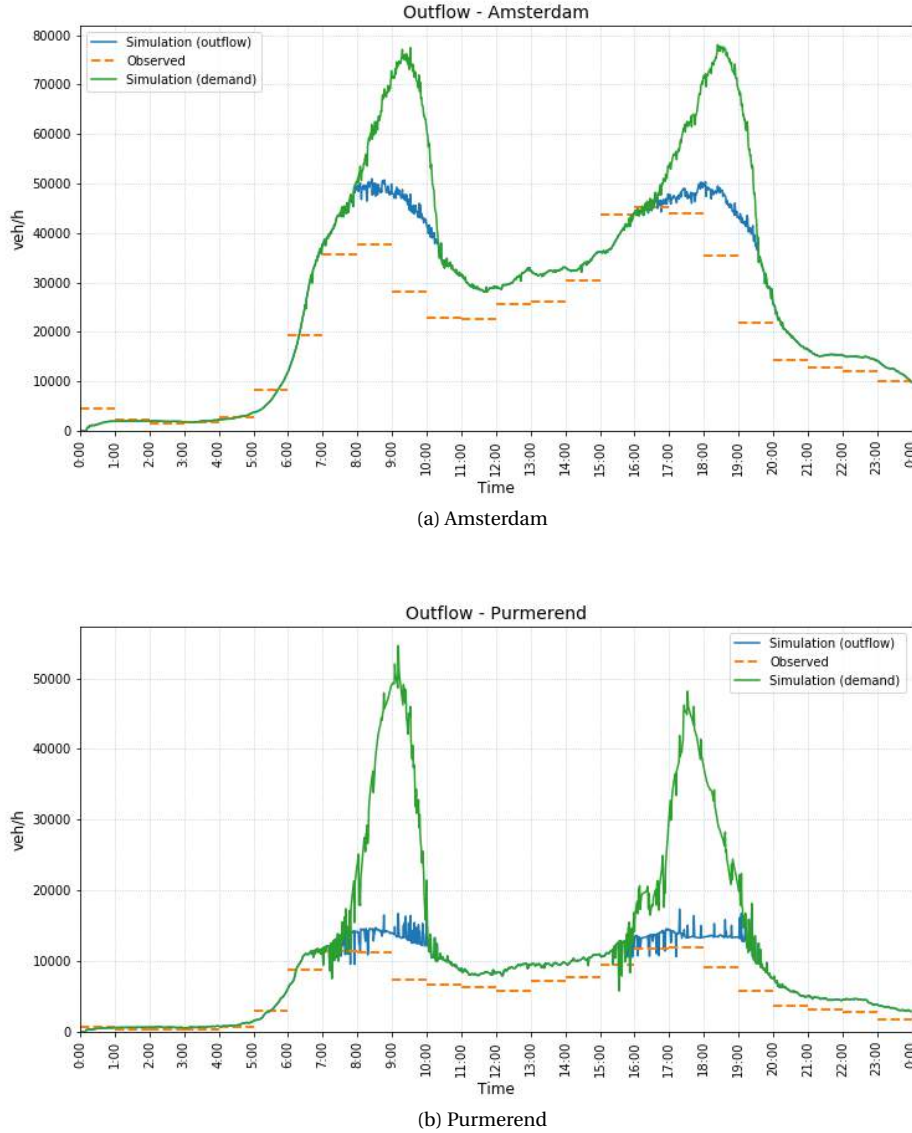


Figure 5.9: The resulting demand and outflow patterns for Amsterdam and Purmerend.

For the other zones, the boundary capacity restriction does not limit the outflow. It can therefore be concluded that the capacity of the roads is sufficient, but it has to be remarked that the boundary capacity between two zones is determined by simply taking the sum of the capacity of all roads connecting those zones, not taking into account that the distribution of traffic over those roads may not be homogeneous. Therefore, the boundary capacity will most likely be smaller in reality.

5.5. CONCLUSION

The results show that the accumulation and outflow patterns obtained by the simulation can be realistic, but is to be fine-tuned.

Deviations in these patterns can probably be solved by distributing traffic over multiple routes, rather than assigning traffic to the fastest route. This could lead to a better distribution of traffic, and improve-

ment in the outflow and accumulation patterns. A part of the zones will then receive less traffic, and others will receive more. The total distance travelled will most likely increase.

The travel times are not realistic, in most cases the travel time is overestimated for long-distance trips and underestimated for short-distance trips. A drawback of this model is that all traffic in a zone drives with the same speed, regardless of the traffic purpose, and the origin or destination. Through traffic on a freeway has then the same speed as the local traffic inside the zone. It would be more realistic to distinguish multiple types of traffic.

The OD matrix also has to be improved. To end up with a feasible solution, the total number of departures and arrivals had to be reduced for some zones before generating the OD-matrix. It could make a difference when the OD-matrix is constructed based on travel times instead of euclidean distances between the OD-pairs.

Summarizing, three options for improvement are suggested:

- Distribute traffic over multiple routes, instead of only assigning traffic to the fastest route.
- Make distinction between through traffic and local traffic, each with an own speed.
- Construct the OD-matrix based on travel times between zones instead of the euclidean distance.

These options will be assessed in chapter 6.

6

IMPROVEMENTS TO THE SIMULATION

Three possible improvements to the simulation model and simulation input have been suggested in section 5.5:

- Distribute traffic over multiple routes, instead of only assigning traffic to the fastest route.
- Make distinction between through traffic and local traffic, each with an own speed.
- Construct the OD-matrix based on travel times between zones instead of the euclidean distance.

These options are tested and analyzed in this chapter.

6.1. MULTIPLE ROUTES

In the original simulation, all traffic was assigned to the shortest path, as explained in section 3.5. Here, traffic is distributed over multiple routes instead of using an all-or-nothing assignment.

6.1.1. METHODOLOGY

For each OD-pair the three fastest routes under free-flow conditions are defined before running the simulation. These routes are determined using the internal distance matrices of the zones. This matrix is a specific matrix for each zone, containing the distances between each pair of its neighbours and the average distance from the zone itself to its neighbours.

During the simulation, the travel times of all three routes are updated according to the travel conditions. Instead of assigning all traffic to the fastest route, in this case the logit model is used to distribute the traffic over these three routes.

p_r gives the share of route r , out of the set of feasible routes R :

$$p_r = \frac{e^{-\alpha \cdot t_r}}{\sum_{\tilde{r} \in R} e^{-\alpha \cdot t_{\tilde{r}}}}$$

R consists of maximum three different routes. These routes are established before the simulation.

α is the parameter of the logit distribution. The larger this parameter, the higher the sensitivity for larger travel times. The shares of two routes with 1, 2 or 5 minutes difference are given in table 6.1 for six logit parameters. For large values of the parameter, the distribution converges to an all-or-nothing assignment.

6.1.2. RESULTS

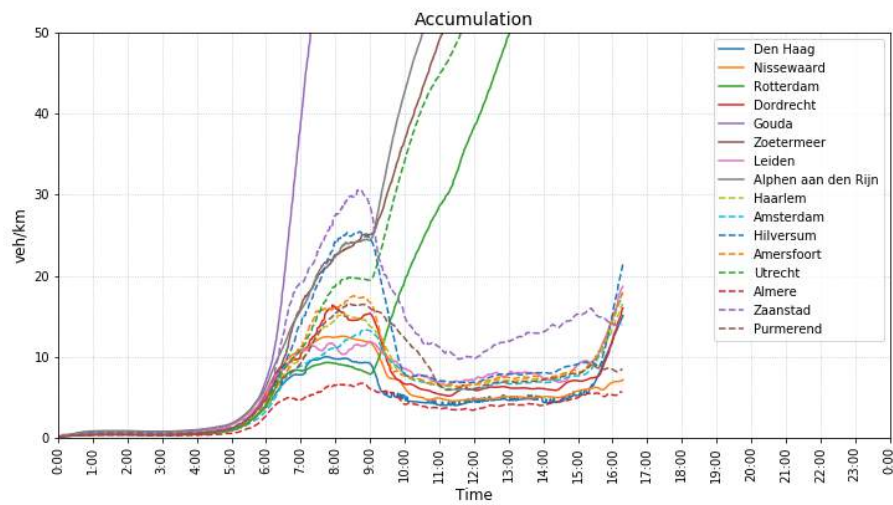
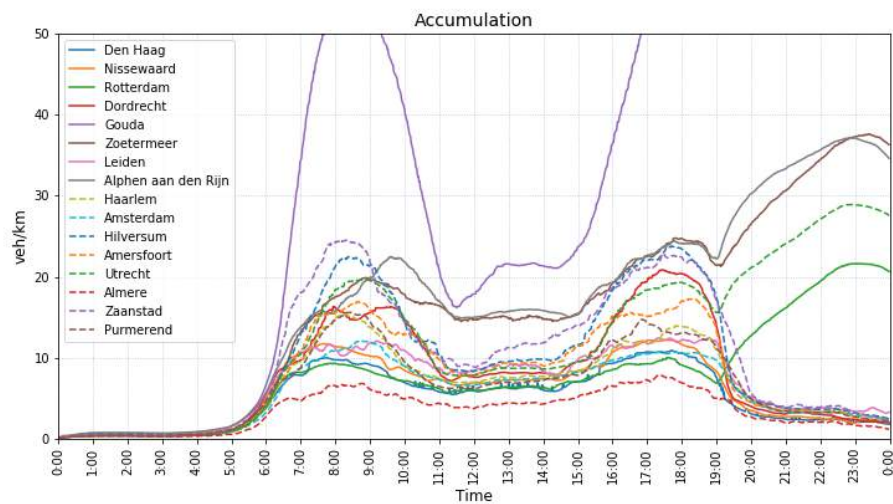
fig. 6.1 and fig. 6.2 show the accumulation patterns for the simulation with a logit model with parameters 2.0min^{-1} and 3.0min^{-1} respectively.

From the plots it can be concluded that the changed distribution of the traffic over a network leads to a gridlock in some of the zones. For the simulation with the parameter equal to 2.0min^{-1} , this already occurs in the morning peak, while for the parameter 3.0min^{-1} it happens during the afternoon peak.

From the results, four possible reasons can be identified:

Table 6.1: Share of two routes with 1 minute difference in travel time

Logit parameter	1 Minute		2 Minutes		5 Minutes	
	Route 1	Route 2	Route 1	Route 2	Route 1	Route 2
0.1min^{-1}	52.5%	47.4%	55.0%	45.0%	62.2%	37.8%
0.2min^{-1}	55.0%	45.0%	59.9%	40.1%	73.1%	26.9%
0.5min^{-1}	62.2%	37.8%	73.1%	26.9%	92.4%	7.6%
1.0min^{-1}	73.1%	26.9%	88.1%	12.1%	99.3%	0.7%
2.0min^{-1}	88.1%	12.1%	99.3%	0.7%		
5.0min^{-1}	99.3%	0.7%				

Figure 6.1: Accumulation plots for the simulation with logit parameter 2.0min^{-1} Figure 6.2: Accumulation plots for the simulation with logit parameter 3.0min^{-1}

- **More kilometers travelled:** When a logit model is used to distribute the traffic over multiple feasible routes, instead of using an all-or-nothing assignment, traffic is diverted to longer routes, which means that the total distance travelled by the system is larger. This might cause to congestion. The total number of vehicles that is generated in the simulation is the same.
- **Discrepancy between feasible routes in the simulation and in real traffic:** For the simulation, the shortest paths are determined based on the internal distance matrices. The internal distance matrices only take into account one previous and one next zone, instead of the full paths. The sum of the internal distances on the path can lead to an unfeasible route or a too optimistic estimate for the path length.
- **Distribution of traffic happens inside the zones rather than on zone level:** When all traffic uses the same path on zone level, it does not necessarily mean that all traffic uses the same roads. An example is traffic between Leiden and Rotterdam via Den Haag. In the zone of Den Haag, traffic can still choose between the A4 and A13, so there are two feasible paths through the same zones.
- **Snowball-effect:** As soon as one zone gets congested, other zones will follow. An example mentioned earlier in this report is Gouda, for which the accumulation is highly overestimated by the simulation. If Gouda receives some more traffic, because the traffic is distributed over the network in a different way, it could lead to a gridlock in the simulation. In real traffic this will not happen, because the accumulation is in fact much smaller than suggested by the simulation.

It has to be remarked that a parameter value of 2.0min^{-1} or 3.0min^{-1} is already quite large, so only small parts of the traffic are sent via a different route than in the case with an all-or-nothing assignment. If the duration of two routes differs by more than 2 minutes, the distribution already close to an all-or-nothing assignment (see table 6.1).

When the logit parameter is further increased, it does not lead to a gridlock, because less traffic is diverted. The accumulations for the logit parameters of 4.0min^{-1} and 5.0min^{-1} are plotted in fig. 6.3 and fig. 6.3.

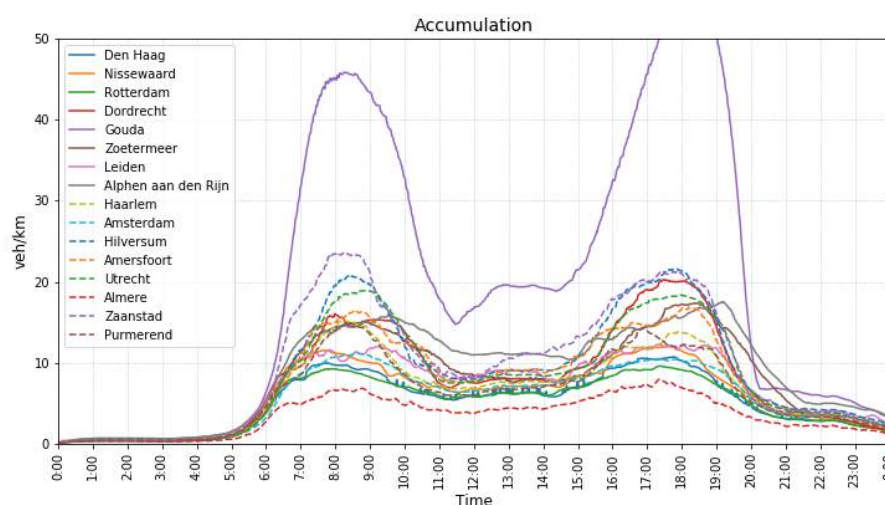


Figure 6.3: Accumulation plots for the simulation with logit parameter 4.0min^{-1}

A comparison of the plots for the four different logit parameters shows that the five zones that are causing the gridlock for the logit parameter of 2.0min^{-1} and 3.0min^{-1} are affected the most by the logit model. One of the zones still has accumulations of more than 40 veh/km with a parameter equal to 5.0min^{-1} . For the eleven other zones, the difference is relatively small compared to the base case.

6.1.3. CONCLUSION

The effect of distributing traffic over multiple routes has been tested using a logit model. The parameter of this model and the difference in travel time between the paths determines the share of each route. The

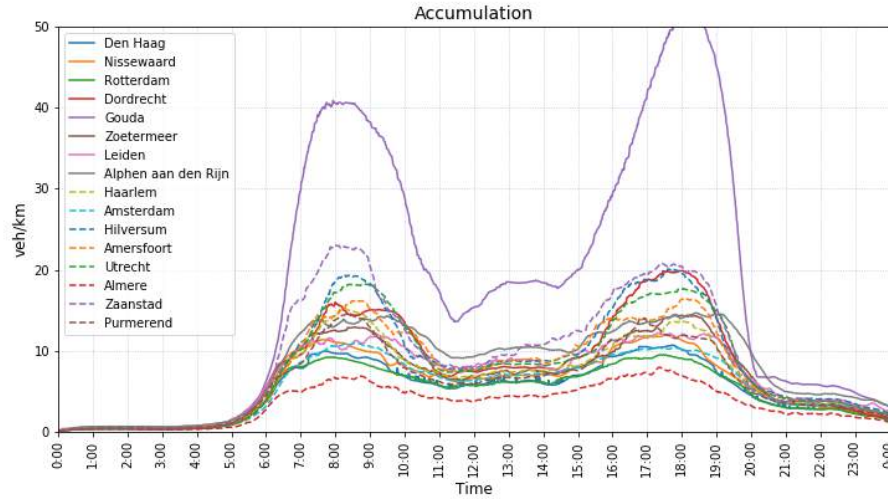


Figure 6.4: Accumulation plots for the simulation with logit parameter 5.0min^{-1}

model has therefore been tested using multiple different parameters. For so far, the distribution of traffic over multiple routes did not have the desired effect. For smaller parameters (3.0min^{-1} or smaller), it leads to a gridlocked network. The results show that diverting only a small amount of traffic to a different route, can lead to severe congestion. With larger parameters (4.0min^{-1} or higher), the effect on most of the zones is small. So, with the current simulation setup and inputs, distributing the traffic over the network using the logit model did not improve the simulation results with respect to the base case. The all-or-nothing assignment gave the best results for so far. This does not mean that the all-or-nothing assignment resembles the way decisions are made in real traffic the best, but it can also be related to the simulation inputs like the internal distance matrix.

6.2. SEPARATION LOCAL AND THROUGH TRAFFIC

From the first simulation results, it was concluded that the simulation model overestimates the travel times, particularly on the longer distances. With free-flow speeds around 60 km/h , the travel times for through traffic become longer than in real traffic, while the travel times for local traffic are shorter. Therefore, it is proposed to make distinction between trips based on the origins and destination. In this section the approach will be explained first, then this approach is tested and lastly the results will be presented and it is discussed whether the approach is an improvement to the model or not.

6.2.1. METHODOLOGY

As described in section 3.1.1, trips are generated in small sets, representing n vehicles, that all have the same destination, same path and the same departure time. Each set of vehicles has a parameter x , which gives the distance to be travelled before the vehicle can leave the current zone. The value of this parameter is set at the moment a vehicle is generated, or when it enters a new zone. During each simulation step, the distance travelled during that step is subtracted from this parameter, which is the duration of one simulation time step (τ) multiplied by the average speed in the current zone at that moment.

In the original simulation, the average speed was the same for all vehicle sets in one zone. In the case that is tested in this section, multiple speeds are used for different types of traffic. The approach that is proposed in this section makes distinction between two main types:

- **Through traffic:** Vehicles crossing a zone with both an external origin and destination.
- **Local traffic:** Vehicles with both an internal origin and destination.

For both types a separate NFD is defined, which gives the relation between the accumulation and the average speed. The accumulation is the total accumulation of the zone, consisting of both the local and the

through traffic.

Apart from through traffic and local traffic, a third type is introduced:

- **Mixed traffic:** Vehicles with either an internal origin and external destination or an external origin and internal destination.

This means that a vehicle is considered as mixed traffic at the first and last zone of its trip, and as through traffic at the zones in between. If a path however consists of one single zone, it is local traffic.

The three traffic types are visualized in fig. 6.5 for a fictional zone map, consisting of hexagons.

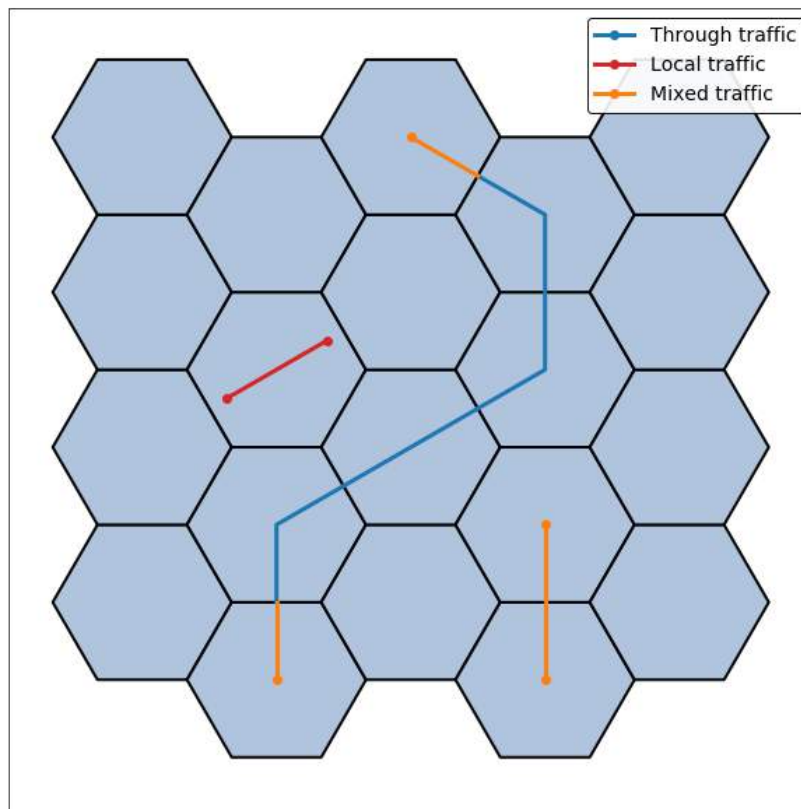


Figure 6.5: Three examples of a path

For mixed traffic no separate NFD is created, but it is assumed that the speed of mixed traffic is the average of the local and through traffic speed. The reason behind this is the idea that mixed traffic starts the trip at the local network, containing lower-hierarchy roads, but it reaches the higher-hierarchy roads already before it leaves the first zone. Imagine a trip starting in the center of The Hague and ending in the center of Amsterdam. This vehicle will use the local network of The Hague to get to the freeway A4. As soon as this vehicle leaves The Hague, it has already travelled some kilometers on the A4. The same counts for the end of the trip in Amsterdam: the vehicle will stay on the freeway network for some kilometers, before it enters the local network.

The rest of the simulation steps are the same as in the original model, described in section 3.1.1. The vehicles can leave the zone as soon as $x = 0$, which is the moment when sum of the travelled distances during each time steps equals the predetermined trip length. The demand of a zone is the number of vehicles inside the zone that has completed this predetermined trip length. Then, it is determined whether the capacities of the boundaries between the zones are sufficient for the demands, and whether the supply of the downstream zones is sufficient. If not, the values for the demand are reduced such that the total demand does not exceed the boundary capacity, conform the method described in section 2.4.2. Lastly, the sets of vehicles are moved

between the zones and the state of each zone is updated according to the sum of the inbound and outbound flows for the zones. The new system state is used in the next time step.

In the remainder of this section, it is explained how the two NFDs for the local and through traffic are created, and how these diagrams are used in the simulation to calculate the state of the network.

NFD CONSTRUCTION

First an assumption has to be made about the way the through and local traffic use the network. Through traffic will mainly use the motorways, while local traffic mainly uses the lower-hierarchy roads. For each road type a distribution between local and through traffic is assumed:

Motorway:	80%	through traffic	-	20%	local traffic
Trunk road:	60%	through traffic	-	40%	local traffic
Primary road:	40%	through traffic	-	60%	local traffic
Secondary road:	20%	through traffic	-	80%	local traffic
Tertiary road:	0%	through traffic	-	100%	local traffic

The accumulation in each zone is split into through traffic and local traffic:

$$K_{\text{through}} = \frac{\sum_{r \in R} k_r \cdot L_r \cdot \phi_r}{\sum_{r \in R} L_r}$$

$$K_{\text{local}} = \frac{\sum_{r \in R} k_r \cdot L_r \cdot (1 - \phi_r)}{\sum_{r \in R} L_r}$$

The total accumulation in the zone is the sum of those accumulations:

$$K_{\text{total}} = K_{\text{through}} + K_{\text{local}}$$

Then, the average speeds are calculated for each accumulation K_{total} :

$$U_{\text{through}}(K_{\text{total}}) = \frac{\sum_{r \in R} P_r(k_r) \cdot L_r \cdot \phi_r}{\sum_{r \in R} k_r \cdot L_r \cdot \phi_r}$$

$$U_{\text{local}}(K_{\text{total}}) = \frac{\sum_{r \in R} P_r(k_r) \cdot L_r \cdot (1 - \phi_r)}{\sum_{r \in R} k_r \cdot L_r \cdot (1 - \phi_r)}$$

In these equations the set of road types is denoted as R and the share of through traffic on road type r is denoted as ϕ_r . This means that the share of local traffic equals $1 - \phi_r$.

NFD FITTING PROCEDURE

The next step is to fit a line through the NFDs. To realize this, the NFDs in terms of speed are multiplied by the total accumulation K_{total} , giving the NFDs in terms of production:

$$P_{\text{through}}(K_{\text{total}}) = U_{\text{through}}(K_{\text{total}}) \cdot K_{\text{total}}$$

$$P_{\text{local}}(K_{\text{total}}) = U_{\text{local}}(K_{\text{total}}) \cdot K_{\text{total}}$$

Normally, the meaning of the production is the internal flow in the zone, but in this case the production is only used to fit a line through the NFD, because the relation between the accumulation and production is multilinear, while the relation between the accumulation and speed consists of multiple inversely proportional lines.

These two production NFDs have no specific meaning, because the two separate NFDs are used to describe the traffic dynamics of one network, with the joint accumulation K_{total} as input variable.

SIMULATION

During the simulation, the speeds are obtained by dividing the production again by the total accumulation:

$$U_{\text{through}}(K_{\text{total}}) = \frac{P_{\text{through}}(K_{\text{total}})}{K_{\text{total}}}$$

$$U_{\text{local}}(K_{\text{total}}) = \frac{P_{\text{local}}(K_{\text{total}})}{K_{\text{total}}}$$

The original NFD shape as determined in section 3.1.1 is still used for the supply restriction in the simulation.

Hysteresis is taken into account by setting a temporary capacity restriction as soon as the third critical density is exceeded, in line with the methodology explained in section 3.3.4. This restriction is only set for through traffic.

6.2.2. APPLICATION

The method described in section 6.2.1 is used to generate the NFDs for the local and through traffic for the sixteen zones. The NFD parameters are given in table 6.2 and table 6.3.

Table 6.2: NFD Parameters for through traffic

Zone	Free-flow speed (km/h)	Critical speed 2 (km/h)	Critical density 1 (veh/km)	Critical density 2 (veh/km)	Critical density 3 (veh/km)	Jam density (veh/km)
Den Haag	92	63.57	6	14	24	85
Nissewaard	89	53.75	8	16	21	80
Rotterdam	92	77.27	8	11	19	90
Dordrecht	100	80.91	6	11	18	80
Gouda	100	72.31	8	13	20	80
Zoetermeer	91	40.91	9	22	22	80
Leiden	94	76.15	7	13	13	80
Alphen a/d Rijn	81	58.82	9	17	21	85
Haarlem	97	64.29	8	14	24	90
Amsterdam	92	66.67	9	15	20	90
Hilversum	102	70.71	8	14	18	85
Amersfoort	97	76.67	7	12	17	85
Utrecht	98	76.15	7	13	17	90
Almere	100	46.00	8	20	20	95
Zaanstad	93	78.89	6	9	23	95
Purmerend	95	97.14	7	7	20	90

Table 6.3: NFD Parameters for local traffic

Zone	Free-flow speed (km/h)	Critical speed 2 (km/h)	Critical density 1 (veh/km)	Critical density 2 (veh/km)	Critical density 3 (veh/km)	Jam density (veh/km)
Den Haag	43	28.14	21	43	58	150
Nissewaard	40	29.74	18	39	52	135
Rotterdam	44	28.13	17	48	65	165
Dordrecht	40	28.30	17	47	57	155
Gouda	42	26.88	18	48	58	150
Zoetermeer	42	26.82	20	44	55	140
Leiden	40	29.05	18	42	55	145
Alphen a/d Rijn	42	28.05	19	41	53	140
Haarlem	45	28.64	20	44	61	155
Amsterdam	45	27.66	19	47	64	155
Hilversum	43	29.56	18	45	60	155
Amersfoort	43	28.64	19	44	60	150
Utrecht	45	27.50	19	48	65	160
Almere	46	30.00	17	45	58	155
Zaanstad	46	26.96	20	46	61	155
Purmerend	39	26.67	18	45	51	135

For Utrecht the NFDs are shown in fig. 6.6, as an example of the relation between the joint accumulation and the speeds for local and through traffic. The joint accumulation is the average density in the zone. The diagrams for the rest of the zones are plotted in appendix B.2.

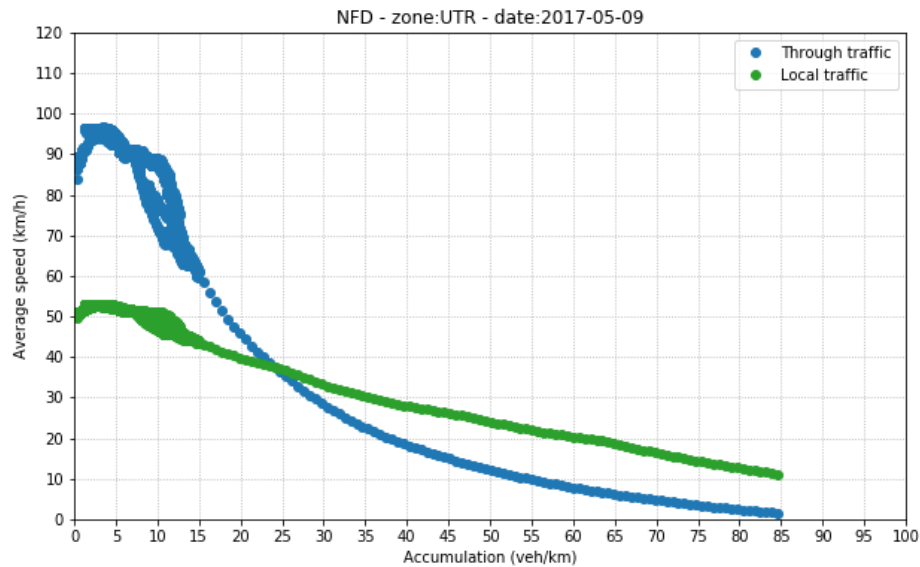


Figure 6.6: Example of an Accumulation-Speed NFD for Utrecht

In line with the expectations, the through speed initially is larger than the local speed. However, with increasing density, the speed of the through traffic drops below the local speed. For Utrecht this happens at an accumulation of around 24 veh/km.

As explained in section 4.2.3, differences in occupancy between the five road types that are distinguished in this research are taken into account by means of a fixed ratio between these densities. The density on motorways is 1.38 times larger than on trunk roads and primary roads 1.90 times larger than on secondary roads, and 2.63 times larger than on tertiary roads.

The relation between the joint accumulation and the accumulation on the different road types is shown in fig. 6.7 for Utrecht. The vertical axis gives the joint accumulation, and the horizontal axis gives the accumulation on the five road types.

When the joint accumulation is 24 veh/km, the accumulation on motorways is already 35 veh/km. At the same time, the accumulation on primary roads and trunk roads is 24 veh/km, around 17 veh/km on secondary roads, and 13 veh/km on tertiary roads. So, the higher-hierarchy roads can already be in congested state, while the lower-hierarchy roads are still in free flow state.

This explains the fact that the speed of through traffic can drop below the local speed, if the accumulation is large enough. Through traffic makes mainly use of the higher-order roads, and for those roads the density is larger than the average density for the zone, while the local traffic makes use of the lower-order roads, which have a smaller density than the average value for the zone.

With respect to the base case simulation (chapter 5) some changes are made to the internal distance matrices. For four zones the internal distances are reduced:

- **Dordrecht:** -10%
- **Gouda:** -20%
- **Zaanstad:** -20%
- **Purmerend:** -10%

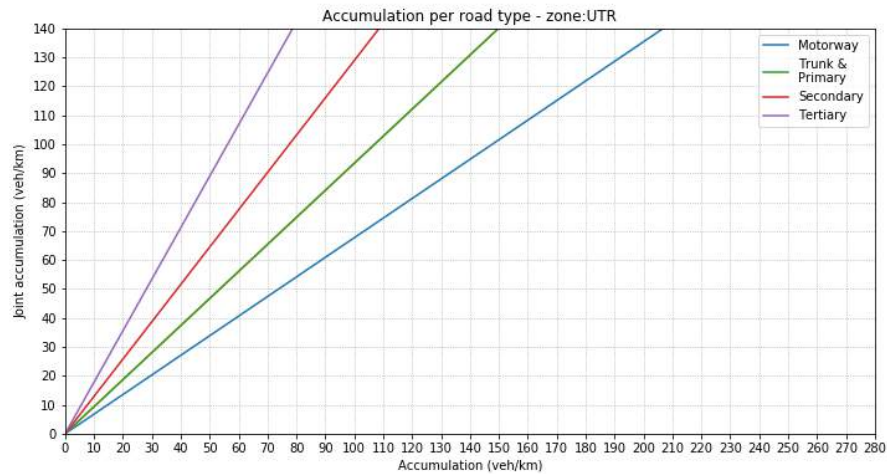


Figure 6.7: Joint accumulation (vertical axis) versus the accumulations for the different road types (horizontal axis)

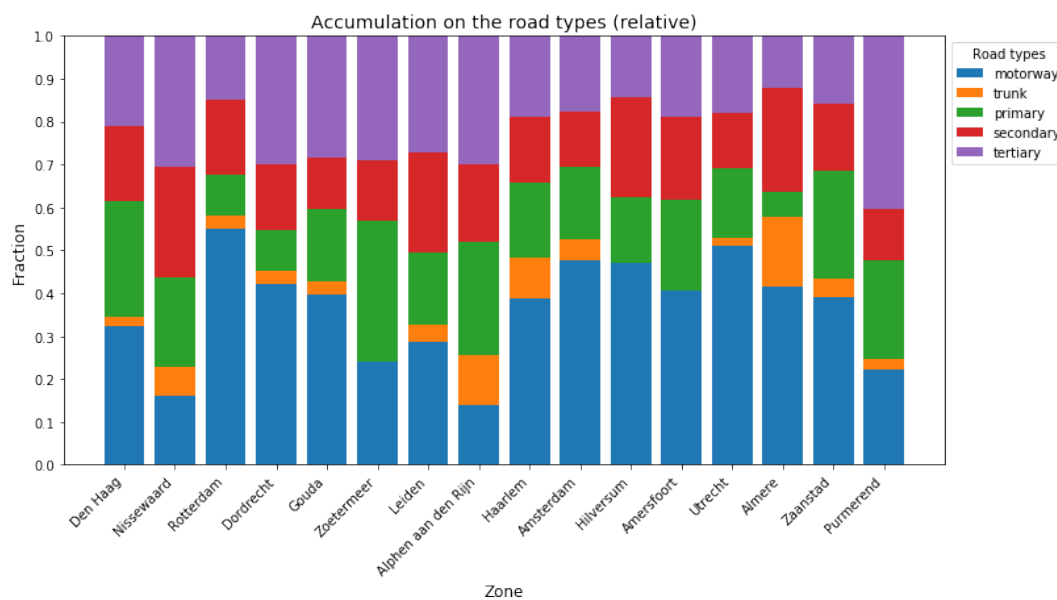


Figure 6.8: Road use percentages per zone

These changes will have a positive effect on the accumulation patterns for these zones.

6.2.3. RESULTS

In this section the effects of separating local and through traffic on the accumulation patterns and the travel times are discussed. Because the OD-matrix remains the same, the outflow patterns will not change significantly. Therefore the outflow patterns are not analyzed again. For the outflow plots is referred to appendix D.

ANALYSIS OF THE ACCUMULATION PATTERNS

In this section, the accumulation patterns are discussed. The results for all zones are summarized in table 6.4. This table gives the ratio between the simulated accumulation patterns and the expected patterns for the base case (A) and the simulation with separation between local and through traffic (B). The closer the values to one, the better the pattern matches the expected results. The columns give the mean values over the day, the minimum and maximum values of the ratio, and the mean values for the morning peak (6:00-10:00)

and the afternoon peak (15:00-19:00).

In section 3.6 it was mentioned that an average deviation of maximum 20% from the expected pattern is desired over 24h and over the morning and afternoon peak periods. The values that fall within this range are shown bold and in green and the values outside this range are underlined and shown in red.

Table 6.4: Ratio between the simulated and expected accumulation for the simulation without separation between local and through traffic (A) and the simulation with separation between local and through traffic (B)

Zone	Mean		Minimum		Maximum		AM peak		PM peak	
	A	B	A	B	A	B	A	B	A	B
Den Haag	0.97	1.01	0.70	0.70	1.51	1.36	0.85	0.90	0.87	0.90
Nissewaard	<u>1.53</u>	1.12	0.70	0.58	2.73	1.97	<u>1.29</u>	0.94	<u>1.52</u>	1.08
Rotterdam	0.98	1.03	0.68	0.70	1.42	1.35	0.92	1.01	0.91	1.00
Dordrecht	<u>1.39</u>	1.20	0.84	0.80	2.80	1.69	<u>1.35</u>	1.08	<u>1.63</u>	1.17
Gouda	<u>2.37</u>	<u>1.74</u>	1.20	1.11	3.65	2.50	<u>2.12</u>	<u>1.45</u>	<u>2.83</u>	<u>1.96</u>
Zoetermeer	<u>1.31</u>	1.16	0.82	0.68	2.31	1.97	1.10	0.97	1.16	1.02
Leiden	0.95	0.99	0.37	0.37	1.67	1.69	<u>0.70</u>	<u>0.76</u>	0.90	0.97
Alphen a/d Rijn	1.08	1.00	0.56	0.53	1.91	1.54	0.90	0.84	1.08	1.02
Haarlem	<u>1.31</u>	<u>1.35</u>	0.80	0.84	1.92	1.85	<u>1.28</u>	<u>1.35</u>	1.16	<u>1.21</u>
Amsterdam	0.94	0.98	0.58	0.60	1.42	1.30	0.91	0.99	<u>0.79</u>	0.85
Hilversum	<u>1.30</u>	<u>1.20</u>	0.77	0.82	1.98	1.74	1.10	1.01	<u>1.48</u>	<u>1.31</u>
Amersfoort	<u>1.22</u>	1.13	0.83	0.71	2.08	1.60	<u>1.23</u>	1.06	<u>1.28</u>	1.04
Utrecht	<u>1.20</u>	<u>1.25</u>	0.83	0.93	1.86	1.81	<u>1.20</u>	1.18	1.13	1.12
Almere	1.00	1.03	0.64	0.67	1.55	1.52	0.90	0.94	0.96	1.01
Zaanstad	<u>2.14</u>	<u>1.49</u>	1.21	0.93	4.27	2.29	<u>2.71</u>	<u>1.67</u>	<u>2.35</u>	<u>1.40</u>
Purmerend	<u>1.69</u>	1.10	0.88	0.54	2.79	1.48	<u>1.87</u>	1.09	<u>1.69</u>	0.98

From this table, it can be concluded that the accumulation patterns overall improved with respect to the base case, because most values in the table are closer to 1 than in the base case, and more values fall in the desired range of 20%. For all zones the plots of the accumulation patterns can be found in appendix E. In this section a few outstanding results are discussed:

- **Nissewaard:** For Dordrecht the accumulation pattern shows a clear improvement compared to the base case. The average deviation over 24 hours decreased from 53% to 12%.
- **Rotterdam:** The model is here able to reproduce the expected pattern accurately, and this is a clear improvement with respect to the base case. The average deviation is now less than 5% over 24 hours and during peak hours.
- **Dordrecht:** For Dordrecht the accumulation pattern also matches the expected pattern quite well, which is an improvement with respect to the base case. The average deviation stays below 20% for 24 hours and during the peak hours.
- **Amsterdam:** For Amsterdam, the accumulation pattern shows a small improvement with respect to the base case. During the morning peak the accumulation matches the expected pattern, but during the afternoon peak there's still a large deviation from the expected pattern. Overall, the results improved.

ANALYSIS OF THE TRAVEL TIMES

The most important reason for making distinction between local and through traffic is the travel times between the zones. Therefore, the travel times between the OD-pairs are compared to data requested from

Google Maps and HERE Maps. The full results can be found in appendix F. The difference in minutes between the free-flow travel times obtained from the simulation and the observed values from Google Maps and HERE Maps are calculated, and the results are summarized in table 6.5. A positive value means that the travel time from the simulation is larger than the observed travel time. The first two columns give the results for the original simulation, and the last two columns for the new case with separation of local and through traffic.

Table 6.5: Statistics of the deviation in free-flow travel times between the simulation and observed values for the base case and the case with separation of local and through traffic. The values are in **minutes**.

Statistic	Base case		New case	
	Google Maps	HERE Maps	Google Maps	HERE Maps
Mean	11.15	11.88	-1.52	-0.78
Median	9.92	10.40	-0.79	-0.67
Std. dev	11.28	11.25	5.32	5.18
Minimum	-11.18	-10.87	-19.02	-14.87
Maximum	41.82	43.07	11.37	12.58

This table shows that the travel times improved, with the average deviation close to zero and the standard deviation has halved with respect to the original simulation case.

The travel times during peak hours are compared to data from Google Maps. For this comparison three routes are selected for the long distance:

- Den Haag - Amsterdam: fig. 6.9
- Den Haag - Amersfoort: fig. 6.10
- Dordrecht - Zaanstad: fig. 6.11

The plots give the average Google Maps travel time based on multiple days of observations. The travel time is measured between the centers of the zones, and an upper and lower bound, which are the travel times between the boundaries of the zones. The full observed travel time patterns are shown in appendix F.2 and appendix F.3.

During the morning peak, the simulated travel time for Den Haag - Amsterdam follows the observed pattern with just a couple of minutes difference. During the afternoon peak, the difference is somewhat larger, but it stays below the upper bound. The peak occurs at the same time moment.

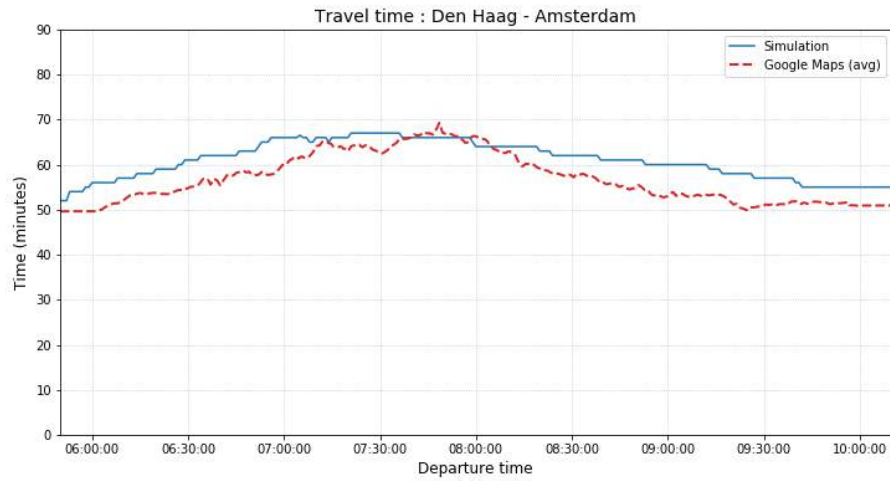
For Den Haag - Amersfoort, during morning the simulation model shows a peak in travel time around 6:45, while the observed travel time has a maximum at 8:30.

For most of the time the simulation model stays between the boundaries, but the travel time is still overestimated. The reason for this is most likely related to the fact that the accumulation for Gouda is still exceeded by the model, and since Gouda is on the path between Den Haag and Amersfoort, traffic on this route is delayed. Near the end of the peak, the estimated travel time matches the observed pattern.

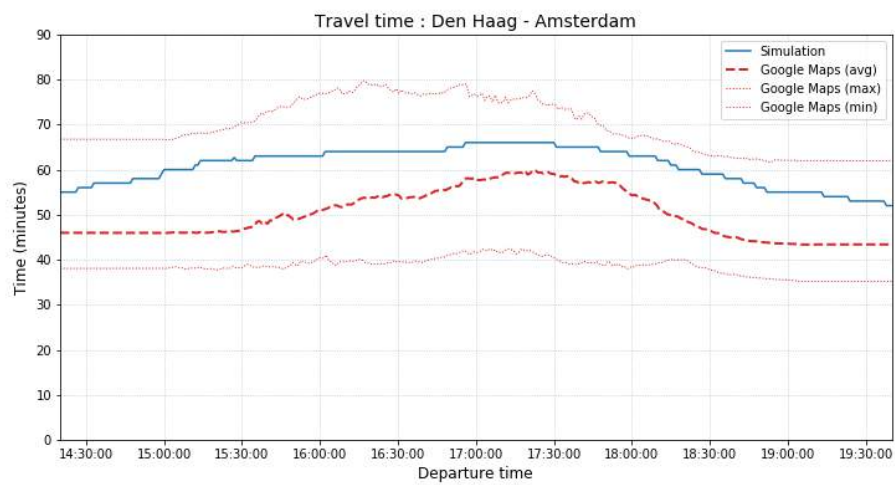
During afternoon peak, the simulated pattern is similar to the observed pattern, and the travel time stays between the boundaries, but there still is a large difference between the travel time from center to center. Only near the end of the afternoon peak, the estimated travel time matches the observed pattern, like in the morning.

The travel time patterns between Dordrecht and Zaanstad also show that during morning the model predicts the peak too early. Around 6:50 there is a drop in travel time, because from that moment another route has become faster. From that moment the travel time decreases and from around 8:00 it follows the observed pattern. The afternoon peak also has a drop in the travel time, around 16:15.

A closer look at the route set shows that traffic between Dordrecht is initially sent via Gouda, Alphen aan den Rijn and Haarlem, which is an unrealistic route in reality. After the drop it is sent via Utrecht and

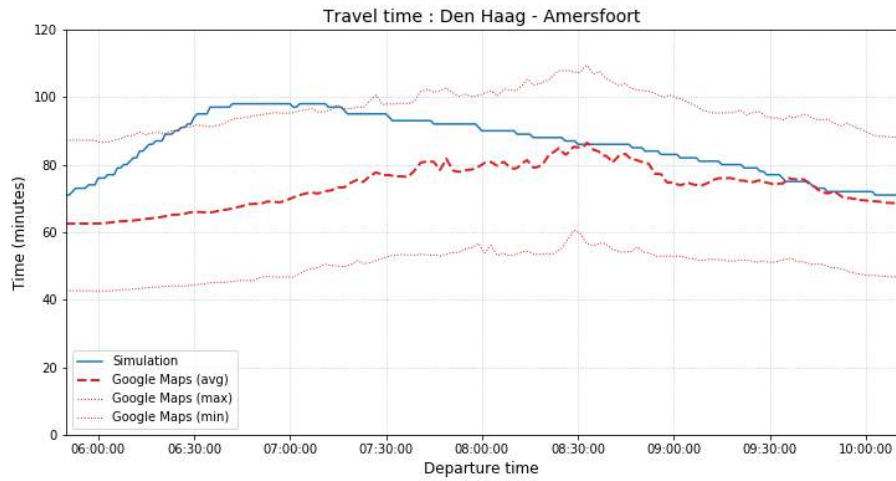


(a) Morning peak

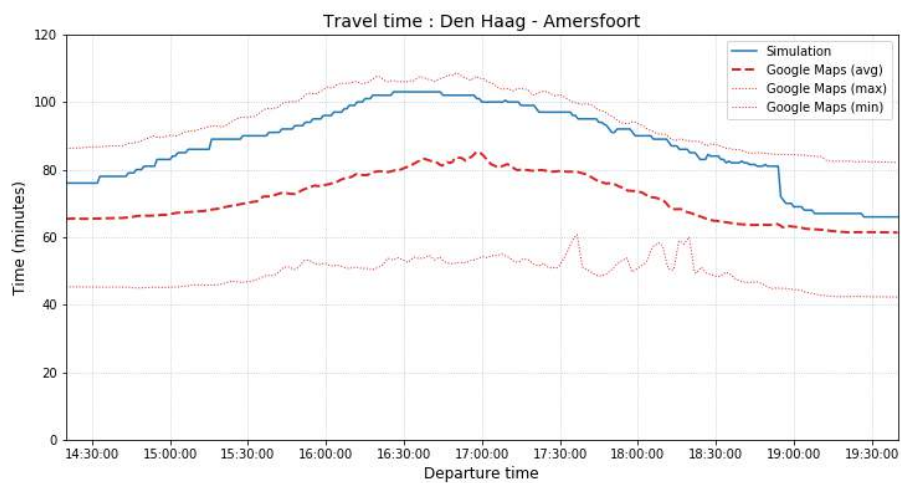


(b) Afternoon peak

Figure 6.9: The travel time plots for the route Den Haag - Amsterdam

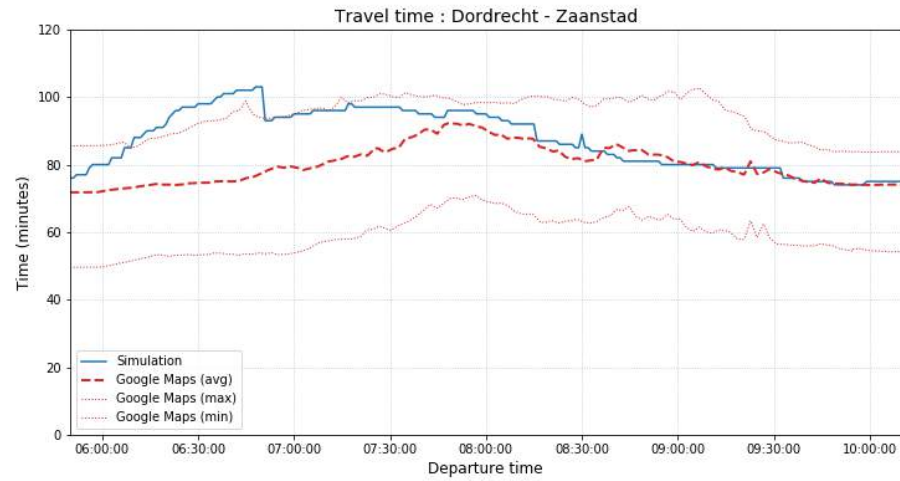


(a) Morning peak

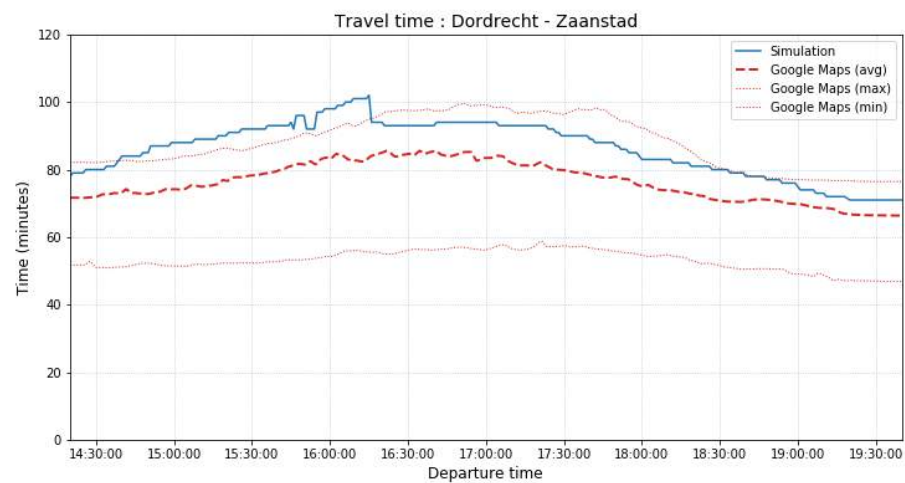


(b) Afternoon peak

Figure 6.10: The travel time plots for the route Den Haag - Amersfoort



(a) Morning peak



(b) Afternoon peak

Figure 6.11: The travel time plots for the route Dordrecht - Zaanstad

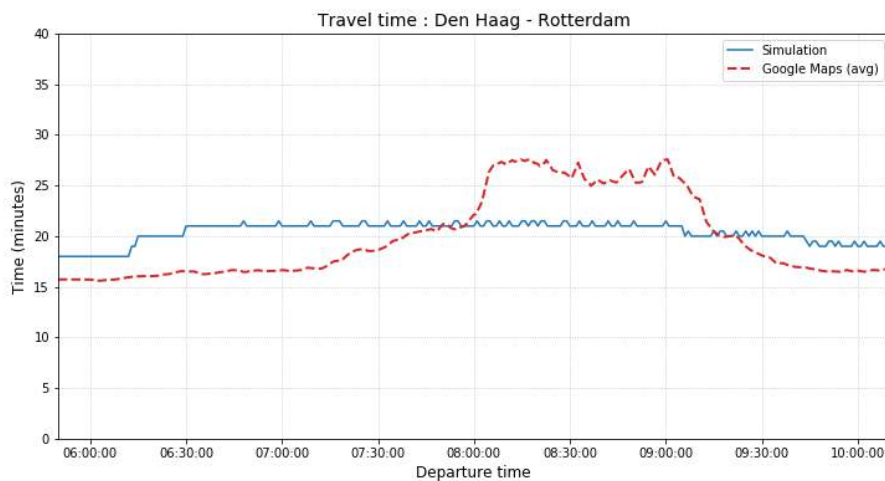
Amsterdam, which is a more realistic path.

This underlines that the used routing strategy, using the internal distance matrix and an all-or-nothing assignment is far from perfect.

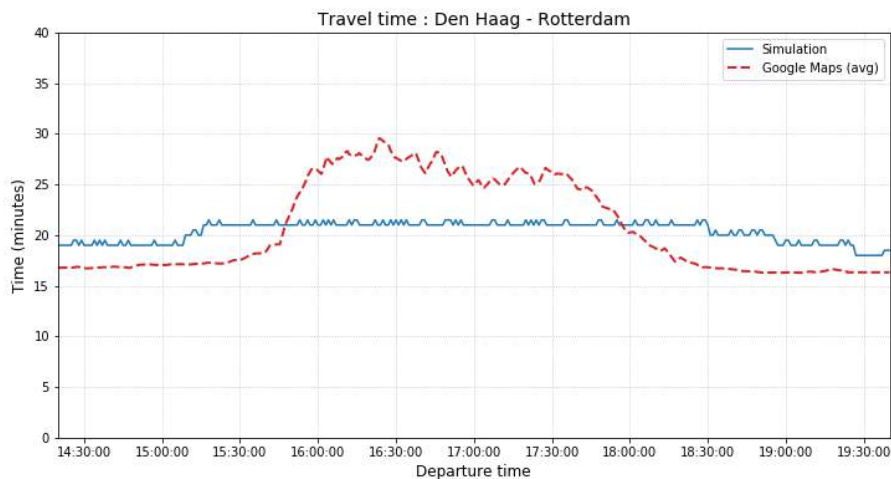
Additionally, three routes for the short distance are tested:

- Den Haag - Rotterdam: fig. 6.12
- Utrecht - Amersfoort: fig. 6.13
- Hilversum - Amsterdam: fig. 6.14

The plots give the average Google Maps travel time between the centers of the zones based on multiple days of observations. The full observed travel time patterns are shown in appendix E2 and appendix E3.



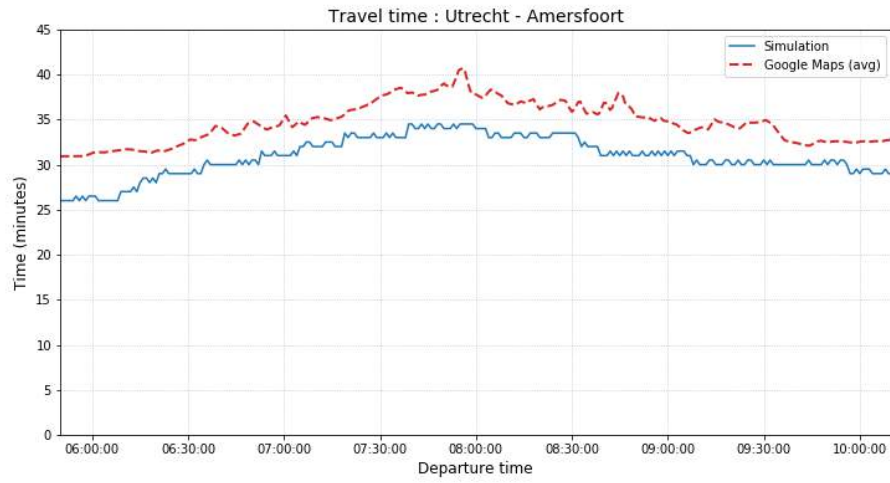
(a) Morning peak



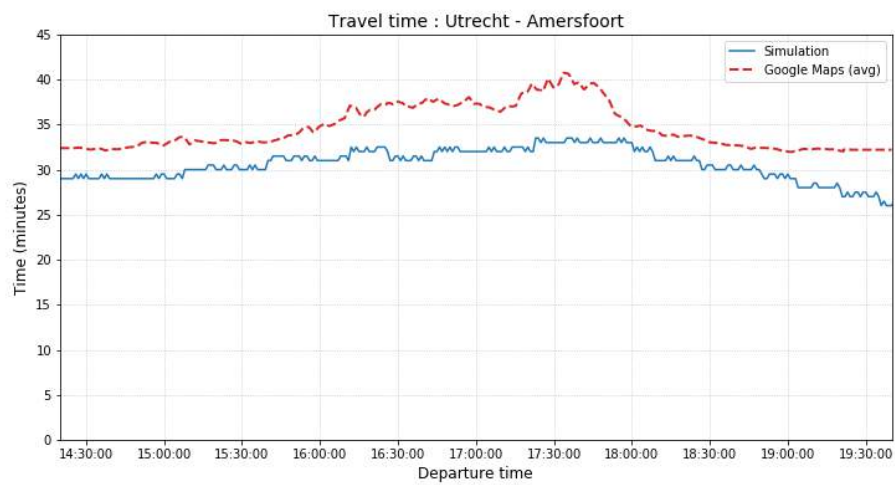
(b) Afternoon peak

Figure 6.12: The travel time plots for the route Den Haag - Rotterdam

The simulated travel time pattern for Utrecht - Amersfoort improved compared to the base case, especially during the morning peak the pattern is similar to the observed pattern, with a couple of minutes difference. For the other two short-distance routes the travel time patterns do not show an improvement with

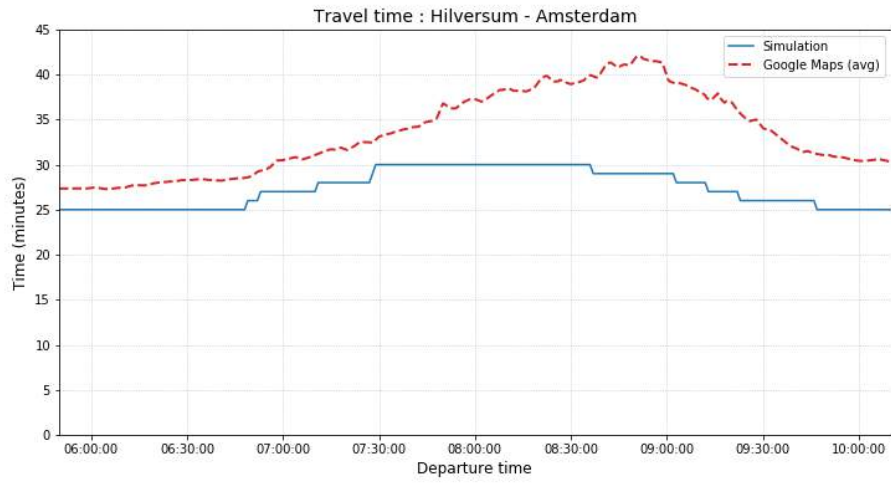


(a) Morning peak

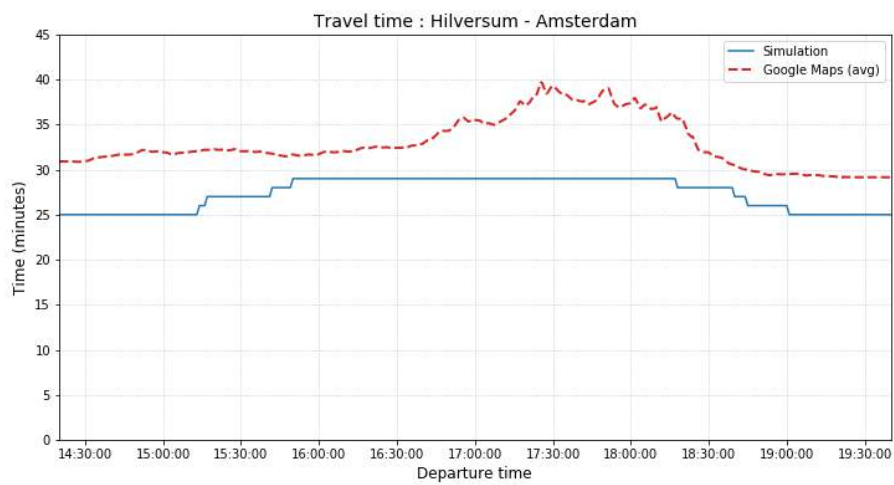


(b) Afternoon peak

Figure 6.13: The travel time plots for the route Utrecht - Amersfoort



(a) Morning peak



(b) Afternoon peak

Figure 6.14: The travel time plots for the route Hilversum - Amsterdam

respect to the base case. A plausible explanation for this conclusion is that the short-distance trips make more use of the local roads, for which the fundamental diagrams were constructed by assumptions rather than observations. Through traffic mainly makes use of freeways, for which the fundamental diagram has been estimated using data from loop-detectors. So it is likely that the NFD for the local traffic is less accurate than the NFD for through traffic, which influences the accuracy of the travel times for short-distance trips.

6.2.4. CONCLUSION

From the statistics for the accumulations and free-flow travel-times it can be concluded that the distinction between local and through traffic improved the simulation results.

The peak-hour patterns of the travel time also show that the travel time patterns for the long-distance trips during peak hours improved with respect to the base case, but for the short-distance trips no clear improvement is visible in the results. The model fails to reconstruct the patterns during for those short-distance trips.

6.3. OD-MATRIX BASED ON TRAVEL TIMES

Originally, the OD-matrix has been estimated using a doubly-constrained gravity model with the euclidean distance between the centers of each OD-pair as the generalized costs for travelling between that OD-pair. When the euclidean distance is used as an estimator for the generalized costs, some important factors are ignored.

The actual path is namely always larger than the euclidean distance, but the size of the detour is different for each OD-pair, because of the differences in the density (degree of meshing) of the road network. Besides that, the differences in speed between the zones are also neglected.

As an alternative, the travel time between the origin and destination can be preferred over the euclidean distance as an estimator for the generalized costs. In this section therefore, the OD-matrix is estimated using the travel time as generalized costs. This OD-matrix is then used in the simulation, and the results are compared to the results with the original OD-matrix. Both cases include the separation between local and through traffic, conform the approach explained in section 6.2.

6.3.1. METHODOLOGY

The OD-matrix is estimated using the first two steps of the four-step model, namely trip generation and trip distribution. In the trip generation step, the total number of departures and arrivals for each zone are estimated. This is done in the same way as in the original simulation (see section 3.4), using a formula based on the number of households and the number of jobs in the zone. The number of departures and arrivals for each zone are equal.

For the trip distribution step the doubly constrained gravity model is used, which distributes traffic based on the generalized costs of travelling between each OD-pair. The deterrence function is a function with the generalized costs of an OD-pair as input, and the attractiveness of this OD-pair as output. Initially, the euclidean distance between the centers of each pair of zones is used as generalized costs. In this case, the travel time of the shortest path is used instead.

In section 3.1, the internal distance matrix is introduced, which gives the length of the path inside a zone z_0 for each combination of a previous zone z_{-1} and next zone z_{+1} . The internal distance matrices are used to construct a shortest path between each OD-pair. The shortest paths have to be determined in terms of travel time, which means that the distances first have to be divided by the speed, resulting in the internal travel time matrices.

In line with section 6.2, three types of traffic are distinguished, each with its own speed. The speeds under free flow conditions are used to transform the internal distance matrices to internal travel time matrices. The travel time of the shortest path from a zone i to a zone j is then used as an input to the OD-estimation process. For the external areas, the travel time is defined as the travel time towards the neighbouring internal zone plus a predefined distance of 40 minutes.

The same shapes for the deterrence functions as mentioned in section 3.4.2 can be used again, but it can be necessary to adapt the parameters of the deterrence function, since the costs are now expressed in a different unit.

The resulting OD-matrix contains the total number of trips for each OD-pair over 24 hours. These values have to be transformed to an OD-pattern for the full day. In section 3.4, the normalized demand patterns are introduced. For each zone, a normalized demand pattern has been determined in section 4.3.4. These patterns, that were used in the original simulation, can also be used in this simulation case. The 24-hour demand pattern for an OD-pair (i, j) is then obtained by multiplying the normalized demand pattern for zone i by the total demand for this OD-pair.

6.3.2. APPLICATION

In the base case simulation, the lognormal function has been used as the deterrence function:

$$f(c_{ij}) = \alpha \cdot e^{-\beta \cdot \ln^2(c_{ij}+1)}$$

The same function is used again in this step, but with new parameters, because the unit of the costs c_{ij} has changed.

After some iterations, the β -parameter is set to a value of 0.62. While in the base case it was necessary to reduce the total departures and arrivals for some zones to obtain a suitable OD matrix (section 4.3.3), in

this case with the travel times as generalized costs it is not necessary to reduce the departures and arrivals. The OD matrix already meets the requirements that the outbound flow for each zone does not exceed the observed outflow.

The final OD-matrix is given in appendix C.2.

6.3.3. RESULTS

In this section the new simulation results are presented and analyzed on three aspects, namely the outflow and accumulation patterns for each zone and the trip duration for each OD-pair.

ANALYSIS OF THE OUTFLOW PATTERNS

The results for all zones are summarized in table 6.6. This table gives the ratio between the simulated outflow patterns and the observed patterns for the simulation case with the original OD matrix (B) and the new OD matrix (C). Both cases include the separation between local and through traffic. The closer the values to one, the better the pattern matches the expected results. The columns give the mean values over the day, the minimum and maximum values of the ratio, and the mean values for the morning peak (6:00-10:00) and the afternoon peak (15:00-19:00).

In section 3.6 it was mentioned that an average deviation of maximum 20% from the expected pattern is desired over 24h and over the morning and afternoon peak periods. The values that fall within this range are shown bold and in green and the values outside this range are underlined and shown in red.

Table 6.6: Ratio between the simulated and observed outflow for the simulation with the original OD matrix (B) and the simulation with the improved OD matrix (C)

Zone	Mean		Minimum		Maximum		AM peak		PM peak	
	B	C	B	C	B	C	B	C	B	C
Den Haag	1.10	1.16	0.85	0.89	1.46	1.58	1.11	1.14	0.98	1.02
Nissewaard	<u>1.27</u>	1.02	0.84	0.65	1.90	1.66	1.14	0.91	<u>1.55</u>	<u>1.24</u>
Rotterdam	1.14	1.04	0.73	0.67	1.51	1.38	<u>1.38</u>	<u>1.26</u>	1.17	1.07
Dordrecht	1.01	0.94	0.69	0.63	1.36	1.29	1.01	0.96	1.03	0.98
Gouda	<u>1.35</u>	<u>1.37</u>	0.95	0.99	1.96	2.00	1.14	1.17	1.08	1.09
Zoetermeer	<u>1.37</u>	<u>1.38</u>	1.06	1.03	2.61	2.66	<u>1.20</u>	<u>1.20</u>	1.20	1.18
Leiden	0.89	<u>0.77</u>	0.70	0.61	1.17	1.02	<u>0.76</u>	<u>0.66</u>	0.83	<u>0.72</u>
Alphen a/d Rijn	<u>1.26</u>	1.08	0.88	0.74	1.77	1.50	1.08	0.98	<u>1.22</u>	1.12
Haarlem	0.90	<u>0.69</u>	0.76	0.58	1.19	0.92	0.93	<u>0.72</u>	0.86	<u>0.69</u>
Amsterdam	1.14	1.03	0.84	0.77	1.58	1.44	<u>1.35</u>	<u>1.21</u>	1.04	0.94
Hilversum	<u>1.22</u>	1.00	0.86	0.71	1.83	1.50	1.16	0.95	1.16	0.95
Amersfoort	<u>1.25</u>	1.19	0.94	0.90	1.69	1.61	1.14	1.09	1.18	1.13
Utrecht	1.10	1.14	0.84	0.89	1.42	1.45	1.10	1.14	0.96	1.00
Almere	<u>1.26</u>	1.00	0.59	0.46	2.78	2.19	0.90	<u>0.71</u>	<u>1.26</u>	1.00
Zaanstad	1.12	0.87	0.87	0.68	1.56	1.22	1.03	<u>0.80</u>	1.06	0.83
Purmerend	<u>1.43</u>	<u>1.47</u>	1.13	1.19	2.07	2.12	<u>1.35</u>	<u>1.38</u>	<u>1.28</u>	<u>1.31</u>

Overall, the effect of the new OD matrix on the outflow patterns is small. For some zones the outflow pattern improves (for example Hilversum), leading to ratios closer to one, but for other zones the situation gets worse (especially for Leiden and Haarlem). But no general conclusion can be drawn from these results. Some examples are discussed in this section:

- **Nissewaard:** Nissewaard was one of the zones for which the outflow during the afternoon peak was

highly overestimated in the previous simulation cases. With the new OD-matrix, the average deviation during the afternoon peak dropped from 55% to 24%. Although this is a major improvement, the deviation is still larger than desired. As discussed in section 5.1, this is probably due to the dominant outbound flow during the morning peak and the dominant inbound flow during the afternoon peak.

- **Hilversum:** Although the pattern already matched the expected pattern quite well during the peak hours, the situation improved with the new OD matrix.
- **Leiden:** The outflow for Leiden is underestimated by the model with the new OD matrix. The most likely reason for this is that with the new OD-matrix there is apparently less traffic on the A4-corridor between Den Haag and Amsterdam.
- **Alphen aan den Rijn:** The outflow plots for Alphen aan den Rijn show improvements during the afternoon peak and between the peaks. In the original simulation cases, the outflow was overestimated in these periods.
- **Haarlem:** Similar to Leiden, the outflow for Haarlem is underestimated by the model with the new OD matrix, so apparently less traffic makes use of the A4-corridor between Den Haag and Amsterdam.

ANALYSIS OF THE ACCUMULATION PATTERNS

For all zones the accumulation patterns can be found in appendix E. The results are summarized in table 6.7. This table gives the ratio between the simulated accumulation patterns and the expected patterns for the simulation case with the original OD matrix (B) and the new OD matrix (C). Both cases include the separation between local and through traffic. The closer the values to one, the better the pattern matches the expected results. The columns give the mean values over the day, the minimum and maximum values of the ratio, and the mean values for the morning peak (6:00-10:00) and the afternoon peak (15:00-19:00).

In section 3.6 it was mentioned that an average deviation of maximum 20% from the expected pattern is desired over 24h and over the morning and afternoon peak periods. The values that fall within this range are shown bold and in green and the values outside this range are underlined and shown in red.

The results do not show a clear improvement in accumulation patterns. While for some zones the results do improve, for other zones the results are worse. The figures in appendix E confirm this.

ANALYSIS OF THE TRAVEL TIMES

The free flow travel times are not discussed again, because the results are exactly the same as for the previous case with separation of local and through traffic, because the same NFDs and internal distance matrices are used. For the results is therefore referred to section 6.2.3.

The travel times during peak hours are compared to data from Google Maps. For this comparison three routes are selected for the long distance:

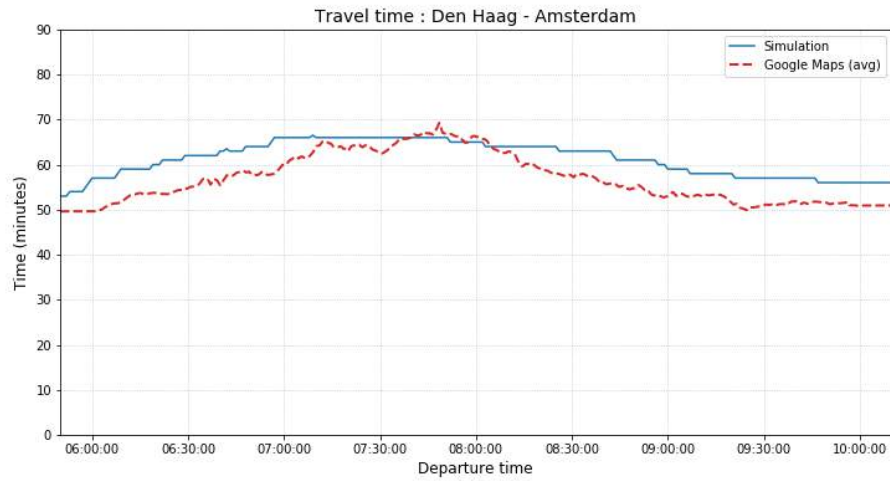
- Den Haag - Amsterdam: fig. 6.15
- Den Haag - Amersfoort: fig. 6.16
- Dordrecht - Zaanstad: fig. 6.17

The plots give the average Google Maps travel time based on multiple days of observations. The travel time is measured between the centers of the zones, and an upper and lower bound, which are the travel time between the boundaries of the zones. The full observed travel time patterns are shown in appendix E2 and appendix E3.

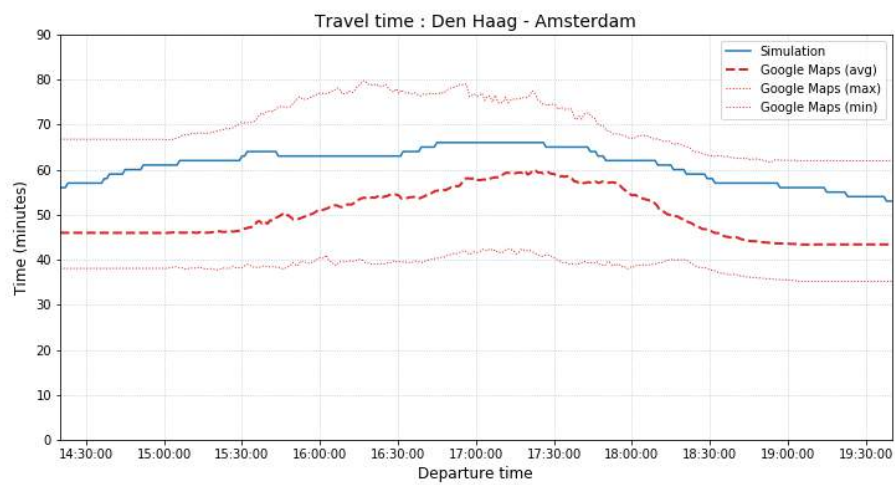
Overall, the patterns are similar to the results of the case with the original OD-matrix (see section 6.2.3). So no new conclusions have to be drawn from these results.

Besides that, three short-distance trips are analyzed:

- Den Haag - Rotterdam: fig. 6.18
- Utrecht - Amersfoort: fig. 6.19
- Hilversum - Amsterdam: fig. 6.20

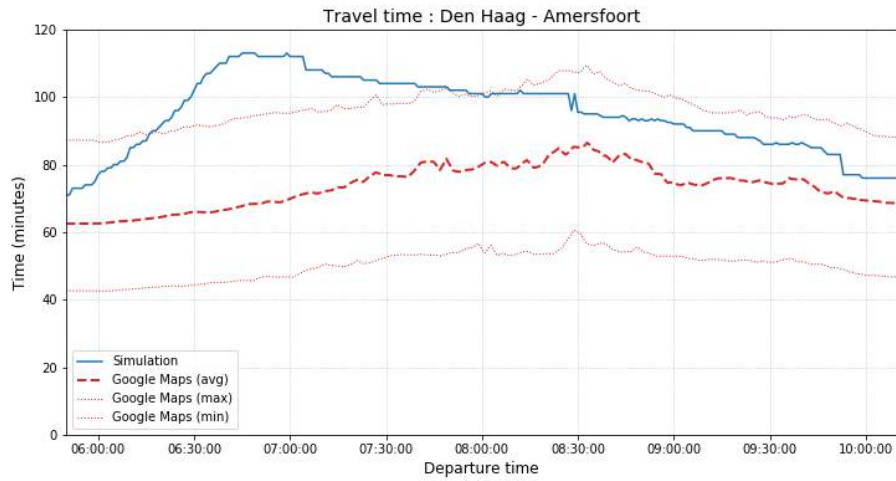


(a) Morning peak

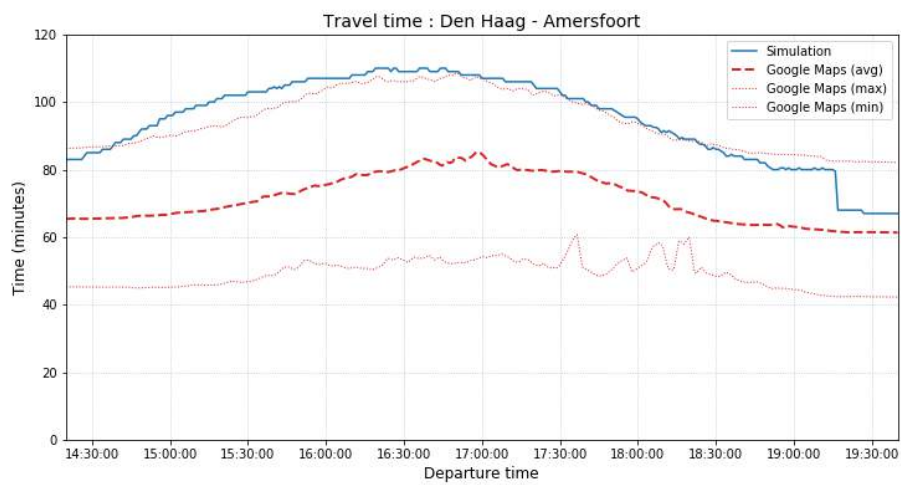


(b) Afternoon peak

Figure 6.15: The travel time plots for the route Den Haag - Amsterdam

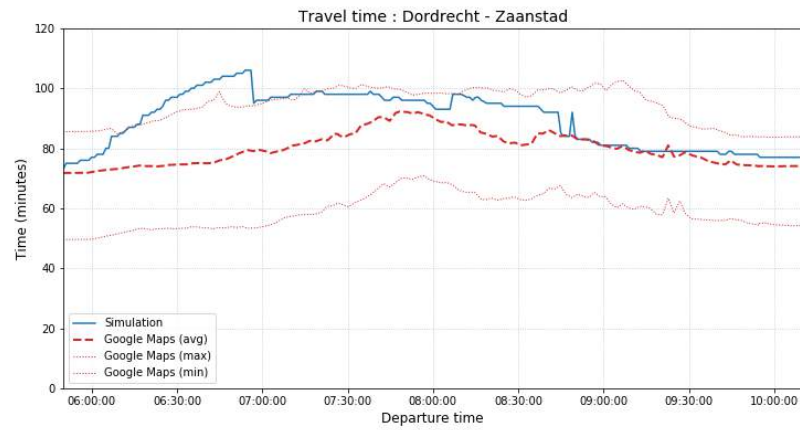


(a) Morning peak

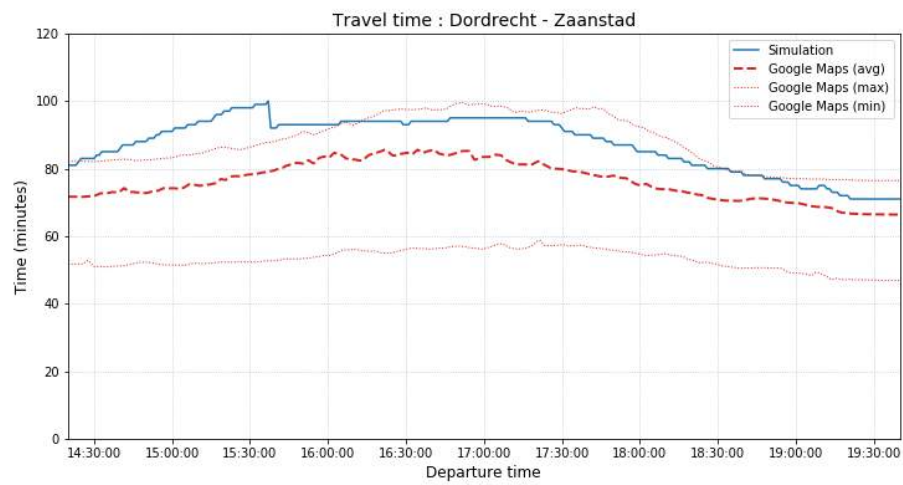


(b) Afternoon peak

Figure 6.16: The travel time plots for the route Den Haag - Amersfoort



(a) Morning peak



(b) Afternoon peak

Figure 6.17: The travel time plots for the route Dordrecht - Zaanstad

Table 6.7: Ratio between the simulated and expected accumulation for the simulation with the original OD matrix (B) and the simulation with the improved OD matrix (C)

Zone	Mean		Minimum		Maximum		AM peak		PM peak	
	B	C	B	C	B	C	B	C	B	C
Den Haag	1.01	<u>1.32</u>	0.70	0.94	1.36	1.74	0.90	1.18	0.90	1.19
Nissewaard	1.12	<u>1.63</u>	0.58	0.89	1.97	2.69	0.94	<u>1.50</u>	1.08	<u>1.72</u>
Rotterdam	1.03	<u>1.27</u>	0.70	0.86	1.35	1.65	1.01	<u>1.28</u>	1.00	<u>1.28</u>
Dordrecht	1.20	1.18	0.80	0.78	1.69	1.68	1.08	1.07	1.17	1.17
Gouda	<u>1.74</u>	<u>1.93</u>	1.11	1.13	2.50	3.05	<u>1.45</u>	<u>1.77</u>	<u>1.96</u>	<u>2.28</u>
Zoetermeer	1.16	<u>1.27</u>	0.68	0.80	1.97	2.10	0.97	1.09	1.02	1.17
Leiden	0.99	0.94	0.37	0.34	1.69	1.57	<u>0.76</u>	<u>0.71</u>	0.97	0.91
Alphen a/d Rijn	1.00	0.88	0.53	0.45	1.54	1.38	0.84	<u>0.76</u>	1.02	0.92
Haarlem	<u>1.35</u>	<u>1.20</u>	0.84	0.72	1.85	1.64	<u>1.35</u>	1.16	<u>1.21</u>	1.05
Amsterdam	0.98	1.18	0.60	0.73	1.30	1.51	0.99	<u>1.22</u>	0.85	1.04
Hilversum	<u>1.20</u>	1.03	0.82	0.67	1.74	1.50	1.01	0.82	<u>1.31</u>	1.04
Amersfoort	1.13	1.09	0.71	0.69	1.60	1.50	1.06	1.01	1.04	1.00
Utrecht	<u>1.25</u>	<u>1.25</u>	0.93	0.92	1.81	1.83	1.18	1.18	1.12	1.11
Almere	1.03	0.94	0.67	0.60	1.52	1.28	0.94	0.85	1.01	0.91
Zaanstad	<u>1.49</u>	<u>1.27</u>	0.93	0.80	2.29	1.71	<u>1.67</u>	<u>1.34</u>	<u>1.40</u>	1.10
Purmerend	1.10	1.12	0.54	0.58	1.48	1.60	1.09	1.16	0.98	1.00

The plots give the average Google Maps travel time between the centers of the zones based on multiple days of observations. The full observed travel time patterns are shown in appendix E2 and appendix E3.

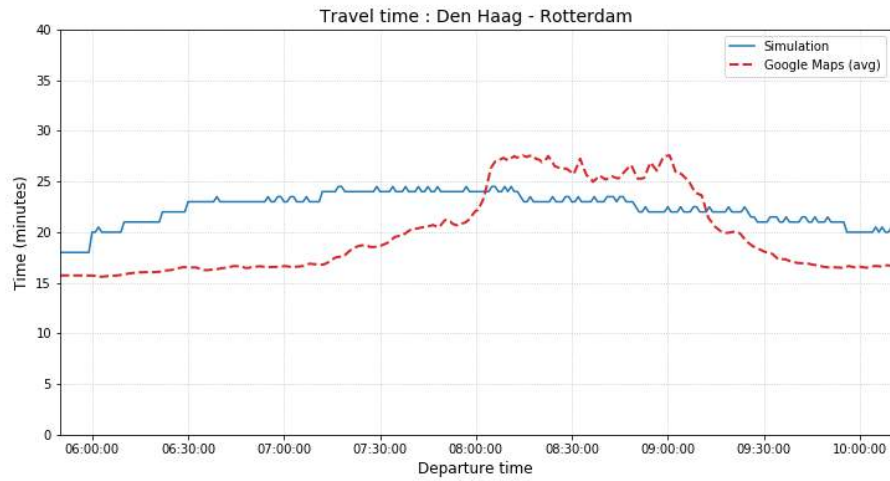
The plots for Den Haag - Rotterdam show a small improvement during the peak hour, but the simulated peak is still less intense, and the duration is much longer than what is observed.

The other two short-distance routes do not show an improvement with respect to the original case, because the results are similar.

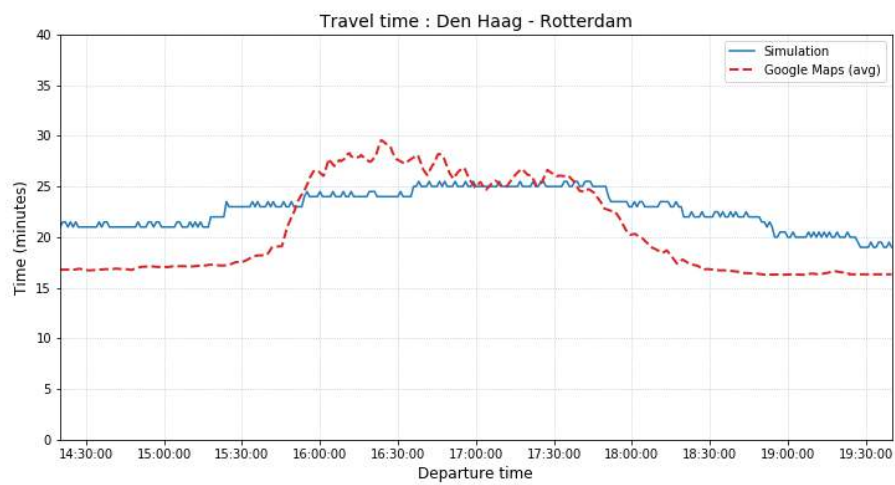
6.3.4. CONCLUSION

Considering the accumulations, outflows and travel times, the OD-matrix constructed using travel times instead of the euclidean distance does not lead to a significant improvement of the results, but the results are equivalent.

Although it did not improve the results, it is still preferred to estimate the OD-matrix using travel times rather than the euclidean distance, because for the original OD matrix a reduction of total departures and arrivals was necessary to end up with a suitable results (see section 3.4.2), while for the new OD-matrix this was not necessary.

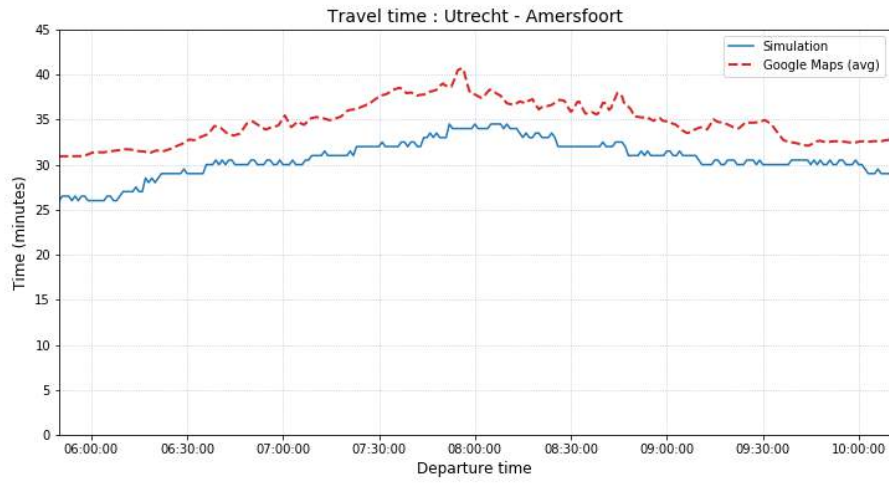


(a) Morning peak

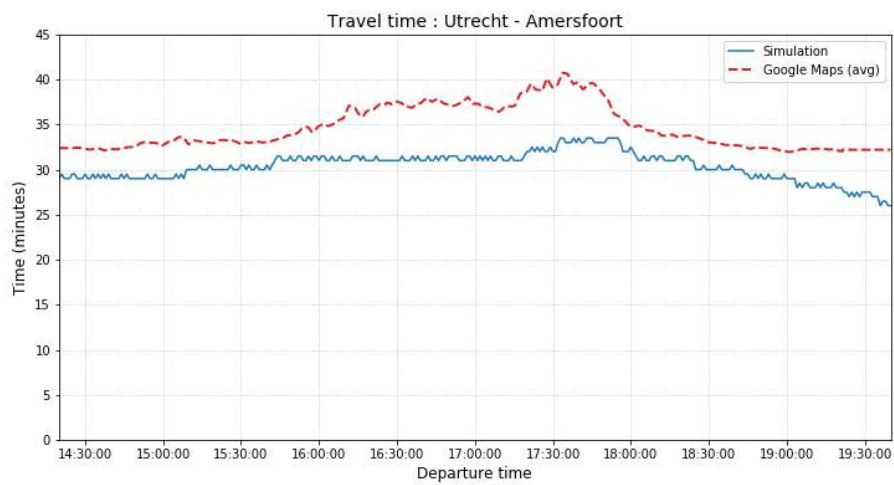


(b) Afternoon peak

Figure 6.18: The travel time plots for the route Den Haag - Rotterdam

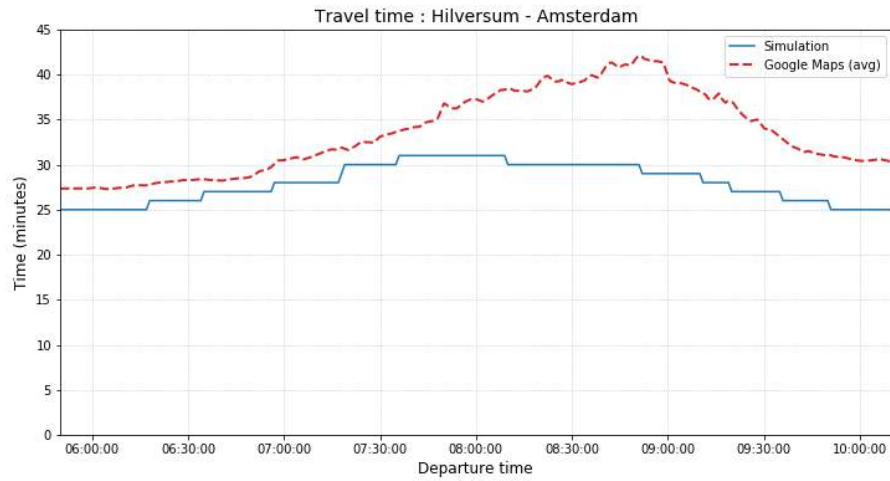


(a) Morning peak

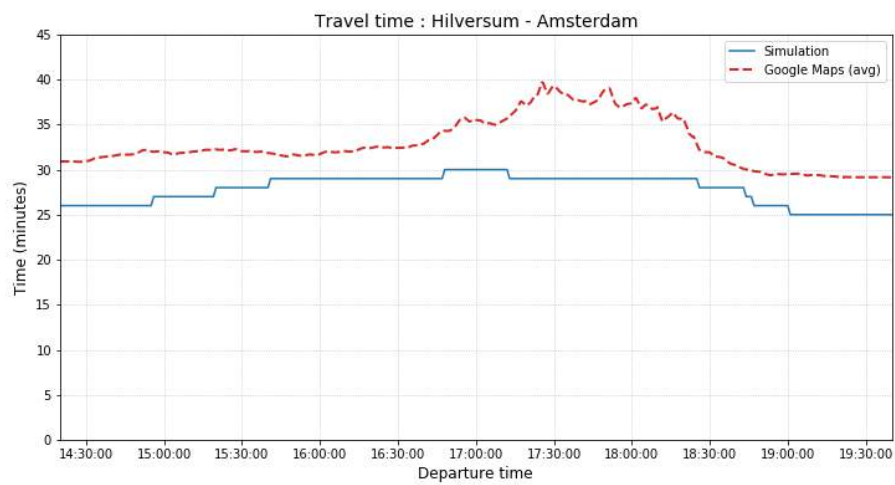


(b) Afternoon peak

Figure 6.19: The travel time plots for the route Utrecht - Amersfoort



(a) Morning peak



(b) Afternoon peak

Figure 6.20: The travel time plots for the route Hilversum - Amsterdam

7

DISCUSSION

In this chapter, the simulation methodology and results are discussed. With regard to the methodology, some shortcomings of the approach are discussed in section 7.1, and it is argued how the approach could have been improved. Then, the relevancy of the results is discussed in section 7.2, and some possible explanations are given for the observations.

7.1. DISCUSSION ON THE METHODOLOGY

The methodology is discussed on five points. On these five points, it is explained how the methodology could be improved, and what the influence can be on the results.

i **NFD construction:**

The NFDs have been constructed by combining data from loop detectors for the freeways with assumed fundamental diagrams for the other roads. The maximum speed was set equal to the speed limit on these roads, and the jam density was assumed to be equal to 125 veh/km, which is a commonly used value for the jam density. The capacity had to be estimated using a minimum time headway, an average vehicle length, and a capacity multiplier. The values for these parameters, mentioned in section 4.2.2, have been assumed without empirical evidence, and the results have not been verified afterwards.

For the Netherlands, municipalities often have data from the traffic signals. This could for example be combined with other data sources like floating car data or results from automatic number plate recognition systems (ANPR). This has not been used in this research, because of the limited availability of the data. The main obstacle is that each municipality stores its own data, instead of making it available via one collective repository.

ii **OD-matrix estimation:**

The OD-matrix is estimated using the first two steps of the four-step model. The number of trips that is generated and attracted by each zone is estimated using a simple formula based on the number of households and jobs in the zone. In the distribution of trips over the OD-pairs, local circumstances are not taken into account. It is for example ignored that the attractiveness of the jobs also depends on the type of job. Large companies or multinationals will attract employees from all over the area, and therefore generate long-distance traffic, while the harbour of Rotterdam for example attracts workers mostly living in the suburbs of Rotterdam. Another example is Hilversum Mediapark, which houses most of the national media companies, providing around 6000 jobs to employees from all over the country. This contrasts with the industrial areas at the west of the same city, which mainly provides jobs to the local residents. It can be beneficial to incorporate these local circumstances in the OD-matrix estimation process.

Besides that, for some of the zones, the observed outflows reveal that there is a dominant inbound flow during one peak and a dominant outbound flow during the other peak. This is for example the case for Nissewaard, which has a dominant outbound flow during the morning, because of the commuting traffic towards Rotterdam. For these zones, it can be beneficial to model the morning peak and afternoon peak separately, instead of using one demand pattern for 24 hours.

iii Demand patterns:

The trip distribution phase leads to an OD-matrix for 24 hours, which has to be translated to a full demand pattern over the day. The internal flow patterns are used to generate these demand patterns. For each zone, a normalized demand pattern is calculated by discretizing the internal flow patterns and dividing it by the total production for 24 hours. The demand pattern for an OD-pair (i, j) is then obtained by multiplying the normalized demand pattern for zone i by the total demand for this OD-pair.

In this approach one fact is ignored, which is that there is a delay between the production in a zone i and the attraction in zone j , equal to the travel time between these zones. This delay is different for each OD couple. This would imply that each origin i has a different demand pattern for each destination j , which all together will give the total demand pattern for zone i . In this research, no distinction is made between the destinations, the pattern only depends on the origin. section 4.3.4 however shows that it may even be possible to define one general demand pattern for all zone, because the demand patterns are similar for all zones. By using one single pattern for all OD-pairs, the input could be more simplified.

iv Supply restriction:

As found in section 5.4, the supply restriction did not limit the flow between two zones at any moment during the simulation. In that section it is mentioned that this means that normally congestion does not propagate from one cell to its neighbours, because zones are never so congested that inflow of traffic is restricted. On the other hand, it is also questionable whether this supply restriction is still valid in the model that is used in this research. The supply restriction was introduced in the Network Transmission Model, defined by Knoop and Hoogendoorn [15]. This model uses a demand and supply scheme inspired by the Cell Transmission Model, for which the demand and supply are given by the NFD. Because the demand is determined in a different way in this research, it can be questioned whether the approach for calculating the supply is still valid in that case.

v Boundary capacity restriction:

Besides the supply restriction, the flow between a pair of zones is also limited by the boundary capacity. In section 5.4 it is shown that the boundary capacity restriction only limits the outflow for two zones: Amsterdam and Purmerend, and for all other zones the outflow is not limited by this restriction. It is mentioned that the way in which the boundary capacity is calculated is probably too simplistic and not in line with the distribution of traffic, because the boundary capacity between two zones is determined by simply taking the sum of the capacity of all roads connecting those zones. The restriction is then only applied when the capacity of all these roads is fully used, but in reality, the flow can already be restricted when the demand is smaller than the total boundary capacity, because some roads are used more heavily than other roads. So, a part of the roads is already fully saturated, while other (often minor) roads are not saturated at all. It is therefore recommended to set the boundary capacity to a reduced level, to account for differences in saturation.

7.2. DISCUSSION ON THE RESULTS

In this master thesis, a dynamic zone model has been developed based on the Network Fundamental Diagrams and it has been applied in a case study for the Randstad. It is found that the model is overall able to reproduce the accumulation and outflow patterns of the zones, but large deviations can occur, as can be found in section 5.2 and section 5.1. These deviations, which were particularly found in the accumulation patterns, are not surprising, because of the high amount of assumptions that had to be made before the simulation, as explained in section 7.1. It is likely that errors in the input are the main reason for the deviations that were found. For the deviations in the accumulation patterns, at least four causes can be identified:

- The zone receives too much traffic in the simulation
- The number of internal trips is overestimated.
- The trip lengths inside the zone are overestimated.
- The shape of the NFD is deviating too much from reality.

When a zone receives too much traffic, the outflow patterns for this zones should also be overestimated by the model. If the outflow pattern for that zone is however close to what could be expected, it is not likely that those zones receive too much traffic. It could however be that the number of internal trips is overestimated, because internal trips are not included in the outflows, since internal trips never leave the zone. Large deviations in the outflow can be explained by errors in the estimated OD-matrix.

The shape of the NFD can also be a reason for these findings. If the traffic speeds are in fact larger than indicated by the NFD, traffic is kept inside the zone for a too long period, and therefore the accumulation remains larger than necessary.

In section 5.2.1 it has been explained that another possible cause for the deviations in the accumulation patterns is that the trip lengths from the internal distance matrix are not realistic, and vehicles are therefore kept in the zone for a too long (or too short, when the accumulation is underestimated) period, leading to an unrealistic accumulation pattern. This possible cause could however not completely explain why the accumulation patterns for some zones (like Gouda and Zaanstad) were highly overestimated.

Considering the travel times, it is found in section 5.3 that the model overestimates the travel times for long-distance trips. On average, the estimated travel time is 10 minutes longer than observed. It also has to be taken into consideration that the travel time depends on the exact location of the origin and destination inside the zones, because the zones are large areas, so the variation in travel time can be multiple minutes. In this travel time comparison, the geographical centers of the zones have been used as origins and destinations, with the presumption that this results in an average travel time for each OD-pair.

In a second simulation (section 6.2), some parts of the methodology have been changed to improve the results. Instead of using one NFD per zone for all traffic inside that zone, two NFDs are used for different types of traffic, so that a larger speed can be assigned to through traffic than to local traffic. This not only lead to an improvement in the travel times, also most of the outflow and accumulation patterns improved. The difference between the estimated and observed travel time is now much smaller in most cases. The average difference is close to zero minutes, and the standard deviation has halved. The problems with excessive accumulations for zones like Gouda and Zaanstad have not been solved however. So, the deviations are probably also related to the NFD, which has been estimated using various assumptions on the traffic behaviour.

The different simulation configurations have shown that changes in the methodology lead to an improvement for some zones or OD-pairs, but the same change can have a negative impact on the results of another zone or OD-pair. This is especially observed in section 6.3, where the OD-matrix has been estimated based on the travel times between the zones rather than euclidean distances. In that case, no general conclusion could be drawn on the results. It also has to be remarked that traffic models always contain many simplifications of the reality. The real traffic behaviour can not be fully captured in a model. Therefore, models will often produce large deviations between simulated results and observations. This is not only the case for dynamic zone models like the model considered in this simulation, but it is also the case for other types of models, like static or quasi-dynamic link models.

8

CONCLUSIONS AND RECOMMENDATIONS

In this final chapter, the conclusions with regard to the research questions are given. From these conclusions, some recommendations are derived for the practical applicability and the possibilities for future research.

The main research question was

- **How can traffic in the Randstad be modelled using a zone-based dynamic traffic model?:**

The model that is developed is inspired by the Network Transmission Model, but some modifications have been made to make the model suitable for large areas like the Randstad. The main difference is that a trip-based approach is used, instead of an accumulation-based approach. With the trip-based approach a specific path with its own trip length can be defined for each vehicle, which has a positive effect on the performance of the model.

Another adjustment is that for each zone two NFDs are defined, one for through traffic and one for local traffic. This addition is necessary for the model to be able to estimate the travel times accurately. For smaller-scale networks this is not necessary, because the speed differences are much smaller.

Six sub-questions have been formulated to answer this main research question. The answers to these questions are discussed in this section.

HOW SHOULD THE RANDSTAD BE DIVIDED INTO ZONES?

The Randstad has been divided into zones by selecting the largest municipalities in the study area (with more than 75,000 inhabitants), and assigning each location in the area to the closest centroid. When smaller zones are desired, the threshold for the number of inhabitants can be set to a smaller value.

In this case study for the Randstad it was necessary to merge some zones that are part of the same agglomeration, and in the more rural area in the center of the Randstad one extra zone has been created, see section 4.1. The reason for these changes is that this approach initially uses a fixed threshold for the number of inhabitants. Agglomerations often consist of multiple municipalities with a large population-density, but in rural areas, the population density is much smaller and the number of inhabitants is often lower than in urban areas. With this approach, more zones than desired are defined in urban areas and too few in rural areas. This is the main shortcoming of this approach.

The approach of defining zones based on the number of inhabitants of each municipality should therefore not be used as a general approach for constructing a zone map, but it could be used as a starting point in defining the zones. It is likely that some changes are needed after this first step. In urban areas, zones can be merged, and in rural areas more zones can be added.

The next step is to shift the boundaries of the zones towards the boundaries of the existing municipalities. Municipalities in the study area that are fully enclosed by the boundaries of one zone, or belong to the agglomeration of a certain city are assigned to the corresponding zone. Other municipalities are assigned to the zone that contains the largest share of their area. It is recommended to make use of the boundaries of existing municipalities, to avoid zone borders crossing urban areas.

Because traffic can enter and leave the study area at the boundaries, it is necessary to add a special zone type, which is the external zone. For each zone that is located at the boundary of the study area, one external

zone is added, adjacent to the original zone. Traffic is only able to move between the external zone and the corresponding zone inside the study area.

CAN A CLEAR NFD BE DEFINED FOR LARGE ZONES?

The concept of the NFD has been developed for urban areas with homogeneous traffic conditions. With larger regions, this homogeneity assumption is not valid, because of the scale of the network and the presence of multiple road types with different characteristics, like speed limit and capacity.

Besides this, a challenge in the NFD estimation process is to incorporate the lower-hierarchy roads, because for those roads no observed data is (publicly) available. Data is available for some provincial roads, but this is just on very specific locations, so it is not enough to construct a reliable NFD, so for these roads assumptions are needed. For freeways, the data is freely available, so it is no problem to construct the NFD.

In section 3.3.2 an approach is therefore proposed to estimate the NFD for the roads for which no data is available. This approach uses information from OpenStreetMap on the lane length of all road types, combined with an assumed fundamental diagram, based on the maximum speed and an assumed capacity value. When multiple road types are combined in one NFD, it gives one speed, which is the weighted average of the speeds on the different road types. The maximum internal flow is also smaller.

In section 4.2.2 it is concluded that it is not recommended to include all roads in the simulation. The residential roads and living streets account for a large part of the total network length, but on the macroscopic traffic flow level, these roads are of minor importance. If these roads are included in the case study, it would have a way too large impact on the shape of the NFD and thus on the traffic speed. These roads therefore have to be left out.

This research has shown in section 4.2.3 that clear NFDs can be defined for large zones, even though multiple road levels are present in the network. The freeway fundamental diagrams show large hysteresis loops for some zones, but when the freeway network is combined with the local network those loops fade away, and only small amounts of scatter are visible in the diagrams. In section 3.3.4 an approach is described to take hysteresis into account by setting temporary speed restrictions to the traffic when the critical density is exceeded. The drawback of this approach is that this restriction is applied to all traffic, while hysteresis is mainly observed on freeways. In section 6.2, an extra simulation case is described, in which distinction is made between local traffic and through traffic. This gives the opportunity to set temporary speed restrictions to the through traffic only, as soon as the critical density is exceeded. Local traffic then remains unrestricted.

WHICH PATHS DOES THE TRAFFIC TAKE INSIDE THE ZONES?

The simulation model is a trip-based approach. This means that each vehicle follows its own path, which is defined at the start of the trip. For each zone that is passed by the vehicle a specific distance is determined that has to be traversed before the vehicle can leave the zone. The speed of the vehicle is determined by the NFD of the zone, and the distance that has to be traversed in a zone is based on the previous and the next on its path.

To realize this, for each zone z_0 an internal distance matrix is defined, containing the path length inside zone z_0 for each combination of a previous zone z_{-1} and next zone z_{+1} . The length of each path is determined using a route planner, like Google Maps. If there are multiple feasible paths, the average of these paths is used. This also means that in the simulation, vehicles with the same previous and next zone will have to cover the same distance. A vehicle can leave the zone when it has completed this predetermined.

HOW CAN AN OD-MATRIX BE ESTIMATED FOR THE RANDSTAD?

This research does not pay particular attention to the OD-matrix estimation process, but it has shown that even a simple approach can be used to reproduce a realistic traffic situation with this simulation model.

The trips are generated in using a simple function with the number of households and jobs in each zone as input. As explained in section 3.4.2, the trips are distributed using the doubly-constrained gravity-model with a lognormal deterrence function, which expresses the attractiveness of an OD-pair as function of the generalized costs. This function has one sensitivity parameter.

In section 4.3.3, it becomes clear that the resulting OD-matrix had to meet one additional requirement, which is that for each zone the number of non-internal trips has to be smaller than the total observed outflow

for that zone, because the outflow of a specific zone is the sum of all non-internal trips and the trips passing through that zone. The outflow should therefore always be larger than the number of non-internal trips.

In first instance, the euclidean distances between the OD-pairs were used as the generalized costs. The sensitivity parameter had to be determined iteratively. This approach did not result in a feasible OD-matrix in first instance, because the requirement for the non-internal trips is not satisfied in section 4.3.3 for all zones. Therefore, the total numbers of trips estimated in section 3.4.1 had to be reduced for some zones, in order to end up with a feasible OD-matrix.

Alternatively, the travel time between the zones could be used as generalized costs. This approach has been tested in section 6.3. From the results of this approach in section 6.3.3, it is concluded that this approach using travel times should be preferred, because it resulted in a more realistic OD-matrix, and the results of the simulation were similar for both the approach using the euclidean distance and the approach using travel times. In this case, the OD-matrix could directly be used in the simulation, because the requirement that the number of non-internal trips does not exceed the observed outflows is satisfied, without reducing the total number of arrivals and departures.

WHAT IS THE ROUTING STRATEGY OF THE TRAFFIC BETWEEN THE ZONES?

With regard to the routing strategy, it is concluded in section 6.1.2 that the all-or-nothing assignment has given the best results for so far. The all-or-nothing assignment means that each vehicle travels with the shortest path from its origin to its destination.

An alternative way is to distribute traffic over multiple routes instead of using an all-or-nothing assignment, by means of a logit model. The results in section 6.1.2 show that the changed distribution of the traffic over a network leads does not have the desired effect. Even though only small amounts of vehicles are rerouted, severe congestion can appear, as it leads to a gridlock in some of the zones for certain logit parameters. When the parameter of the logit distribution is increased however, the results converge to an all-or-nothing assignment. So, with the current simulation setup and inputs, distributing the traffic over the network using the logit model has not lead to an improvement in the simulation results. This does not mean yet that all traffic for one OD-pair uses the same roads, because traffic can choose from multiple routes within the zones.

WHAT IS THE PERFORMANCE OF THE MODEL FOR THE RANDSTAD?

In section 3.6 it was stated that it is desired that the model can reconstruct the accumulation patterns of the real traffic. It is desired that the average deviation between the simulated and observed patterns is less than 20% over 24 hours, and also specifically during the peak hours (6:00 - 10:00 and 15:00 - 19:00).

With regard to the accumulation patterns it was concluded in section 5.2 that the model is able to reproduce the shapes of the accumulation patterns, but large deviations occur during the peak hours, with a difference of more than 20%. For the majority of the zones, the deviation from the expected patterns during peak hours is larger than desired. Especially for Gouda and Zaanstad, the simulation results show an accumulation pattern that is about 2 or 3 times higher then the expected pattern based on the observed values. Multiple reasons can be given for these results. The most likely cause is that the trip lengths inside the zones are overestimated. In section 5.2.1 it was shown that reducing these internal trip lengths improves the results, but it does not fully explain the differences.

In section 5.1 it was found that in general the model is able to reproduce the shapes of the outflow patterns, taking into account the desired range of 20%. For some larger cities like Den Haag and Rotterdam, the simulated outflow pattern exceeds the observed pattern by more than 20% during the morning peak. This could be solved by adapting the OD-matrix, for example by reducing the total demand for these zones. Another conclusion from the results is that some specific zones have a dominant outbound flow during morning peak, but a dominant inbound flow during afternoon peak, or vice versa. For this reason, the outflow is overestimated during one of the peaks. This could possibly be solved by estimating separate OD-matrices for both peak periods, instead of estimating one OD-matrix for 24 hours.

The comparison of the traveltimes in section 5.3 showed that the simulation produces unrealistic travel times. In most cases the travel time is overestimated for long-distance trips and underestimated for short-distance trips. This is caused by the fact that all traffic in a zone drives with the same speed, which means that through traffic on a freeway has then the same speed as the local traffic on the urban roads.

Therefore, section 6.2 proposed to make distinction between two types of traffic: Local traffic and through

traffic. Both types have their own NFD. In section 6.2.3 it is found that the approach to make distinction between two traffic types improved the simulation results, both for the accumulation patterns and the travel times. Especially for the long-distance trips during peak hours the travel time patterns improved with respect to the base case, but for the short-distance trips no clear improvement is visible in the results. The accumulation patterns show that for more zones, the average deviation with respect to the expected patterns falls within the desired range of 20%. Overall, the distinction between local and through traffic lead to a major improvement in the results, and it is therefore concluded that it is absolutely necessary to distinguish multiple traffic types when modelling large areas like the Randstad.

Based on the simulation results, it can be concluded that the results are promising, despite the high number of assumptions that has to be made before the simulation could be executed. Considering the simulated accumulation and outflow patterns and the observed values, it is found that for most zones the difference falls within an acceptable range of 20%.

The results have also shown that it is absolutely necessary to distinguish multiple types of traffic, each with its own NFD. When one single NFD is used for all traffic, it results in inaccurate travel times. For through traffic, the travel times are overestimated, while for local traffic the travel times are underestimated. In general, the model works the best for long-distance trips. The model is then able to estimate the travel times with a deviation of a few minutes. On the shorter distance however further improvement is needed, because the model generally underestimates the travel times, especially during the peak hours.

With regard to the practical applicability, it can be concluded that quite some steps have to be taken before the model could be applied. Especially the NFD generation step is a time-consuming job on this scale, and adding data for urban roads would take even more time, because no general database exists for this data for the Netherlands. Besides that, the OD-estimation remains a challenge at this large scale. The calculation times of the simulation are however short, under normal circumstances the simulations took about five minutes for one full day. This calculation time can however grow rapidly when more zones are used or when a smaller time step is used.

RECOMMENDATIONS

Based on this research, three recommendations for practice are given and four recommendations for future research are proposed.

RECOMMENDATIONS FOR PRACTICE

i **OD-matrix estimation:**

In this research no particular attention has been paid to the OD-estimation process, but only a simple approach has been used to construct the OD-matrix. It is recommended to improve the OD-matrix estimation process.

ii **Route sets:**

The simulation results have shown that unfeasible or unrealistic routes may be present in the route set, because it is constructed based on the internal distance matrix. If more attention is paid to the route sets, unrealistic simulation results can be prevented, by excluding infeasible routes.

iii **NFDs for local traffic:**

For this thesis, the fundamental diagrams for non-freeway roads were estimated using an assumed free-flow speed and capacity. These assumptions mainly influence the NFDs for local traffic, but the assumptions have not been verified yet, which could be the reason for the inaccurate travel times for short-distance trips. It is recommended to verify these assumptions and improve the NFD estimation process. If the model is applied to an area for which data from observations is also available for the local traffic, the same approach as used for motorways should be preferred over the analytical approach.

RECOMMENDATIONS FOR FUTURE RESEARCH

i **Multiple traffic types:**

In the last part of this research, it is proposed to make distinction between two traffic types: local traffic and through traffic. Several assumptions have been made to construct the NFD for both traffic types.

Although it was concluded that this approach has a positive effect on the simulation results, the approach can further be improved and tested. The assumptions on how traffic is divided over the different road types in section 6.2.1, have to be verified and probably also adjusted.

ii **Hysteresis:**

In this research, hysteresis is incorporated by setting a temporary capacity restriction as soon as the network reaches its congested state. The effect of this temporary capacity restriction is however not analyzed in this research, so it is unknown yet whether this approach represents the hysteresis phenomenon realistically. It is therefore recommended to study the effect of this approach.

iii **Zone size:**

The zone map has been created based on all municipalities in the area with more than 75,000 inhabitants. This finally resulted in sixteen zones for the study area. It is recommended to study the effect of the zone size on the outcomes of the simulation. How does the model perform with smaller zones, or even with larger zones?

iv **Other areas:**

The Randstad is the first area for which this simulation model has been tested. It is recommended to apply this model to other large areas, to check whether this approach could be used as a universal approach for modelling traffic on a macroscopic level.

BIBLIOGRAPHY

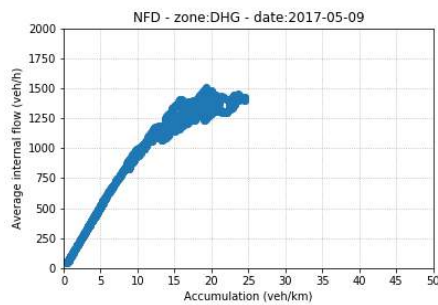
- [1] L. Brederode, M. Bliemer, and L. Wismans. *STAQ: Static Traffic Assignment with Queing*. Association for European Transport (AET), 2010. URL <http://resolver.tudelft.nl/uuid:2e241e08-1851-4259-8ef8-67f3c4676221>.
- [2] L. Brederode, A. Pel, L. Wismans, E. De Romph, and S.P. Hoogendoorn. Static Traffic Assignment with Queuing: model properties and applications. *Transportmetrica A: Transport Science*, 0(0):1–36, 2018. doi: 10.1080/23249935.2018.1453561.
- [3] C. Buisson and C. Ladier. Exploring the Impact of Homogeneity of Traffic Measurements on the Existence of Macroscopic Fundamental Diagrams. *Transportation Research Record*, 2124(1):127–136, 2009. doi: 10.3141/2124-12. URL <https://doi.org/10.3141/2124-12>.
- [4] Centraal Bureau voor Statistiek (CBS). Aantal huishoudens - gemeenten, 2017. data retrieved from CBS, http://www.cbsinuwbuurt.nl/#sub-gemeenten2017_aantal_huishoudens.
- [5] T. Courbon and L. Leclercq. Cross-comparison of Macroscopic Fundamental Diagram Estimation Methods. *Procedia - Social and Behavioral Sciences*, 20:417–426, 2011. ISSN 1877-0428. doi: 10.1016/j.sbspro.2011.08.048. URL <http://www.sciencedirect.com/science/article/pii/S1877042811014285>. The State of the Art in the European Quantitative Oriented Transportation and Logistics Research – 14th Euro Working Group on Transportation & 26th Mini Euro Conference & 1st European Scientific Conference on Air Transport.
- [6] C.F. Daganzo. The cell transmission model: A dynamic representation of highway traffic consistent with the hydrodynamic theory. *Transportation Research Part B: Methodological*, 28(4):269–287, 1994. ISSN 0191-2615. doi: [https://doi.org/10.1016/0191-2615\(94\)90002-7](https://doi.org/10.1016/0191-2615(94)90002-7). URL <http://www.sciencedirect.com/science/article/pii/0191261594900027>.
- [7] C.F. Daganzo. The cell transmission model, part II: Network traffic. *Transportation Research Part B: Methodological*, 29(2):79–93, 1995. ISSN 0191-2615. doi: [https://doi.org/10.1016/0191-2615\(94\)00022-R](https://doi.org/10.1016/0191-2615(94)00022-R). URL <http://www.sciencedirect.com/science/article/pii/019126159400022R>.
- [8] C.F. Daganzo and N. Geroliminis. An analytical approximation for the macroscopic fundamental diagram of urban traffic. *Transportation Research Part B: Methodological*, 42(9):771 – 781, 2008. ISSN 0191-2615. doi: 10.1016/j.trb.2008.06.008. URL <http://www.sciencedirect.com/science/article/pii/S0191261508000799>.
- [9] EPOMM. TEMS - The EPOMM Modal Split Tool, 2008-2014. data retrieved from EPOMM, <http://www.epomm.eu/tems/index.phtml>.
- [10] V.V. Gayah and C.F. Daganzo. Clockwise hysteresis loops in the Macroscopic Fundamental Diagram: An effect of network instability. *Transportation Research Part B: Methodological*, 45(4):643–655, 2011. ISSN 0191-2615. doi: <https://doi.org/10.1016/j.trb.2010.11.006>. URL <http://www.sciencedirect.com/science/article/pii/S0191261510001396>.
- [11] N. Geroliminis and C.F. Daganzo. Macroscopic modeling of traffic in cities. In *86th Annual Meeting Transportation Research Board*, Washington, D.C., January 2007.
- [12] N. Geroliminis and C.F. Daganzo. Existence of urban-scale macroscopic fundamental diagrams: Some experimental findings. *Transportation Research Part B: Methodological*, 42(9):759–770, 2008. ISSN 0191-2615. doi: 10.1016/j.trb.2008.02.002. URL <http://www.sciencedirect.com/science/article/pii/S0191261508000180>.

- [13] N. Geroliminis and J. Sun. Properties of a well-defined macroscopic fundamental diagram for urban traffic. *Transportation Research Part B: Methodological*, 45(3):605–617, 2011. ISSN 0191-2615. doi: 10.1016/j.trb.2010.11.004. URL <http://www.sciencedirect.com/science/article/pii/S0191261510001372>.
- [14] N. Geroliminis and J. Sun. Hysteresis phenomena of a Macroscopic Fundamental Diagram in free-way networks. *Transportation Research Part A: Policy and Practice*, 45(9):966–979, 2011. ISSN 0965-8564. doi: 10.1016/j.tra.2011.04.004. URL <http://www.sciencedirect.com/science/article/pii/S0965856411000620>. Select Papers from the 19th International Symposium on Transportation and Traffic Theory (ISTTT).
- [15] V.L. Knoop and S.P. Hoogendoorn. An Area-Aggregated Dynamic Traffic Simulation Model. *European Journal of Transport and Infrastructure Research (EJTIR)*, 15:226–242, 2015. ISSN 1567-7141. URL <https://repository.tudelft.nl/islandora/object/uuid:cfe6d923-6676-4cf7-b60d-a4ab1a949dad?collection=research>.
- [16] V.L. Knoop, J.W.C Van Lint, and S.P. Hoogendoorn. Traffic dynamics: Its impact on the Macroscopic Fundamental Diagram. *Physica A: Statistical Mechanics and its Applications*, 438:236–250, 2015. ISSN 0378-4371. doi: 10.1016/j.physa.2015.06.016. URL <http://www.sciencedirect.com/science/article/pii/S0378437115005695>.
- [17] V.L. Knoop, P. van Erp, L. Leclercq, and S.P. Hoogendoorn. Empirical MFDs using Google Traffic Data. In *21st IEEE International Conference on Intelligent Transportation Systems*, Hawaii, USA, November 2018. IEEE.
- [18] Knoop, V.L., Tamminga, G.F., and Leclercq, L. Network Transmission Model: Application to a Real World City. In *95th Annual Meeting Transportation Research Board*, pages 1–15, Washington, D.C., 2016.
- [19] R. Lamotte and N. Geroliminis. The morning commute in urban areas with heterogeneous trip lengths. *Transportation Research Part B: Methodological*, 2017. ISSN 0191-2615. doi: 10.1016/j.trb.2017.08.023. URL <http://www.sciencedirect.com/science/article/pii/S0191261517307208>.
- [20] H. Mahmassani, J.C. Williams, and R. Herman. Investigation of Network-Level Traffic Flow Relationships: Some Simulation Results. *Transportation Research Record*, pages 121–130, 1 1984. ISSN 0361-1981.
- [21] G. Mariotte, J. Leclercq, and J.A. Laval. Macroscopic urban dynamics: Analytical and numerical comparisons of existing models. *Transportation Research Part B: Methodological*, 101:245–267, 2017. ISSN 0191-2615. doi: 10.1016/j.trb.2017.04.002. URL <http://www.sciencedirect.com/science/article/pii/S0191261516307846>.
- [22] OpenStreetMap Wiki. Overpass API — OpenStreetMap Wiki, 2018. [Online], Available: <http://wiki.openstreetmap.org/w/index.php?oldid=1699607>, [Accessed: November 30, 2018].
- [23] OpenStreetMap Wiki. Key:highway — OpenStreetMap Wiki, 2018. [Online]. Available: <http://wiki.openstreetmap.org/w/index.php?oldid=1687287> [Accessed: November 17, 2018].
- [24] Publieke Dienstverlening Op de Kaart (PDOK). Dataset: Basisregistratie Topografie (BRT) TOPNL, 2018. data retrieved from PDOK, <https://www.pdok.nl/downloads?articleid=1976855>.
- [25] X Shi and H Lin. Research on the Macroscopic Fundamental Diagram for Shanghai urban expressway network. *Transportation Research Procedia*, 25:1300–1316, 2017. ISSN 2352-1465. doi: <https://doi.org/10.1016/j.trpro.2017.05.153>. URL <http://www.sciencedirect.com/science/article/pii/S2352146517304453>. World Conference on Transport Research - WCTR 2016 Shanghai. 10-15 July 2016.
- [26] Stichting Lisa. Overzicht lisa-data per gemeente, 2016. data retrieved from LISA, <https://www.lisa.nl/data/gratis-data/overzicht-lisa-data-per-gemeente>.
- [27] US Bureau of Public Roads. Traffic assignment manual, 1964.

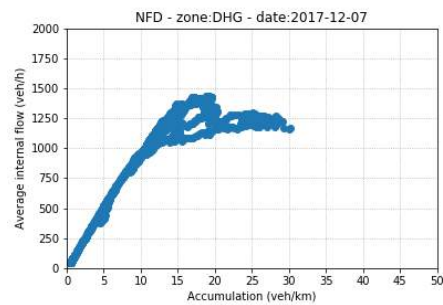
-
- [28] R. Van Nes. Trip generation. Lecture, 2016. CIE4801 Transportation and Spatial Modelling, Technische Universiteit Delft, delivered 12 September 2016.
 - [29] J. G. Wardrop. Some Theoretical Aspects of Road Traffic Research. *Proceedings of the Institution of Civil Engineers, Part II*, pages 325–378, 1952.

A

FREEWAY NFDs

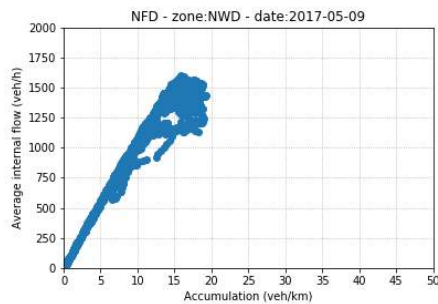


(a) 9 May 2017

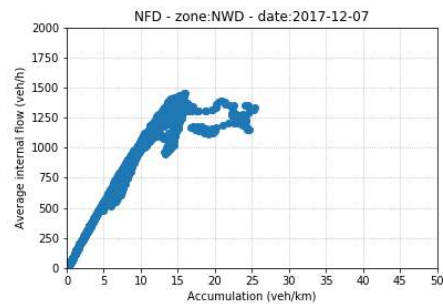


(b) 7 December 2017

Figure A.1: Network Fundamental Diagrams for the freeway network of Den Haag



(a) 09 May 2017



(b) 07 December 2017

Figure A.2: Network Fundamental Diagrams for the freeway network of Nissewaard

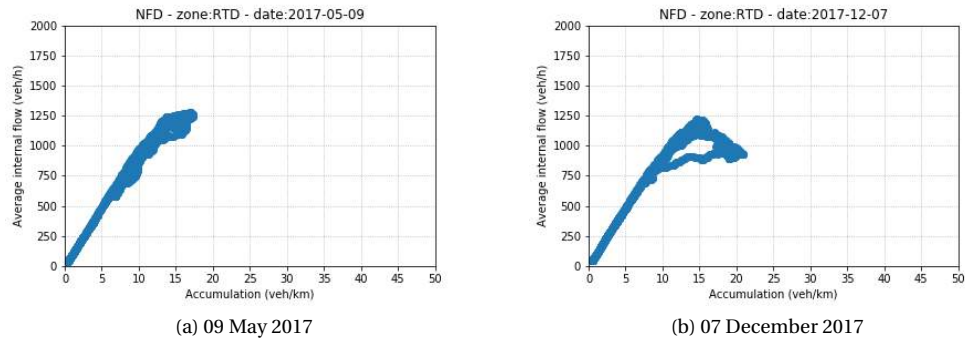


Figure A.3: Network Fundamental Diagrams for the freeway network of Rotterdam

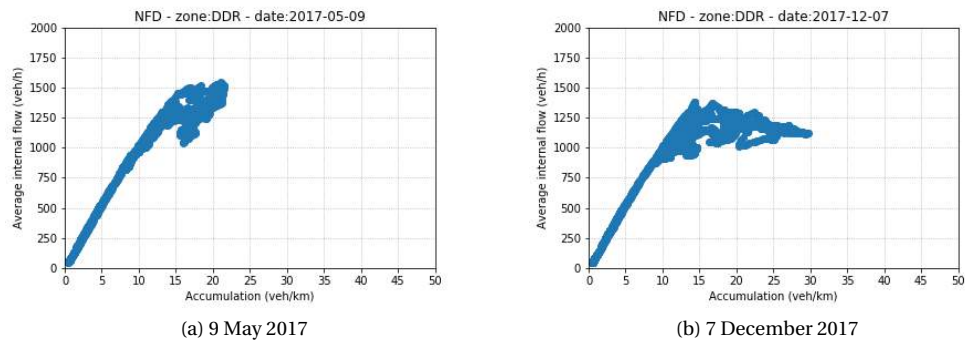


Figure A.4: Network Fundamental Diagrams for the freeway network of Dordrecht

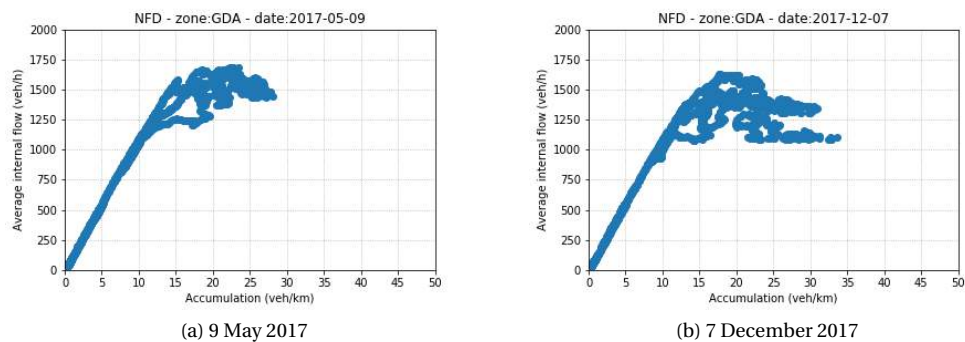
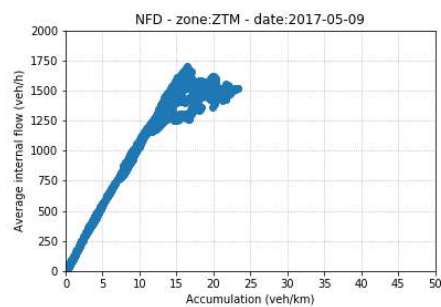
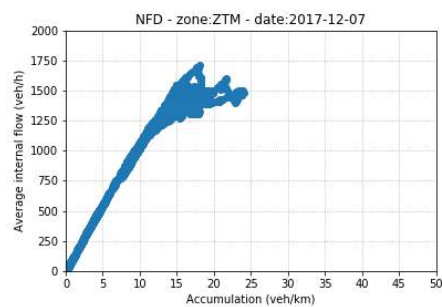


Figure A.5: Network Fundamental Diagrams for the freeway network of Gouda

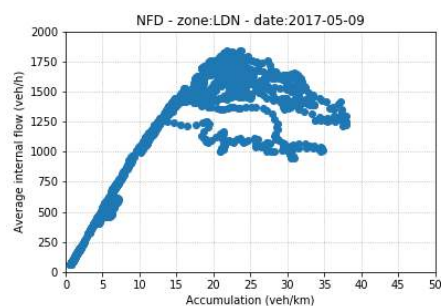


(a) 9 May 2017

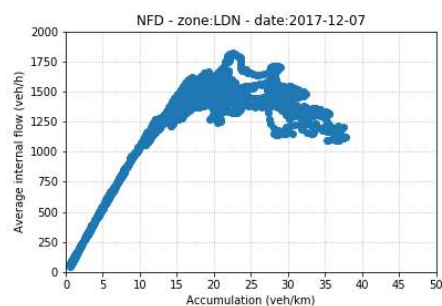


(b) 7 December 2017

Figure A.6: Network Fundamental Diagrams for the freeway network of Zoetermeer

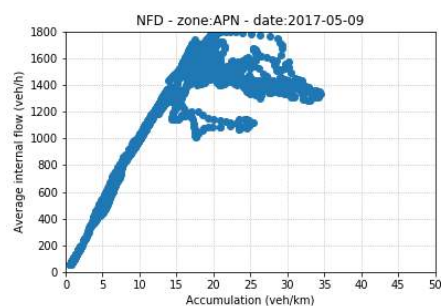


(a) 9 May 2017

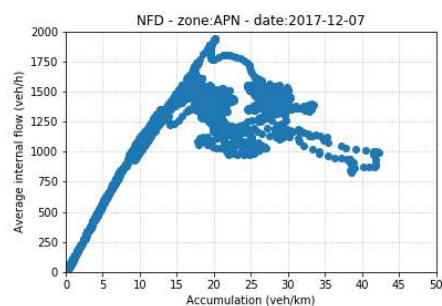


(b) 7 December 2017

Figure A.7: Network Fundamental Diagrams for the freeway network of Leiden



(a) 9 May 2017



(b) 7 December 2017

Figure A.8: Network Fundamental Diagrams for the freeway network of Alphen a/d Rijn

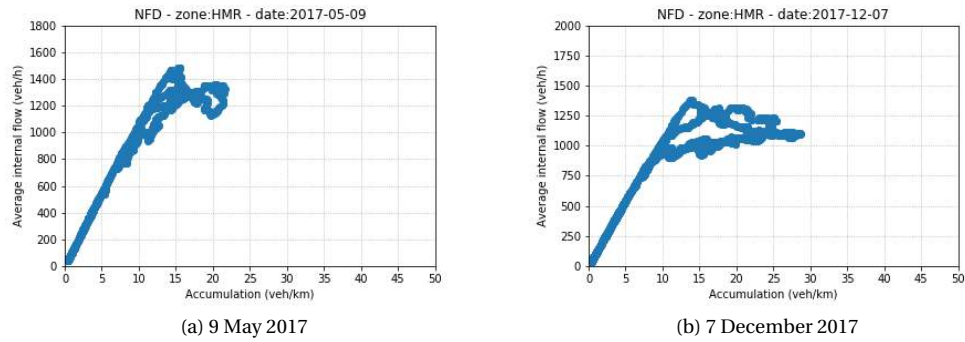


Figure A.9: Network Fundamental Diagrams for the freeway network of Haarlem

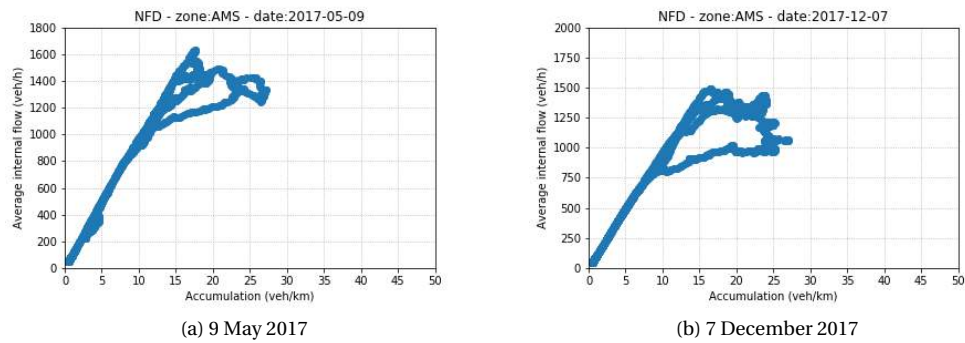


Figure A.10: Network Fundamental Diagrams for the freeway network of Amsterdam

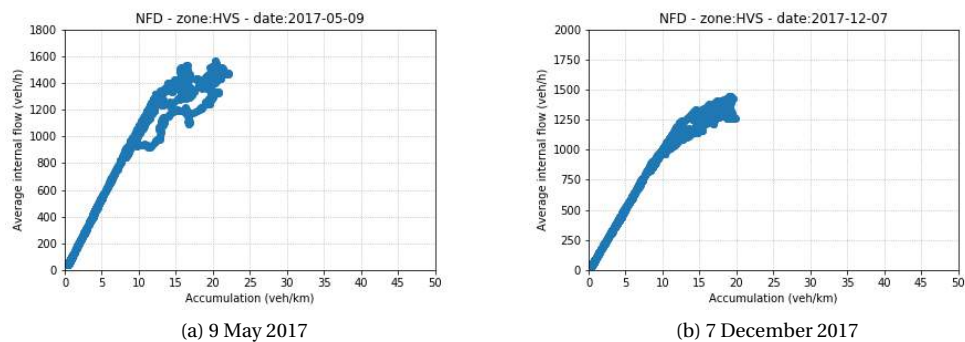
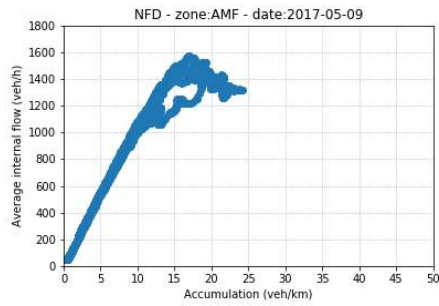
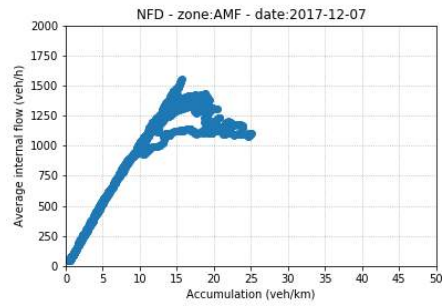


Figure A.11: Network Fundamental Diagrams for the freeway network of Hilversum

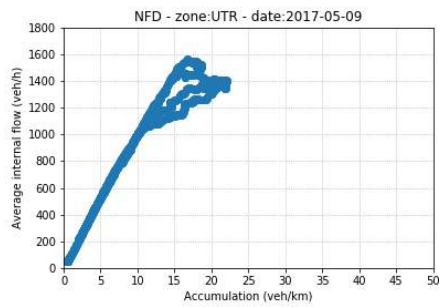


(a) 9 May 2017

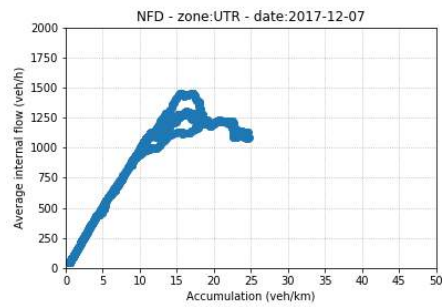


(b) 7 December 2017

Figure A.12: Network Fundamental Diagrams for the freeway network of Amersfoort

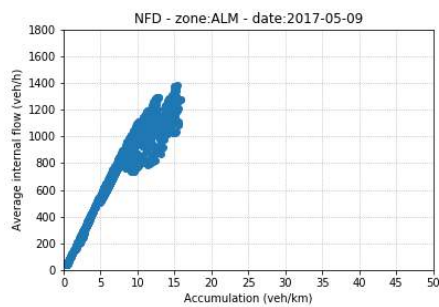


(a) 9 May 2017

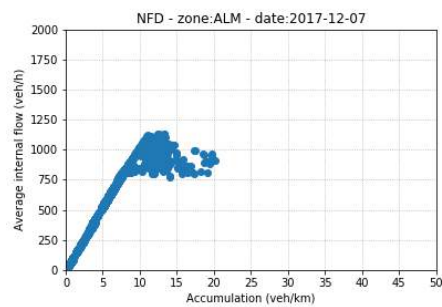


(b) 7 December 2017

Figure A.13: Network Fundamental Diagrams for the freeway network of Utrecht



(a) 9 May 2017



(b) 7 December 2017

Figure A.14: Network Fundamental Diagrams for the freeway network of Almere

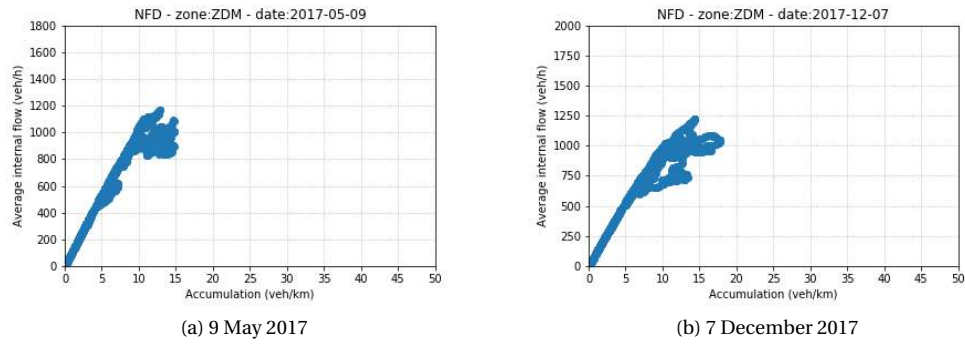


Figure A.15: Network Fundamental Diagrams for the freeway network of Zaanstad

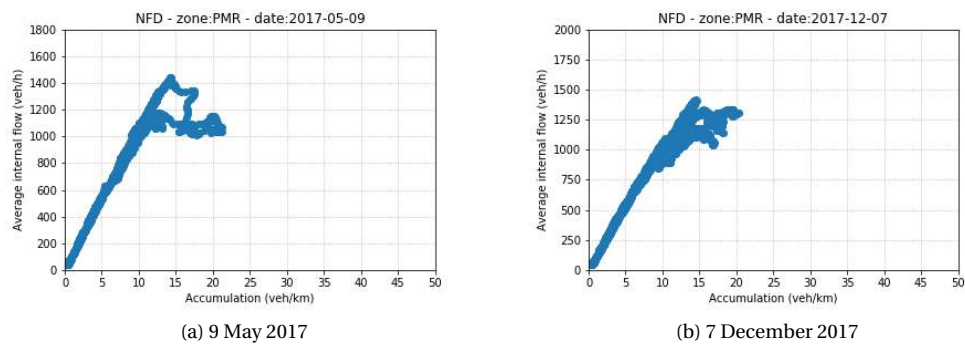


Figure A.16: Network Fundamental Diagrams for the freeway network of Purmerend

B

NFD PLOTS

B.1. FULL NETWORK

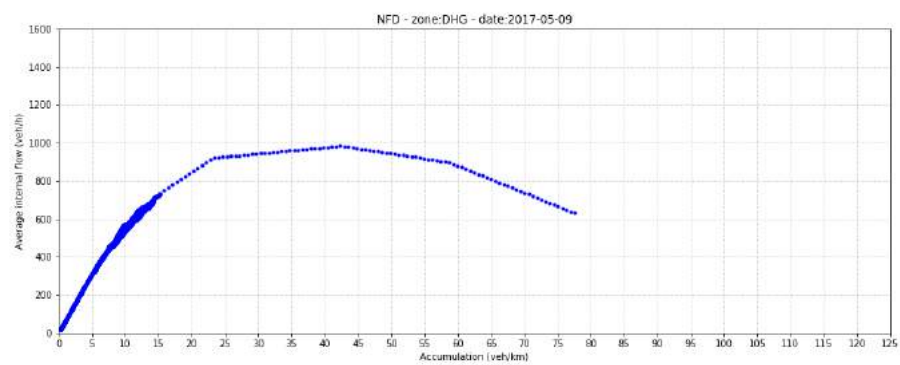


Figure B.1: Network Fundamental Diagram for Den Haag

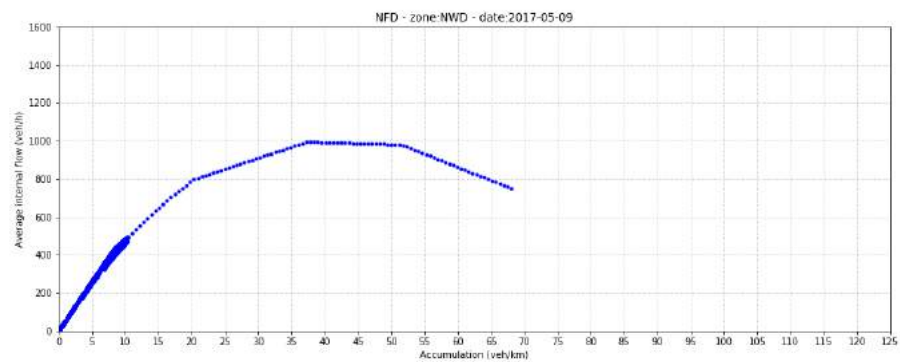


Figure B.2: Network Fundamental Diagram for Nissewaard

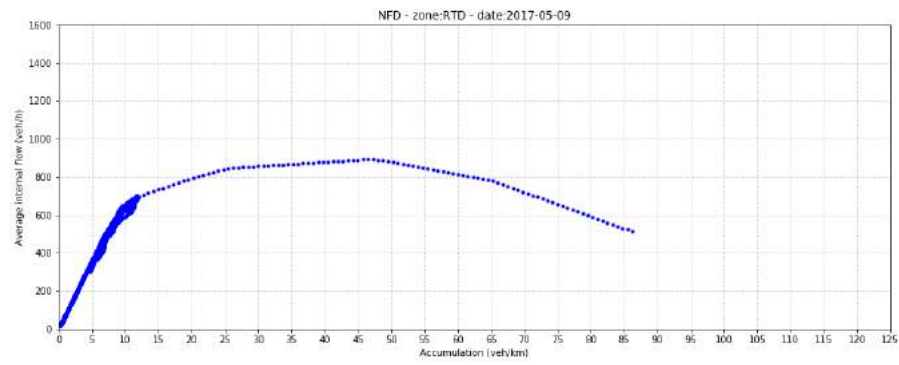


Figure B.3: Network Fundamental Diagram for Rotterdam

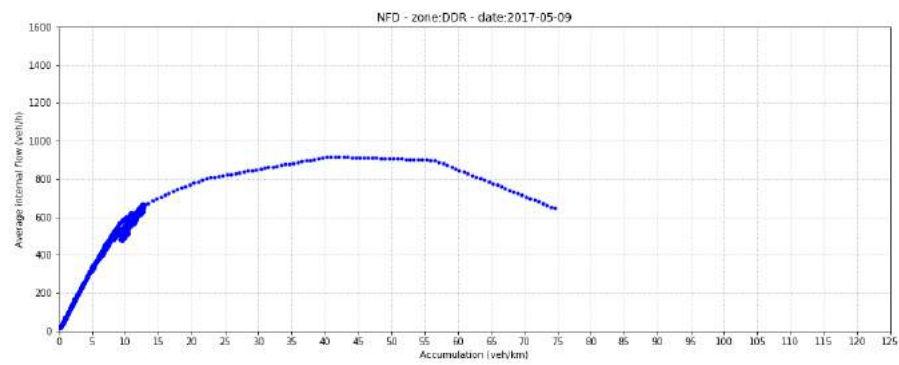


Figure B.4: Network Fundamental Diagram for Dordrecht

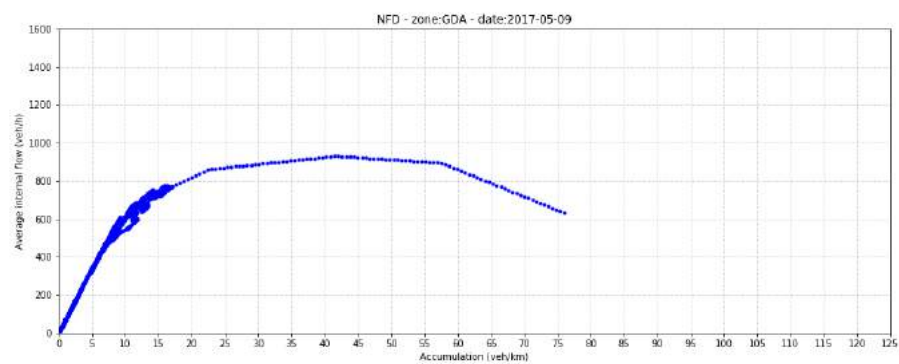


Figure B.5: Network Fundamental Diagram for Gouda

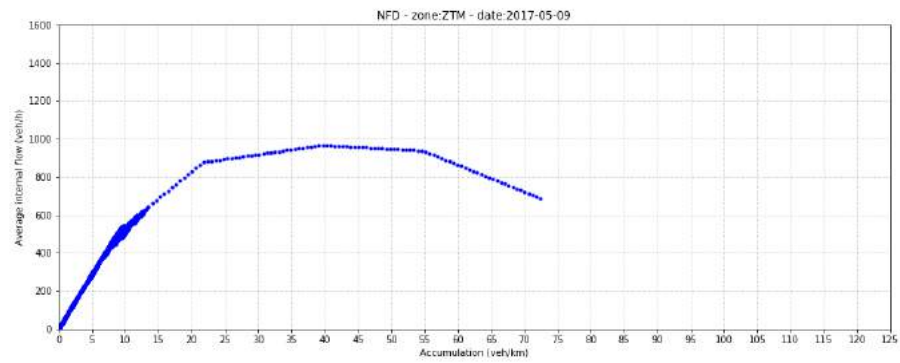


Figure B.6: Network Fundamental Diagram for Zoetermeer

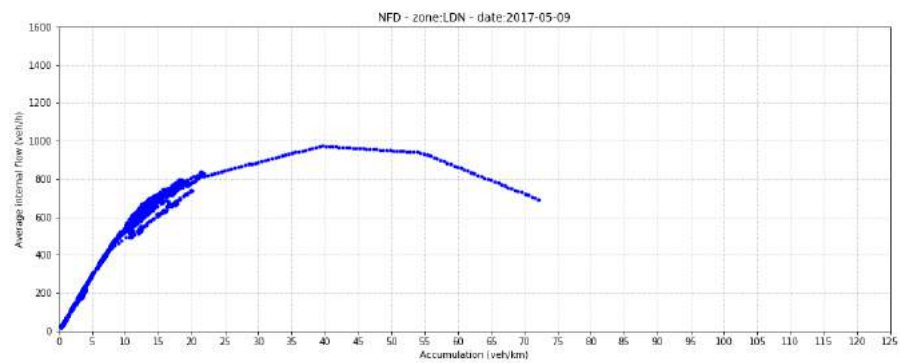


Figure B.7: Network Fundamental Diagram for Leiden

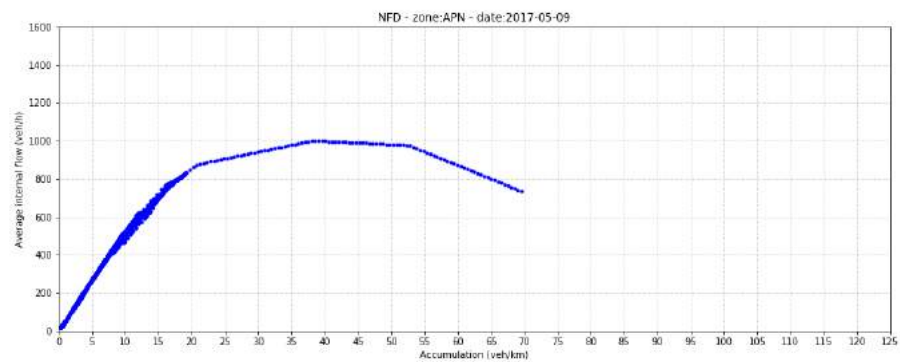


Figure B.8: Network Fundamental Diagram for Alphen a/d Rijn

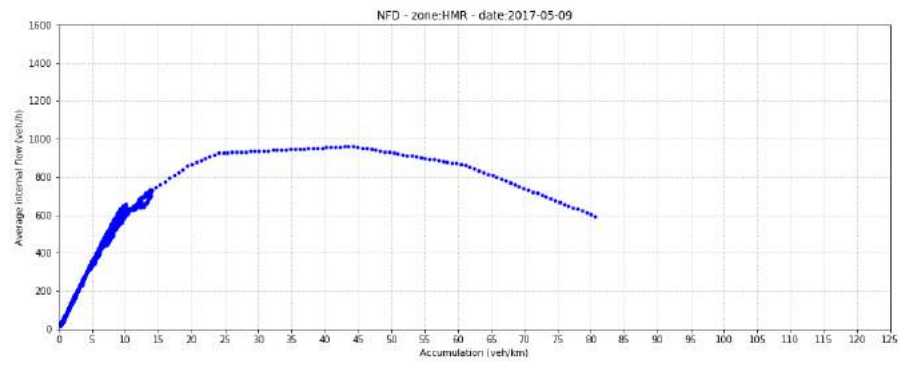


Figure B.9: Network Fundamental Diagram for Haarlem

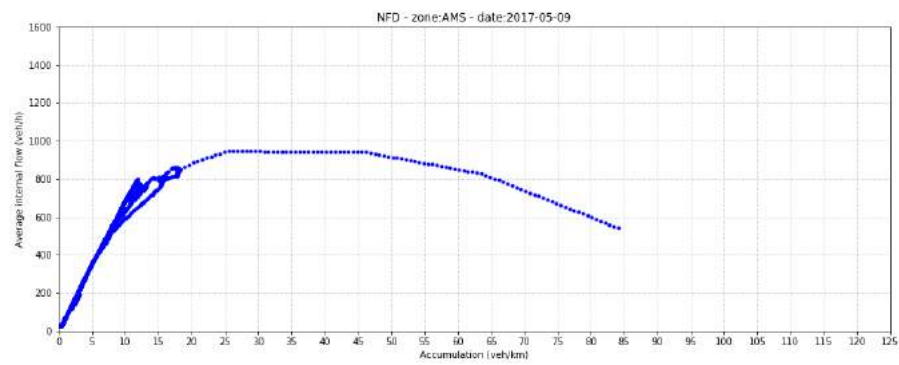


Figure B.10: Network Fundamental Diagram for Amsterdam

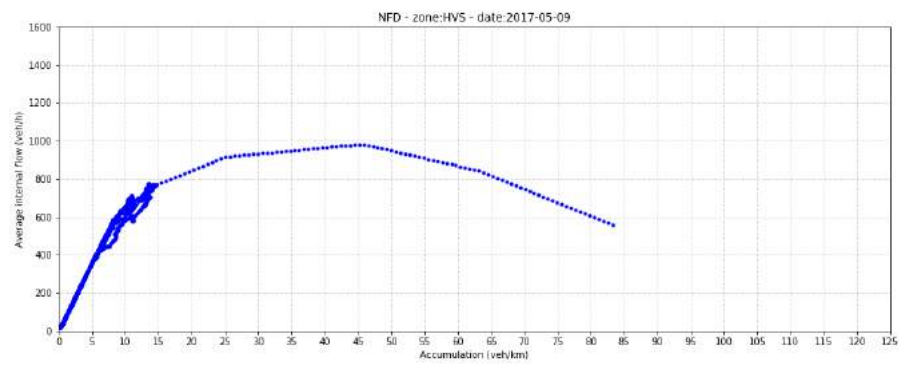


Figure B.11: Network Fundamental Diagram for Hilversum

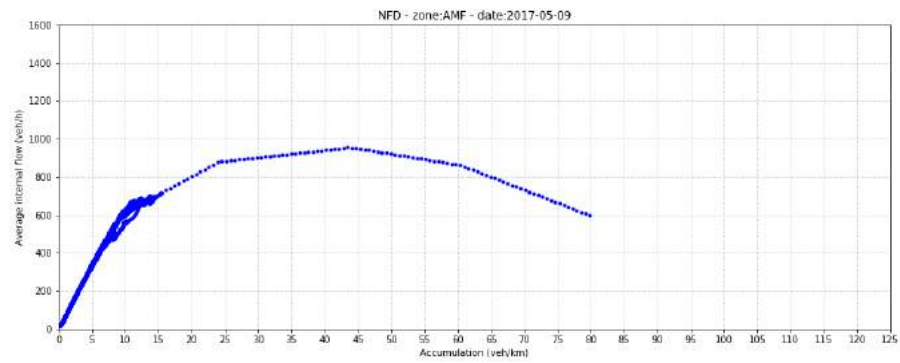


Figure B.12: Network Fundamental Diagram for Amersfoort

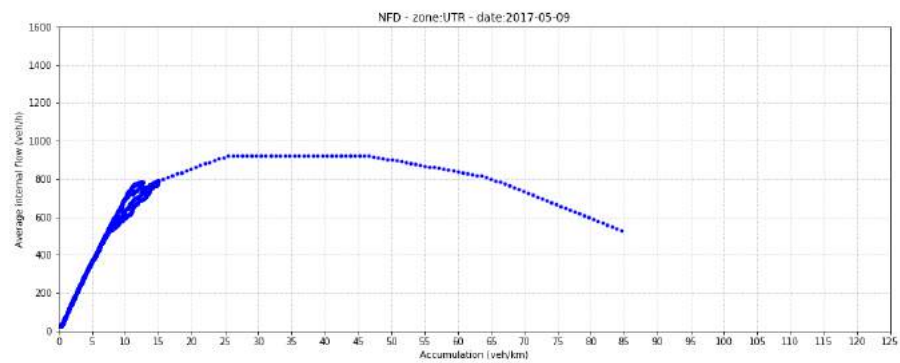


Figure B.13: Network Fundamental Diagram for Utrecht

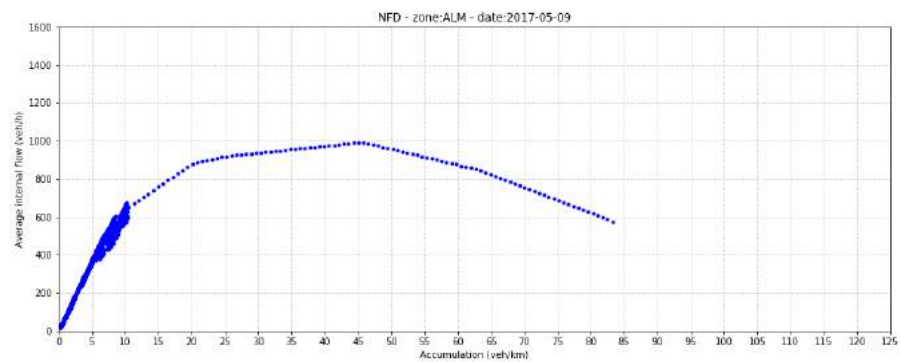


Figure B.14: Network Fundamental Diagram for Almere

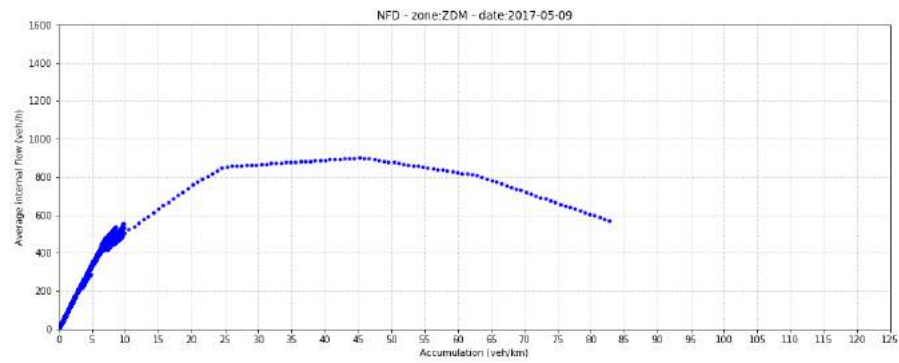


Figure B.15: Network Fundamental Diagram for Zaanstad

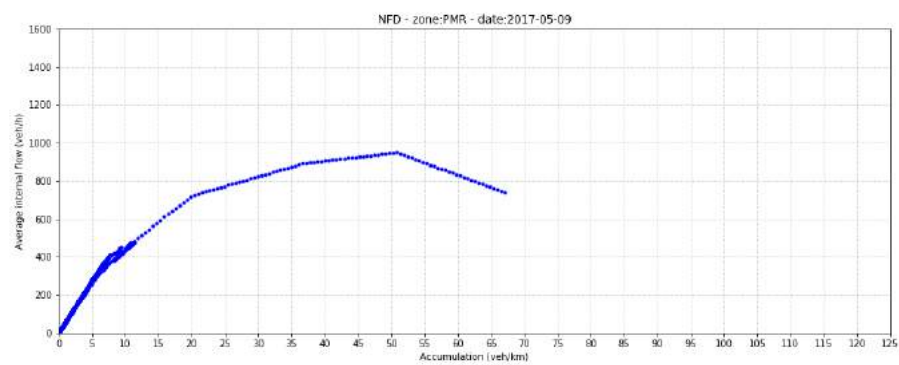


Figure B.16: Network Fundamental Diagram for Purmerend

B.2. LOCAL & THROUGH TRAFFIC

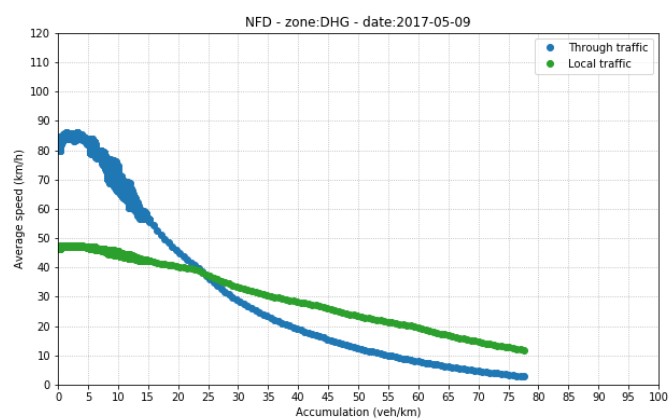


Figure B.17: Network Fundamental Diagrams for the local and through traffic of Den Haag

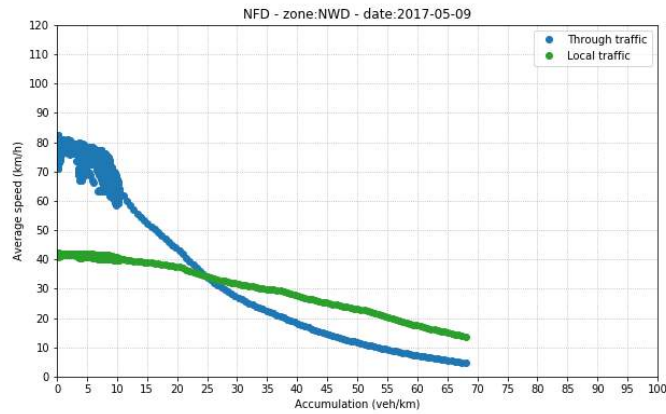


Figure B.18: Network Fundamental Diagrams for the local and through traffic of Nissewaard

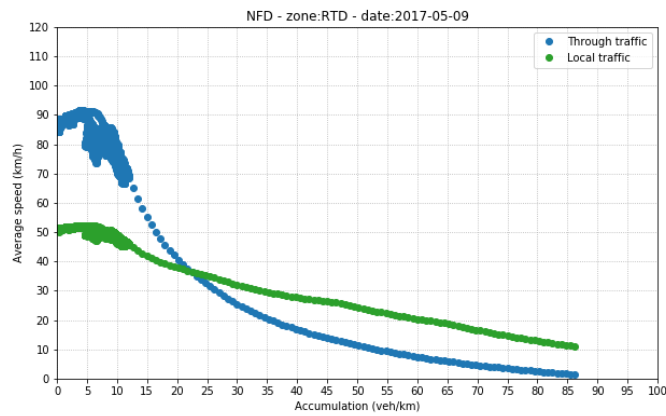


Figure B.19: Network Fundamental Diagrams for the local and through traffic of Rotterdam

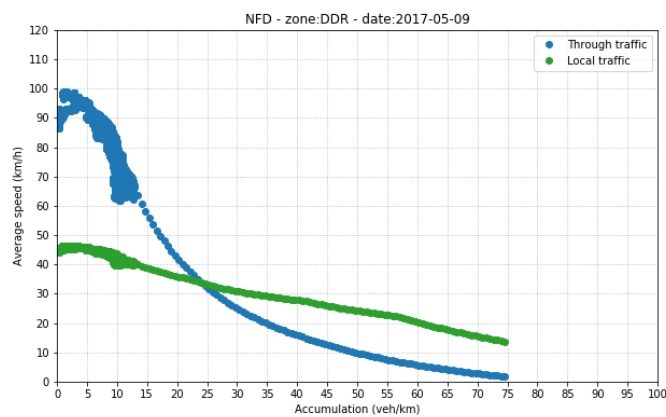


Figure B.20: Network Fundamental Diagrams for the local and through traffic of Dordrecht

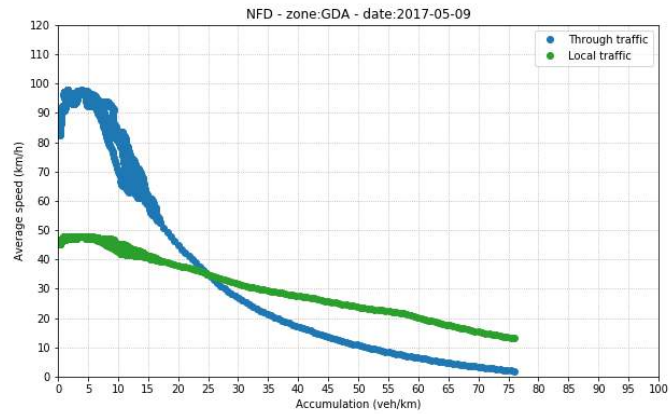


Figure B.21: Network Fundamental Diagrams for the local and through traffic of Gouda

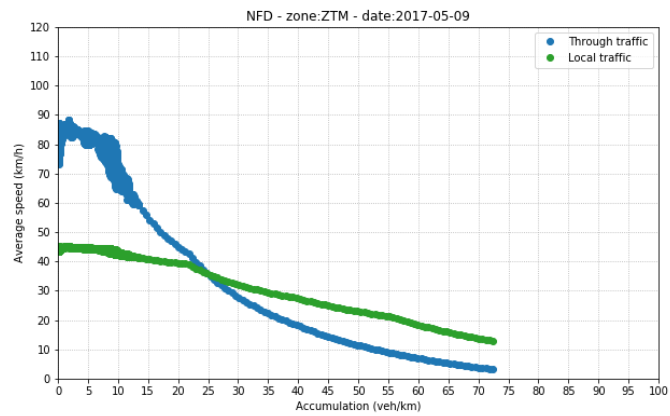


Figure B.22: Network Fundamental Diagrams for the local and through traffic of Zoetermeer

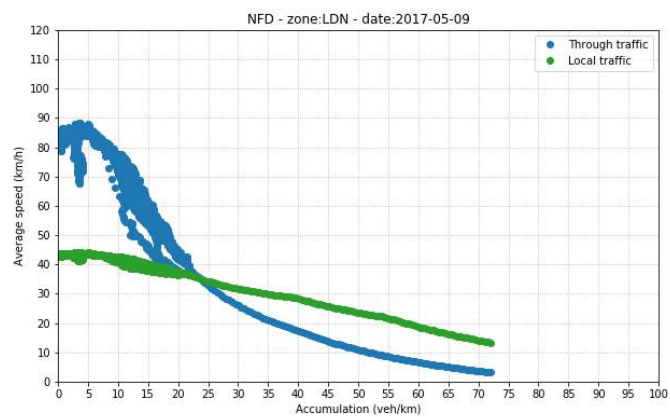


Figure B.23: Network Fundamental Diagrams for the local and through traffic of Leiden

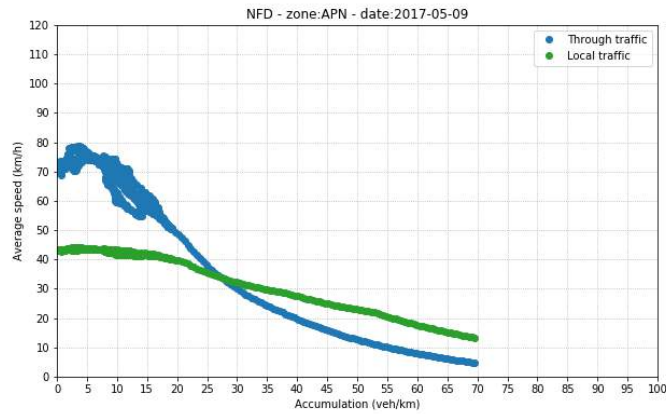


Figure B.24: Network Fundamental Diagrams for the local and through traffic of Alphen a/d Rijn

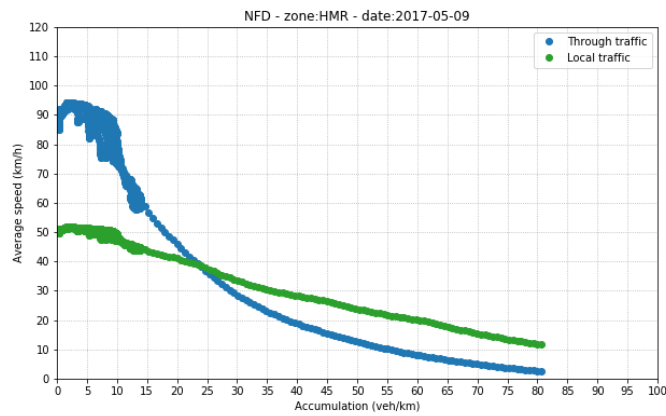


Figure B.25: Network Fundamental Diagrams for the local and through traffic of Haarlem

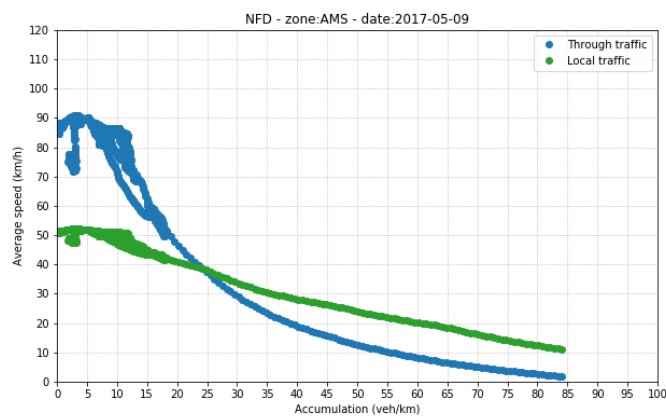


Figure B.26: Network Fundamental Diagrams for the local and through traffic of Amsterdam

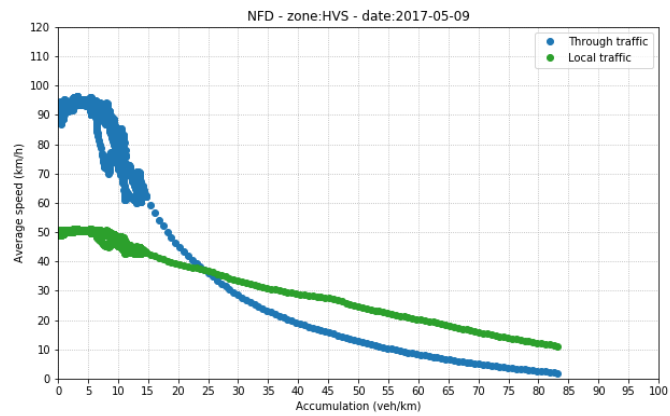


Figure B.27: Network Fundamental Diagrams for the local and through traffic of Hilversum

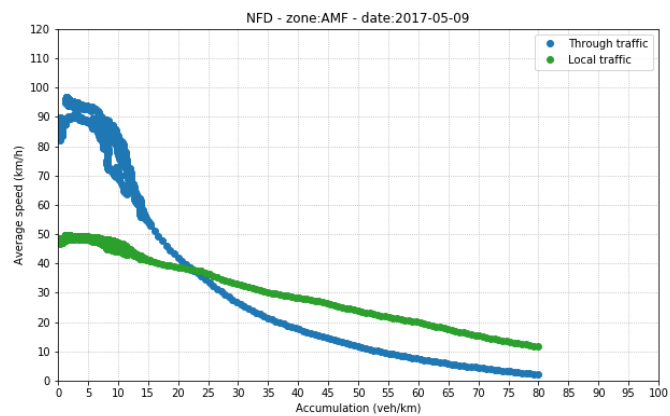


Figure B.28: Network Fundamental Diagrams for the local and through traffic of Amersfoort

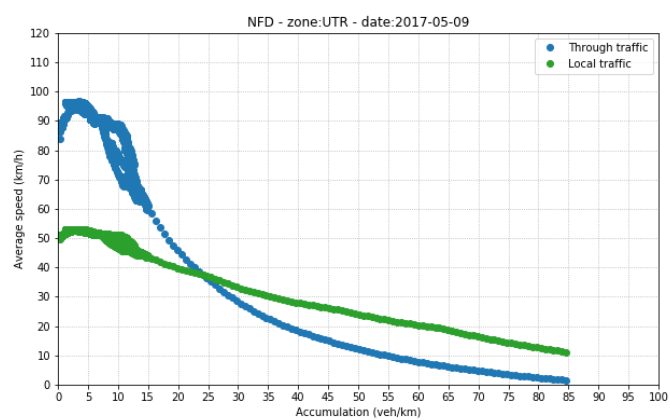


Figure B.29: Network Fundamental Diagrams for the local and through traffic of Utrecht

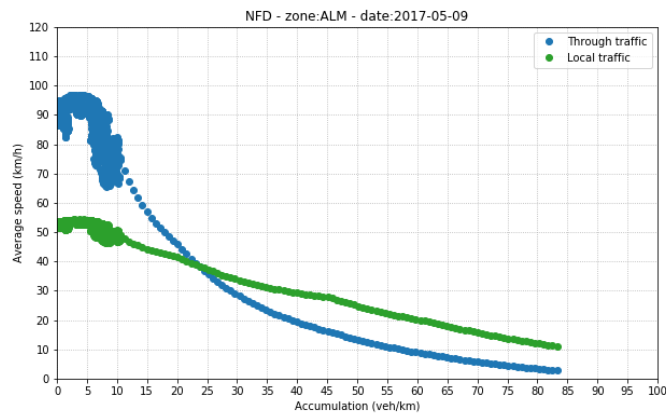


Figure B.30: Network Fundamental Diagrams for the local and through traffic of Almere

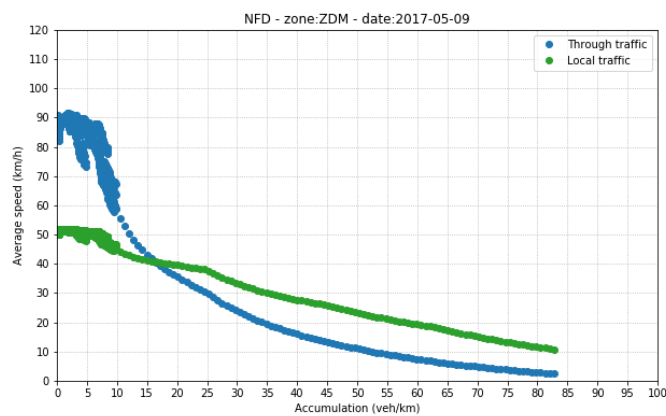


Figure B.31: Network Fundamental Diagrams for the local and through traffic of Zaanstad

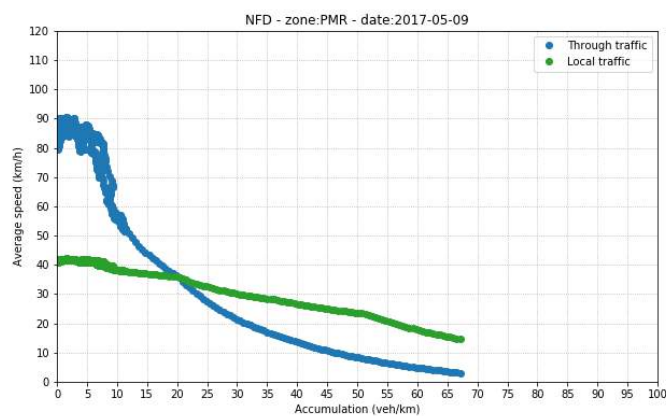


Figure B.32: Network Fundamental Diagrams for the local and through traffic of Purmerend

C

OD-MATRIX

C.1. BASE-CASE

Table C.1: OD matrix (×1000)

nr.	Name	1	2	3	4	5	6	7	8	9	10	11	12	13	14	15	16
1	Den Haag	452.9	11	147	7.1	9.6	53.1	30.5	7.2	7	3.3	0.6	0.5	4.5	0.3	0.9	0.4
2	Nissewaard	11	38.1	69.7	5.2	2.2	3.1	1.3	0.7	0.6	0.5	0.1	0.1	1.2	0.1	0.1	0.1
3	Rotterdam	147	69.7	425.3	19.3	15.6	43.9	11.5	5.5	4.2	2.8	0.6	0.6	6.1	0.3	0.6	0.3
4	Dordrecht	7.1	5.2	19.3	366.9	38.9	5.9	3.2	4.3	2.7	3.4	1.3	1.7	27	0.5	0.5	0.3
5	Gouda	9.6	2.2	15.6	38.9	119.4	13.7	7.9	18.4	5.6	6.6	1.7	1.5	32	0.6	0.8	0.5
6	Zoetermeer	53.1	3.1	43.9	5.9	13.7	94	15.1	7.7	3.7	2.2	0.4	0.3	3.8	0.2	0.4	0.2
7	Leiden	30.5	1.3	11.5	3.2	7.9	15.1	290.5	26.2	36.6	9.7	1	0.7	5.8	0.6	2.8	1
8	Alphen a/d Rijn	7.2	0.7	5.5	4.3	18.4	7.7	26.2	72.8	21.9	16.2	1.8	1	13.6	0.8	1.8	0.9
9	Haarlem	7	0.6	4.2	2.7	5.6	3.7	36.6	21.9	540.1	99.4	4.6	2.2	12.1	3.3	48.4	10.7
10	Amsterdam	3.3	0.5	2.8	3.4	6.6	2.2	9.7	16.2	99.4	462	30.3	8.4	36.8	16.1	26.2	20
11	Hilversum	0.6	0.1	0.6	1.3	1.7	0.4	1	1.8	4.6	30.3	119.7	28.6	31.3	23.2	1.8	2.6
12	Amersfoort	0.5	0.1	0.6	1.7	1.5	0.3	0.7	1	2.2	8.4	28.6	247.8	36.3	10.4	0.8	1.2
13	Utrecht	4.5	1.2	6.1	27	32	3.8	5.8	13.6	12.1	36.8	31.3	36.3	549	7.1	2.7	2.4
14	Almere	0.3	0.1	0.3	0.5	0.6	0.2	0.6	0.8	3.3	16.1	23.2	10.4	7.1	172.8	2.2	5.5
15	Zaanstad	0.9	0.1	0.6	0.5	0.8	0.4	2.8	1.8	48.4	26.2	1.8	0.8	2.7	2.2	212.5	28
16	Purmerend	0.4	0.1	0.3	0.3	0.5	0.2	1	0.9	10.7	20	2.6	1.2	2.4	5.5	28	106.2

Table C.2: OD matrix (×1000) for the external areas. External zones have numbers above 100. Zone 112 for example means the external area near zone 12 (Amersfoort).

nr.	Name	102	104	112	113	114	115	116
1	Den Haag	5.8	6.5	1.6	4	0.5	1.2	0.9
2	Nissewaard	5.4	3.5	0.4	1.2	0.1	0.2	0.2
3	Rotterdam	13.8	12	1.8	5	0.5	0.9	0.8
4	Dordrecht	3.9	40.7	3.7	11.7	0.7	0.8	0.8
5	Gouda	1.9	12.1	2.8	9.8	0.7	0.9	0.9
6	Zoetermeer	1.8	3.6	0.8	2.4	0.2	0.5	0.4
7	Leiden	1.5	3.5	1.7	4	0.7	2.1	1.5
8	Alphen a/d Rijn	0.8	3.3	2	5.3	0.7	1.3	1.1
9	Haarlem	1.2	3.8	4.7	8.1	2.5	12.3	7.8
10	Amsterdam	0.9	4.5	10.8	15.2	6.1	9.2	10.7
11	Hilversum	0.3	1.7	12	8.6	4.2	1.4	2.3
12	Amersfoort	0.3	2.3	33	11.2	3.6	1	1.7
13	Utrecht	2	17.6	27.4	62.3	4.5	2.9	3.7
14	Almere	0.2	0.9	7.6	3.9	8.3	1.6	3.4
15	Zaanstad	0.3	0.9	1.9	2.3	1.4	12.3	8
16	Purmerend	0.2	0.7	2.3	2	2.2	5.5	11.6

C.2. OD-MATRIX BASED ON TRAVEL TIMES

Table C.3: OD matrix (×1000)

nr.	Name	1	2	3	4	5	6	7	8	9	10	11	12	13	14	15	16
1	Den Haag	765	5.1	197.1	8.4	11.4	29.1	23.1	5.6	6.1	3.6	0.3	0.3	6.4	0.2	0.6	0.5
2	Nissewaard	5.1	204.7	34.7	8.6	2.3	2.2	0.9	0.7	0.5	0.4	0.1	0.1	1.9	0	0.1	0.1
3	Rotterdam	197.1	34.7	716.9	29.1	17.9	53.1	16.3	5.4	5	3.1	0.4	0.4	9.9	0.2	0.5	0.4
4	Dordrecht	8.4	8.6	29.1	382.6	14.8	5.4	1.4	3.4	1.2	2.5	1	1.5	21.7	0.3	0.2	0.2
5	Gouda	11.4	2.3	17.9	14.8	101.3	33.1	6.8	35.2	4.4	3.9	0.9	1.1	46.8	0.3	0.4	0.3
6	Zoetermeer	29.1	2.2	53.1	5.4	33.1	162.1	6.7	6.6	1.8	1.1	0.3	0.3	9.6	0.1	0.2	0.1
7	Leiden	23.1	0.9	16.3	1.4	6.8	6.7	318.7	18.3	35.5	11	0.5	0.2	5.4	0.4	1.8	1.3
8	Alphen a/d Rijn	5.6	0.7	5.4	3.4	35.2	6.6	18.3	84.6	10.8	12.5	0.5	0.5	17	0.3	0.8	0.6
9	Haarlem	6.1	0.5	5	1.2	4.4	1.8	35.5	10.8	632	72.3	2.4	1	8.9	1.7	23	7
10	Amsterdam	3.6	0.4	3.1	2.5	3.9	1.1	11	12.5	72.3	796.9	29.1	7.8	69.9	18.1	12.9	29.8
11	Hilversum	0.3	0.1	0.4	1	0.9	0.3	0.5	0.5	2.4	29.1	149.2	27	26.2	10.7	1.5	3.3
12	Amersfoort	0.3	0.1	0.4	1.5	1.1	0.3	0.2	0.5	1	7.8	27	259.4	37.3	6.4	0.5	1.1
13	Utrecht	6.4	1.9	9.9	21.7	46.8	9.6	5.4	17	8.9	69.9	26.2	37.3	496.7	5.5	2.1	3.7
14	Almere	0.2	0	0.2	0.3	0.3	0.1	0.4	0.3	1.7	18.1	10.7	6.4	5.5	201.6	1	2.2
15	Zaanstad	0.6	0.1	0.5	0.2	0.4	0.2	1.8	0.8	23	12.9	1.5	0.5	2.1	1	258.5	28.2
16	Purmerend	0.5	0.1	0.4	0.2	0.3	0.1	1.3	0.6	7	29.8	3.3	1.1	3.7	2.2	28.2	100.4

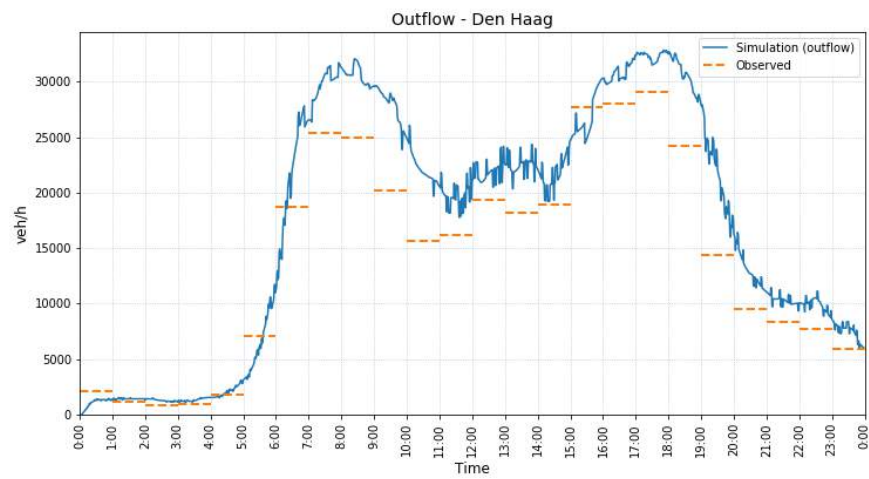
Table C.4: OD matrix (×1000) for the external areas. External zones have numbers above 100. Zone 112 for example means the external area near zone 12 (Amersfoort).

nr.	Name	102	104	112	113	114	115	116
1	Den Haag	2.7	6.7	1.3	4.4	0.4	1.2	1.1
2	Nissewaard	17.9	6.7	0.8	2	0.1	0.2	0.2
3	Rotterdam	8.9	15.3	1.8	6.4	0.4	1.2	1.1
4	Dordrecht	3.8	49	3.9	9.7	0.7	0.5	0.6
5	Gouda	1.3	7	2.4	10.5	0.5	0.7	0.7
6	Zoetermeer	1	3.2	0.9	3.6	0.2	0.4	0.3
7	Leiden	0.7	1.8	0.9	3.3	0.6	1.9	1.6
8	Alphen a/d Rijn	0.5	2.7	1.3	5.5	0.4	1	0.9
9	Haarlem	0.6	2	3.1	5.8	2	10.5	5.9
10	Amsterdam	0.6	3.6	12.3	21.6	8.6	8.8	14.5
11	Hilversum	0.1	1.2	11.7	6.5	3.2	1.4	2.3
12	Amersfoort	0.2	1.7	34.1	9	2.9	0.8	1.4
13	Utrecht	1.7	15	31.1	62.3	4.8	3.3	4.8
14	Almere	0.1	0.6	5.4	2.6	9.7	1	1.7
15	Zaanstad	0.1	0.3	1.4	1.5	0.9	14.3	6.7
16	Purmerend	0.1	0.5	2.2	2.3	1.5	6.7	12.2

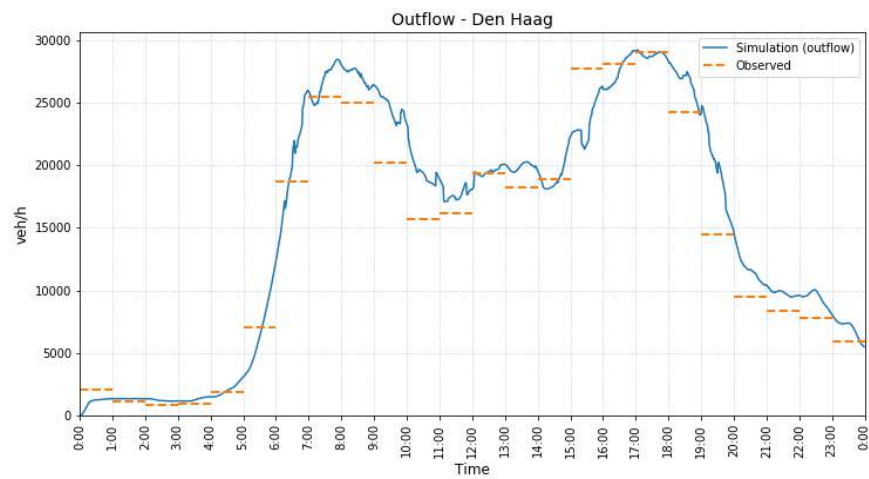
D

OUTFLOW PLOTS

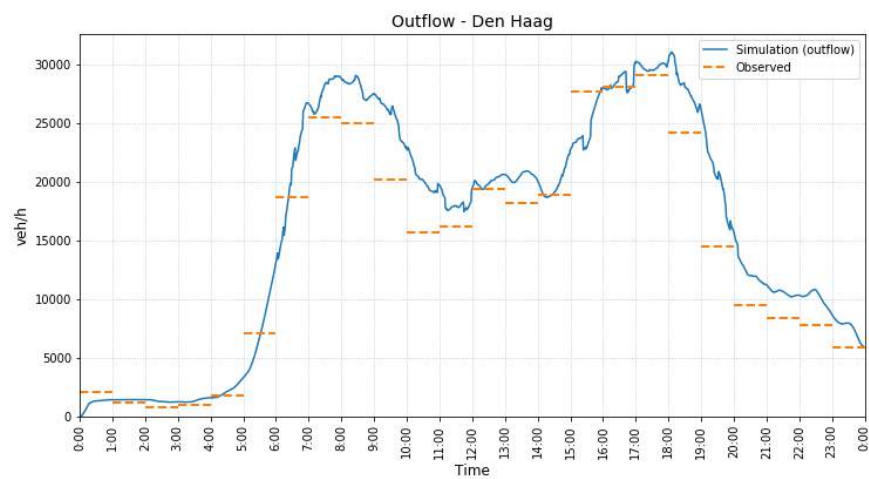
DEN HAAG



(a) Base case



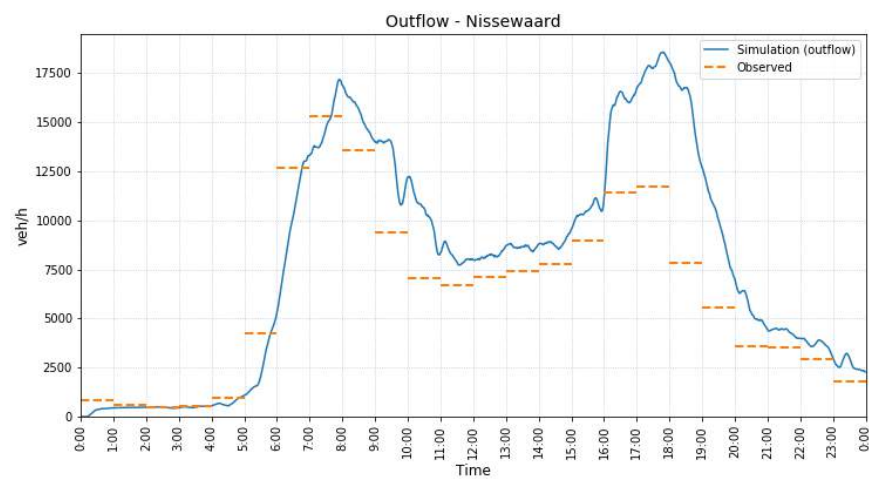
(b) Case with separation of local and through traffic



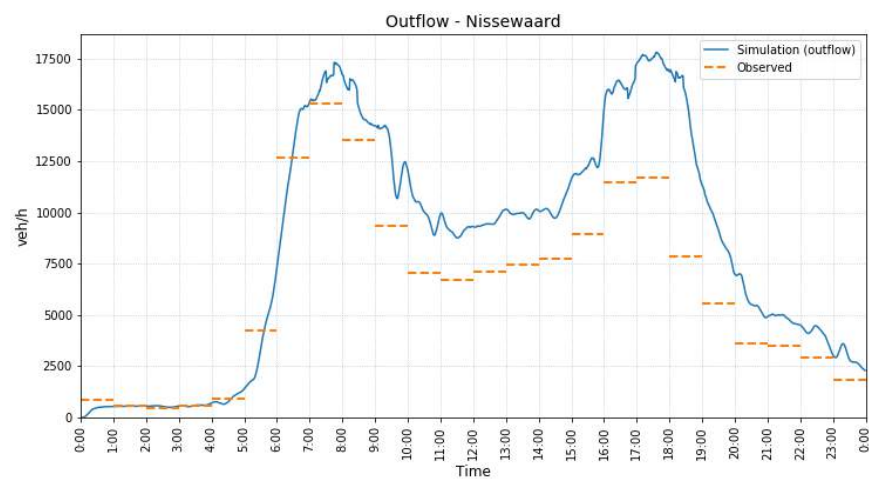
(c) Case with OD matrix based on travel times

Figure D.1: Outflow plots for Den Haag

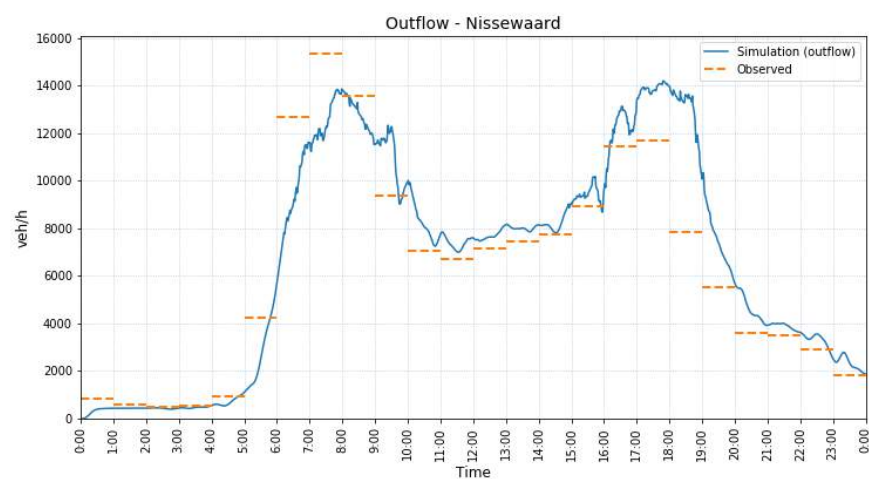
NISSEWAARD



(a) Base case



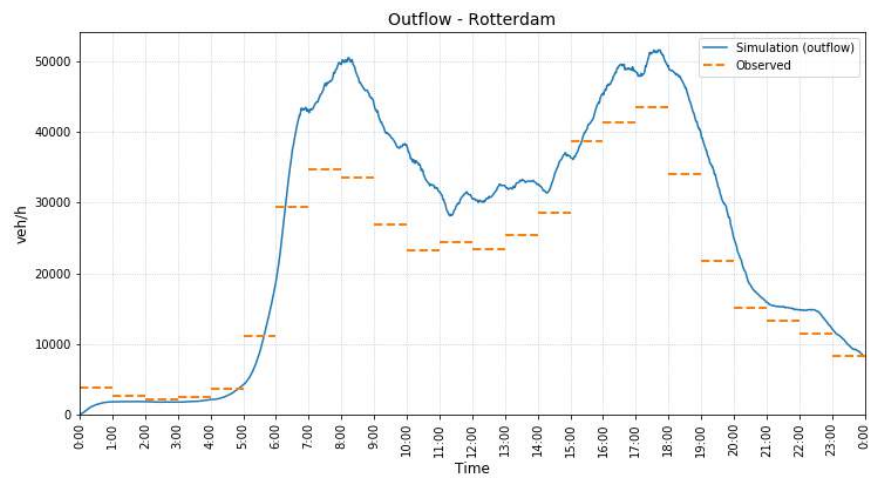
(b) Case with separation of local and through traffic



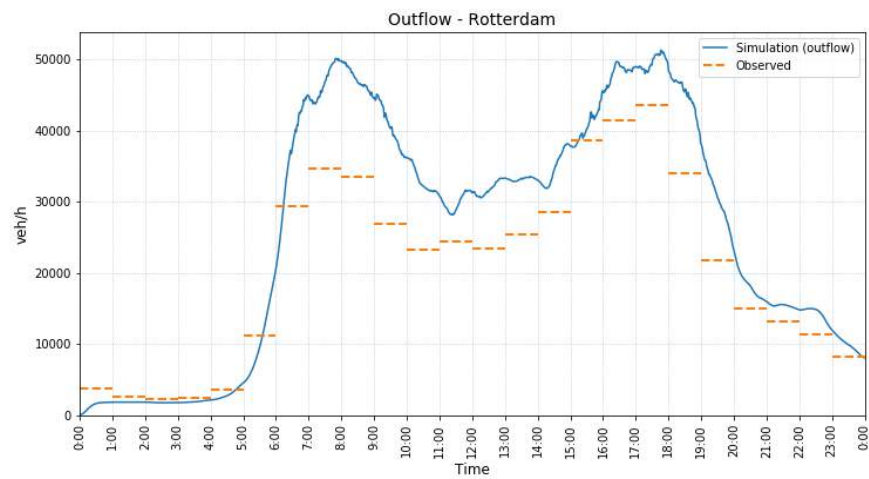
(c) Case with OD matrix based on travel times

Figure D.2: Outflow plots for Nissewaard

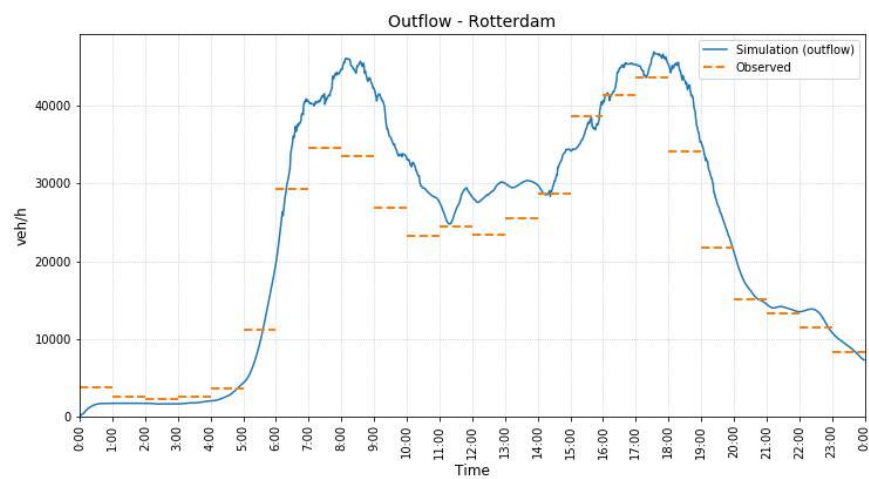
ROTTERDAM



(a) Base case



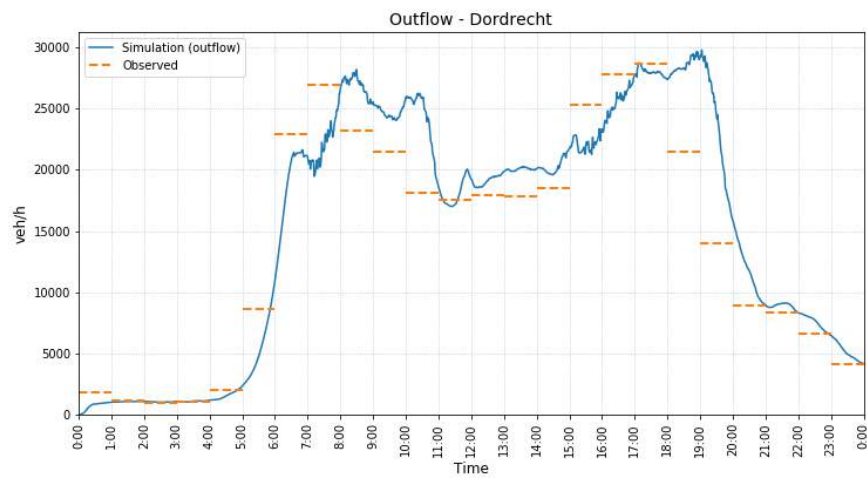
(b) Case with separation of local and through traffic



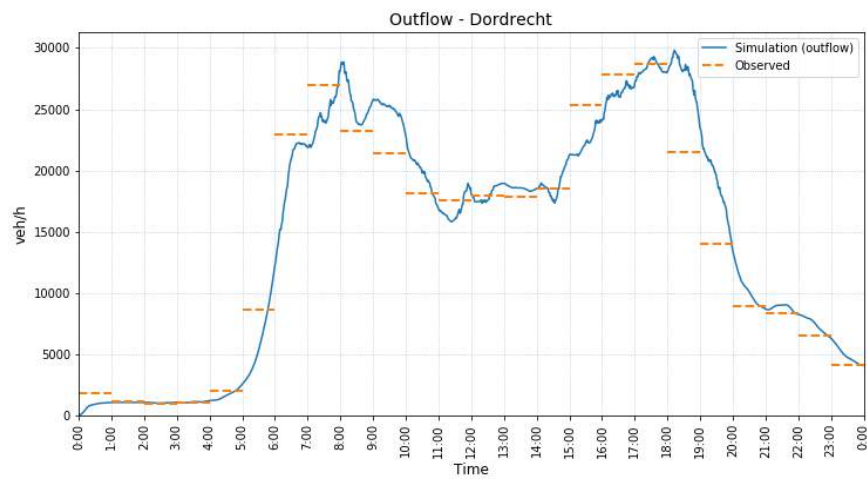
(c) Case with OD matrix based on travel times

Figure D.3: Outflow plots for Rotterdam

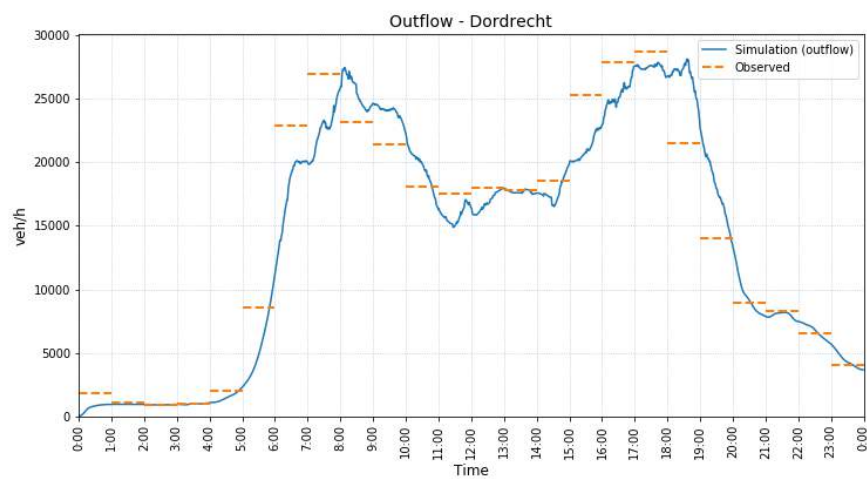
DORDRECHT



(a) Base case



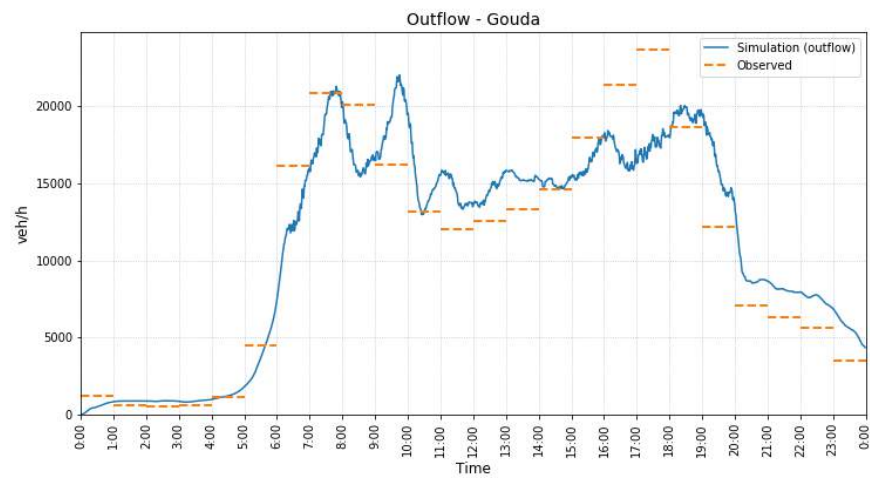
(b) Case with separation of local and through traffic



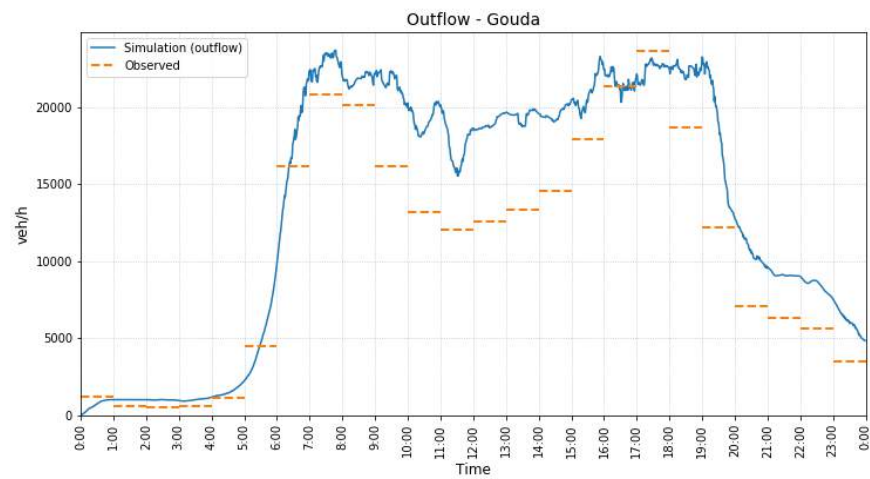
(c) Case with OD matrix based on travel times

Figure D.4: Outflow plots for Dordrecht

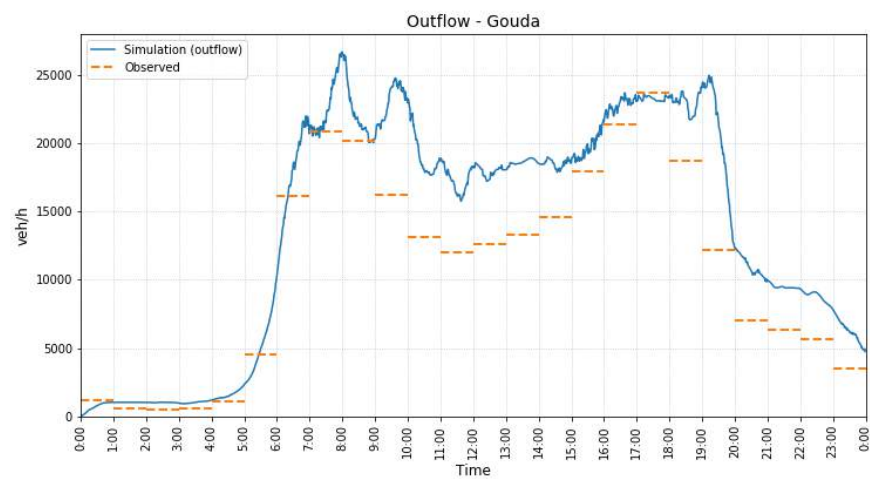
GOUDA



(a) Base case



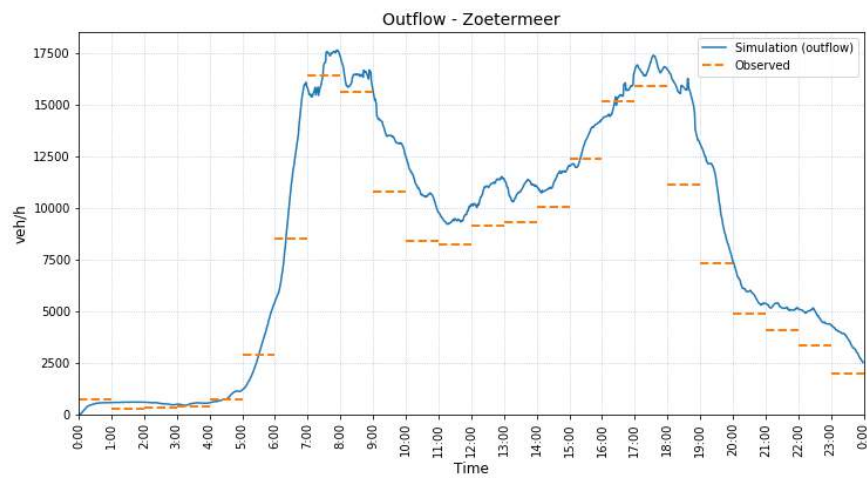
(b) Case with separation of local and through traffic



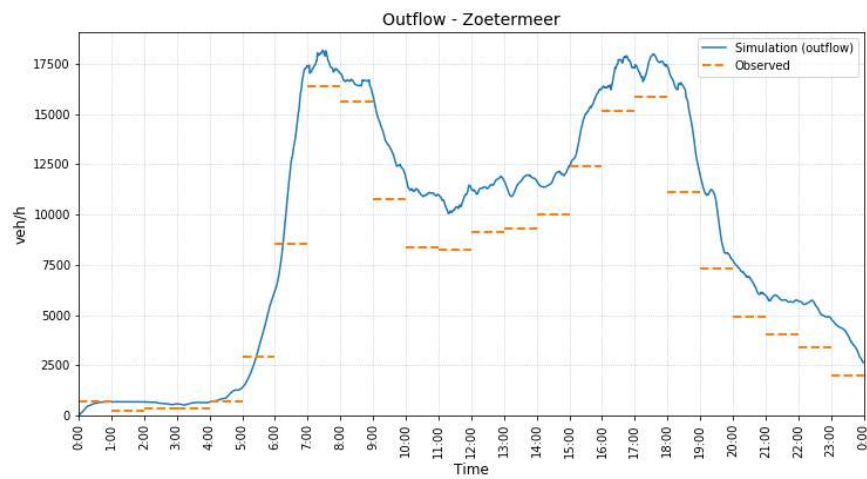
(c) Case with OD matrix based on travel times

Figure D.5: Outflow plots for Gouda

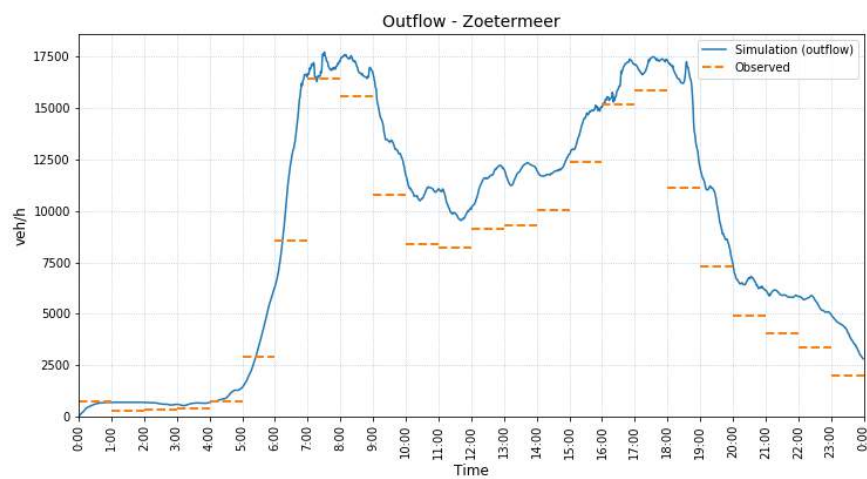
ZOETERMEER



(a) Base case



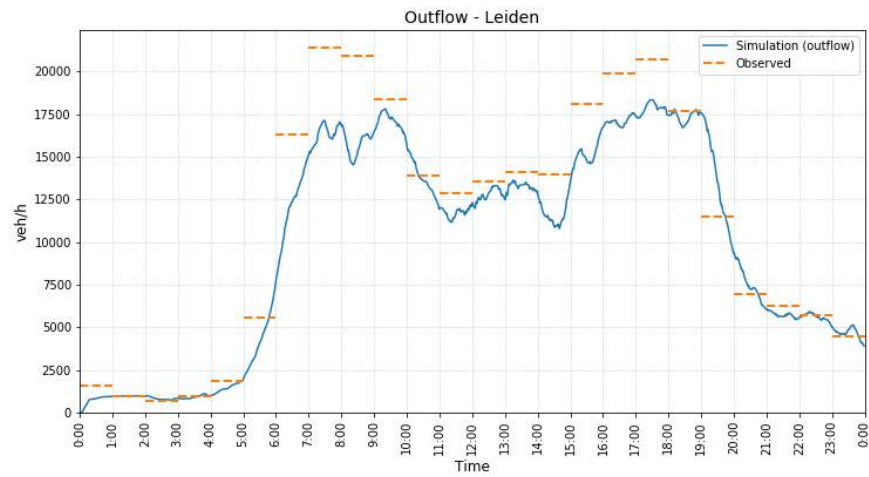
(b) Case with separation of local and through traffic



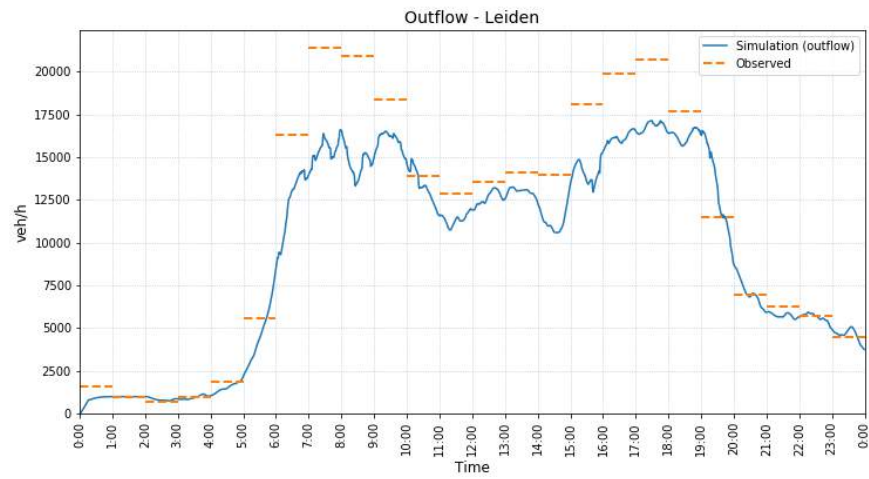
(c) Case with OD matrix based on travel times

Figure D.6: Outflow plots for Zoetermeer

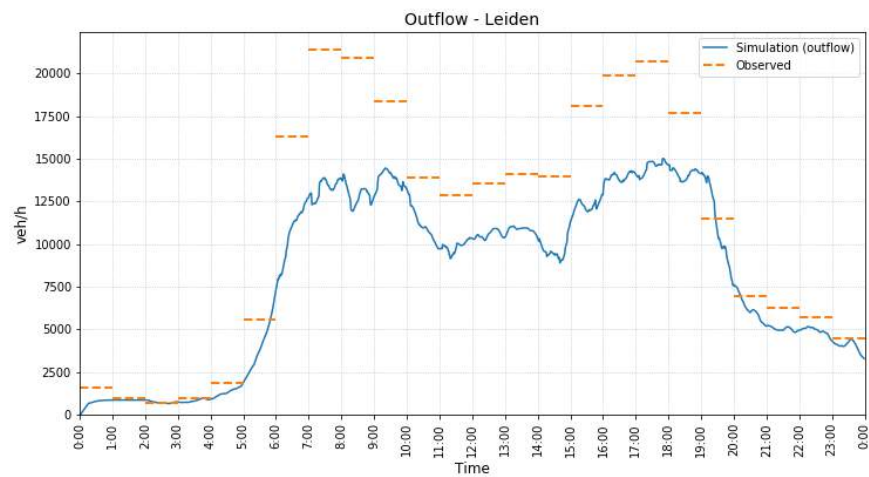
LEIDEN



(a) Base case



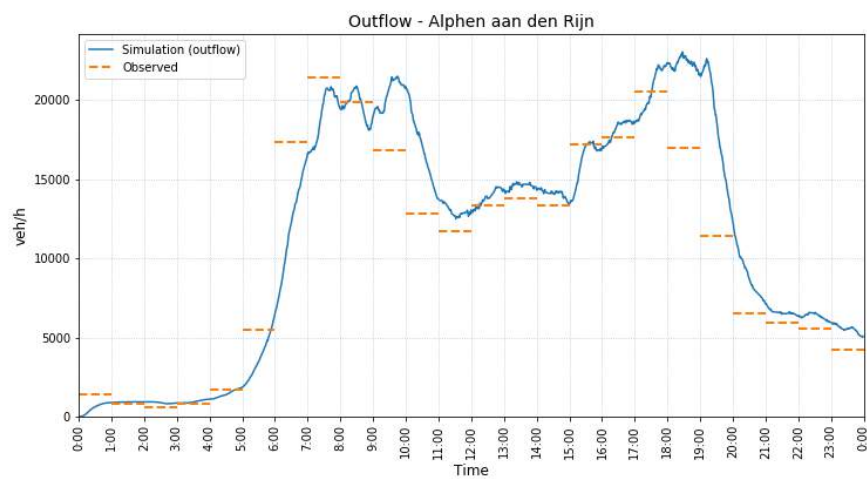
(b) Case with separation of local and through traffic



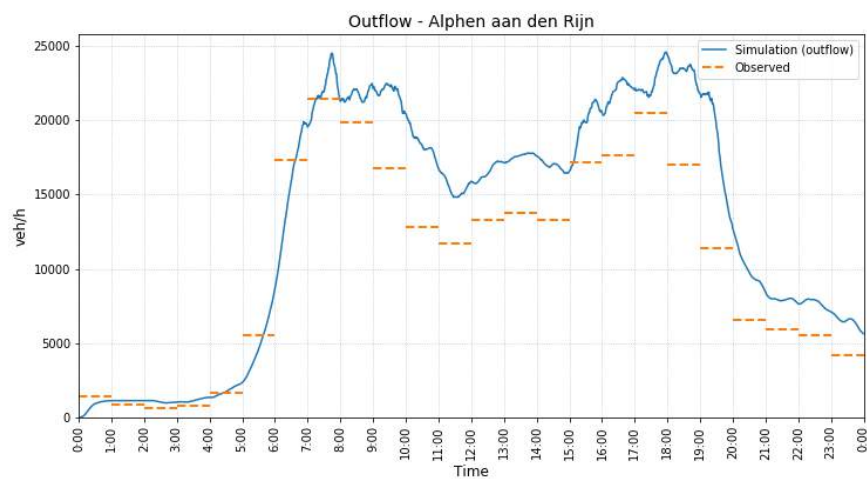
(c) Case with OD matrix based on travel times

Figure D.7: Outflow plots for Leiden

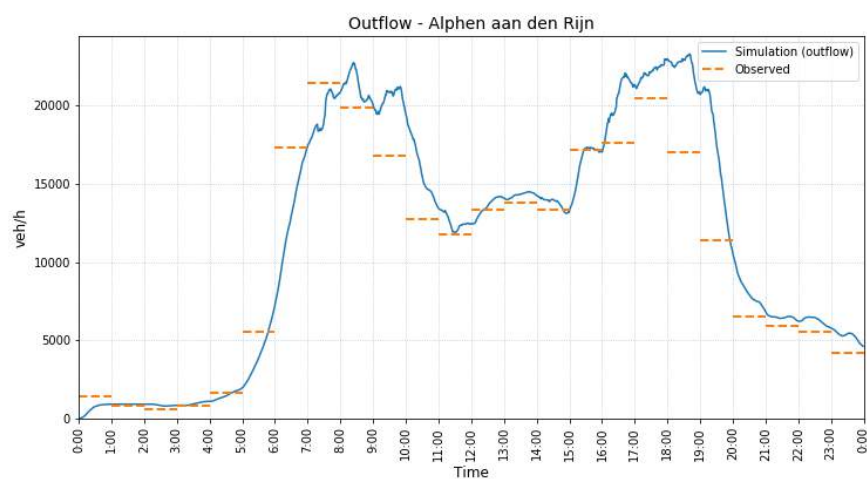
ALPHEN AAN DEN RIJN



(a) Base case



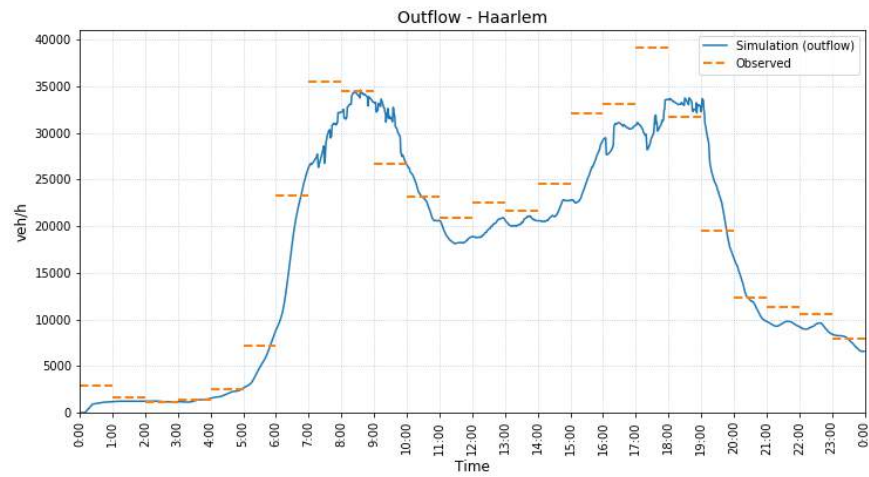
(b) Case with separation of local and through traffic



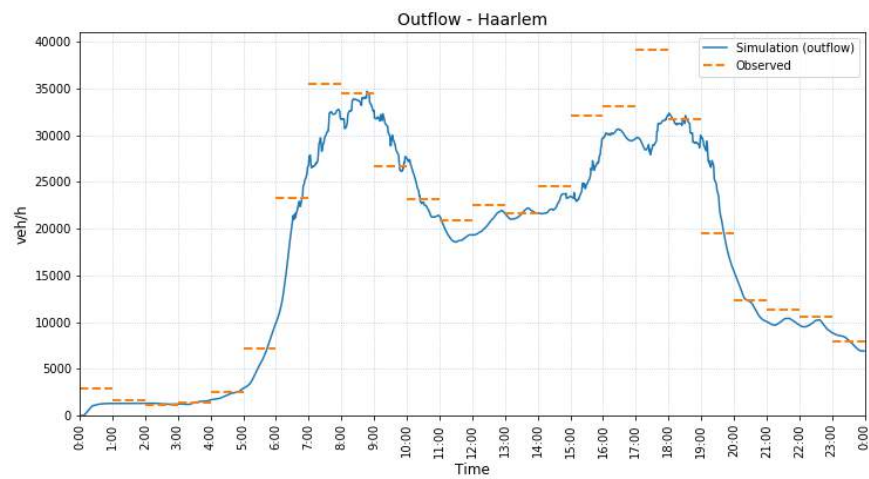
(c) Case with OD matrix based on travel times

Figure D.8: Outflow plots for Alphen aan den Rijn

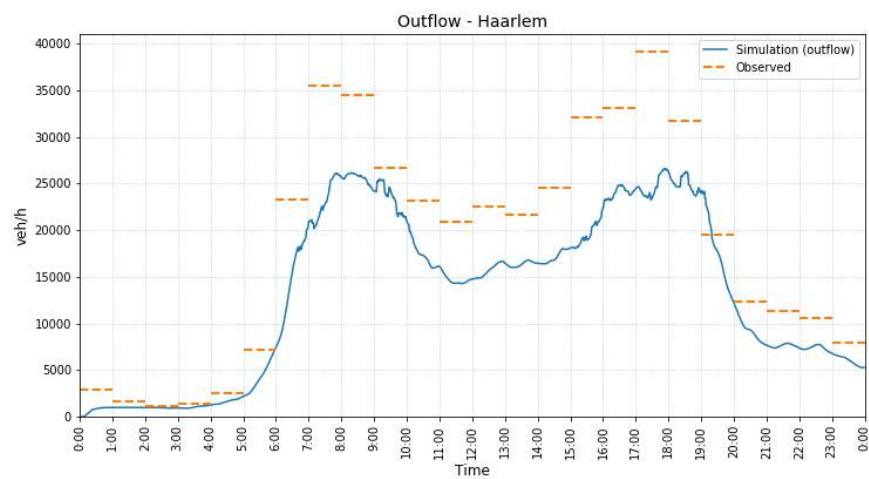
HAARLEM



(a) Base case



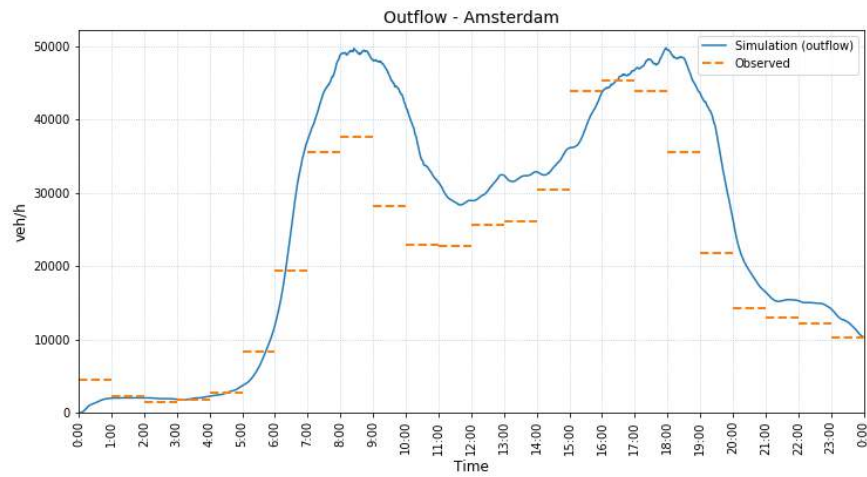
(b) Case with separation of local and through traffic



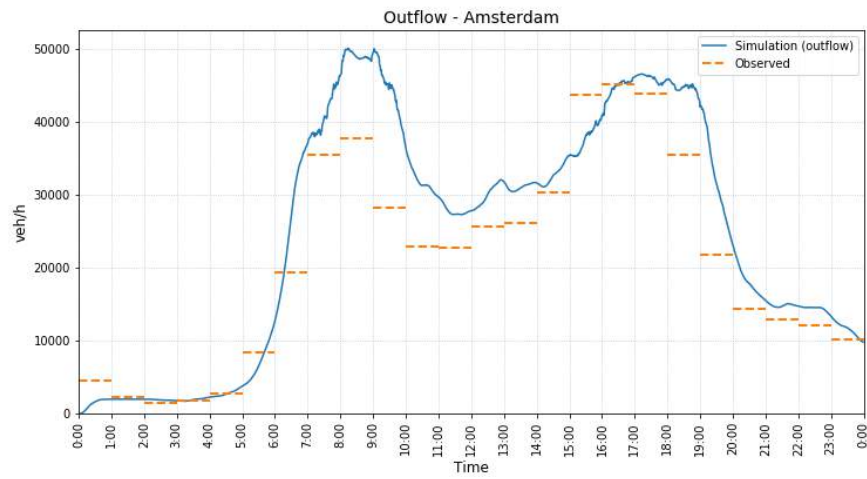
(c) Case with OD matrix based on travel times

Figure D.9: Outflow plots for Haarlem

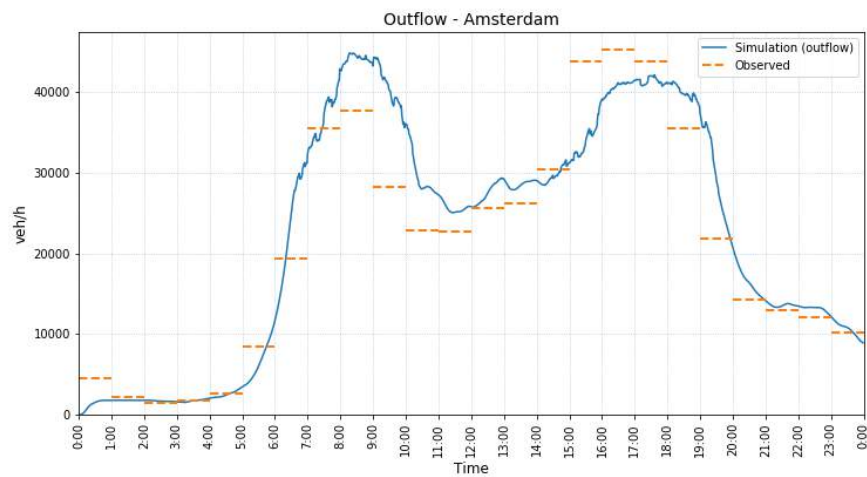
AMSTERDAM



(a) Base case



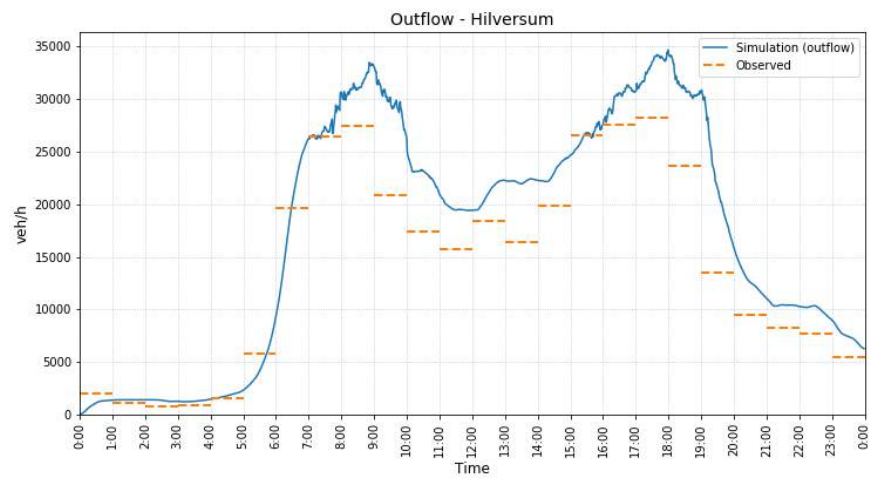
(b) Case with separation of local and through traffic



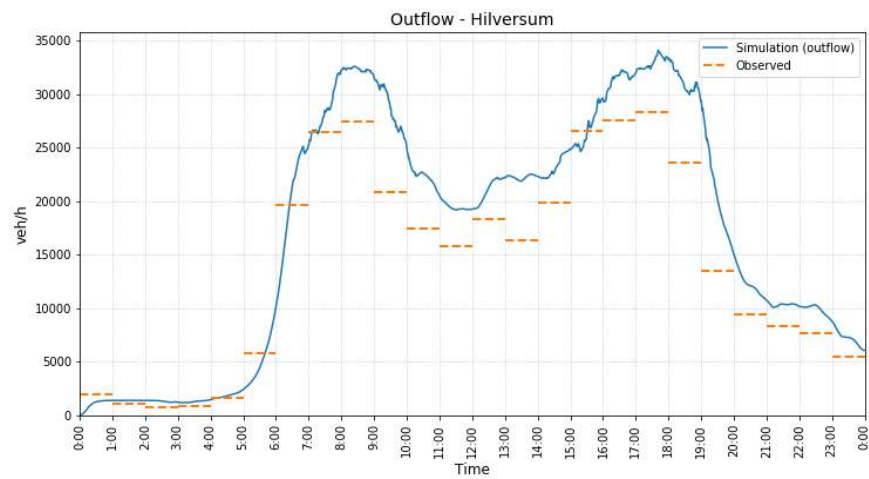
(c) Case with OD matrix based on travel times

Figure D.10: Outflow plots for Amsterdam

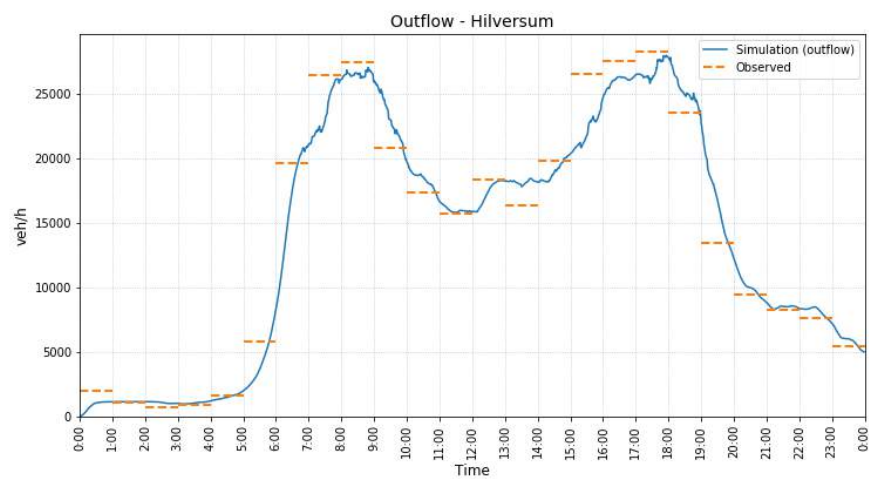
HILVERSUM



(a) Base case



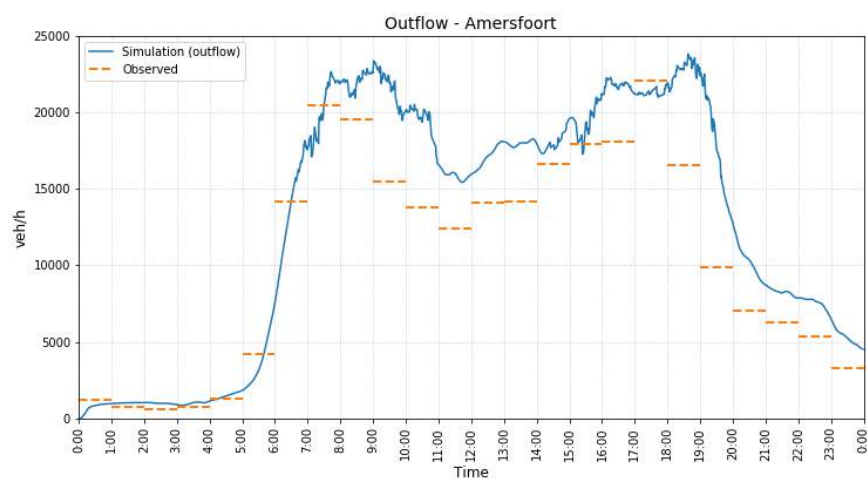
(b) Case with separation of local and through traffic



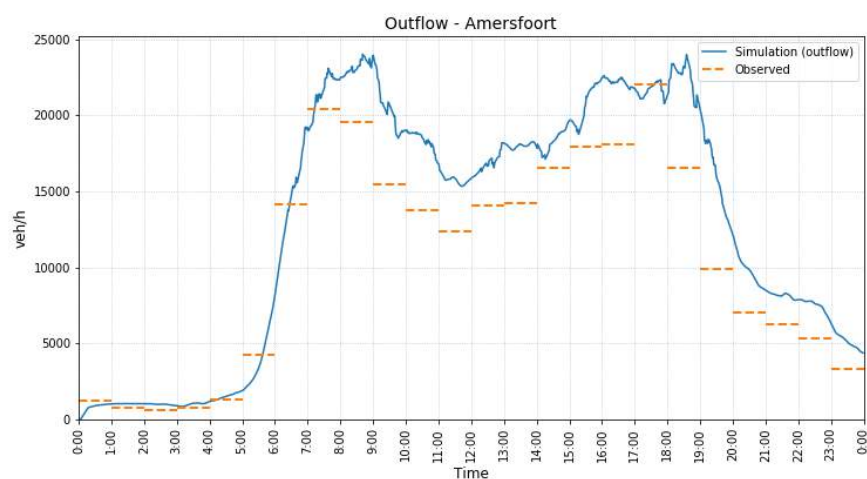
(c) Case with OD matrix based on travel times

Figure D.11: Outflow plots for Hilversum

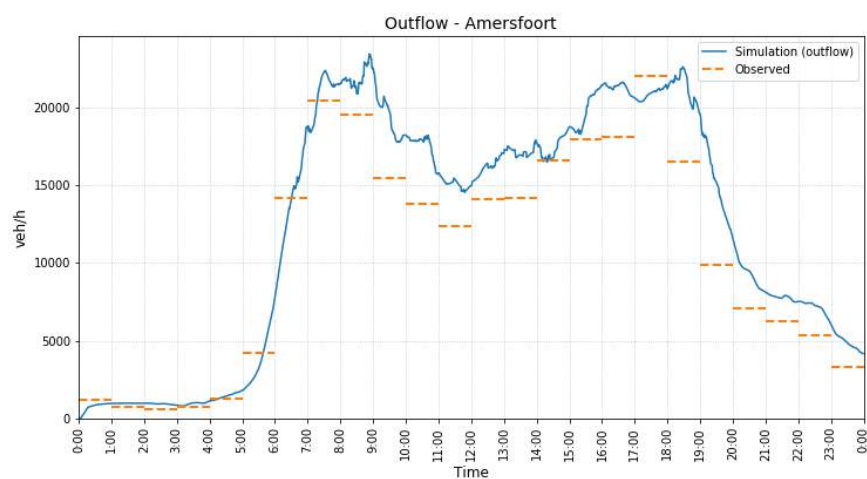
AMERSFOORT



(a) Base case



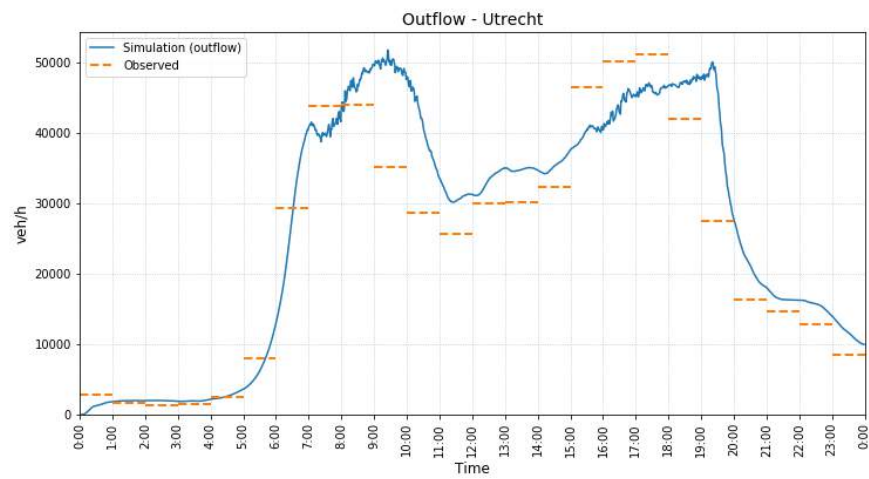
(b) Case with separation of local and through traffic



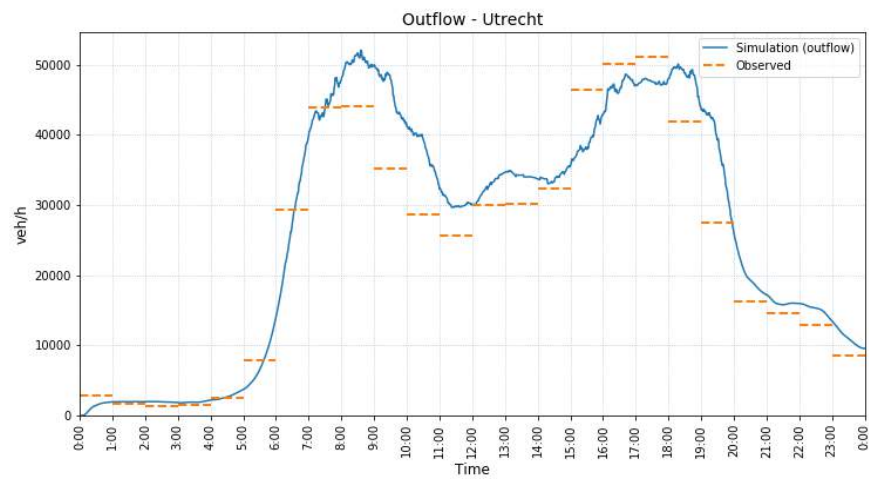
(c) Case with OD matrix based on travel times

Figure D.12: Outflow plots for Amersfoort

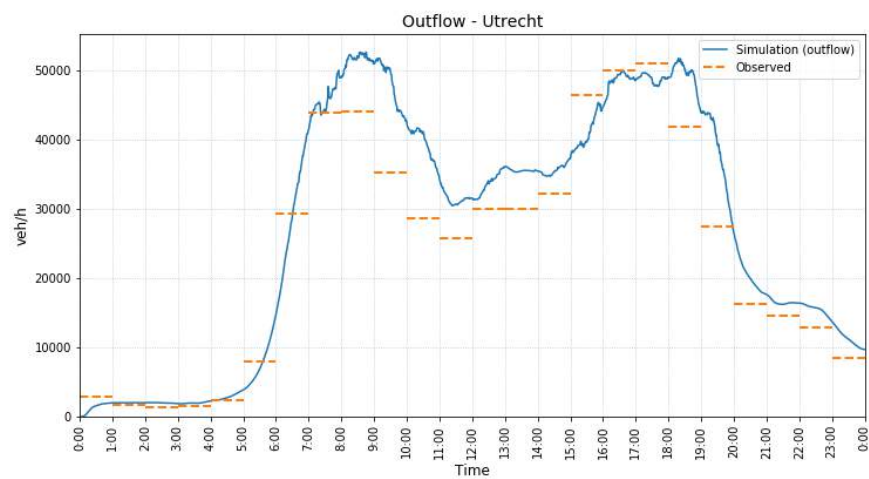
UTRECHT



(a) Base case



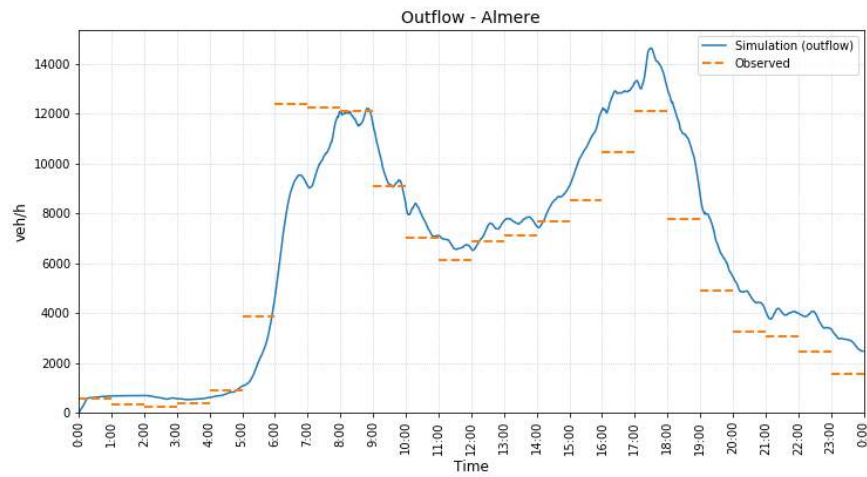
(b) Case with separation of local and through traffic



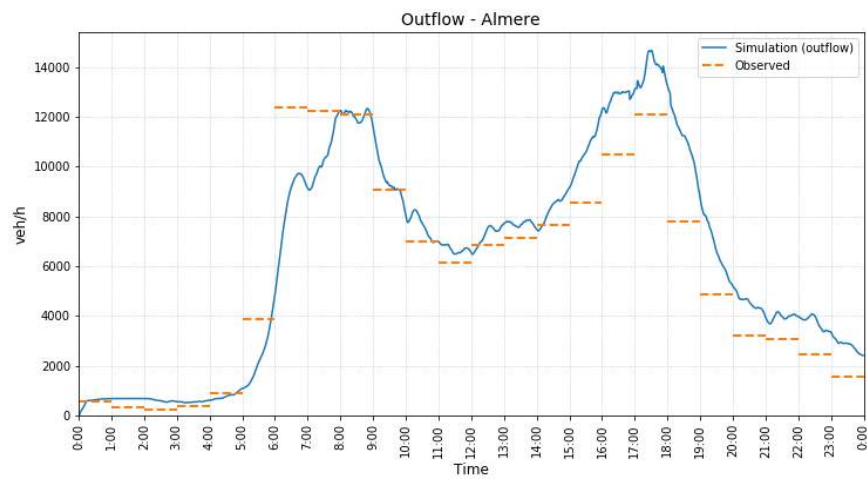
(c) Case with OD matrix based on travel times

Figure D.13: Outflow plots for Utrecht

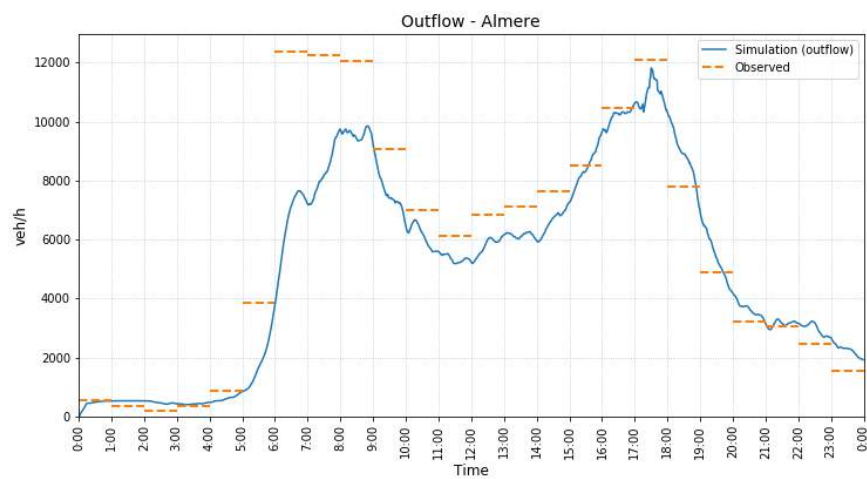
ALMERE



(a) Base case



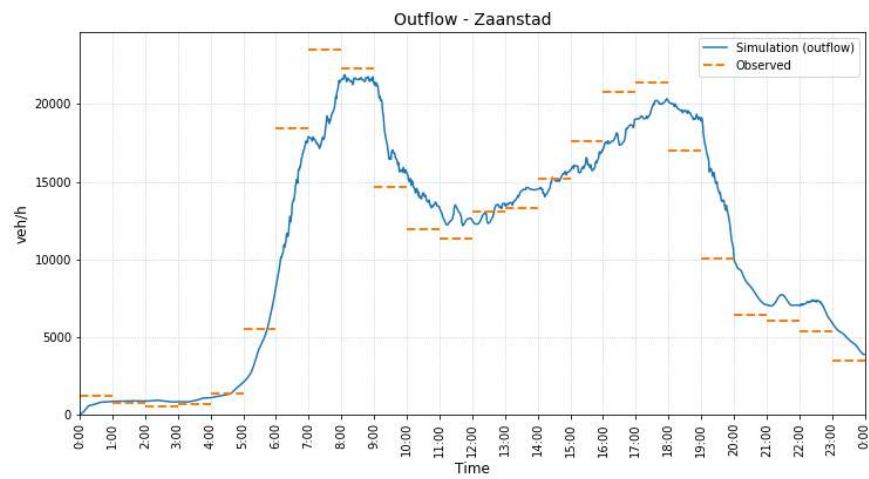
(b) Case with separation of local and through traffic



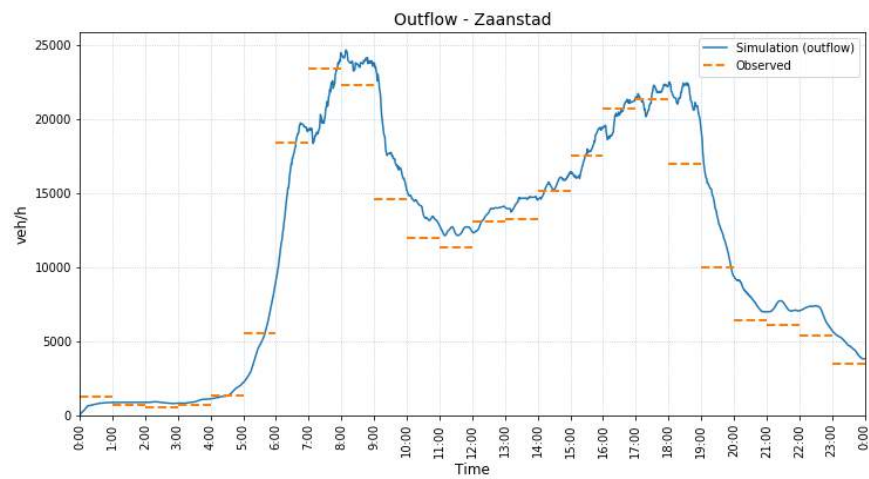
(c) Case with OD matrix based on travel times

Figure D.14: Outflow plots for Almere

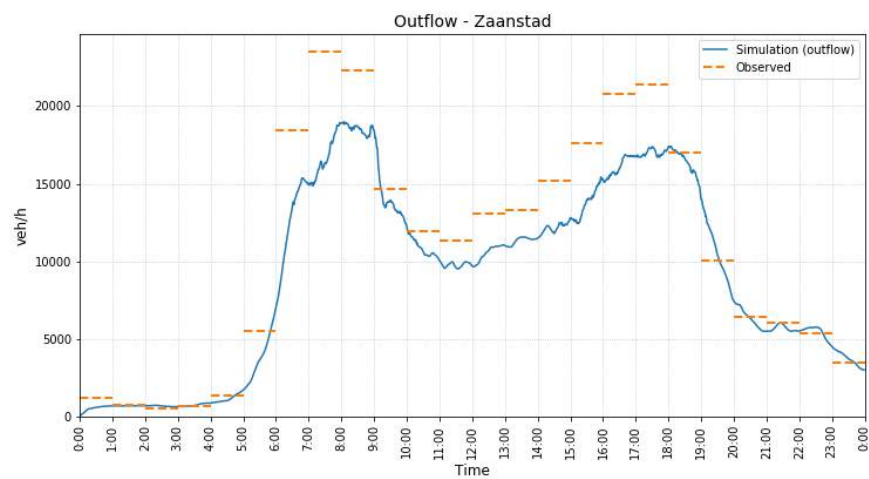
ZAASTAD



(a) Base case



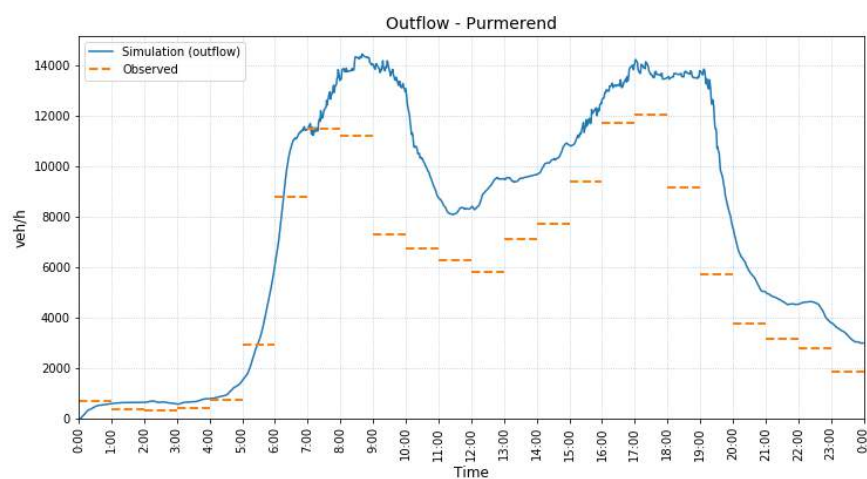
(b) Case with separation of local and through traffic



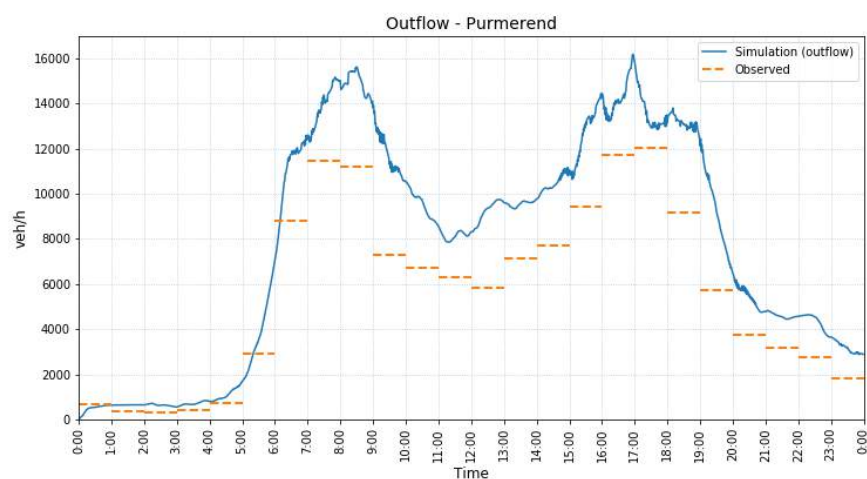
(c) Case with OD matrix based on travel times

Figure D.15: Outflow plots for Zaanstad

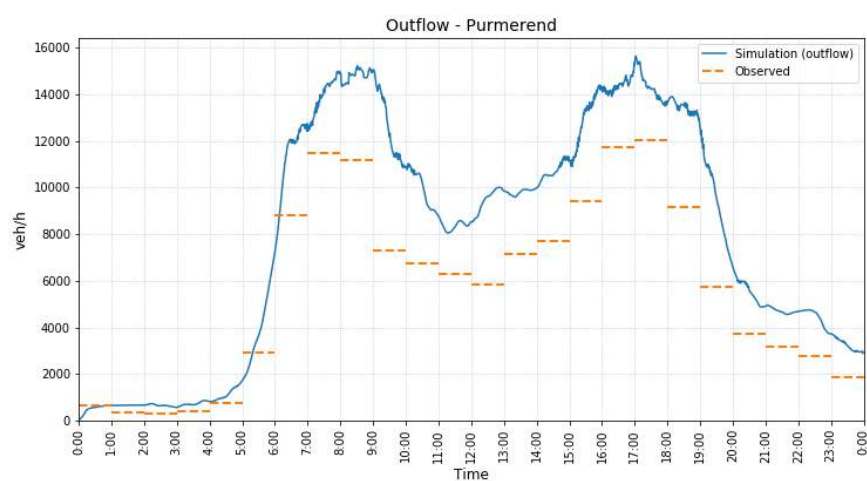
PURMEREND



(a) Base case



(b) Case with separation of local and through traffic



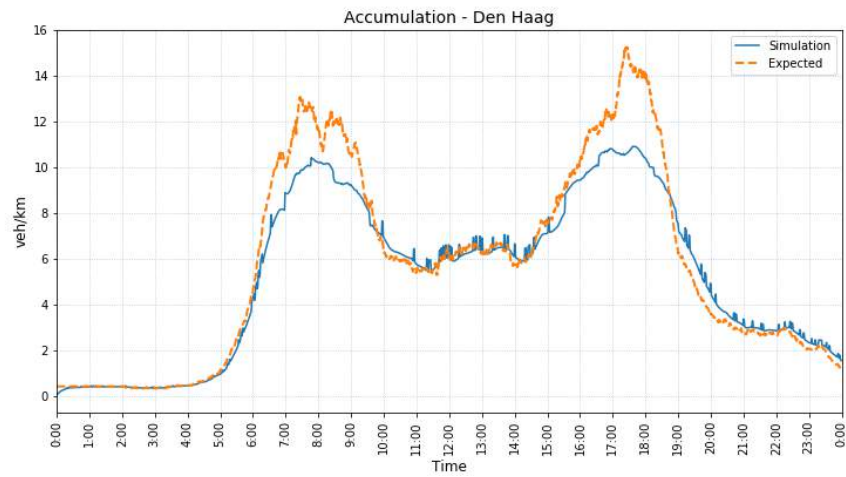
(c) Case with OD matrix based on travel times

Figure D.16: Outflow plots for Purmerend

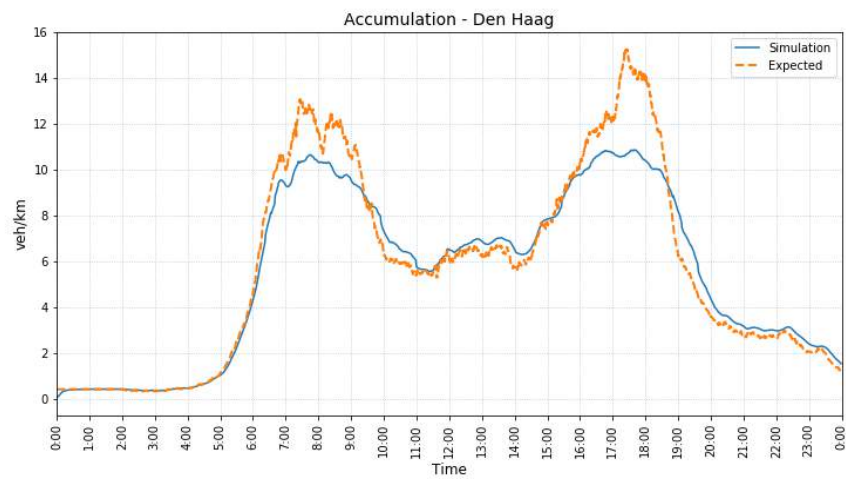
E

ACCUMULATION PLOTS

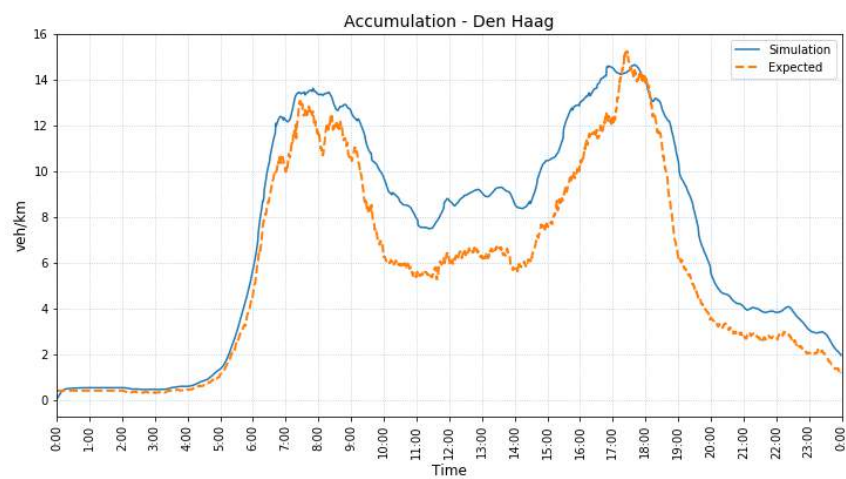
DEN HAAG



(a) Base case



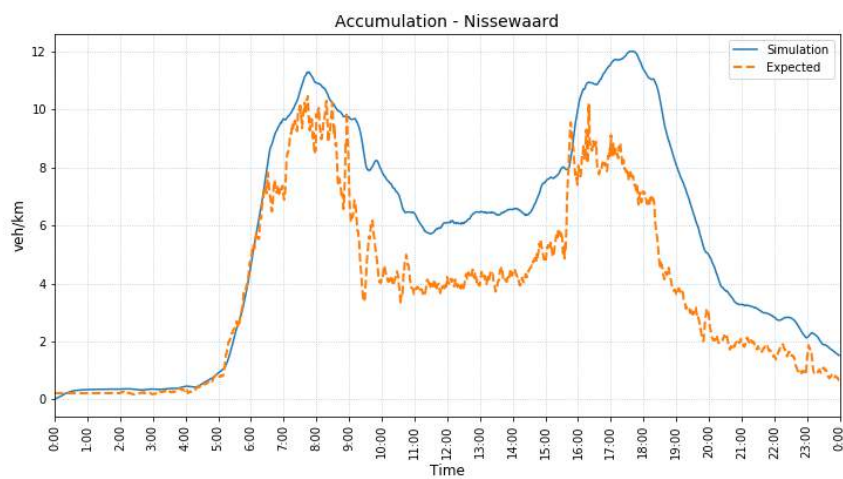
(b) Case with separation of local and through traffic



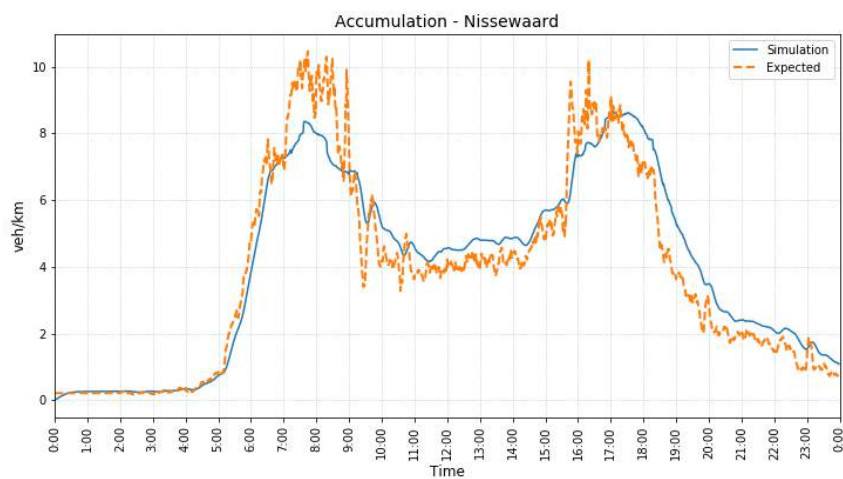
(c) Case with OD matrix based on travel times

Figure E.1: Accumulation plots for Den Haag

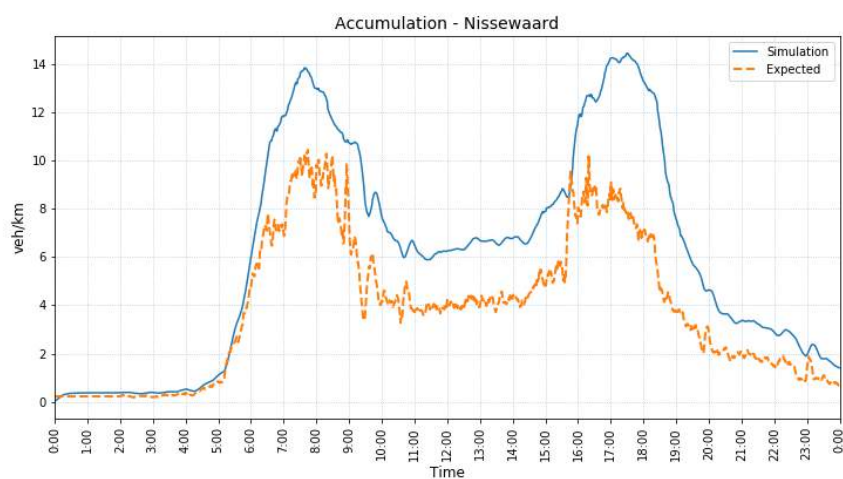
NISSEWAARD



(a) Base case



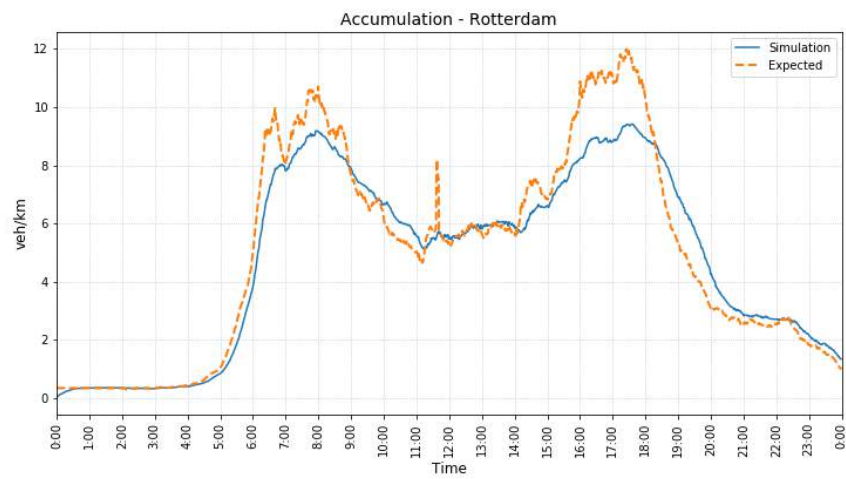
(b) Case with separation of local and through traffic



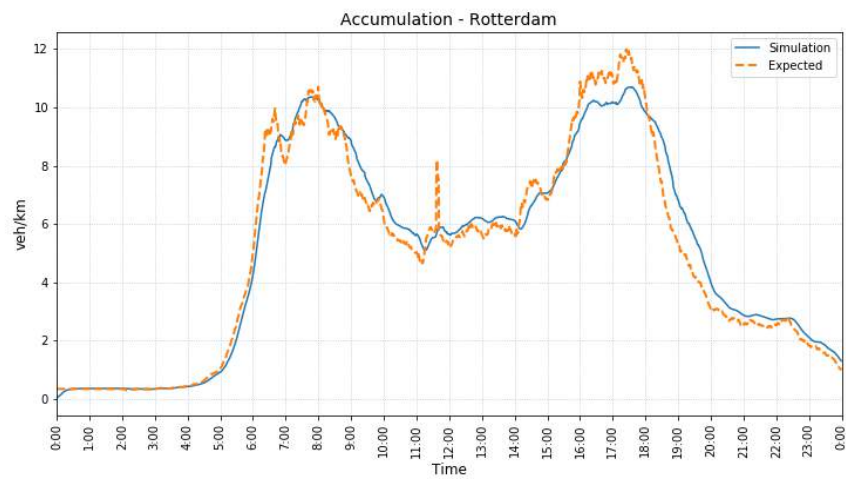
(c) Case with OD matrix based on travel times

Figure E.2: Accumulation plots for Nissewaard

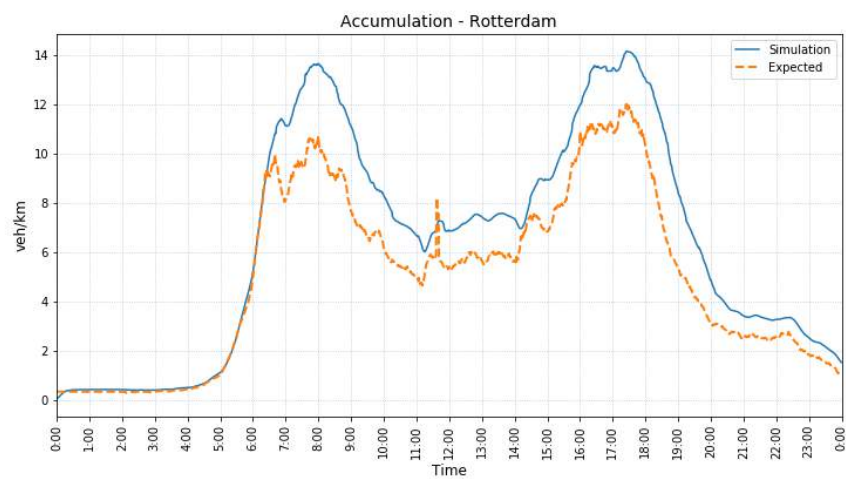
ROTTERDAM



(a) Base case



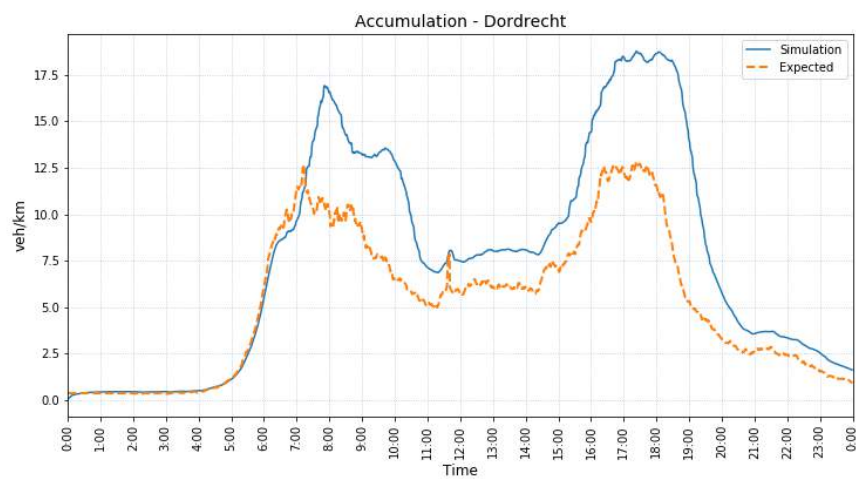
(b) Case with separation of local and through traffic



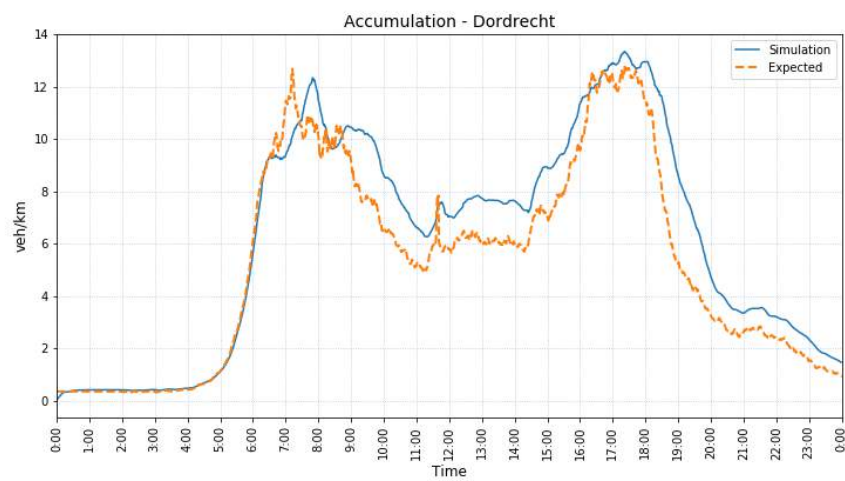
(c) Case with OD matrix based on travel times

Figure E.3: Accumulation plots for Rotterdam

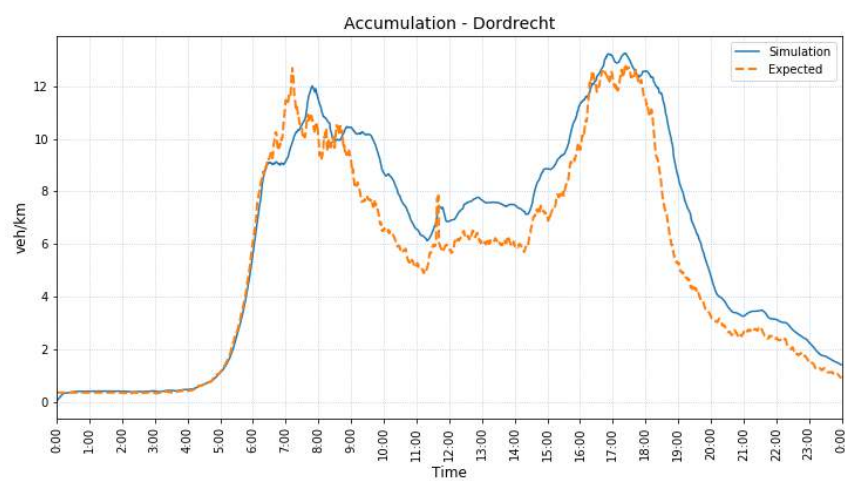
DORDRECHT



(a) Base case



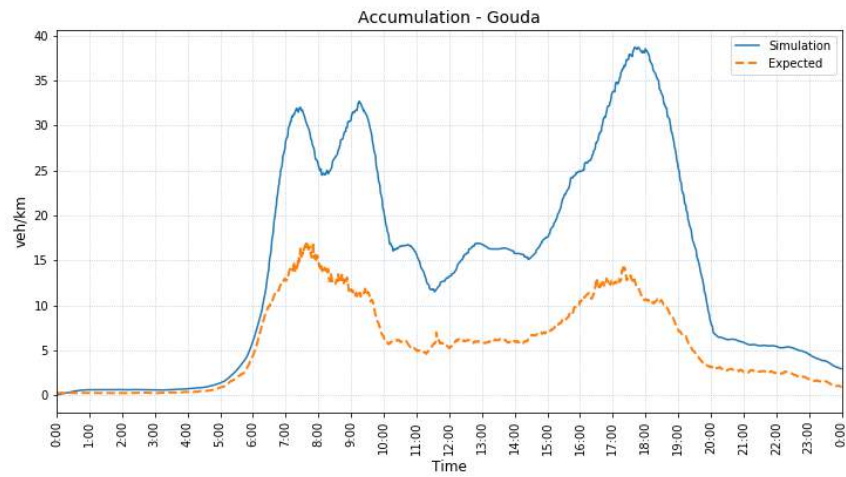
(b) Case with separation of local and through traffic



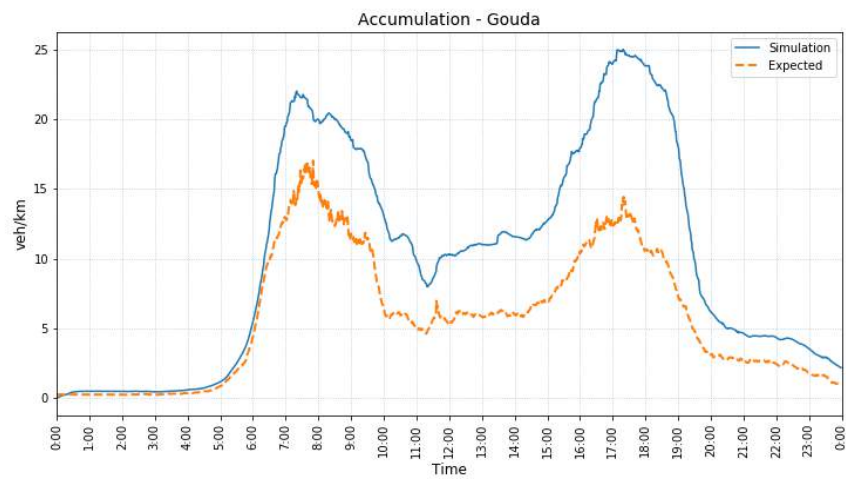
(c) Case with OD matrix based on travel times

Figure E.4: Accumulation plots for Dordrecht

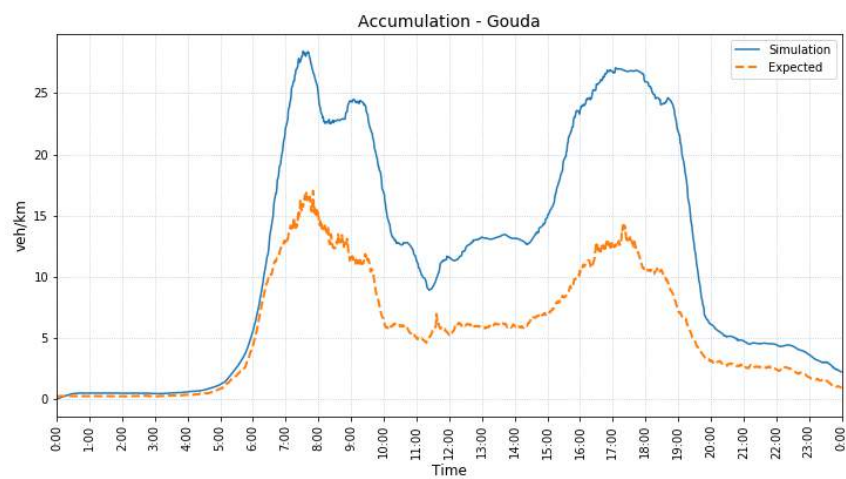
GOUDA



(a) Base case



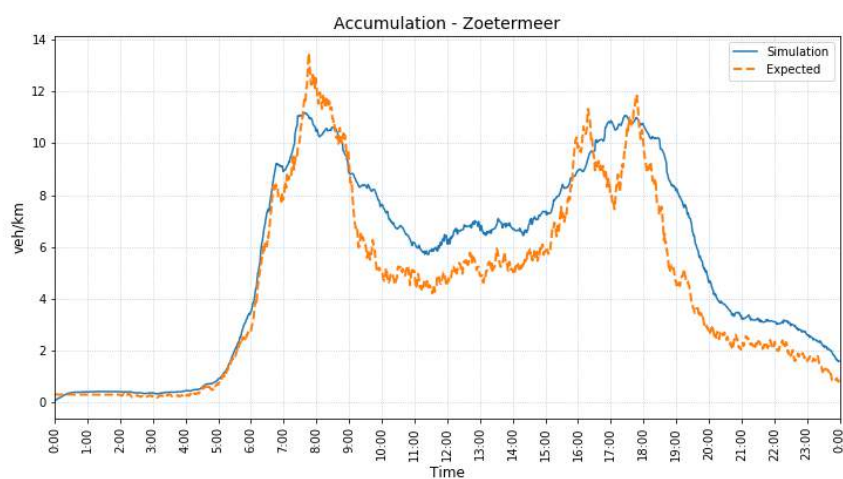
(b) Case with separation of local and through traffic



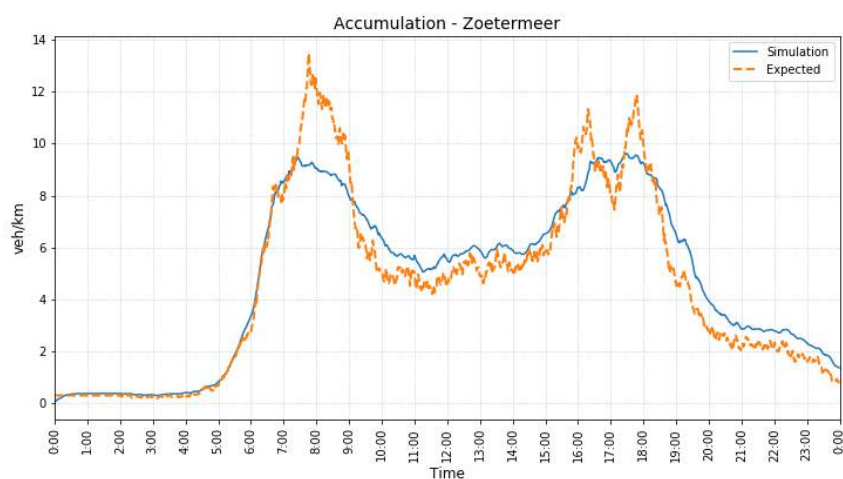
(c) Case with OD matrix based on travel times

Figure E.5: Accumulation plots for Gouda

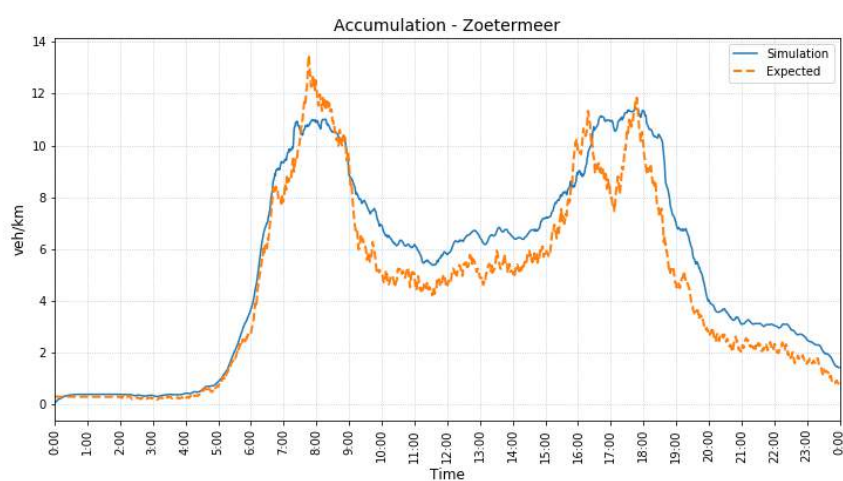
ZOETERMEER



(a) Base case



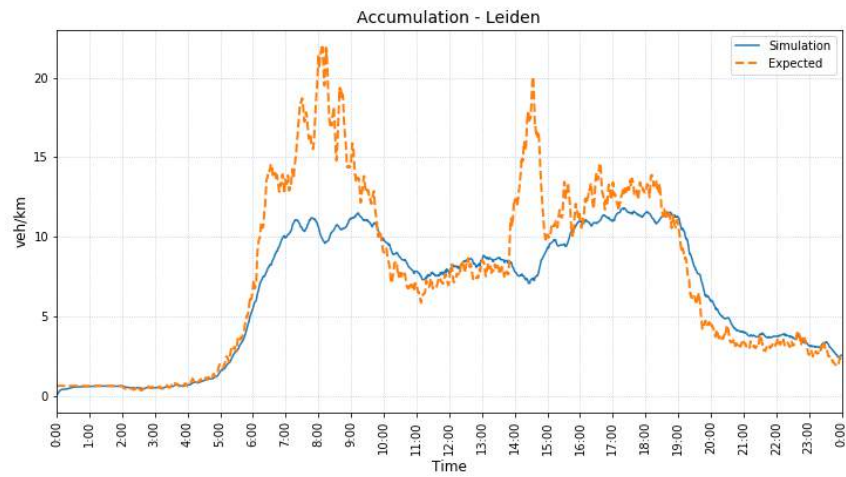
(b) Case with separation of local and through traffic



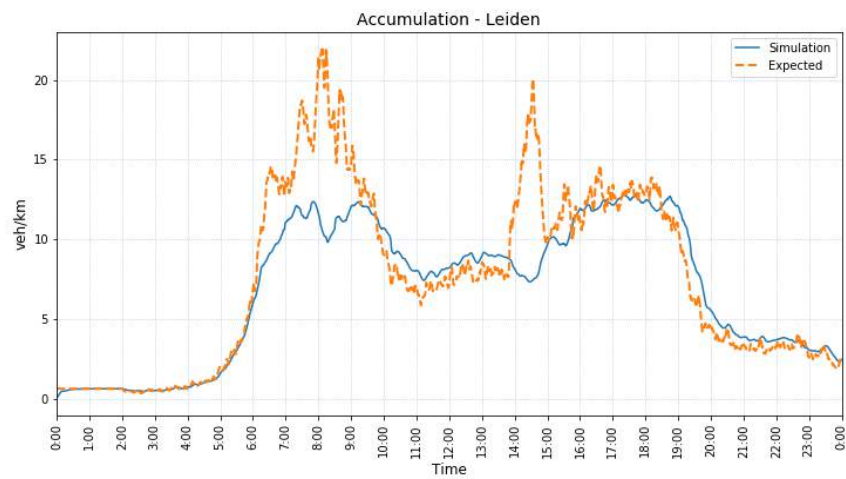
(c) Case with OD matrix based on travel times

Figure E.6: Accumulation plots for Zoetermeer

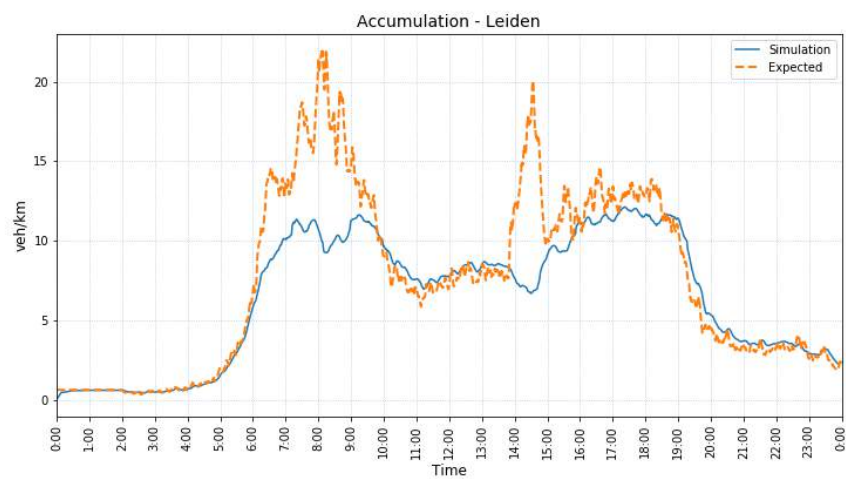
LEIDEN



(a) Base case



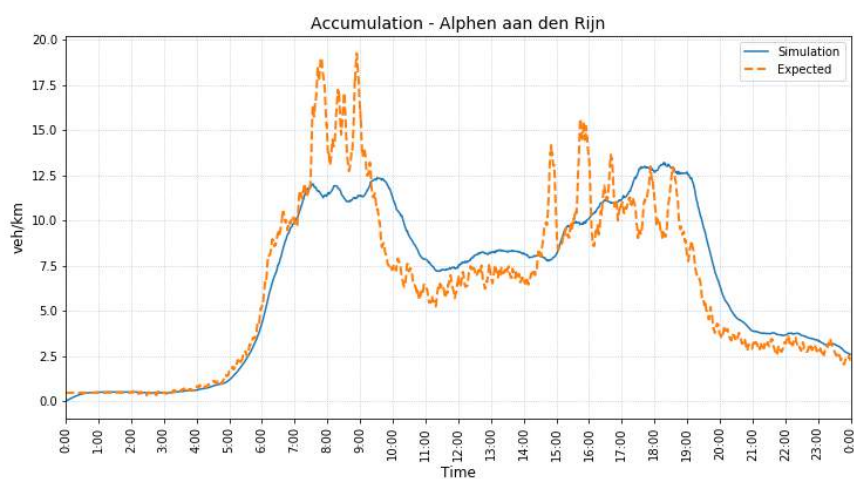
(b) Case with separation of local and through traffic



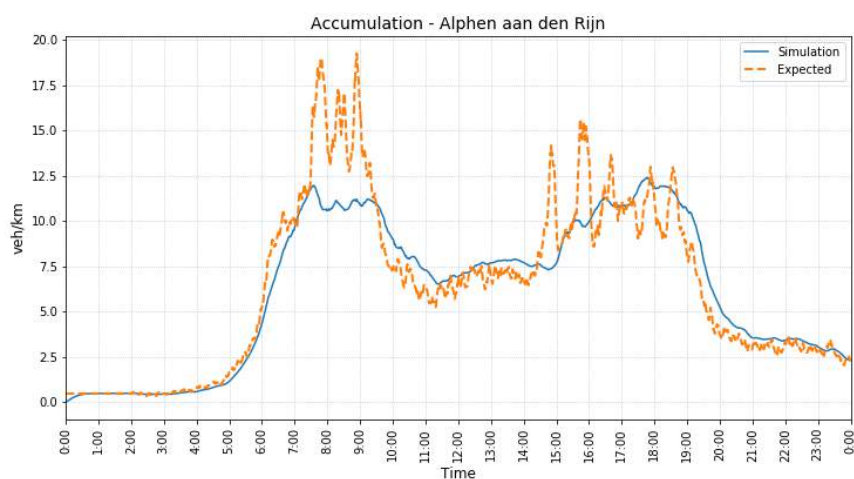
(c) Case with OD matrix based on travel times

Figure E.7: Accumulation plots for Leiden

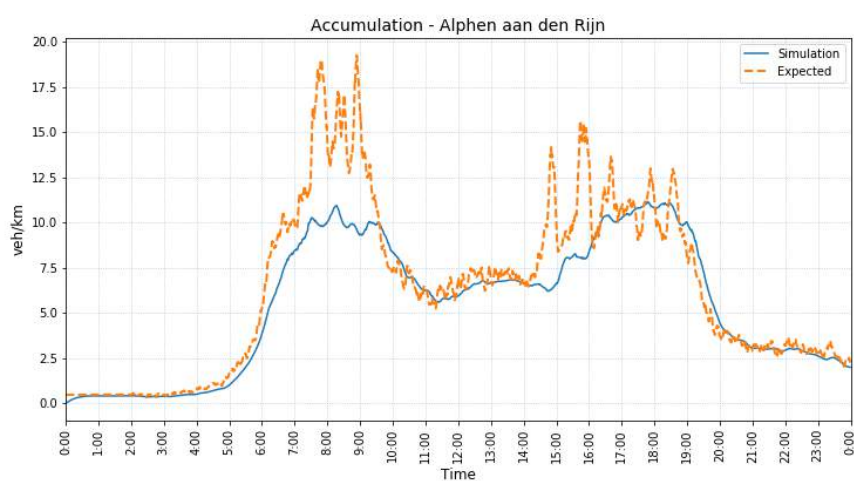
ALPHEN AAN DEN RIJN



(a) Base case



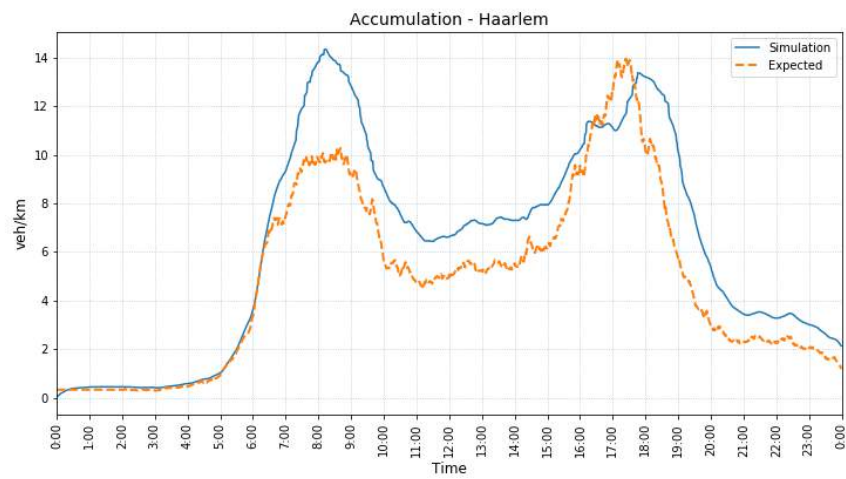
(b) Case with separation of local and through traffic



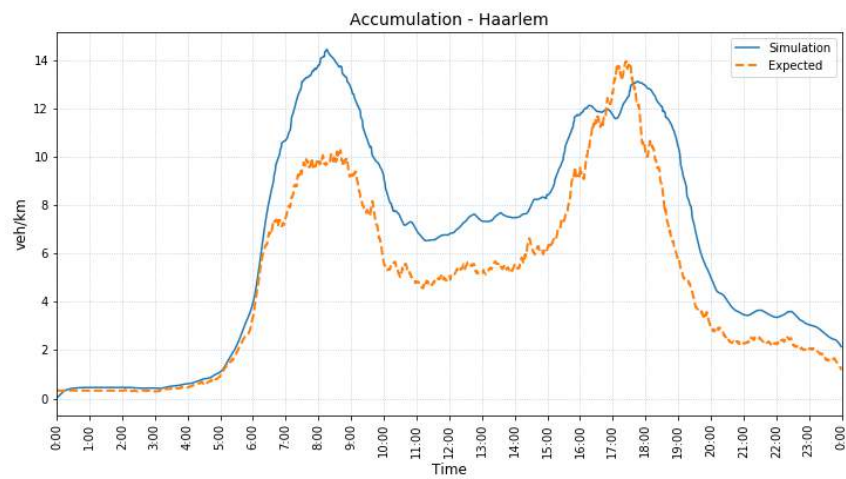
(c) Case with OD matrix based on travel times

Figure E.8: Accumulation plots for Alphen aan den Rijn

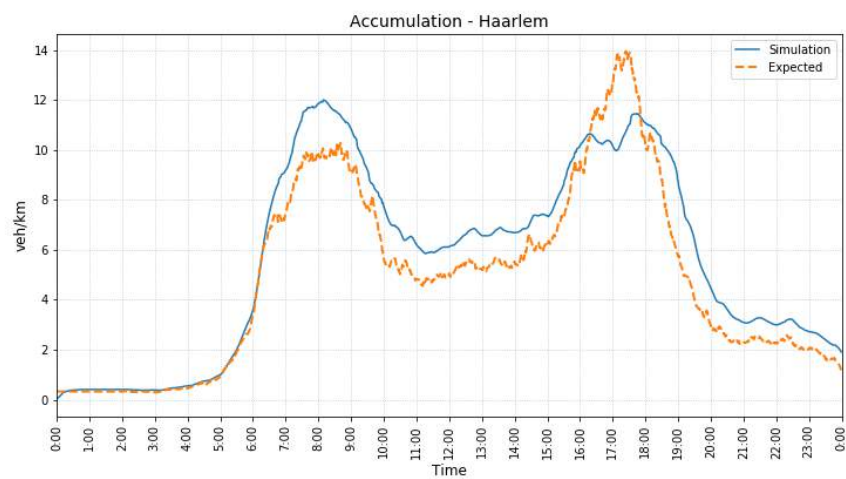
HAARLEM



(a) Base case



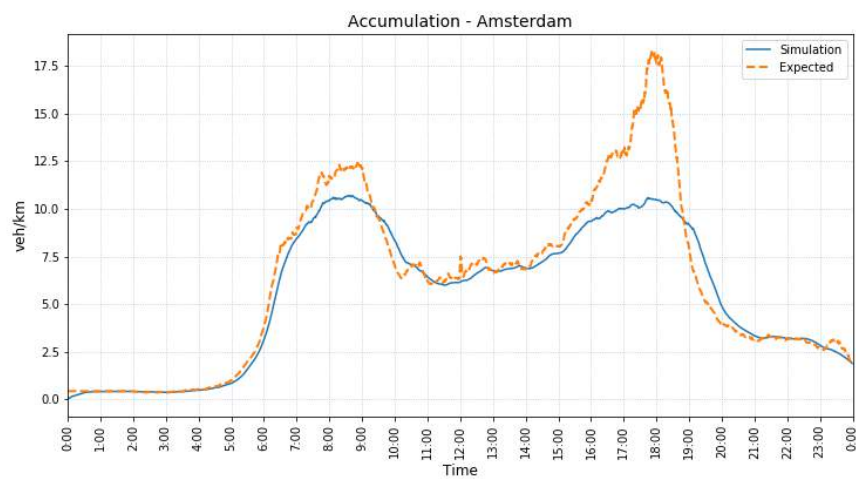
(b) Case with separation of local and through traffic



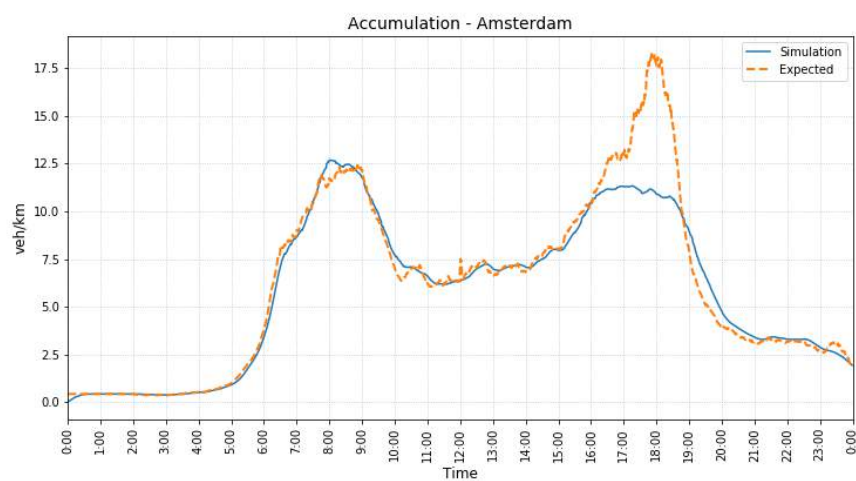
(c) Case with OD matrix based on travel times

Figure E.9: Accumulation plots for Haarlem

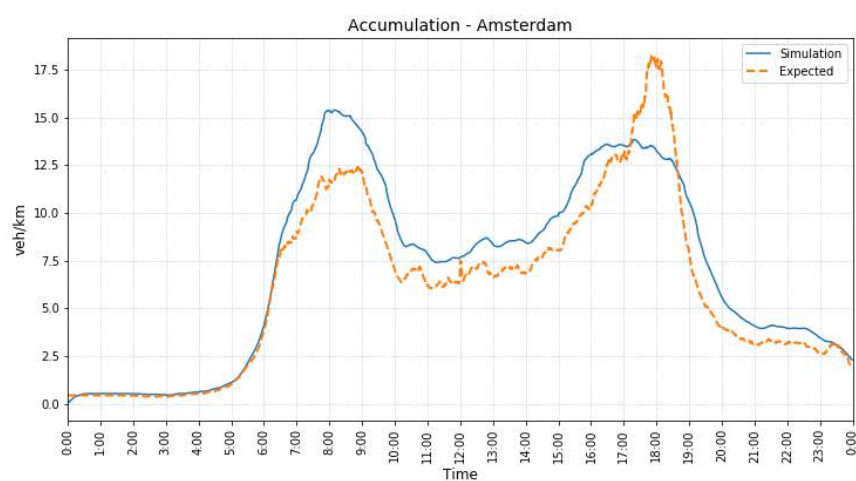
AMSTERDAM



(a) Base case



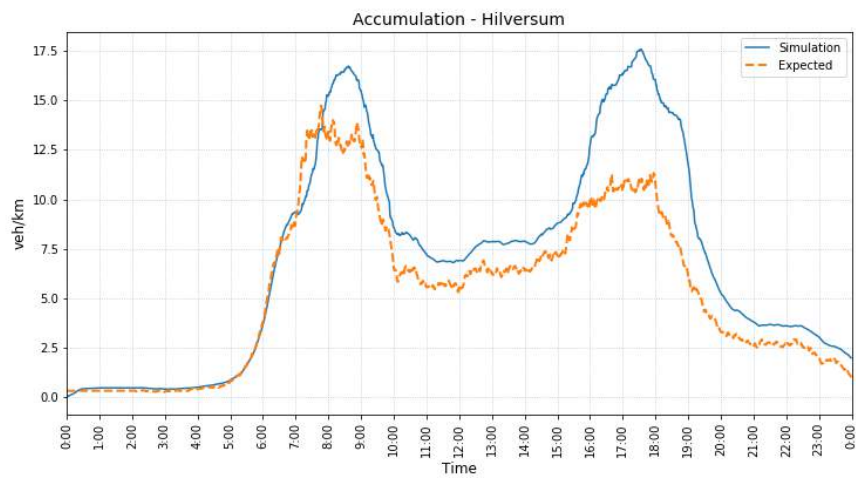
(b) Case with separation of local and through traffic



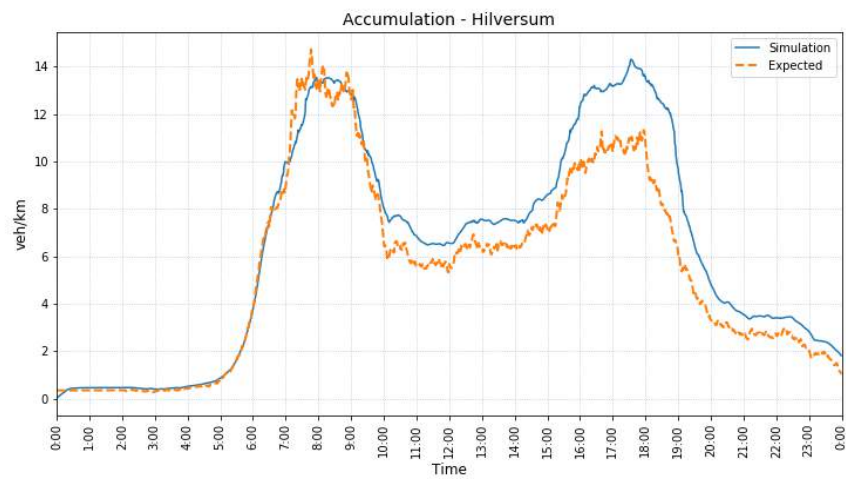
(c) Case with OD matrix based on travel times

Figure E.10: Accumulation plots for Amsterdam

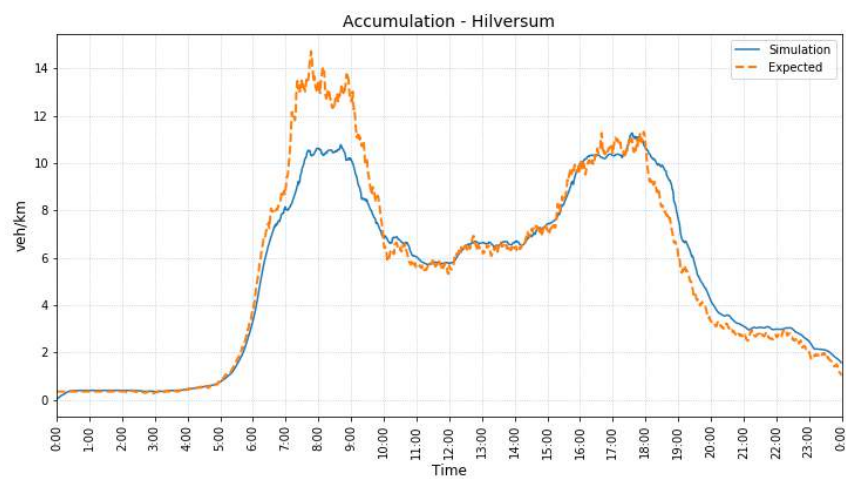
HILVERSUM



(a) Base case



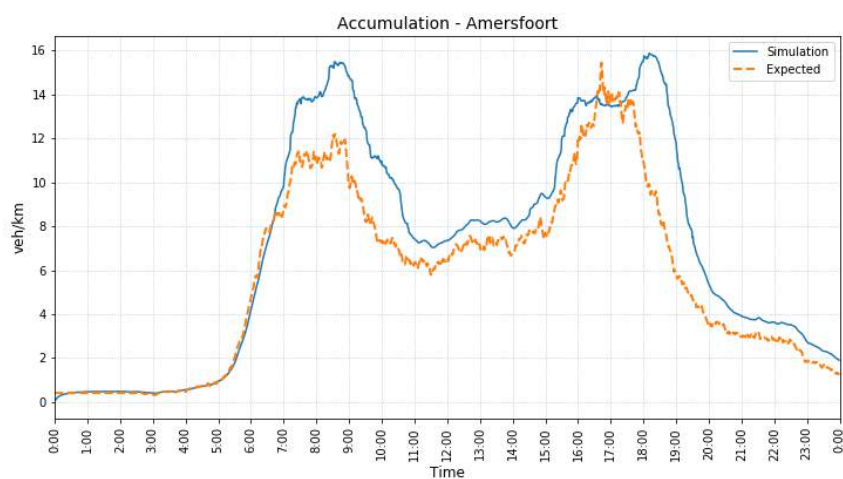
(b) Case with separation of local and through traffic



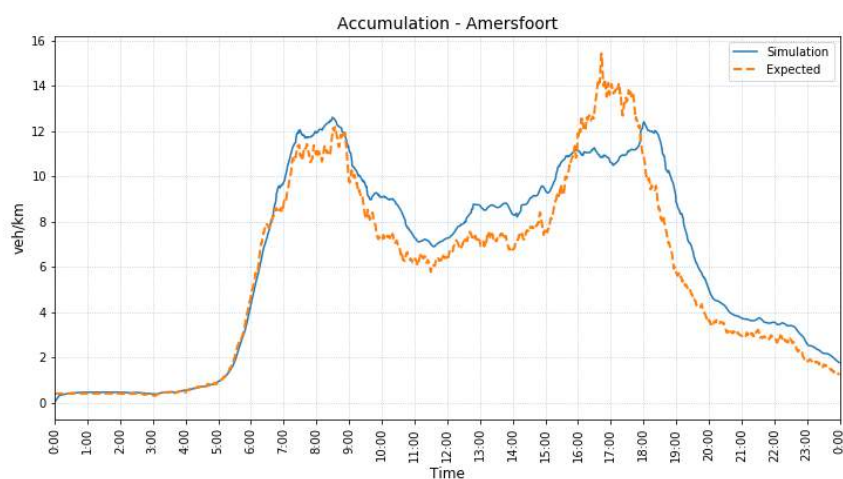
(c) Case with OD matrix based on travel times

Figure E.11: Accumulation plots for Hilversum

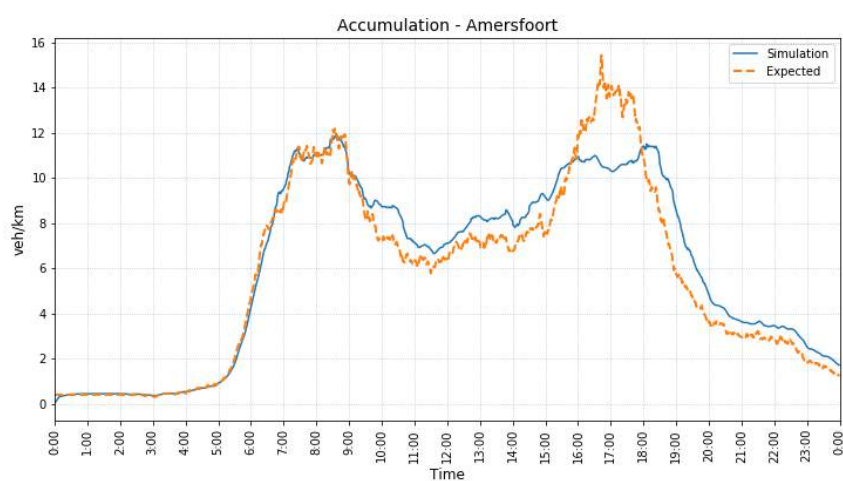
AMERSFOORT



(a) Base case



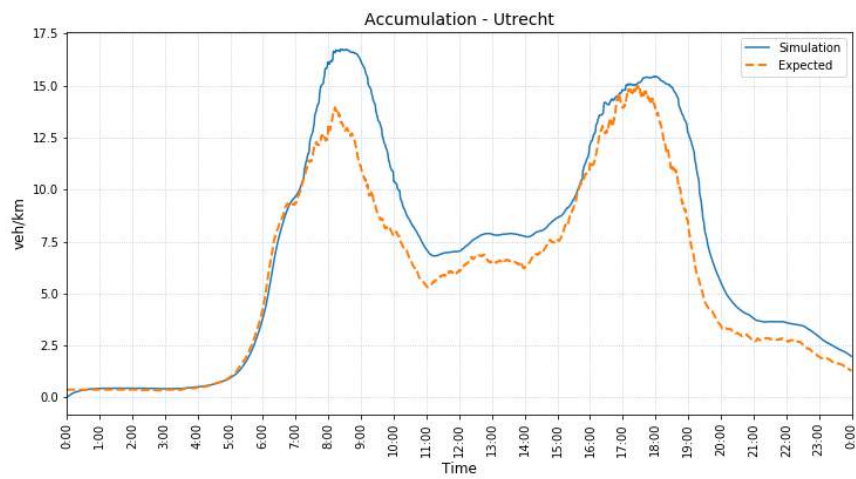
(b) Case with separation of local and through traffic



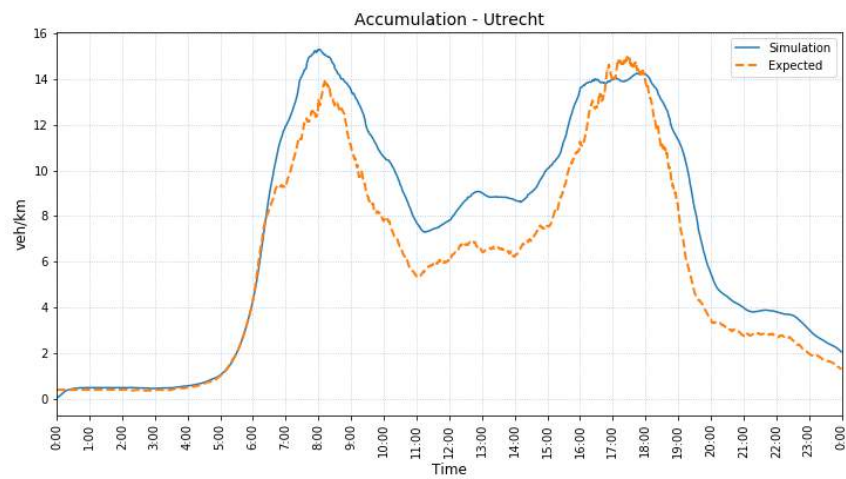
(c) Case with OD matrix based on travel times

Figure E.12: Accumulation plots for Amersfoort

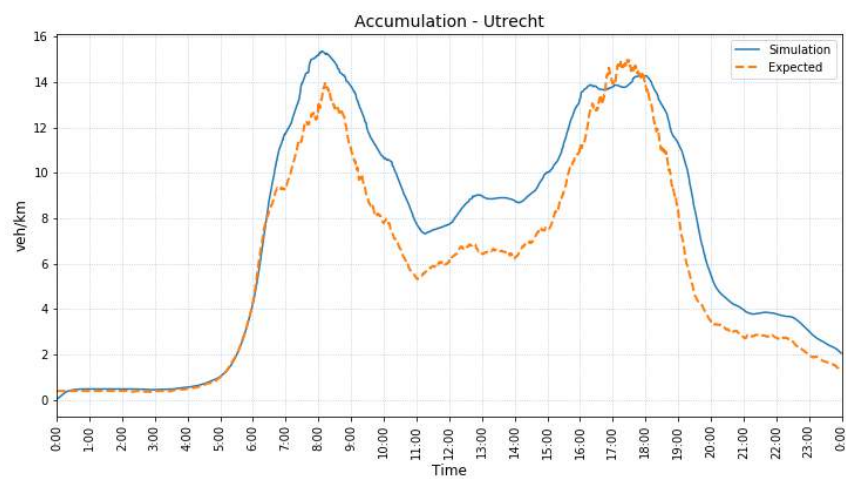
UTRECHT



(a) Base case



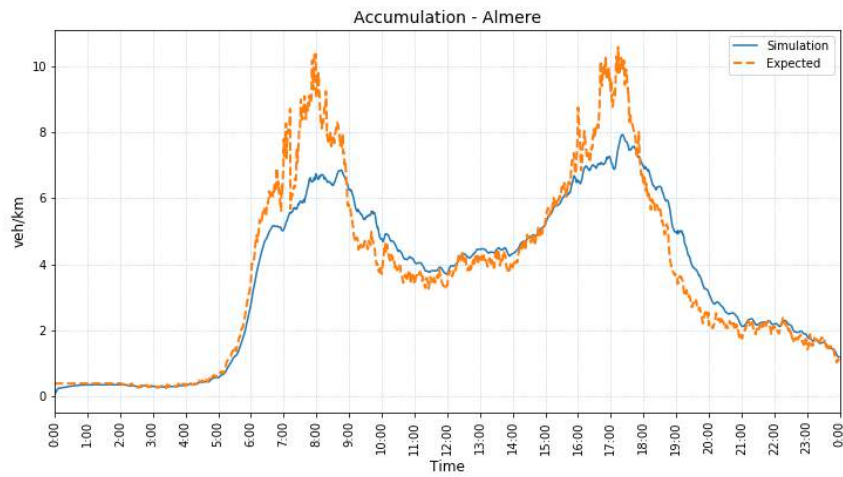
(b) Case with separation of local and through traffic



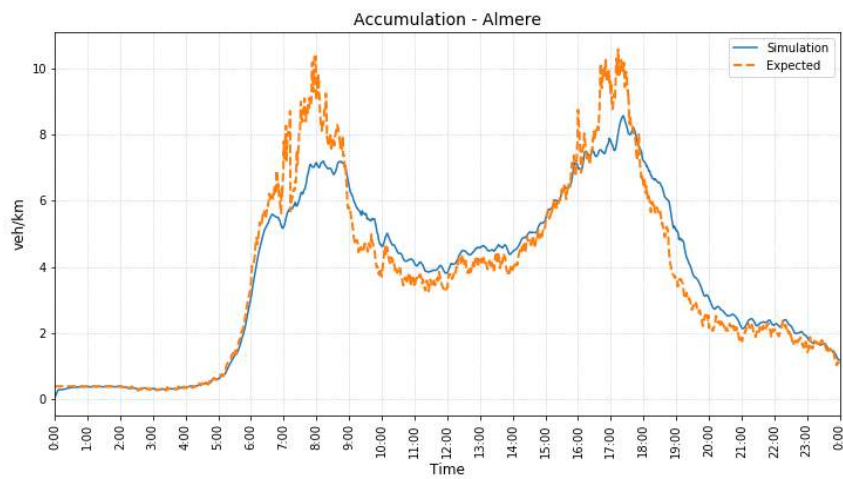
(c) Case with OD matrix based on travel times

Figure E.13: Accumulation plots for Utrecht

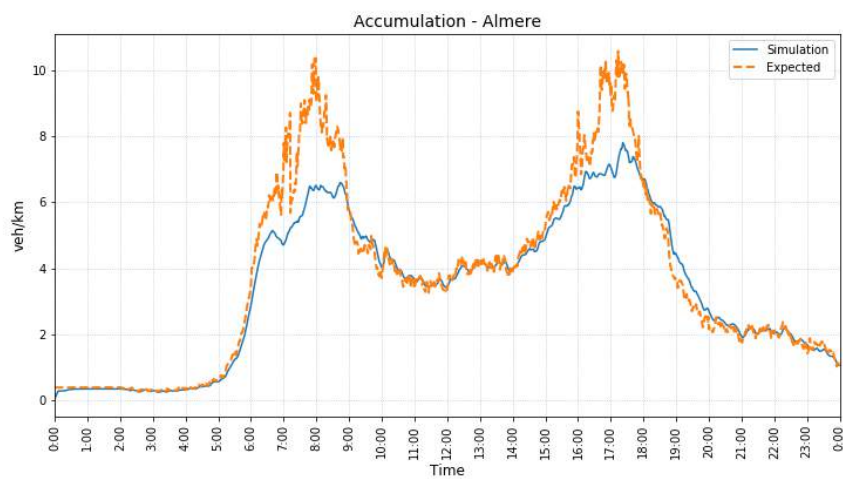
ALMERE



(a) Base case



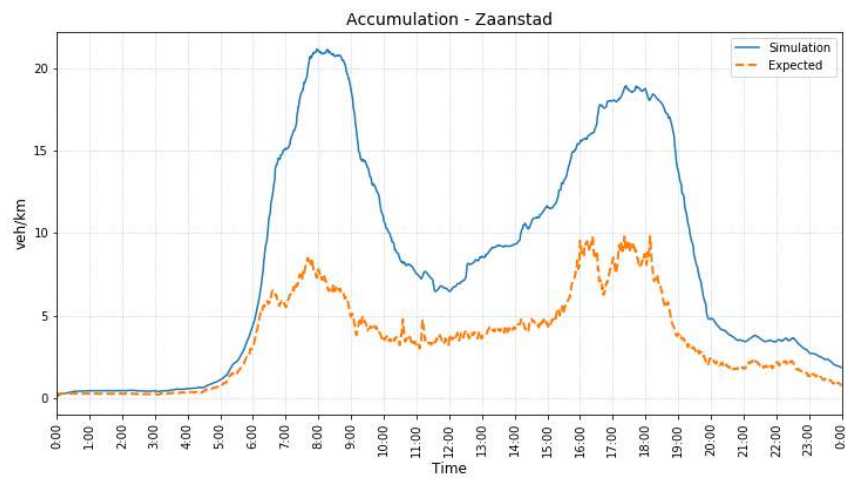
(b) Case with separation of local and through traffic



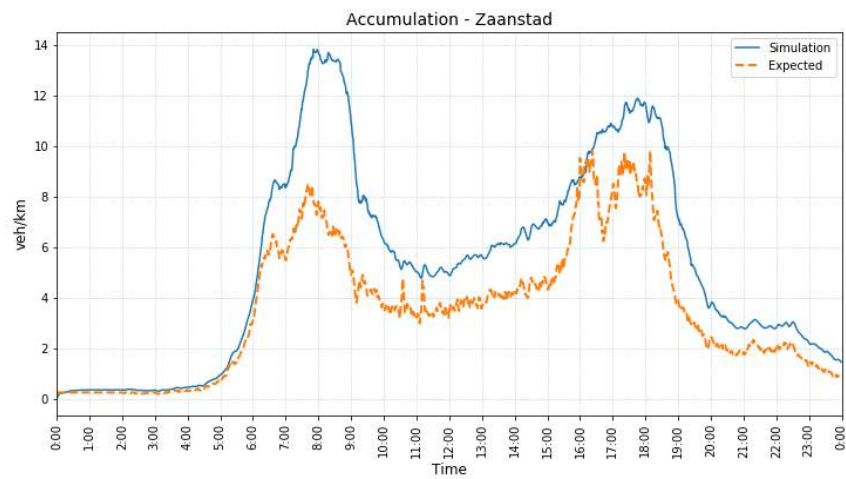
(c) Case with OD matrix based on travel times

Figure E.14: Accumulation plots for Almere

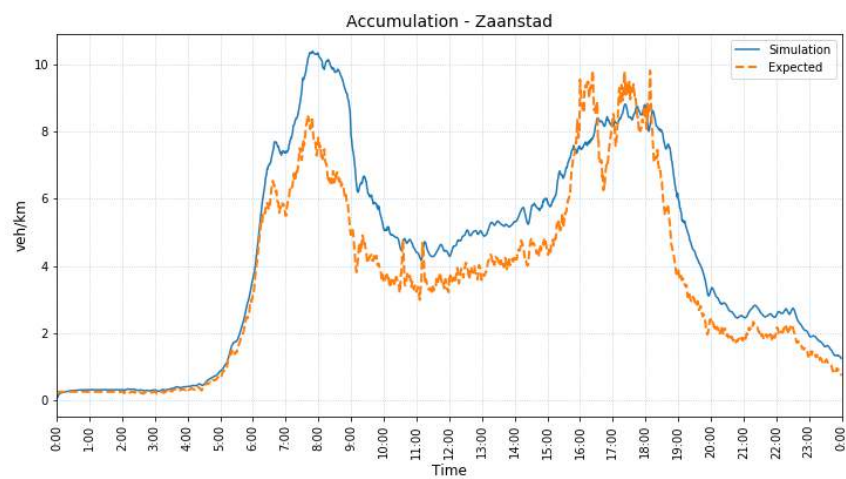
ZAAANSTAD



(a) Base case



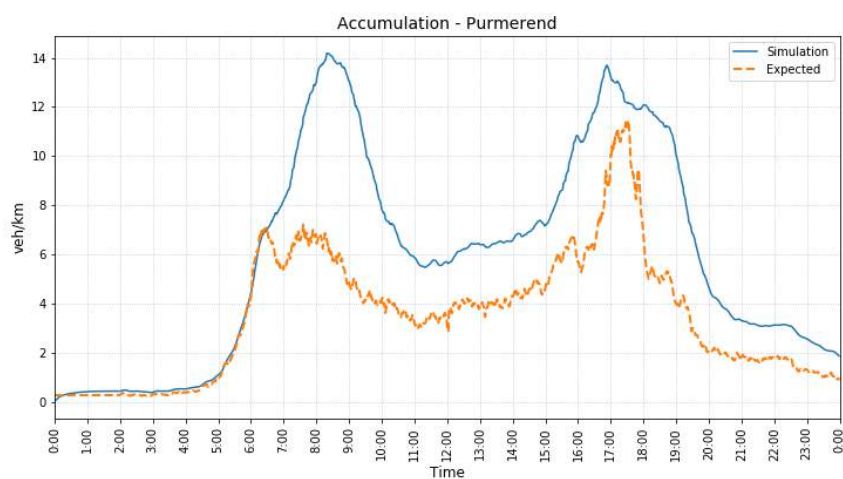
(b) Case with separation of local and through traffic



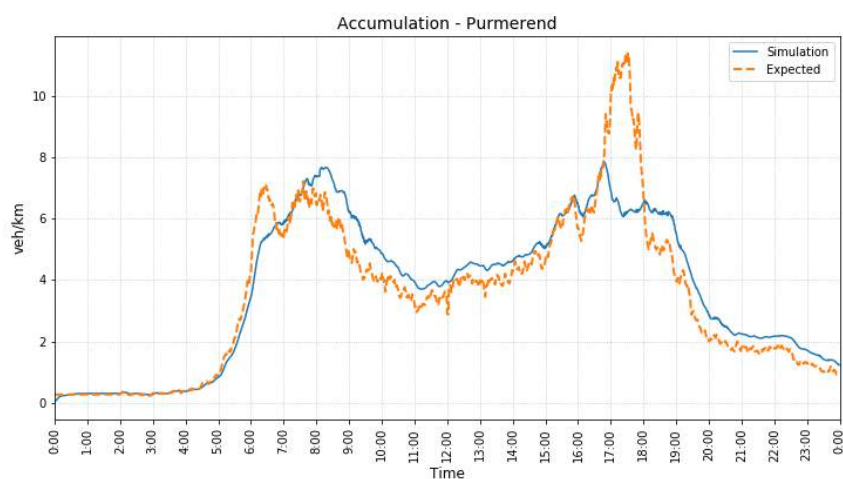
(c) Case with OD matrix based on travel times

Figure E.15: Accumulation plots for Zaanstad

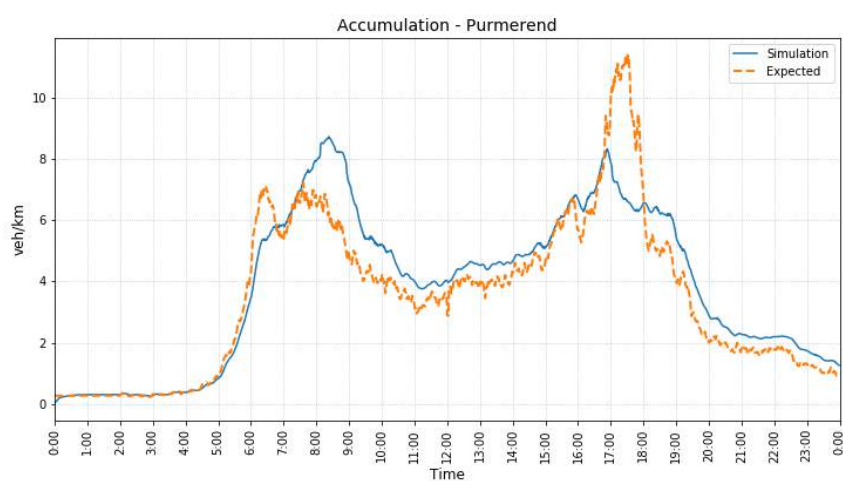
PURMEREND



(a) Base case



(b) Case with separation of local and through traffic



(c) Case with OD matrix based on travel times

Figure E.16: Accumulation plots for Purmerend

F

TRAVEL TIMES

F.1. FREE-FLOW TRAVEL TIMES

DEN HAAG

Table F1: Free-flow travel times in minutes from Den Haag for the simulation cases without (A) and with (B) separation of local and through traffic, and the free-flow travel times from Google Maps and HERE Maps

Destination	Simulation A	Simulation B	Google Maps	HERE Maps
Nissewaard	55	42	40	41
Rotterdam	19	18	17	17
Dordrecht	47	39	38	38
Gouda	38	29	32	31
Zoetermeer	24	21	22	21
Leiden	30	26	31	30
Alphen a/d Rijn	40	35	35	35
Haarlem	55	44	46	41
Amsterdam	68	52	46	44
Hilversum	87	63	63	63
Amersfoort	90	65	64	63
Utrecht	61	44	41	39
Almere	95	71	61	60
Zaanstad	75	54	51	51
Purmerend	83	59	55	53

NISSEWAARD

Table E2: Free-flow travel times in minutes from Nissewaard for the simulation cases without (A) and with (B) separation of local and through traffic, and the free-flow travel times from Google Maps and HERE Maps

Destination	Simulation A	Simulation B	Google Maps	HERE Maps
Den Haag	55	42	40	43
Rotterdam	35	29	33	33
Dordrecht	48	37	36	39
Gouda	57	42	42	44
Zoetermeer	53	40	46	49
Leiden	75	55	60	62
Alphen a/d Rijn	74	52	57	60
Haarlem	100	73	75	73
Amsterdam	104	75	74	76
Hilversum	105	75	80	80
Amersfoort	104	76	77	79
Utrecht	79	56	54	56
Almere	122	86	83	86
Zaanstad	120	83	80	83
Purmerend	126	90	84	85

ROTTERDAM

Table E3: Free-flow travel times in minutes from Rotterdam for the simulation cases without (A) and with (B) separation of local and through traffic, and the free-flow travel times from Google Maps and HERE Maps

Destination	Simulation A	Simulation B	Google Maps	HERE Maps
Den Haag	19	18	15	15
Nissewaard	35	29	31	31
Dordrecht	32	31	28	28
Gouda	30	28	26	26
Zoetermeer	21	20	24	24
Leiden	39	31	35	34
Alphen a/d Rijn	45	37	39	39
Haarlem	64	49	50	45
Amsterdam	77	57	49	48
Hilversum	78	61	64	62
Amersfoort	81	63	61	61
Utrecht	52	42	38	37
Almere	95	76	65	64
Zaanstad	84	59	55	55
Purmerend	92	64	59	57

DORDRECHT

Table F4: Free-flow travel times in minutes from Dordrecht for the simulation cases without (A) and with (B) separation of local and through traffic, and the free-flow travel times from Google Maps and HERE Maps

Destination	Simulation A	Simulation B	Google Maps	HERE Maps
Den Haag	47	39	37	38
Nissewaard	48	37	36	37
Rotterdam	32	31	30	28
Gouda	34	28	34	34
Zoetermeer	41	33	38	38
Leiden	67	51	56	56
Alphen a/d Rijn	51	38	49	50
Haarlem	83	61	72	67
Amsterdam	67	55	55	51
Hilversum	61	50	53	51
Amersfoort	60	48	50	50
Utrecht	37	35	36	36
Almere	78	61	56	57
Zaanstad	92	71	70	71
Purmerend	89	68	71	69

GOUDA

Table E5: Free-flow travel times in minutes from Gouda for the simulation cases without (A) and with (B) separation of local and through traffic, and the free-flow travel times from Google Maps and HERE Maps

Destination	Simulation A	Simulation B	Google Maps	HERE Maps
Den Haag	38	29	31	29
Nissewaard	57	42	43	43
Rotterdam	30	28	27	26
Dordrecht	34	28	36	35
Zoetermeer	19	15	23	22
Leiden	40	29	43	41
Alphen a/d Rijn	20	16	30	31
Haarlem	52	39	58	51
Amsterdam	51	41	53	48
Hilversum	52	41	55	51
Amersfoort	55	43	52	50
Utrecht	26	22	29	26
Almere	69	52	58	57
Zaanstad	72	49	63	62
Purmerend	73	54	67	63

ZOETERMEER

Table E6: Free-flow travel times in minutes from Zoetermeer for the simulation cases without (A) and with (B) separation of local and through traffic, and the free-flow travel times from Google Maps and HERE Maps

Destination	Simulation A	Simulation B	Google Maps	HERE Maps
Den Haag	24	21	21	21
Nissewaard	53	40	47	48
Rotterdam	21	20	25	25
Dordrecht	41	33	40	40
Gouda	19	15	22	22
Leiden	34	29	33	32
Alphen a/d Rijn	30	26	33	34
Haarlem	59	45	48	43
Amsterdam	67	49	47	46
Hilversum	68	49	57	54
Amersfoort	71	51	54	54
Utrecht	42	30	31	30
Almere	85	60	60	61
Zaanstad	79	55	53	53
Purmerend	87	60	57	55

LEIDEN

Table E7: Free-flow travel times in minutes from Leiden for the simulation cases without (A) and with (B) separation of local and through traffic, and the free-flow travel times from Google Maps and HERE Maps

Destination	Simulation A	Simulation B	Google Maps	HERE Maps
Den Haag	30	26	29	27
Nissewaard	75	55	59	59
Rotterdam	39	31	36	34
Dordrecht	67	51	57	55
Gouda	40	29	43	39
Zoetermeer	34	29	32	30
Alphen a/d Rijn	26	22	27	27
Haarlem	29	25	31	28
Amsterdam	45	36	31	31
Hilversum	68	52	48	50
Amersfoort	84	63	55	56
Utrecht	57	42	49	43
Almere	72	55	46	47
Zaanstad	52	37	37	38
Purmerend	60	43	41	40

ALPHEN AAN DEN RIJN

Table F8: Free-flow travel times in minutes from Alphen aan den Rijn for the simulation cases without (A) and with (B) separation of local and through traffic, and the free-flow travel times from Google Maps and HERE Maps

Destination	Simulation A	Simulation B	Google Maps	HERE Maps
Den Haag	40	35	35	34
Nissewaard	74	52	56	57
Rotterdam	45	37	42	41
Dordrecht	51	38	49	49
Gouda	20	16	31	31
Zoetermeer	30	25	33	33
Leiden	26	22	27	26
Haarlem	36	31	33	30
Amsterdam	34	32	32	33
Hilversum	60	50	50	52
Amersfoort	66	50	53	53
Utrecht	44	41	30	30
Almere	65	53	48	49
Zaanstad	55	41	38	40
Purmerend	64	46	42	42

HAARLEM

Table F9: Free-flow travel times in minutes from Haarlem for the simulation cases without (A) and with (B) separation of local and through traffic, and the free-flow travel times from Google Maps and HERE Maps

Destination	Simulation A	Simulation B	Google Maps	HERE Maps
Den Haag	55	44	40	37
Nissewaard	100	73	71	68
Rotterdam	64	49	48	44
Dordrecht	83	61	67	64
Gouda	52	39	55	49
Zoetermeer	59	45	43	39
Leiden	29	25	27	25
Alphen a/d Rijn	36	31	30	28
Amsterdam	29	27	25	24
Hilversum	52	43	43	44
Amersfoort	68	55	50	49
Utrecht	52	46	43	40
Almere	56	46	41	40
Zaanstad	27	23	24	24
Purmerend	44	34	32	30

AMSTERDAM

Table F.10: Free-flow travel times in minutes from Amsterdam for the simulation cases without (A) and with (B) separation of local and through traffic, and the free-flow travel times from Google Maps and HERE Maps

Destination	Simulation A	Simulation B	Google Maps	HERE Maps
Den Haag	68	52	45	42
Nissewaard	104	75	75	74
Rotterdam	77	57	52	49
Dordrecht	67	55	54	51
Gouda	51	41	52	47
Zoetermeer	67	49	47	45
Leiden	45	36	31	30
Alphen a/d Rijn	34	32	34	33
Haarlem	29	27	29	25
Hilversum	25	25	29	30
Amersfoort	41	37	36	36
Utrecht	30	30	30	27
Almere	29	28	27	27
Zaanstad	31	29	29	31
Purmerend	28	25	30	29

HILVERSUM

Table F.11: Free-flow travel times in minutes from Hilversum for the simulation cases without (A) and with (B) separation of local and through traffic, and the free-flow travel times from Google Maps and HERE Maps

Destination	Simulation A	Simulation B	Google Maps	HERE Maps
Den Haag	87	63	63	63
Nissewaard	105	75	78	79
Rotterdam	78	61	62	63
Dordrecht	61	50	51	52
Gouda	52	41	53	52
Zoetermeer	68	49	55	55
Leiden	68	52	50	51
Alphen a/d Rijn	60	50	53	54
Haarlem	52	43	49	47
Amsterdam	25	25	31	31
Amersfoort	19	19	22	23
Utrecht	27	27	32	34
Almere	22	22	25	27
Zaanstad	43	35	39	43
Purmerend	39	31	40	41

AMERSFOORT

Table F.12: Free-flow travel times in minutes from Amersfoort for the simulation cases without (A) and with (B) separation of local and through traffic, and the free-flow travel times from Google Maps and HERE Maps

Destination	Simulation A	Simulation B	Google Maps	HERE Maps
Den Haag	90	65	63	61
Nissewaard	104	76	78	77
Rotterdam	81	63	62	61
Dordrecht	60	48	51	50
Gouda	55	43	53	50
Zoetermeer	71	51	55	53
Leiden	84	63	57	57
Alphen a/d Rijn	66	50	53	52
Haarlem	68	55	55	54
Amsterdam	41	37	37	37
Hilversum	19	19	25	25
Utrecht	27	26	32	32
Almere	31	28	29	29
Zaanstad	59	47	46	49
Purmerend	55	43	47	47

UTRECHT

Table F.13: Free-flow travel times in minutes from Utrecht for the simulation cases without (A) and with (B) separation of local and through traffic, and the free-flow travel times from Google Maps and HERE Maps

Destination	Simulation A	Simulation B	Google Maps	HERE Maps
Den Haag	61	44	41	39
Nissewaard	79	56	55	55
Rotterdam	52	43	40	38
Dordrecht	37	35	36	34
Gouda	26	22	30	28
Zoetermeer	42	30	33	31
Leiden	57	42	50	44
Alphen a/d Rijn	44	41	30	30
Haarlem	52	46	48	43
Amsterdam	30	30	31	28
Hilversum	27	27	36	33
Amersfoort	27	26	32	32
Almere	44	38	39	39
Zaanstad	55	46	46	47
Purmerend	52	43	46	45

ALMERE

Table F.14: Free-flow travel times in minutes from Almere for the simulation cases without (A) and with (B) separation of local and through traffic, and the free-flow travel times from Google Maps and HERE Maps

Destination	Simulation A	Simulation B	Google Maps	HERE Maps
Den Haag	95	71	60	58
Nissewaard	122	86	84	84
Rotterdam	95	76	67	65
Dordrecht	78	61	57	57
Gouda	69	52	58	56
Zoetermeer	85	60	61	60
Leiden	72	55	46	46
Alphen a/d Rijn	65	53	49	50
Haarlem	56	46	45	43
Amsterdam	29	28	27	26
Hilversum	22	22	25	27
Amersfoort	31	28	28	28
Utrecht	44	38	38	38
Zaanstad	47	38	35	38
Purmerend	43	34	36	36

ZAA NSTAD

Table F.15: Free-flow travel times in minutes from Zaanstad for the simulation cases without (A) and with (B) separation of local and through traffic, and the free-flow travel times from Google Maps and HERE Maps

Destination	Simulation A	Simulation B	Google Maps	HERE Maps
Den Haag	75	54	50	49
Nissewaard	120	83	81	81
Rotterdam	84	59	57	56
Dordrecht	92	71	70	71
Gouda	72	49	64	61
Zoetermeer	79	55	53	52
Leiden	52	37	37	37
Alphen a/d Rijn	55	41	40	40
Haarlem	27	23	29	26
Amsterdam	31	29	30	31
Hilversum	43	35	39	43
Amersfoort	59	47	46	49
Utrecht	55	46	46	47
Almere	47	38	37	40
Purmerend	20	15	18	19

PURMEREND

Table F.16: Free-flow travel times in minutes from Purmerend for the simulation cases without (A) and with (B) separation of local and through traffic, and the free-flow travel times from Google Maps and HERE Maps

Destination	Simulation A	Simulation B	Google Maps	HERE Maps
Den Haag	83	59	54	51
Nissewaard	126	90	84	83
Rotterdam	92	64	61	58
Dordrecht	89	68	71	69
Gouda	73	54	68	64
Zoetermeer	87	60	57	54
Leiden	60	43	40	39
Alphen a/d Rijn	64	46	43	42
Haarlem	44	34	36	32
Amsterdam	28	25	30	29
Hilversum	39	31	39	41
Amersfoort	55	43	46	47
Utrecht	52	43	47	45
Almere	43	34	37	38
Zaanstad	20	15	17	18

F.2. MORNING PEAK TRAVEL TIMES

DEN HAAG - AMSTERDAM

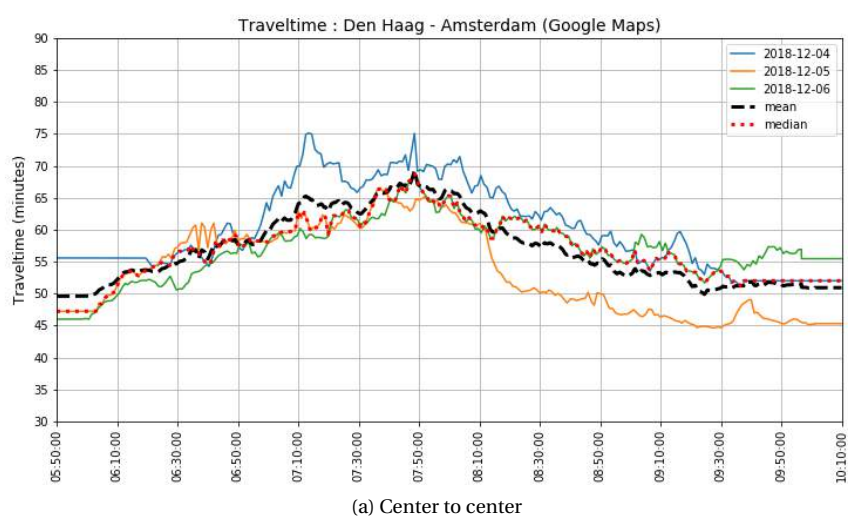
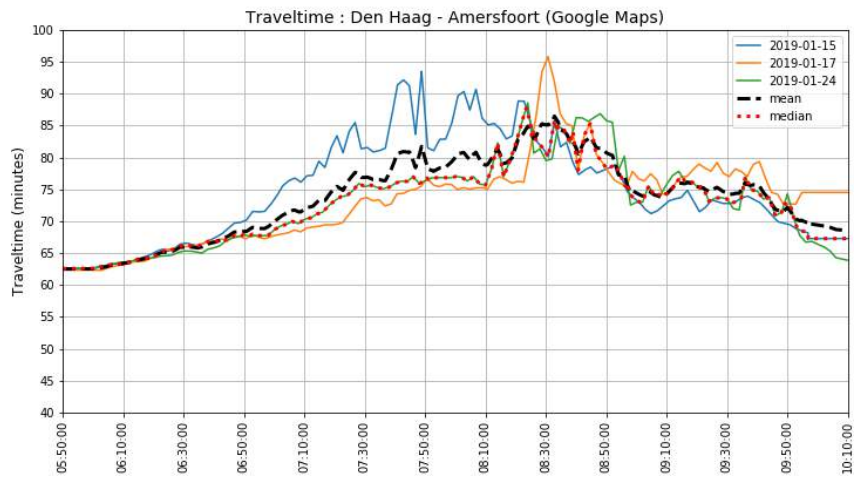
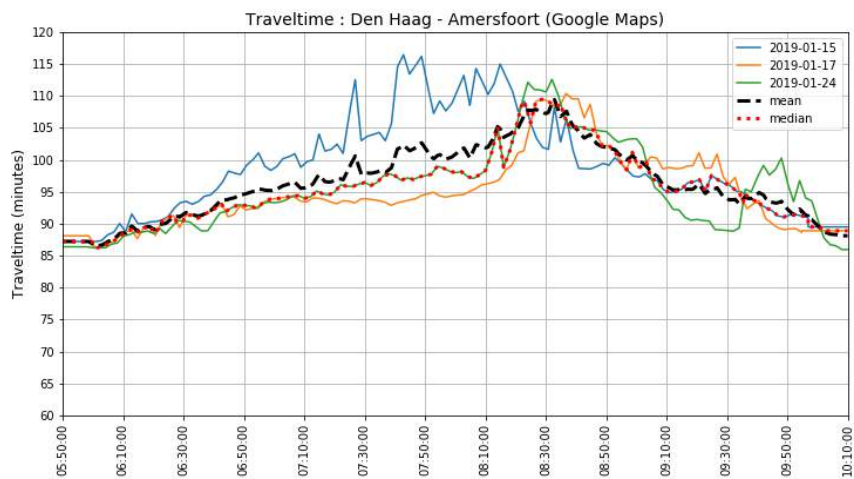


Figure F.1: Travel times Den Haag - Amsterdam during morning peak

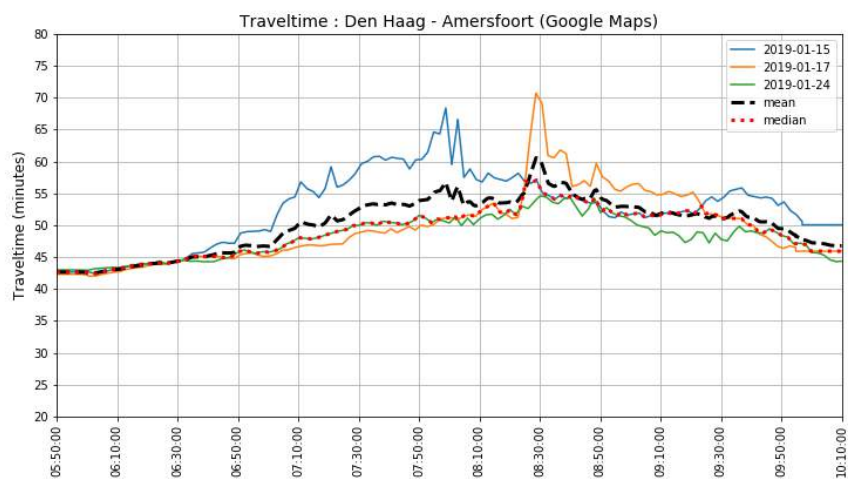
DEN HAAG - AMERSFOORT



(a) Center to center



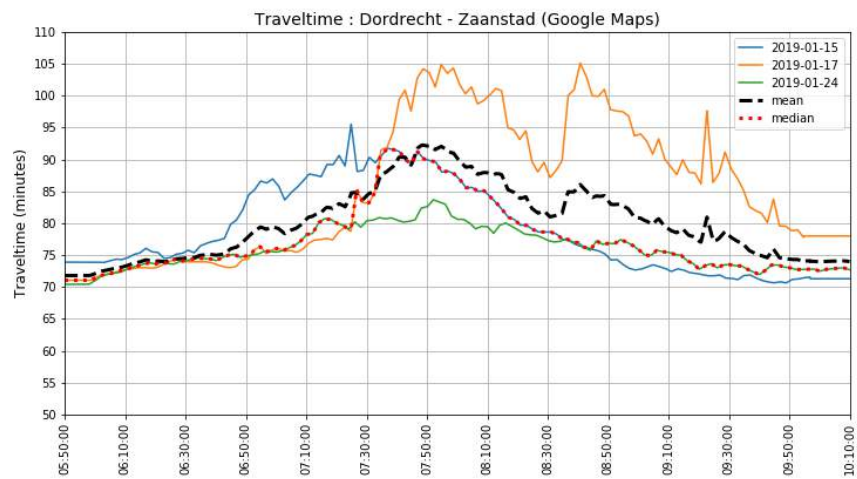
(b) Upper bound



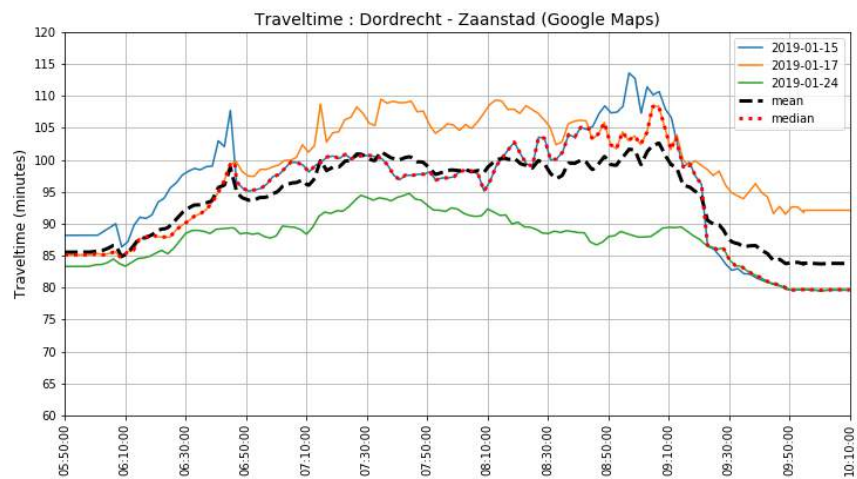
(c) Lower bound

Figure E2: Travel times Den Haag - Amersfoort during morning peak

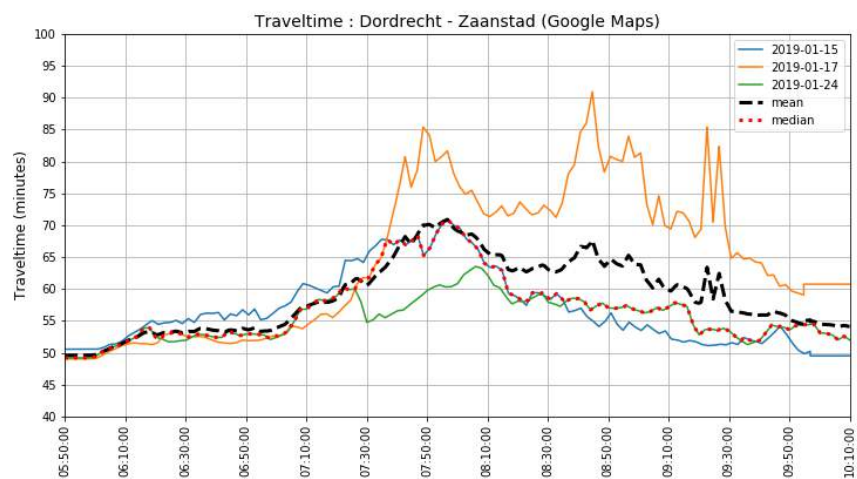
DORDRECHT - ZAASTAD



(a) Center to center



(b) Upper bound



(c) Lower bound

Figure E3: Travel times Dordrecht - Zaanstad during morning peak

DEN HAAG - ROTTERDAM

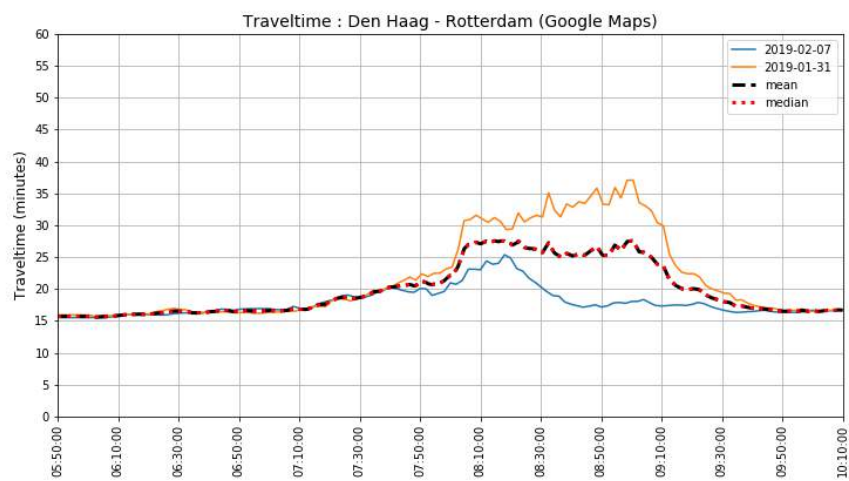


Figure E4: Travel times Den Haag - Rotterdam during morning peak

UTRECHT - AMERSFOORT

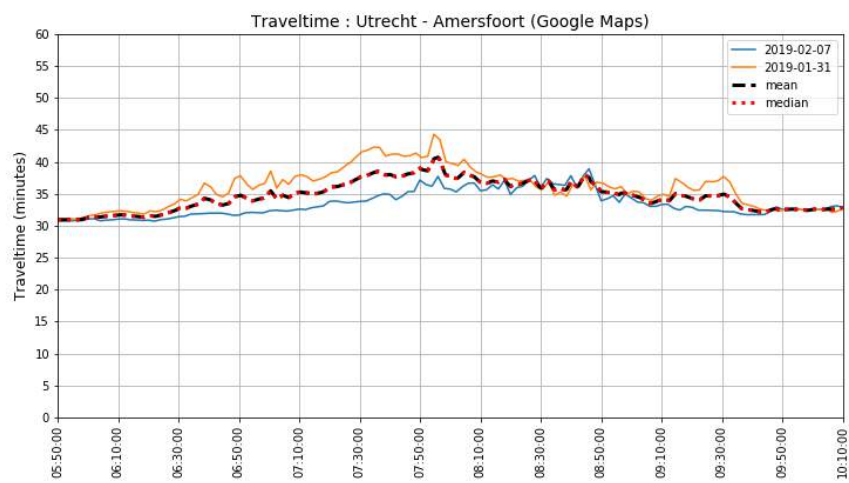


Figure E5: Travel times Utrecht - Amersfoort during morning peak

HILVERSUM - AMERSFOORT

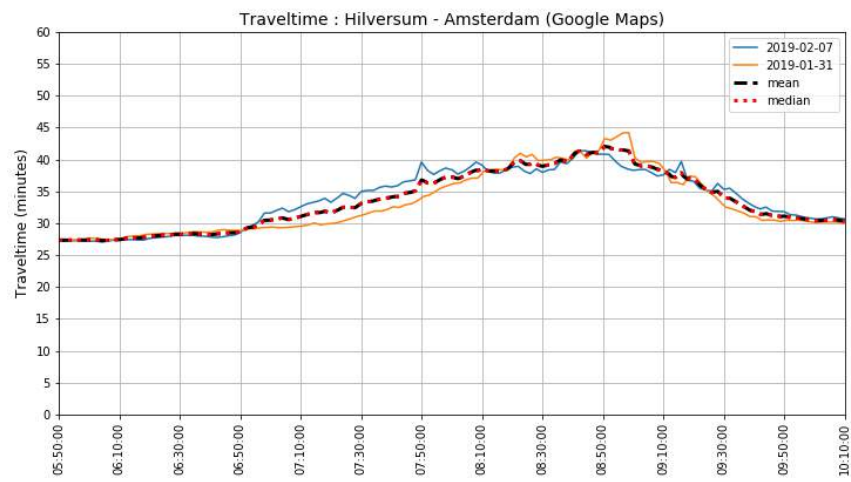


Figure F6: Travel times Hilversum-Amsterdam during morning peak

F.3. AFTERNOON PEAK TRAVEL TIMES

DEN HAAG - AMSTERDAM

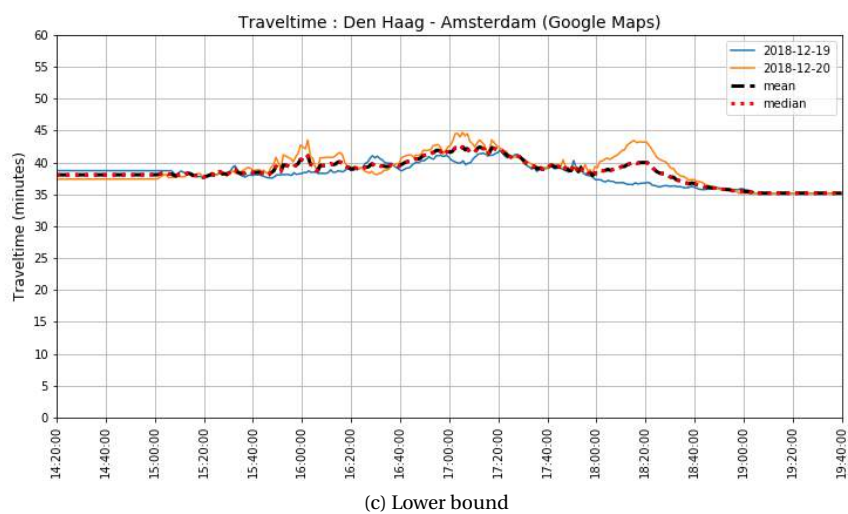
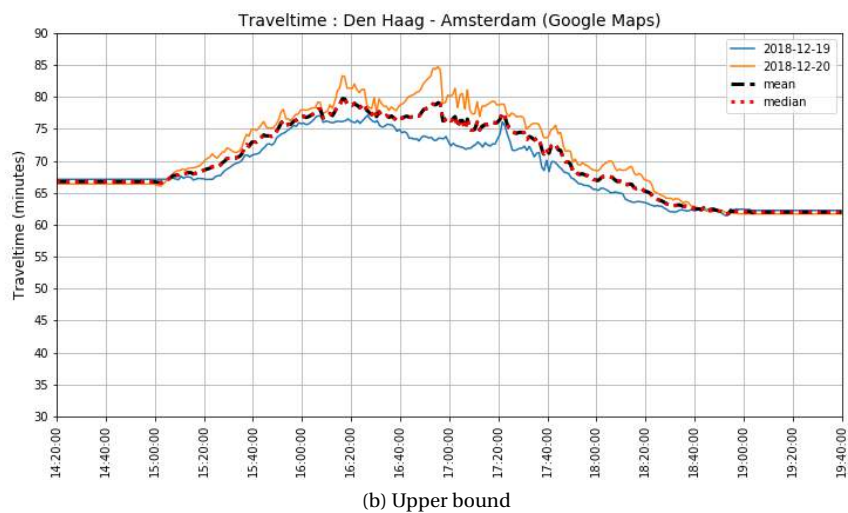
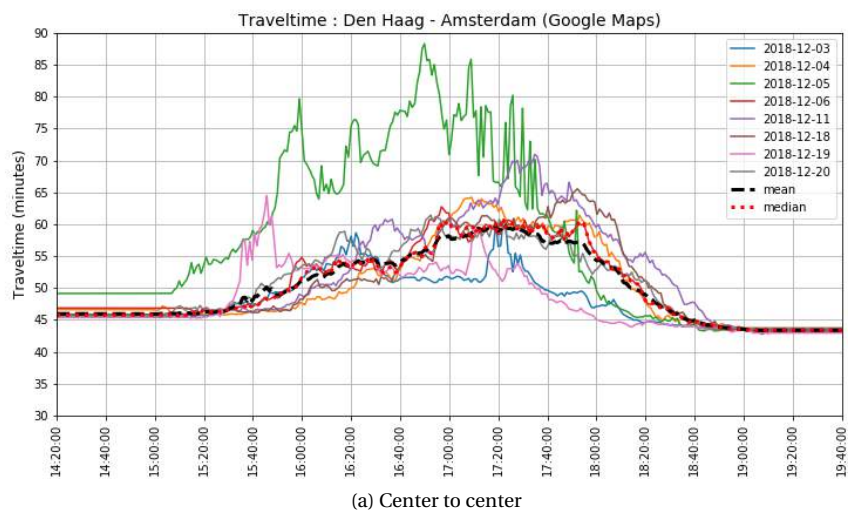
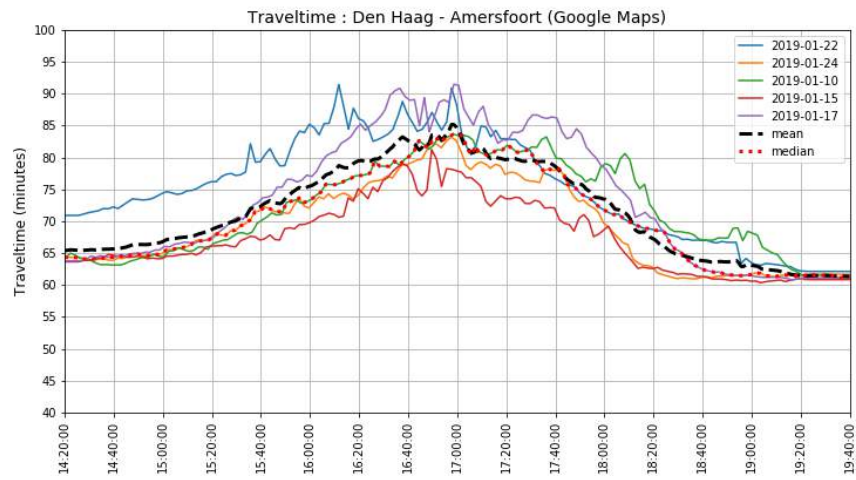
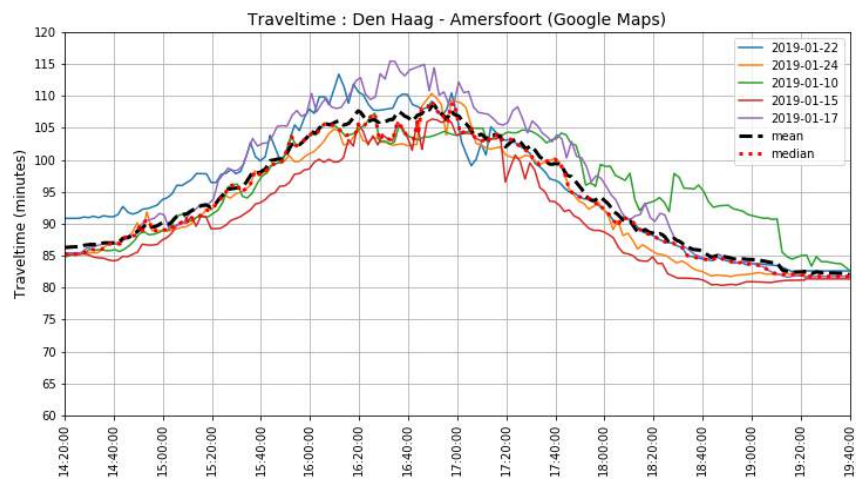


Figure F7: Travel times Den Haag - Amsterdam during afternoon peak

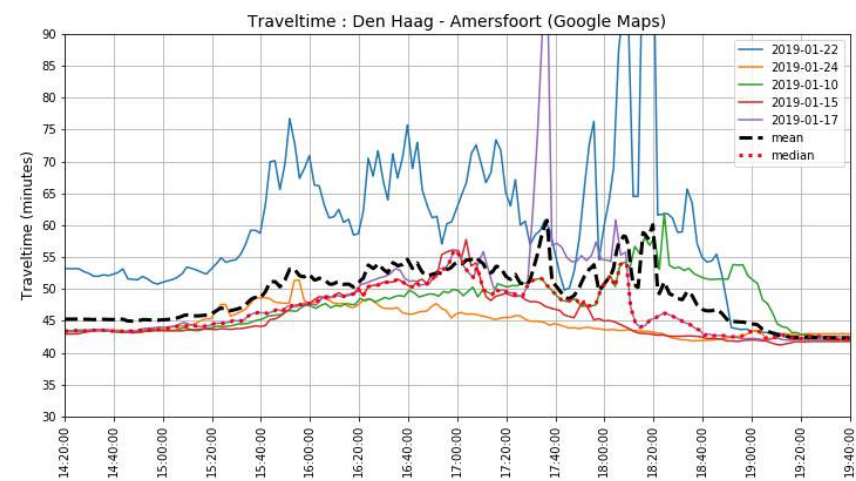
DEN HAAG - AMERSFOORT



(a) Center to center



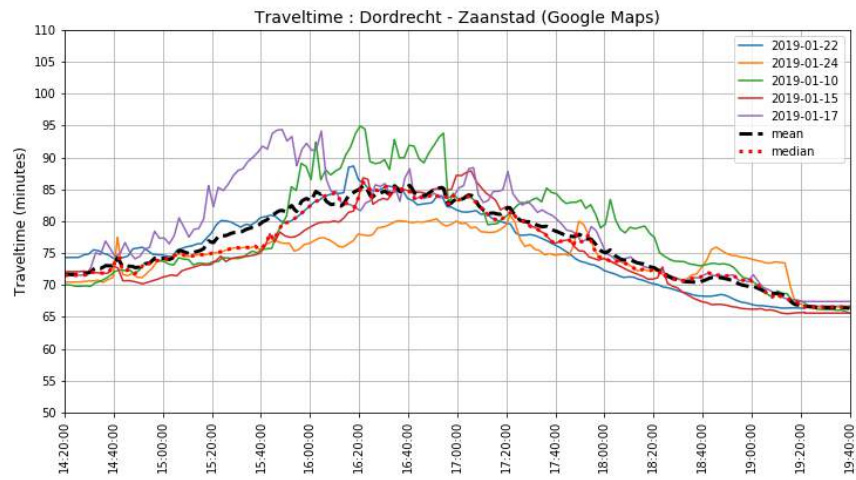
(b) Upper bound



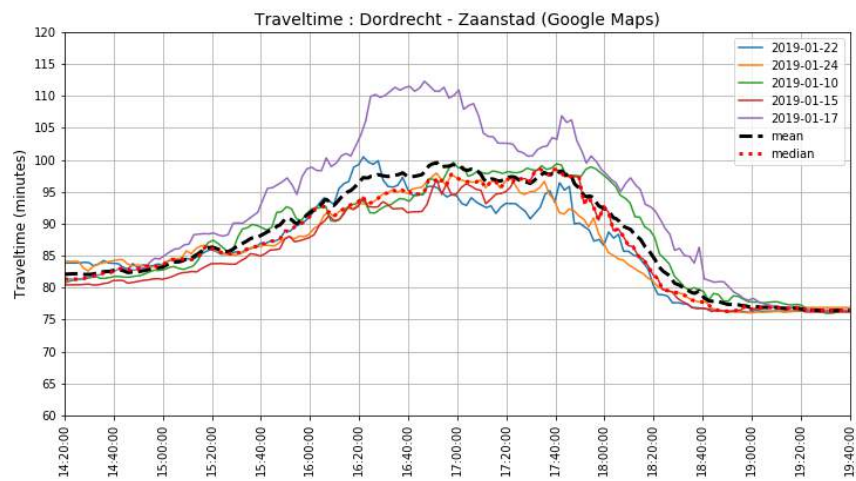
(c) Lower bound

Figure F8: Travel times Den Haag - Amersfoort during afternoon peak

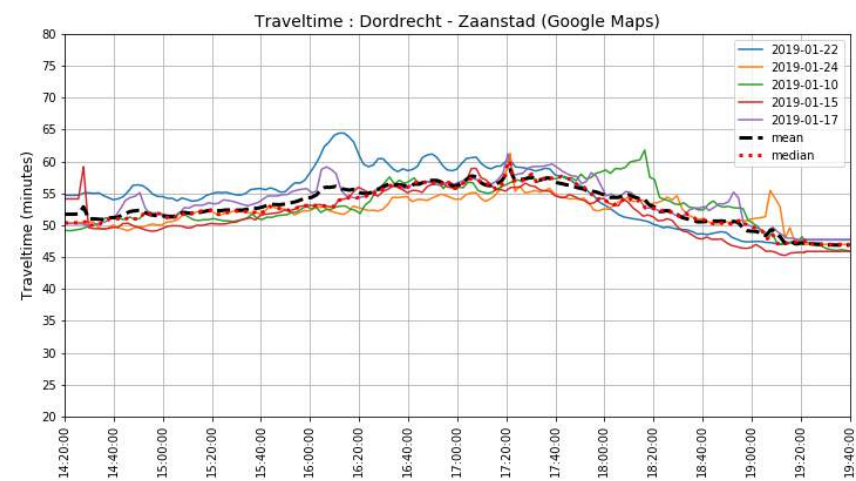
DORDRECHT - ZAA NSTAD



(a) Center to center



(b) Upper bound



(c) Lower bound

Figure E9: Travel times Dordrecht - Zaanstad during afternoon peak

DEN HAAG - ROTTERDAM

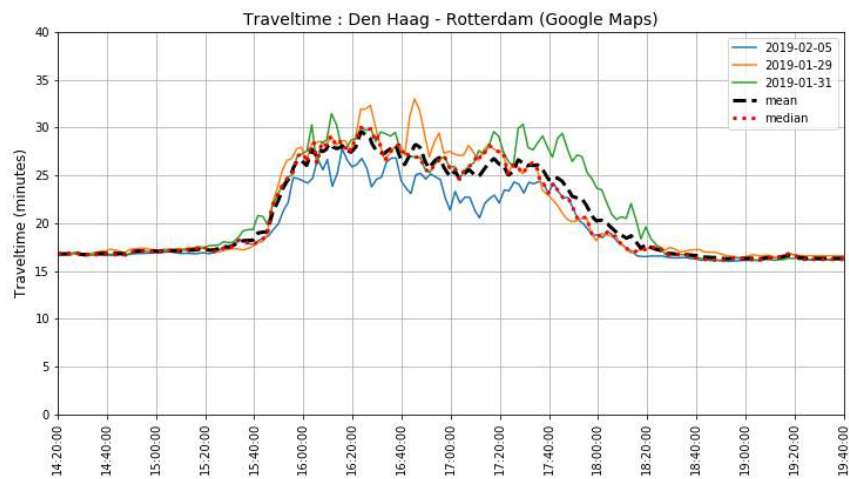


Figure F.10: Travel times Den Haag - Rotterdam during afternoon peak

UTRECHT - AMERSFOORT

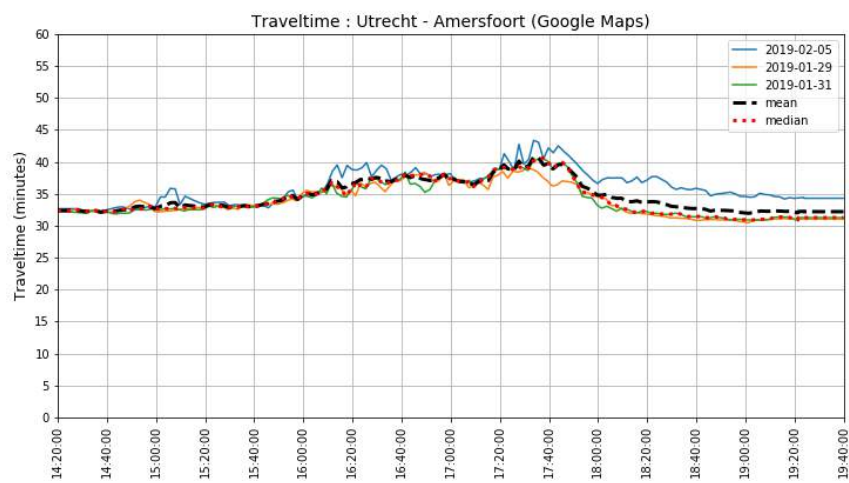


Figure F.11: Travel times Utrecht - Amersfoort during afternoon peak

HILVERSUM - AMERSFOORT

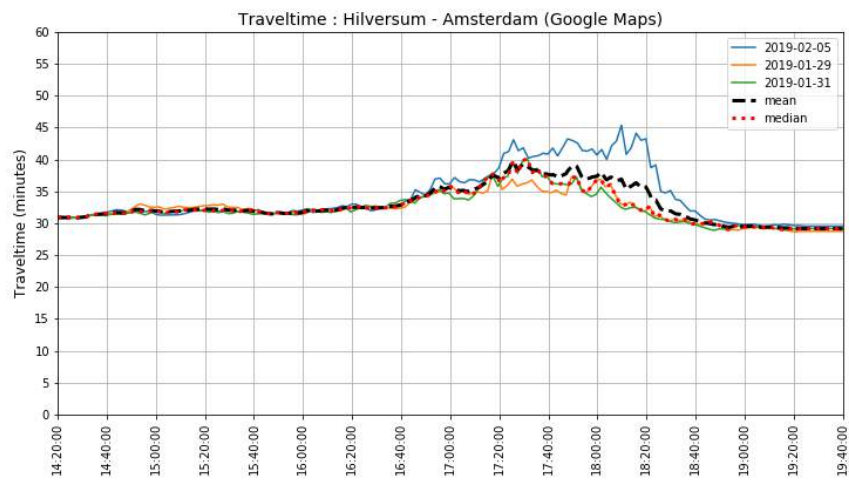


Figure F.12: Travel times Hilversum-Amsterdam during afternoon peak



TECHNICAL INFORMATION

COMPUTATION TIMES

Table G.1: Computation times per simulation

#	Simulation name	Computation time
1	Base case	5min 53sec
2	Base case with reduced internal distances	5min 15sec
3	Logit parameter 2.0	15 min 0sec
4	Logit parameter 3.0	18 min 18sec
5	Logit parameter 4.0	16 min 17sec
6	Logit parameter 5.0	14 min 56sec
7	Separation local & through traffic	4min 49sec
8	OD-matrix based on travel times	4min 36sec

COMPUTER SPECIFICATIONS

Table G.2: Computer specifications

Processor	Intel Core i7-4710HQ @ 2.50GHz
RAM	8.00 GB
OS	Windows 10 Home 64bit

